

**Peraryl-substituted Cyclotrisilene ($c\text{-Si}_3\text{R}_4$) as a Precursor for
Ring Opening and Expansion**

Dissertation

Zur Erlangung des Grades
des Doktors der Naturwissenschaften
der Naturwissenschaftlich-Technischen Fakultät,
der Universität des Saarlandes

vorgelegt von

M. Sc. Hui Zhao

Saarbrücken

08.2018

Tag des Kolloquiums:	06. 12. 2018
Dekan:	Prof. Dr. Guido Kickelbick
Berichterstatter:	Prof. Dr. David Scheschkewitz Prof. Dr. Guido Kickelbick
Vorsitz:	Prof. Dr. Michael Springborg
Akademischer Mitarbeiter:	Dr. Volker Huch

Die vorliegende Arbeit entstand in der Zeit von Oktober 2014 bis August 2018 an der Universität des Saarlandes, Naturwissenschaftlich-Technische Fakultät, Fachrichtung Chemie, im Arbeitskreis von Herrn Prof. Dr. David Scheschkewitz.

Kurzzusammenfassung

Hauptaugenmerk dieser Arbeit liegt auf dem Untersuchen der Reaktivität von peraryl-substituierten Cyclotrisilenen ($c\text{-Si}_3\text{Tip}_4$) gegenüber verschiedenen kleinen Molekülen. Die Reaktion von $c\text{-Si}_3\text{Tip}_4$ mit Styrol und Diketon liefert zugleich weitere Hinweise auf einen dritten Reaktionsmechanismus, die Ringöffnungsreaktion zu Disilylsilylenen, die Siliciumversion von vinyl-Carbenen. Die beschriebene Synthese von 1,2,3-Trisilacyclopentadienederivaten, durch die Reaktion von $c\text{-Si}_3\text{Tip}_4$ mit Alkinen, stellt eine neue Methode zur Herstellung von cyclischen, konjugierten C=C–Si=Si Systemen dar. Si_3E -bicyclo[1.1.0]butane and Si_3E_2 -bicyclo[1.1.1]pentane (E = S, Se, Te) werden erhalten durch die Additionsreaktionen von $c\text{-Si}_3\text{Tip}_4$ mit Chalkogenen. Die thermische Isomerisierung zu 2-Chalcogena-1,3,4-trisilacyclobutenen wird durch die NMR-spektroskopischen Daten nahegelegt und durch die Isolierung des Hydrolyseprodukts 2-Tellura-1,3,4-trisilacyclobuten gestützt.

Abstract

This thesis concentrates mainly on the reactivity study of a peraryl-substituted cyclotrisilene ($c\text{-Si}_3\text{Tip}_4$) towards various small molecules. The reaction of $c\text{-Si}_3\text{Tip}_4$ with styrene and diketone provides further evidence for a third reaction mode, namely the ring opening to disilylenyl silylene, a silicon version of vinyl carbene. The synthesis of 1,2,3-trisilacyclopentadiene derivatives that achieved by reaction of $c\text{-Si}_3\text{Tip}_4$ with alkynes, constitutes a new method to access cyclic conjugated $\text{C}=\text{C}-\text{Si}=\text{Si}$ systems. π -addition reactions of $c\text{-Si}_3\text{Tip}_4$ with chalcogen elements resulting in the Si_3E -bicyclo[1.1.0]butane and Si_3E_2 -bicyclo[1.1.1]pentane ($\text{E} = \text{S}, \text{Se}, \text{Te}$) derivatives. In addition, thermal isomerization to 2-chalcogena-1,3,4-trisilacyclobutenes is achieved as suggested by NMR spectroscopic data and supported by the isolation of the hydrolysis product of 2-tellura-1,3,4-trisilacyclobutene.

Annotation

This thesis has been published in parts in:

- Hui. Zhao, Kinga. Leszczyńska, Lukas. Klemmer, Volker. Huch, Michael. Zimmer and David. Scheschkewitz, Disilyl Silylene Reactivity of a Cyclotrisilene, *Angew. Chem. Int. Ed.* **2018**, *57*, 2445-2449. [DOI:10.1002/anie.201711833](https://doi.org/10.1002/anie.201711833)
Angew. Chem. **2018**, *130*, 2470-2474. [DOI:10.1002/ange.201711833](https://doi.org/10.1002/ange.201711833)
- Hui Zhao, Lukas Klemmer, Michael J. Cowley, Moumita Majumdar, Volker Huch, Michael Zimmer and David Scheschkewitz, Phenylene-bridged cross-conjugated 1,2,3-trisilacyclopentadienes, *Chem. Commun.*, **2018**, *54*, 8399-8402. [DOI: 10.1039/C8CC03297A](https://doi.org/10.1039/C8CC03297A)
- Hui Zhao, Lukas Klemmer, Michael J. Cowley, Volker Huch, Michael Zimmer and David Scheschkewitz, Reactivity of a Peraryl Cyclotrisilene (*c*-Si₃R₄) Toward Chalcogens, *Z. Anorg. Allg. Chem.* **2018**, *644*, 999-1005. [DOI: 10.1002/zaac.201800182](https://doi.org/10.1002/zaac.201800182)

Acknowledgements

Firstly I would like to express my deepest gratitude to my research supervisor **Prof. Dr. Scheschkewitz** who was despite being rather busy with his duties, took time to listen, discuss and keep me on the correct path of my research. This thesis would not have been possible without the professional guidance, enthusiastic encouragement and useful critiques of **Prof. Dr. Scheschkewitz** throughout my entire PhD study.

I would also like to thank **Prof. Dr. Guido Kickelbick** for taking the duty as an examiner of this thesis.

Special acknowledgement goes towards the **Saarland University, China Scholarship Council**, and **COST Action CM1302** (Smart Inorganic Polymers) for helping and providing funding for this work.

I am grateful to **Lukas Klemmer** for performing DFT calculations. It was delighted to have the opportunity to collaborate with him and learn calculations.

I would like to thank **Dr. Volker Huch** for his effort in collecting and analysing the X-ray crystal data.

Many thanks to **Dr. Michael Zimmer** for performing the VT NMR and solid-state CP-MAS NMR experiments. As well as to **Susanne Harling** for the measurement of elemental analyses.

A special mention to our secretary **Bianca Iannuzzi**, I would like to thank you for your kind support in various routines.

My special thanks are extended to all other former and current group members: **Dr. Moumita Majumdar, Dr. Michael Cowley, Dr. Prasenjit Bag, Dr. Philipp Willmes, Dr. David Nieder, Dr. Naim M. Obeid, Isabell Omlor, Bettina Piro, Günther Berlin, Dr. Carsten Präsang, Dr. Andreas Rammo, Dr. Diego Andrea,**

Marcel Lambert, Yvonne Kaiser, Andreas Kell, Yannic Heider, Thomas Bütter, Evelyne Altmeyer and **Andreas Adolf**, for their generous support and friendly working atmosphere that we shared in our lab.

I would especially like to thank **Dr. Kinga Leszczyńska** and **Nadine Poitiers**, with whom I have had the pleasure to work. They gave me much valuable advice and assistance during my PhD projects.

I wish to thank my best friend **Yunjie He**, who always gives me warm-hearted encouragement during the writing and personal guidance during my stay in Germany.

Last but by no means the least, a very special thank goes out to all **the members of my Family**, who have been supportive of my career goals and providing me with undisturbed time to pursue those goals.

Background

Silicon is the second most common element on Earth by mass (about 28%) after oxygen (47%)¹ as more than ninety percent of the Earth's crust, e.g. dusts and sands, are composed of silicon dioxide or silicates in various forms. Even though silicate minerals have been used by human beings over hundreds of years in the form of clay, porcelain, glasses, etc., silicon in its elemental form had not attracted attention until the year 1823 when amorphous silicon was prepared by Jöns Jacob Berzelius via heating of silicon tetrafluoride in the presence of potassium.² Almost 31 years later in 1854 the crystalline form of silicon was prepared by Deville.³ Since there is no organosilicon material containing C–Si bonds in nature except for silicon carbide in meteorites,¹ the real flourish of silicon chemistry only began in the early 20th century when a detailed investigation of hydrides of silicon and organosilicon compounds was carried out by Alfred Stock⁴ and Frederick Stanley Kipping.⁵ In the wake of these pioneering endeavors, many thousands of organosilicon compounds were prepared, for instance for the polysiloxane industry. Nowadays, the manufacture of high-purity elemental silicon and inorganic and organic silicon compounds sustains diverse applications, e.g. in microprocessors, photovoltaics and not least the building industry (waterproofing treatment and sealants).⁶

In parallel with the development of the silicon and silicone industries, scientific research in silicon chemistry has grown rapidly in recent decades, in particular since the so-called classical double-bond rule⁷ (stating that elements of the third row of the periodic table and below cannot sustain multiple bonds)^{8,9} was disproven through the first isolation of P=P, Si=Si and Si=C doubly bonded diphosphene, disilene and silene in 1980s by Yoshifuji,¹⁰ R. West¹¹ and A. G. Brook,¹² respectively. These milestone achievements were enabled by the use of sterically and electronically stabilizing substituents. In subsequent years various subvalent silicon compounds including silylenes,¹³ trivalent silyl radicals,¹⁴ acyclic- and cyclic disilenes¹⁵, compounds with

Si=E double bond (E = S, Se, Te, N, P, Bi, etc.), etc. were isolated and characterized by spectroscopic means and X-ray crystallography.

Trisilaallenes,¹⁶ and disilynes¹⁷ are prime examples that the properties of unsaturated silicon species often substantially differ from those of the corresponding carbon species. Robinson's disilicon(0)¹⁸ species draws its stability from the near-perpendicular coordination of N-heterocyclic carbenes (NHCs), while the corresponding carbon species adopt linear allene structures. Similarly, the geometries around the Si=Si double bond and Si≡Si triple bonds of disilene and disilyne are *trans*-bent in contrast to the planar C=C double and C≡C triple bonds. Moreover, silicon combines with other elements to form various types of structures completely unknown to carbon chemistry. Two tricyclic unsaturated isomers of hexasilabenzene¹⁹ perfectly illustrate that unhybridized bonding situations are preferred for heavier elements. Theoretical studies predict that repeating units in pure silicon nanosheets do not exhibit a planar hexagonal geometry like in graphene, but a non-classical bridged propellane motif instead.²⁰ These differences reflect the well-established propensity of silicon for single bonding even in the element: while a variety of allotropes of carbon besides diamond, such as graphite, fullerenes, and carbon nanotubes, are known as a stable material mainly consisting of sp²-hybridized carbon atoms, silicon's only stable element modification to date has a diamond-type structure based on tetracoordinate silicon atoms.

Among these low-valent silicon species, small and thus highly strained ring systems consisting of silicon have been attractive synthetic challenges both for fundamental curiosity and their anticipated potential in synthesis. Until the early 1980s, when the synthesis of first stable cyclotrisilane was achieved by Masamune,²¹ they were considered as non-isolable reactive intermediates. The significant ring strain and the weakness of endocyclic Si–Si single bond make the cycloreversion of cyclotrisilane one of the major methods to generate silylenes and disilenes as reactive intermediates.²² The cyclotrisilene, with the Si=Si double bond incorporated into the

skeleton of cyclotrisilane, was obtained in the late 1990s by Kira²³ and Sekiguchi,²⁴ independently, taking advantage of bulky silyl substituents and exocyclic π - σ^* interaction.

**“Chemistry itself knows altogether too well that
– given the real fear that the scarcity of global
resources and energy might threaten the unity of
mankind – chemistry is in a position to make a
contribution towards securing a true peace on earth.”**

Kenichi Fukui

Table of Contents

List of Abbreviations	1
List of Figures.....	3
List of Schemes.....	5
List of Tables	9
1 Introduction	11
1.1 Pioneering Works	11
1.1.1 Synthesis of the first stable disilene	11
1.1.2 Synthesis of the first stable cyclotrisilene	12
1.2 The Carter-Goddard-Malrieu-Trinquier (CGMT) Model.....	13
1.3 Strain Energy (SE) of Cyclic Disilenes.....	15
1.4 Routes to Cyclotrisilene	17
1.4.1 Reductive Dehalogenation	17
1.4.2 Condensation	19
1.4.3 Valence Isomerization	20
1.4.4 Cleavage of Si=Si double bond in Tetrasilene-1,3-diene.....	21
1.4.5 Synthesis of Aryl-substituted Cyclotrisilene	22
1.4.6 Silicon Analogue of Spiropentadiene.....	23
1.4.7 1-Disilagermirene and 2-Disilagermirene	24
1.4.8 Recent Advances	24
1.5 UV/vis Spectroscopy	26
1.6 ²⁹ Si NMR Spectroscopy	27
1.7 Reactions of Stable Cyclotrisilenes	29
1.7.1 Halogen Abstraction	29
1.7.2 Cycloaddition.....	29
1.7.3 Si-Si single bond insertion.....	33
1.7.4 Miscellaneous Reactions.....	35
2 Aims and Scope.....	43
3 Results and Discussion.....	47
3.1 Disilyl Silylene like Reactivity of Cyclotrisilene.....	47

3.2	Supplementary Results.....	51
3.2.1	[2+2] and [2+4] Cycloaddition.....	51
3.2.2	Reaction of cyclotrisilene with benzoyl chloride	55
3.2.3	Reaction with azobenzene	57
3.2.4	Attempt reaction of cyclotrisilene with phenyl isocyanate.....	59
3.3	Phenylene-Bridged Cross-conjugated 1,2,3-Trisilacyclopentadienes	61
3.4	Reactivity of peraryl Cyclotrisilene towards Chalcogens.....	67
3.5	Supplementary Results: Reactivity of Cyclotrisilene towards Divalent Species of Group 14 Elements.....	71
3.5.1	Reactions of 24 with SnCl ₂	72
3.5.2	Reduction of 98 with NpLi	75
3.5.3	Attempted reactions of cyclotrisilene 24 with silylenes	78
3.5.4	Reaction of 24 with Roesky silylene	79
4	Summary.....	87
5	Outlook.....	93
6	Supplementary Experiments	94
6.1	General.....	95
6.1.1	Experiential Conditions.....	95
6.1.2	Purification of Solvents.....	95
6.1.3	Methods of Analysis and Measurement.....	95
6.1.4	Computational Details	96
6.2	Synthesis of Starting Materials	97
6.2.1	Synthesis of TipBr	97
6.2.2	Preparation of Lithium Naphthalene (Li/C ₁₀ H ₈).....	97
6.2.3	Synthesis of Tip ₂ SiCl ₂	98
6.2.4	Synthesis of disilenide 20	99
6.2.5	Synthesis of TipSiCl ₃	99
6.2.6	Synthesis of trisilaallyl chloride 23	100
6.2.7	Synthesis of cyclotrisilene 24	101
6.3	Reactivity of 24 towards 1,3-butadiene and imine	102
6.3.1	Synthesis of 82	102

6.3.2	Synthesis of 84	103
6.3.3	Synthesis of 85	104
6.3.4	Synthesis of 88	105
6.3.5	Synthesis of 98	106
6.3.6	Synthesis of 100	107
6.3.7	Synthesis of 104 and 105	108
7	References.....	111
8	Supporting Information.....	119
8.1	Disilyl Silylene Reactivity of a Cyclotrisilene	119
8.2	Phenylene-bridged cross-conjugated 1,2,3-trisilacyclopentadienes	121
8.3	Reactivity of a peraryl cyclotrisilene (<i>c</i> -Si ₃ R ₄) toward chalcogens	123
9	Appendix.....	125
9.1	Overview of numbered compounds	125
9.2	Absorption spectra.....	133
9.2.1	UV/vis Spectra and Determination of ϵ for 84	133
9.2.2	UV/vis Spectra and Determination of ϵ for 98	134
9.2.3	UV/vis Spectra and Determination of ϵ for 104	135
9.2.4	UV/vis Spectra and Determination of ϵ for 105	136
9.3	X-ray Structure Determination	137
9.3.1	Crystal Data and Structure Refinement for 82	137
9.3.2	Crystal Data and Structure Refinement for 85	139
9.3.3	Crystal Data and Structure Refinement for 88	141
	Curriculum Vitae.....	143

List of Abbreviations

Å	A ngstrom
Ar	A romatic substituent
BDE	B ond D issociation E nergy
BP86	The gradient-corrected exchange functionals of B ecke 88 and P erdew 86
CGMT	C arter- G oddard- M alrieu- T rinquier
C	C elsius
Cp*	Pentamethylcyclopentadienyl $\eta^5\text{-C}_5\text{H}_5$
Cy	C yclohexyl
CP-MAS	C ross P olarization M agic A ngle S pinning
Dip	2,6- D iisopropylphenyl
DME	1,2- D imethoxyethylene
DMAP	4-(<i>N,N</i> - d imethylamino)pyridine
DFT	D ensity F unctional T heory
Dsi	CH(SiMe ₃) ₂
dec.	d ecomposition
d	d oublet
equiv.	e quivalents
Eq.	E quation
Et	E thyl, -C ₂ H ₅
EMind	1,1,3,3,7,7-Hexaethyl-5,5-dimethyl-s-hydridacen-4-yl
Hal.	H alide
hrs	h ours
HMBC	H eteronuclear M ultiple B ond C orrelation
HMQC	H eteronuclear M ultiple Q uantum C orrelation
HOMO	H ighest O ccupied M olecular O rbital
<i>i</i> Pr	<i>i</i> so- P ropyl, -C ₃ H ₇
LUMO	L owest U noccupied M olecular O rbital
Me	M ethyl

Mes	2,4,6-Trimethylphenyl
MO	M olecular O rbital
mmol	m illimole
mp.	m elting p oint
m	m ultiply
min	m inute(s)
NHC	N - H eterocyclic c arbene
NMR	N uclear M agnetic R esonance
Ph	P henyl
ppm	p arts p er m illion
rt	r oom t emperature
SE	S train E nergy
s	s inglet
^t Bu	t ert- B utyl, -C ₄ H ₉
Tip	1,3,5- T riisopropylphenyl
TMS	T rimethylsilyl
TMSOTf	T rimethylsilyl trifluoromethanesulfonate
thf	t etrahydrofuran
UV	U ltraviolet
vis	v isible
VT	V ariable T emperature
Xyl	X yl, 2,6-Me ₂ C ₆ H ₂
λ_{\max}	m aximum absorption wavelength
μL	microliter
$\Sigma\Delta E_{\text{S-T}}$	S inglet- T riplet energy splitting

List of Figures

Figure 1. (a) Energy profile for coupling of two triplet carbenes to form an olefin; curve a shows two carbene fragments with a triplet state, curve b describes the interaction of two carbene fragments with excited triplet state. (b) Energy profile for coupling of two singlet carbene fragments into an excited olefin	13
Figure 2. Interaction diagram of the formation of planar and <i>trans</i> -bent double bond from carbene and silylene fragments according to CGMT model.....	14
Figure 3. Structural parameters for characterization of Si=Si double bond (d = bond length, θ = <i>trans</i> -bent angle, τ = twist angle, ψ = dihedral angle in cyclotrisilene).....	15
Figure 4. Cyclic delocalization of π electrons through the σ conjugation.....	17
Figure 5. Frontier orbitals and their energy levels of ethylene and disilene at the B3LYP/6-311++G(2d,p)//B3LYP/6-31G(d) level of theory.....	26
Figure 6. Approximate orientation of the principal shielding tensor components in disilenes.....	29
Figure 7. Molecular structure of 82 ·C ₇ H ₈ in solid state.....	52
Figure 8. Molecular structure of 84 in solid state.....	53
Figure 9. 2D ¹ H/ ¹³ C HMQC spectrum (C ₆ D ₆ , 300 K) of 84	54
Figure 10. Molecular structure of 85 ·C ₆ H ₁₄ in solid state.....	56
Figure 11. Molecular structure of 88 ·C ₅ H ₁₂ in solid state.....	58
Figure 12. ²⁹ Si NMR spectrum (59.6 MHz, 300 K, C ₆ D ₆) of the reaction mixture of 24 with phenyl isocyanate.....	60
Figure 13. ²⁹ Si CP-MAS NMR spectrum (79.5 MHz, 300 K) of 98	74
Figure 14. Molecular structure of 98 in solid state.....	75
Figure 15. ²⁹ Si NMR spectrum (79.5 MHz, C ₆ D ₆ , 300 K) of the reaction mixture of 24 with SnCl ₂ and NpLi.....	76
Figure 16. Molecular structure of 100 in solid state.....	77
Figure 17. ¹ H NMR spectrum (300.13 MHz, C ₆ D ₆ , 300 K) of the reaction mixture of 24 with 102	79
Figure 18. ²⁹ Si NMR spectrum (59.6 MHz, C ₆ D ₆ , 300 K) of the reaction mixture of 24 with 103	80
Figure 19. ²⁹ Si CP-MAS NMR spectrum (79.5 MHz, 300 K) of 104 (up) and ²⁹ Si NMR spectrum (59.6 MHz, C ₆ D ₆ , 300 K) of 105 (below).....	81
Figure 20. Molecular structure of 104 in solid state.....	83
Figure 21. Stabilizing donor-acceptor interaction of 104	84
Figure 22. ¹ H NMR spectrum of 104 in C ₆ D ₆ , at 300 K (black), over two days (red) and heated at 50 °C overnight (green).....	85
Figure 23. UV/vis spectra of 84 ($\lambda_{\text{max}} = 353$ nm) in hexane at different concentrations ($1.6 \cdot 10^{-3}$ – $3.0 \cdot 10^{-3}$ mol L ⁻¹).....	133
Figure 24. Determination of ϵ (8367 L mol ⁻¹ cm ⁻¹) at $\lambda = 353$ nm through a graphical draw of absorptions of 84 against their concentrations.....	133
Figure 25. UV/vis spectra of 98 in thf at different concentrations ($0.6 \cdot 10^{-3}$ – $2.0 \cdot 10^{-3}$ mol L ⁻¹). λ : 271 nm, 450 nm (shoulder).....	134
Figure 26. Determination of ϵ (36350 L mol ⁻¹ cm ⁻¹) at $\lambda = 271$ nm through a graphical draw of absorptions of 98 against their concentrations.....	134

Figure 27. UV/vis spectra of 104 ($\lambda_{\text{max}} = 422 \text{ nm}$) in toluene at different concentrations ($0.6 \cdot 10^{-3} - 1.2 \cdot 10^{-3} \text{ mol L}^{-1}$).	135
Figure 28. Determination of ε ($5820 \text{ L mol}^{-1}\text{cm}^{-1}$) at $\lambda = 422 \text{ nm}$ through a graphical draw of absorptions of 104 against their concentrations.	135
Figure 29. UV/vis spectra of 105 in hexane at different concentrations ($0.4 \cdot 10^{-3} - 1.2 \cdot 10^{-3} \text{ mol L}^{-1}$). $\lambda(\varepsilon)$: 328 nm ($14350 \text{ L mol}^{-1}\text{cm}^{-1}$), 410 nm (shoulder).....	136
Figure 30. Determination of ε ($14350 \text{ L mol}^{-1}\text{cm}^{-1}$) at $\lambda = 328 \text{ nm}$ through a graphical draw of absorptions of 105 against their concentrations.	136

List of Schemes

Scheme 1. Trapping of the transient tetramethyldisilene B .	11
Scheme 2. Synthesis of the first isolable disilene 1 .	11
Scheme 3. Synthesis of the first stable cyclotrisilene 2 .	12
Scheme 4. Homodesmotic reactions of cyclic alkenes and cyclic disilenes.	16
Scheme 5. Synthesis of Sekiguchi's cyclotrisilene 3 (R = SiMe ^t Bu ₂).	18
Scheme 6. Reduce of 4 with different reductive reagent resulting in cyclotrisilene 2 and cyclotetrasilene 5 (R = SiMe ₂ ^t Bu).	18
Scheme 7. Synthesis of bicyclo[4.1.0]heptasil-1(6)-ene 6 (R = ^t Bu).	18
Scheme 8. Synthesis of cyclotrisilene 9 by condensation of dilithio- and halogensilanes (R ₁ = SiMe ^t Bu ₂ , R ₂ = Si ^t Bu ₃).	19
Scheme 9. Interconversion between 10a,b and cyclotrisilene 3 .	19
Scheme 10. Synthesis of trisila-bicyclo[1.1.0]butane 12 followed by thermal isomerization to cyclotrisilene 13 (R = SiMe ^t Bu ₂).	20
Scheme 11. Thermal isomerization of trisilaallene 14 yields cyclotrisilene 3 (R = SiMe ^t Bu ₂).	20
Scheme 12. Thermal isomerization of disilyne 15a,b yields cyclotrisilene 16a,b , respectively (15a : R ₁ = R ₂ = SiMe(Si ^t Bu ₃) ₂ , 16a : R ₃ = Si(^t Bu ₃), R ₄ = Me, R ₅ = R ₂ ; 15b : R ₁ = Si ⁱ PrDsi ₂ , R ₂ = SiNpDsi ₂ ; 16b : R ₃ = Dsi, R ₄ = Np, R ₅ = R ₁ ; Np = CH ₂ ^t Bu, Dsi = CH(SiMe ₃) ₂).	21
Scheme 13. Thermo- and photolysis of tetrasila-1,3-diene 17 yields cyclotrisilene 18 (R = SiMe ₃).	21
Scheme 14. Synthesis of cyclotrisilene 21 with carbon-based substituents via postulated disilynylsilylene intermediate 22 (Cp* = C ₅ Me ₅).	22
Scheme 15. Synthesis of peraryl-substituted cyclotrisilene 24 .	23
Scheme 16. Reduction of trihalosilane with KC ₈ results in spiropentasiladiene 25 and cyclotrisilene 2 .	23
Scheme 17. Synthesis of 1-disilagermirene 26 and 2-disilagermirene 27 (R = SiMe ^t Bu ₂).	24
Scheme 18. Synthesis of silicon analogue of bicyclo[1.1.0]but-1(2)-ene (BBE) 30 ·DMAP and the canonical structure 30z .	25
Scheme 19. Synthesis of cyclotrisilene 32 with heteroatom substituent (R = SiMe ^t Bu ₂).	26
Scheme 20. Reaction of cyclotrisilene 2 , 3 with CCl ₄ and BrCH ₂ CH ₂ Br (2 : R = SiMe ₂ ^t Bu, R ₁ = SiR ₃ ; 33 : X = Cl; 3 : R = R ₁ = SiMe ^t Bu ₂ ; 10a : X = Cl; 10b : X = Br).	29
Scheme 21. Reactions of cyclotrisilene 3 and 24 with 1,3-butadiene and ketone affording cycloaddition adduct 34 and 35a,b (34 : R = SiMe ^t Bu ₂ ; 35a : R = Tip, R ₁ = H; 35b : R = Tip, R ₁ = H).	30
Scheme 22. Reactions of cyclotrisilene 3 and 24 with isocyanides and carbon monoxide (36a : R = SiMe ^t Bu ₂ , R' = cyclohexyl; 36b : R = SiMe ^t Bu ₂ , R' = Xyl; 36c : R = Tip, R' = ^t Bu; 36d : R = Tip, R' = Xyl; 37/37'a : R = SiMe ^t Bu ₂ ; 37/37'b : R = Tip; 38 : R = Tip; 39a : R = SiMe ^t Bu ₂ , R' = H, X = OH; 39b : R = SiMe ^t Bu ₂ , R' = H, X = OMe; 39c : R = Tip, R' = TMS, X = OTf).	31
Scheme 23. Reactions of cyclotrisilene 3 , 24 and 32 with chalcogen elements yielding	

40/41a-c , and 42a , followed by formation of 43a and 44a,b (40 , 43 : R = R ₁ = SiMe ^t Bu ₂ , 41 , 44 : R = R ₁ = Tip; 42 : R ₁ = SR, R = SiMe ^t Bu ₂ ; a : E = S; b : E = Se; c : E = Te).....	32
Scheme 24. Reaction of cyclotrisilene 3 with phenylacetylene yields 45	33
Scheme 25. σ-insertion of Si-Si single bond of cyclotrisilene results in ring-expanded products 49-51 (49a : R = SiMe ^t Bu ₂ , R' = Xyl; 49b : R = Tip, R' = ^t Bu; 50 : R = SiMe ^t Bu ₂ ; 51 , 52 : R = Tip; a : E = S, b : E = Se, c : E = Te).....	34
Scheme 26. Reaction of 21 with N-heterocyclic carbene yields 54	35
Scheme 27. Reaction of 26 with N-heterocyclic carbene 53 yields ring-opening product 55	36
Scheme 28. Reaction of 24 with benzil and styrene affords ring-opening product 57-58 and cycloaddition product 59	37
Scheme 29. Synthesize 1,2,3-trisilacyclopenta-2,4-diene derivative 60-61 via reaction of 24 with alkyne and the proposed reaction mechanism.....	37
Scheme 30. Photochemical isomerization of cyclotrisilene 2 to tetrasilabicyclo[1.1.0]butane derivative 65 (R = SiMe ₂ ^t Bu).....	38
Scheme 31. Synthesize cyclotetra- and cyclotrisilenylium ion 67⁺ , 70⁺ by oxidative removal of substituent of cyclotrisilene 3 and 9 , respectively.....	39
Scheme 32. Reaction of 24 with 2-phosphaethynolate anion 71 yields 72 followed by photolysis to 73	40
Scheme 33. Synthesize Donor-Acceptor adduct of 1,3-disila-2-oxyallyl zwitterion 74 and 75	41
Scheme 34. Alternative synthetic route to hexasilabenzene 76 by the reaction of disilenide 20 with Cp*Si ⁺ cation via cyclotrisilene 21	41
Scheme 35. Relative energies (kcal/mol) of singlet Si ₃ H ₄	43
Scheme 36. Synthesis of disilanyl silylene derivative 55 and possible reaction yields ring-opening and cycloaddition products.....	44
Scheme 37. Generic examples of conjugated Si=Si-C=C systems (Ar = aromatic unit, LU = linking unit).....	44
Scheme 38. Synthesis of cyclic Ge=Si-C=C system and the possible reactions of cyclotrisilene 24 with acetylene and 1,4-diethynylbenzene (Ar = aromatic unit, LU = linking unit).....	45
Scheme 39. Possible reactions of cyclotrisilene 24 with chalcogen elements (R = Tip, Ch, Ch' = S, Se, Te).....	46
Scheme 40. Possible reactions of cyclotrisilene 24 with divalent Group 14 species (R = Tip).....	46
Scheme 41. Generic products of cyclotrisilenes reactions.....	47
Scheme 42. Representatives of reactions of disilene with alkene and carbonyl compound.....	48
Scheme 43. Cycloadduct 35 , 59 and ring-opening product 57-58	49
Scheme 44. [2+4]/[2+2] cycloaddition of 24 with 1,3-butadiene and diimine yields adduct 82 and 84 , respectively (R ₁ = Dip).....	51
Scheme 45. Reaction of 24 with benzoyl chloride yields 85	55
Scheme 46. Reaction of 24 with azobenzene results in 88	57
Scheme 47. Cyclotrisilene 24 is inert towards phenyl isocyanate.....	60

Scheme 48. Generic examples of molecule with conjugated Si=Si-C=C systems (LU = linking units).	62
Scheme 49. 1,2,3-Trisilacyclopentadiene derivatives 60 , 61 and ring-opening intermediate 62	63
Scheme 50. Products resulting from reaction of 24 with chalcogen element (a: E = S, b: E = Se, c: E = Te).	67
Scheme 51. Reaction of 1-disilagermirene 26 and 2-disilagermirene 27 with GeCl ₂ /SnCl ₂ ·dioxane yields 91 and 92 , respectively, and the proposed mechanism	72
Scheme 52. Reaction of 24 with SnCl ₂ results in 98	73
Scheme 53. Reduce the mixture of 24 and SnCl ₂ with NpLi affording Si/Sn cluster 100 in a non-stoichiometric manner.	76
Scheme 54. Attempted reactions of 24 with silylenes 101 and 102	78
Scheme 55. Reaction of 24 with Roesky silylene 103 yields 104 and 105	80
Scheme 56. Ring-opening and π-addition reactions of 24 (c-Si ₃ Tip ₄).....	88
Scheme 57. Reactions of cyclotrisilene 24 with benzoyl chloride and azobenzene.	89
Scheme 58. Synthesis of 60-61	89
Scheme 59. Reactions of 24 with chalcogen elements.	90
Scheme 60. Reactions of 24 with SnCl ₂ and Roesky silylene 103	92

List of Tables

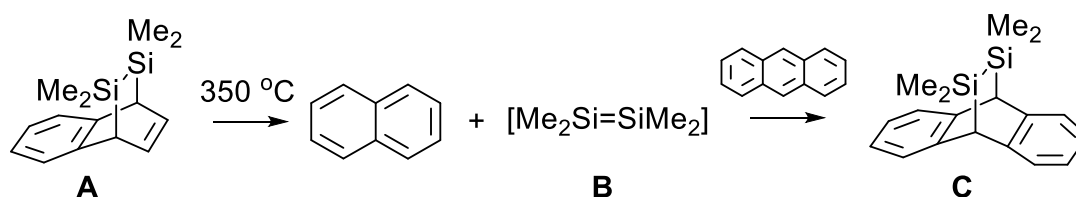
Table 1. Strain energy of cyclic alkenes and disilenes (kcal mol ⁻¹)	16
Table 2. λ_{\max} of selected cyclotrisilenes. <i>a</i>) in hexane, nm; <i>b</i>) L mol ⁻¹ cm ⁻¹	27
Table 3. ²⁹ Si NMR chemical shifts of selected cyclotrisilenes. <i>a</i>) in d ₆ -benzene, ppm...	28
Table 4. Selected ²⁹ Si NMR shifts, structure parameters as well as physical properties of 82-88 . <i>a</i>) ring Si-Si single bond length; <i>b</i>) in d ₆ -benzene; <i>c</i>) in solid state.....	59

1 Introduction

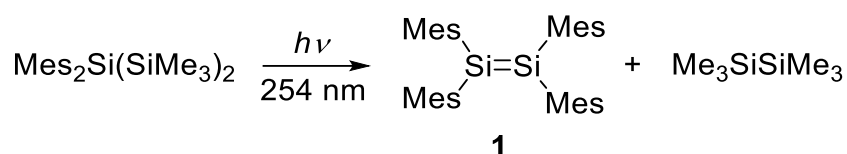
1.1 Pioneering Works

1.1.1 Synthesis of the first stable disilene

Prior to the isolation of a stable disilene, circumstantial evidence regarding the existence of a transient disilene had been released by Peddle and Roark. Tetramethyldisilene **B** was generated during the thermolysis of disilane-bridged naphthalene **A** at 350 °C and was trapped in the presence of anthracene giving the disilane-bridged octa-2,5-diene **C** (Scheme 1).²⁵ The first synthesis of the isolable tetramesityldisilene **1** was achieved by West, Michl and Fink in 1981 via photolysis of 2,2-bis(mesityl)hexamethyltrisilane in hydrocarbon solution (Scheme 2).¹¹ Stable disilene **1** was isolated as a bright-yellow crystalline solid showing a strong absorption band in the visible at $\lambda_{\text{max}} = 420$ nm. The Si=Si double bond is sterically stabilized by the presence of two mesityl (2,4,6-trimethylphenyl) groups at each silicon atom, whereas the considerable red-shift and consequently smaller excitation energy compared to that of olefins suggests that the Si=Si π bond is distinctly weaker than the C=C π bond.



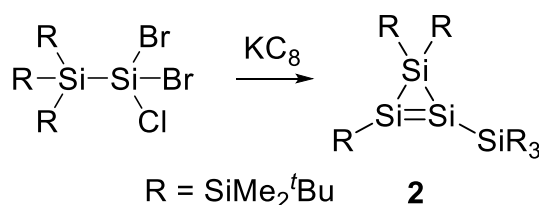
Scheme 1. Trapping of the transient tetramethyldisilene **B**.²⁵



Scheme 2. Synthesis of the first isolable disilene **1**.¹¹

1.1.2 Synthesis of the first stable cyclotrisilene

In carbon chemistry, cyclopropene (C₃H₄) as the simplest cycloalkene was always a subject of curiosity due to its high ring strain and the resulting high reactivity.²⁶ In contrast, even substituted cyclotrisilenes (c-Si₃R₄) were not isolated until the year 1999, although numerous disilenes as well as a few cyclic disilenes had been previously described. The first stable cyclotrisilene **2** was serendipitously obtained by Kira and co-workers in an attempt to synthesize a silicon version of an alkyne by reduction of a trihalosilane with potassium graphite (Scheme 3).²³ The bulky silyl substituents in **2** kinetically protect the reactive core of the molecule. π - σ^* interactions between the Si=Si bond and the antibonding orbitals of the substituents contribute significantly to the stability of **2**, which was isolated as dark-red crystals and shows a maximum absorption wavelength at $\lambda_{\max} = 482$ nm, red-shifted by $\Delta\lambda = 62$ nm compared with that of the first disilene **1** ($\lambda_{\max} = 420$ nm).¹¹ The ²⁹Si NMR signals of the tricoordinate silicon atoms are found at δ 81.9 (Si-R) and 99.8 (Si-SiR₃) ppm, and thus significantly high-field shifted relative to those for the acyclic tetrasilyldisilenes (142-154 ppm).²⁷



Scheme 3. Synthesis of the first stable cyclotrisilene **2**.²³

The isolation of acyclic disilenes and the smallest cyclic derivative – cyclotrisilene – enabled the comparison of their properties with those of their carbon analogues, the alkenes and cyclopropene, respectively. In the following, the CGMT model will therefore be presented, which allows for a correlation of the singlet-triplet excitation energy of the constituting carbene-analogous fragments with the characteristics of the double bond. In addition, the subsequent section (Section 1.4) will address the

added complication of strain in small cyclic alkenes and their heavier homologues.

1.2 The Carter-Goddard-Malrieu-Trinquier (CGMT) Model

The CGMT model was developed by Malrieu and Trinquier based on earlier work by Carter and Goddard III and is widely accepted to allow for qualitative understanding of the geometry of doubly bonded systems of heavier Group 14 elements. In this model, instead of considering the dissociation of a multiply bonded system, the combination of two carbene-like fragments was investigated as a function of their spin multiplicity.²⁸ It is well known that methylene (CH_2) has a triplet ground state with respect to the 9 kcal mol⁻¹ higher lying singlet state.²⁹ In contrast, theoretical and experimental evidence supports that the singlet state of silylene (SiH_2) is energetically more favorable than the triplet state by ~18-21 kcal mol⁻¹.³⁰⁻³¹

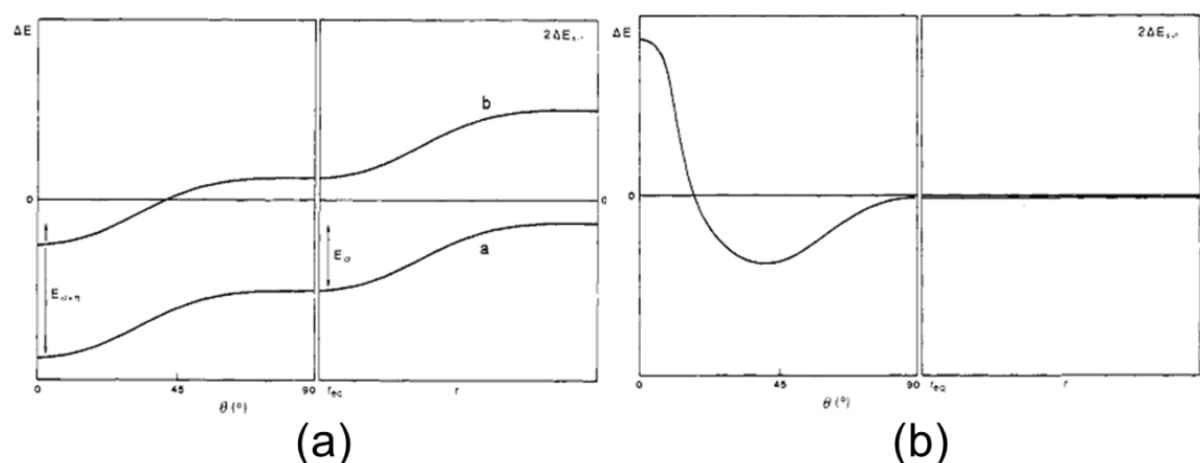


Figure 1. (a) Energy profile for coupling of two triplet carbenes to form an olefin; curve a shows two carbene fragments with a triplet state, curve b describes the interaction of two carbene fragments with excited triplet state. (b) Energy profile for coupling of two singlet carbene fragments into an excited olefin. Reproduced from the literature.^{28b}

In Carter and Goddard III's computational model, the triplet-singlet excitation, ΔE_{ST} , is taken as a measure for the preparation energy required to create a reactive state, ready for barrier-less combination of the two fragments. Figure 1 shows the energy profile of the coupling of both triplet and singlet carbene fragments to form an

olefin-like double bond. The energy gain in the resulting “classical” planar doubly bonded system equals the total interaction energy of both σ - and π -components, $E_{\sigma+\pi}$ (Figure 1a). When $\sum E_{ST} < 1/2 E_{\sigma+\pi}$ a planar doubly bonded system is formed. Conversely, a *trans*-bent orientation becomes more favorable when $\sum E_{ST} > 1/2 E_{\sigma+\pi}$.^[28b]

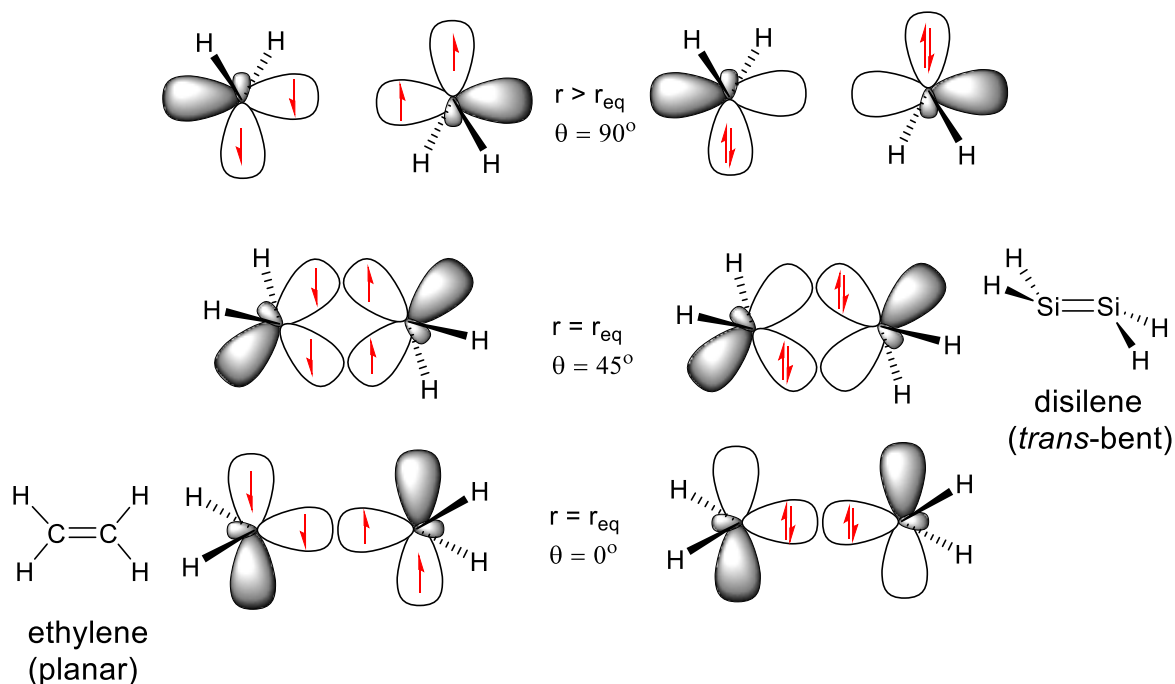


Figure 2. Interaction diagram of the formation of planar and *trans*-bent double bond from carbene and silylene fragments according to CGMT model.

Figure 2 shows the interaction diagram of two carbene and its heavier analogue SiH₂ fragments as a function of the positional parameter r (distance) and θ (bending angle). The maximal stabilization of two triplet carbene fragments is achieved at an angle $\theta = 0^\circ$, forming a “classical” planar ethylene system. In contrast, in case of SiH₂ this maximum is reached at an angle $\theta = 45^\circ$ at which the electron density of the lone pairs of electrons of the singlet fragments is effectively donated into the vacant $p(\pi)$ orbitals. With decreasing angle θ the formation of a bond becomes impossible due to the strong Coulomb repulsion between the lone pairs of electrons (two-center-four-electron interaction).³² The non-planar or *trans*-bent geometry of disilene is the consequence. Thus apart from the bond length d , deviation of Si=Si

double bond from planarity is generally characterized by two angular parameters: the *trans*-bent angle θ , which describes the degree of deviation between the Si=Si double bond vector and the plane defined by silicon and its adjacent substituents, and the twist angle τ , which represents the dihedral distortion of two R–Si(sp²)–R planes with respect to each other. Such Si=Si double bond twist is also observed in cyclic disilenes represented by the dihedral angle ψ along the R–Si=Si–R bond (Figure 3).

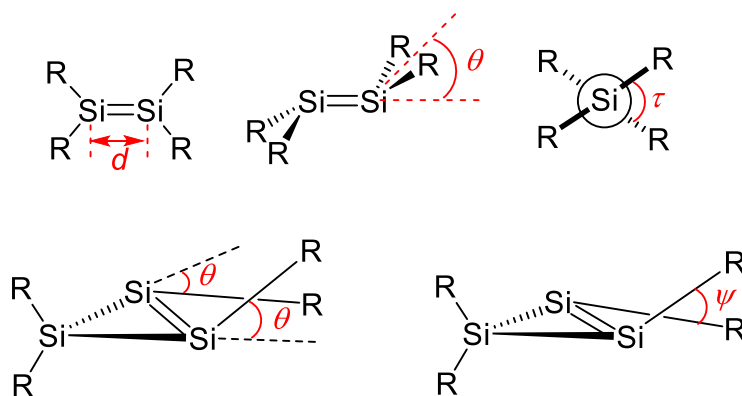
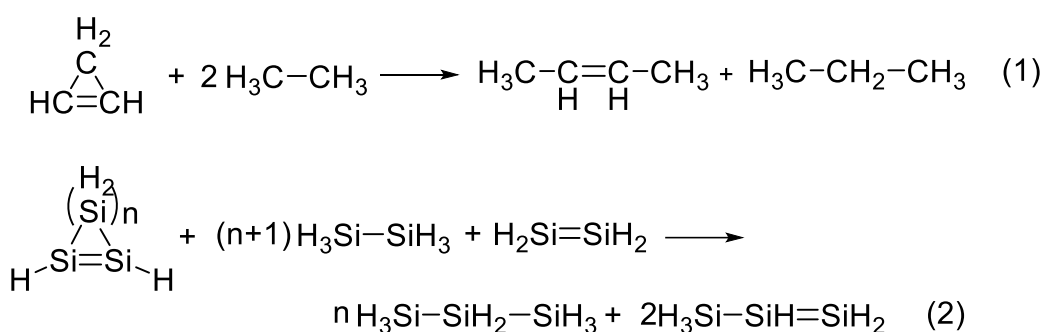


Figure 3. Structural parameters for characterization of Si=Si double bond (d = bond length, θ = *trans*-bent angle, τ = twist angle, ψ = dihedral angle in cyclotrisilene).

1.3 Strain Energy (SE) of Cyclic Disilenes

Strain energy (SE) has proven to be valuable for the evaluation of the inherent reactivity of organic compounds with unusual geometries or intramolecular interactions.³³ A general theoretical method for the accurate assessment of strain energy in cyclic hydrocarbons is the use of homodesmotic reaction equations, in which there are equal numbers of carbon atoms for each state of hybridization as well as equal numbers of bonds involving any two elements in reactants and products (Scheme 4, Eq. 1).³⁴ With the report on the isolation of stable cyclic disilenes, their strain energy was determined by the homodesmotic method (Scheme 4, Eq. 2).³⁵⁻³⁶ Table 1 shows the calculated strain energy of selected cyclic alkenes and disilenes.³⁶ Notably, the ring size has a different effects on the SE values of cyclooligosilanes and cycloalkanes. Calculations by Inagaki and co-workers also demonstrated that the

introduction of a double bond into three- (35.4 to 34.5 kcal mol⁻¹), four- (12.9 to 9.1 kcal mol⁻¹), and five-membered (3.0 to 0.9 kcal mol⁻¹) saturated cyclic oligosilanes relaxes the ring strain to a large extent. This is in marked contrast to their carbon analogues, wherein the strain energy is even increased (cyclopropene 55.5 kcal mol⁻¹ to cyclopropane 25.5 kcal mol⁻¹) by the introduction of the double bond (Table 1).³⁶



Scheme 4. Homodesmotic reactions of cyclic alkenes and cyclic disilenes.³⁴⁻³⁵

Table 1. Strain energy of cyclic alkenes and disilenes (kcal mol⁻¹).³⁶

E						
C	25.5	55.5	22.6	28.7	4.7	4.5
Si	35.5	34.5	12.9	9.1	3.0	0.9

The more relaxed ring strain in cyclic disilenes is in good agreement with the more elastic feature of Si=Si double bond than C=C double bond. The effective relaxation could be theoretically interpreted by the in-phase π - σ^* interaction between the π -bond of three-coordinated silicon atom and σ -bonds on the saturated atom in the ring.³⁶ The π -electrons delocalize through σ_{EH} bonds in a cyclic manner due to the cyclic interaction of π and σ_{EH}^* (Figure 4).³⁷

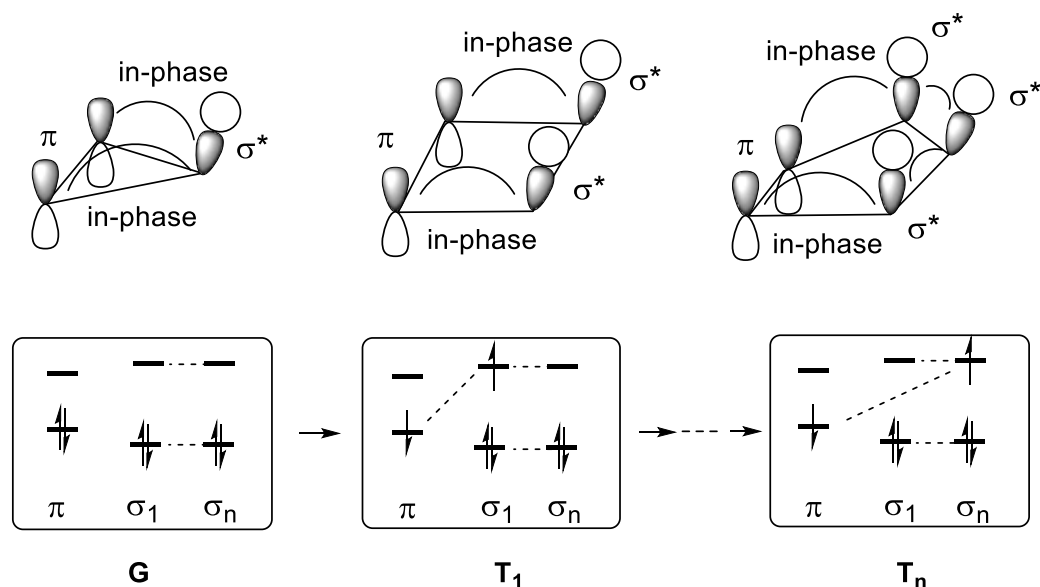
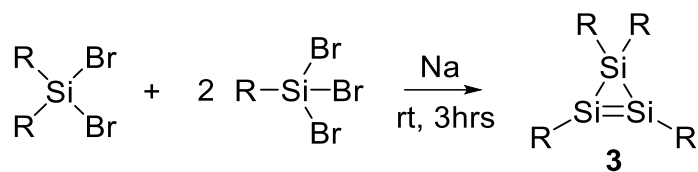


Figure 4. Cyclic delocalization of π electrons through the σ conjugation.³⁶

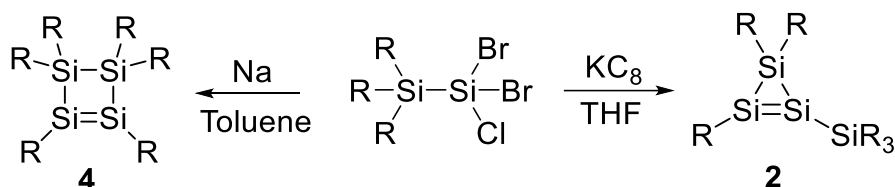
1.4 Routes to Cyclotrisilene

1.4.1 Reductive Dehalogenation

Reductive coupling is the most general used method to synthesize cyclotrisilenes, albeit the yields are typically moderate at best due to the inherent difficulties of hetero coupling two different precursors. Soon after the publication of Kira's cyclotrisilene,²³ Sekiguchi and co-workers reported the synthesis of persilyl-substituted cyclotrisilene **3** by reduction of one equivalent of 2,2-dibromo-1,1,3,3-tetra(tert-butyl)-1,3-dimethyltrisilane and two equivalents of 2,2,2-tribromo-1,1-di(tert-butyl)-1-methyldisilane with sodium in toluene (Scheme 5).²⁴ The reaction led to immediate formation of a dark red solution from which cyclotrisilene **3** was isolated as red-orange crystals at 9.4% yield after recrystallization from hexane.²⁴

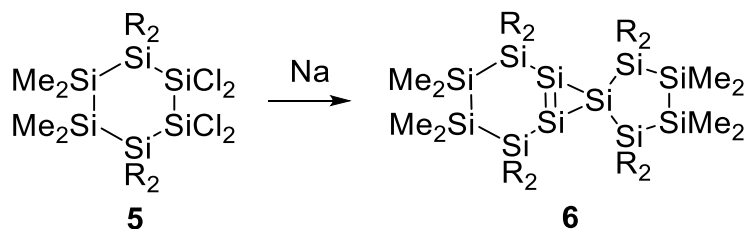


Scheme 5. Synthesis of Sekiguchi's cyclotrisilene **3** (R = SiMe^tBu₂).²⁴



Scheme 6. Reduce of **4** with different reductive reagent resulting in cyclotrisilene **2** and cyclotetrasilene **5** (R = SiMe₂^tBu).²³

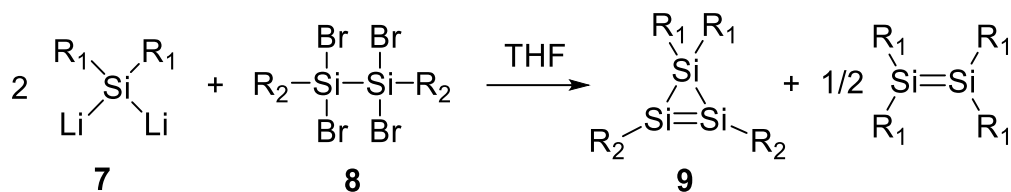
The major product of reductive coupling depends significantly on the reducing agent as well as the reaction time. Reaction of a suitable trihalosilane with potassium graphite in tetrahydrofuran produces cyclotrisilene **2**, while its reaction with sodium in toluene results in cyclotetrasilene **4** (Scheme 6).²³ A short reaction time is also crucial for the successful isolation of **3**, prolonged reaction time results in over-reduction.



Scheme 7. Synthesis of bicyclo[4.1.0]heptasil-1(6)-ene **6** (R = ^tBu).³⁸

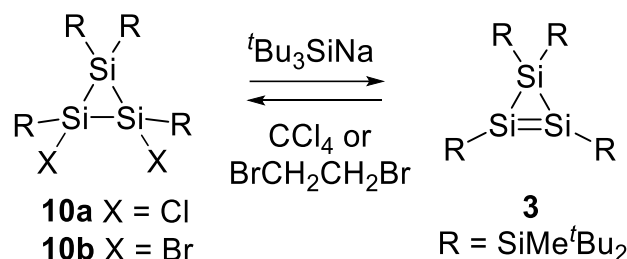
The tetrasilane-bridged bicyclo[4.1.0]heptasil-1(6)-ene **6** was also obtained by reduction of 1,1,2,2-tetrachlorocyclohexasilane **5** with four equivalents of sodium dispersion in toluene (Scheme 7).³⁸ Notably, the reddish crystals of **6** are very stable and can be heated to 238 °C in argon atmosphere without decomposition.

1.4.2 Condensation



Scheme 8. Synthesis of cyclotrisilene **9** by condensation of dilithio- and halogensilanes ($R_1 = \text{SiMe}^t\text{Bu}_2$, $R_2 = \text{Si}^t\text{Bu}_3$).³⁹

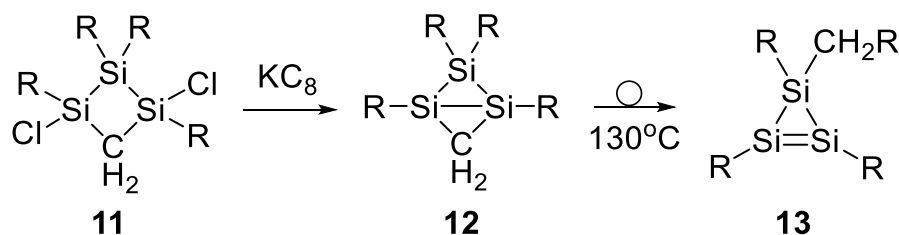
Sekiguchi and co-workers reported the synthesis of a highly crowded cyclotrisilene **9** by reaction of dilithiosilane **7** with bromotetrasilane **8** at a ratio of 2:1 (Scheme 8).³⁹ The second equivalent of dilithiosilane acts as a reductant towards the intermittent 1,2-dibromo cyclotrisilane. The introduction of extremely bulky tri-*tert*-butylsilyl groups at the unsaturated silicon atoms of cyclotrisilenes has a planarizing effect on the Si=Si double bond as shown by the comparatively small $^t\text{Bu}_3\text{Si-Si=Si-Si}^t\text{Bu}_3$ dihedral angle ψ of 4.8° for **9**, in marked contrast to the highly *trans*-bent structure of **3** (dihedral angle $\psi^t\text{BuMe}_2\text{Si-Si=Si-Si}^t\text{BuMe}_2$ 31.9°).²⁴



Scheme 9. Interconversion between **10a,b** and cyclotrisilene **3**.⁴⁰

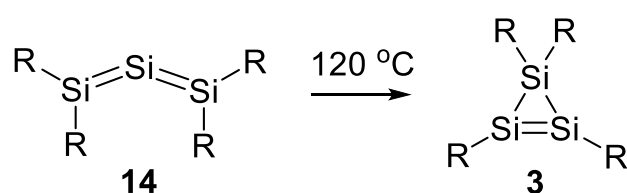
1,2-Dichloro- or 1,2-dibromo- cyclotrisilane **10a,b** were prepared by the reaction of cyclotrisilene **3** with CCl_4 and 1,2-dibromoethane, respectively. Interestingly, conversion of **10a,b** by reduction with $^t\text{Bu}_3\text{SiNa}$ to **3** was also proven to be an efficient, albeit non-productive method to produce cyclotrisilene (Scheme 9).⁴⁰ It is likely that the reaction pathway includes an electron transfer step with a halogen-sodium exchange to form an anionic intermediate, which then quickly undergoes elimination of NaX to form the final cyclotrisilene **3**.

1.4.3 Valence Isomerization



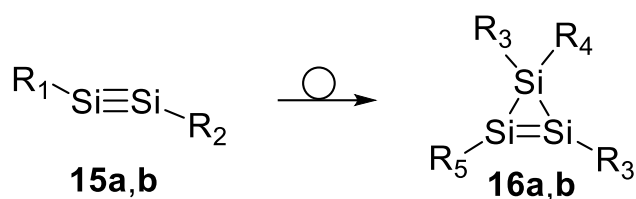
Scheme 10. Synthesis of trisila-bicyclo[1.1.0]butane **12** followed by thermal isomerization to cyclotrisilene **13** ($R = SiMe^tBu_2$).⁴²

Currently reported valence isomerizations to cyclotrisilenes generally occur with precursors with silyl substituents, which can be rationalized by the higher migration tendency of silyl group compared to alkyl and aryl substituent.⁴¹ Cyclotrisilene **13** with three silyl and one alkyl substituent was prepared by reduction of dichloro-trisilacyclobutene **11** with potassium graphite followed by heating of the thus obtained trisila-bicyclo[1.1.0]butane **12** at $130^\circ C$ (Scheme 10).⁴² The cleavage of the bridging Si-C single bond accompanied with silyl substituent migration results in formation of **13**. Due to the introduction of alkyl substituents **13** exhibits both upfield sp^3-Si and downfield sp^2-Si signals for the skeletal silicon atoms at -71.7 and 122.8 ppm in comparison to those of cyclotrisilene **3** at -127.3 and 97.7 ppm.²⁴



Scheme 11. Thermal isomerization of trisilaallene **14** yields cyclotrisilene **3** ($R = SiMe^tBu_2$).⁴³

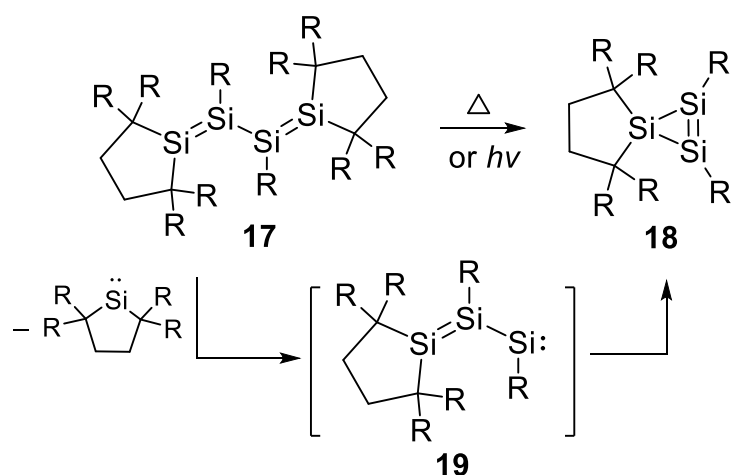
The trisilaallene **14** was also observed to undergo thermal rearrangement yielding cyclotrisilene **3** in 30% isolated yield (Scheme 11).⁴³ However, compared with the reductive dehalogenation (Scheme 5),²⁴ this method of cyclotrisilene generation is less straightforward due to the relative low yield of the synthesis of **14** (40%).



Scheme 12. Thermal isomerization of disilyne **15a,b** yields cyclotrisilene **16a,b**, respectively (**15a**: $R_1 = R_2 = \text{SiMe}(\text{Si}^t\text{Bu}_3)_2$, **16a**: $R_3 = \text{Si}^t\text{Bu}_3$, $R_4 = \text{Me}$, $R_5 = R_2$; **15b**: $R_1 = \text{Si}^i\text{PrDsi}_2$, $R_2 = \text{SiNpDsi}_2$; **16b**: $R_3 = \text{Dsi}$, $R_4 = \text{Np}$, $R_5 = R_1$; $\text{Np} = \text{CH}_2^t\text{Bu}$, $\text{Dsi} = \text{CH}(\text{SiMe}_3)_2$).⁴⁴⁻⁴⁵

Thermal isomerization of disilyne to cyclotrisilene was initially reported by Wiberg *et al.* in 2004 involving the transformation of the symmetrically substituted disilyne **15a** to cyclotrisilene **16a** (Scheme 12).⁴⁴ Unfortunately, no spectroscopy data was published. In 2010 Sekiguchi and co-workers reported the synthesis of unsymmetrically substituted disilyne **15b** and its isomerization in solution to yield cyclotrisilene **16b** quantitatively (Scheme 12), which was characterized spectroscopically by NMR and HRMS.⁴⁵ In the three-membered skeleton of **16b** the $\text{sp}^3\text{-Si}$ exhibits signal at -14.1 ppm while the two $\text{sp}^2\text{-Si}$ display signal at 70.0 ($\text{R}_5\text{-Si}=\text{Si}$) and 130.1 ($\text{R}_3\text{-Si}=\text{Si}$) ppm.

1.4.4 Cleavage of Si=Si double bond in Tetrasila-1,3-diene



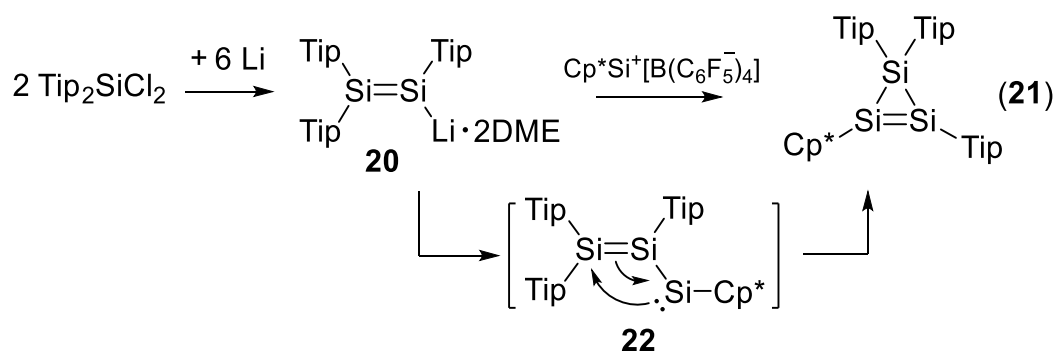
Scheme 13. Thermo- and photolysis of tetrasila-1,3-diene **17** yields cyclotrisilene **18** ($R = \text{SiMe}_3$).⁴⁹

In carbon chemistry, 1,3-butadienes are known to undergo a Diels-Alder type

dimerization⁴⁶ or the cleavage of the C2-C3 bond upon heating.⁴⁷ Upon irradiation with UV light, isomerization to bicyclo[1.1.0]butane or cyclobutene takes place.⁴⁸ In contrast, both thermolysis and irradiation of tetrasiladiene **17** in benzene affords cyclotrisilene **18** as yellow crystals in 87% and 51% yield, respectively (Scheme 13).⁴⁹ The formation mechanism was rationalized by the ring closure of a disilyl silylene **19** formed by homolytic cleavage of one of the Si=Si double bonds of tetrasiladiene **17**.

1.4.5 Synthesis of Aryl-substituted Cyclotrisilene

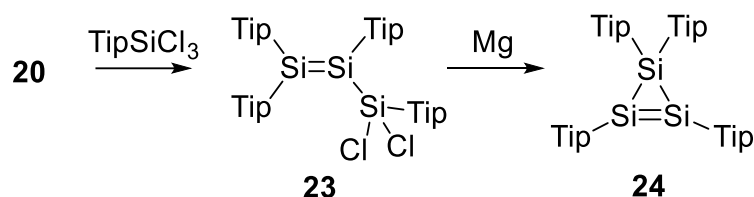
In 2004, Scheschkewitz synthesized disilenide **20** by direct reaction of $\text{Tip}_2\text{SiCl}_2$ with an excess amount of lithium powder (Scheme 14).⁵⁰ The surprising stability (mp. 121 °C), acceptable isolated yield (51% from hexane) and the presence of an anionic reactive site turn **20** into an efficient nucleophilic Si=Si transfer reagent.^{15a,c,e,51} As shown in Scheme 14, by reaction of **20** with silicon(II) tetrakis(pentafluorophenyl)borate accompanied with the elimination of $\text{Li}[\text{B}(\text{C}_6\text{F}_5)_4]$, Scheschkewitz and Jutzi *et al.* synthesized cyclotrisilene **21**, the first cyclotrisilene with carbon-based substituents.⁵² The reaction process can be readily explained by the formation of intermediate disilyl silylene **22** which subsequently undergoes intramolecular isomerization to the final product **21** isolated as orange-brown oil.



Scheme 14. Synthesis of cyclotrisilene **21** with carbon-based substituents via postulated disilylsilylene intermediate **22** ($\text{Cp}^* = \text{C}_5\text{Me}_5$).^{50,52}

Synthesis of the first peraryl-substituted cyclotrisilene **24** was also achieved by

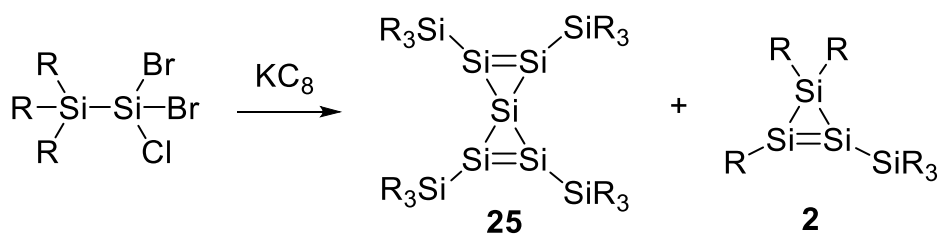
Scheschkewitz's group taking advantage of the homoleptic trisilaallyl chloride precursor **23** obtained by reaction of disilenide **20** with TipSiCl_3 .⁵² After reduction of **23** with magnesium powder, cyclotrisilene **24** is isolated from pentane solution as orange crystals in 51% yield (Scheme 15). It should be mentioned that the reduction time must be critically limited to seven hours as otherwise the over-reduced product magnesium salt of trisilene-1,3-diide is generated as an impurity.⁵³



Scheme 15. Synthesis of peraryl-substituted cyclotrisilene **24**.⁵²

1.4.6 Silicon Analogue of Spiropentadiene

The reaction of trihalosilane with potassium graphite at $-78\text{ }^\circ\text{C}$ gives a brownish red solid, which contains spiropentadiene **25** and cyclotrisilene **2** in a ratio of 1:8 as determined by ^1H NMR. Crystallization from hexane gave the dark red crystals of **25** in 3.5% yield (Scheme 16).⁵⁴

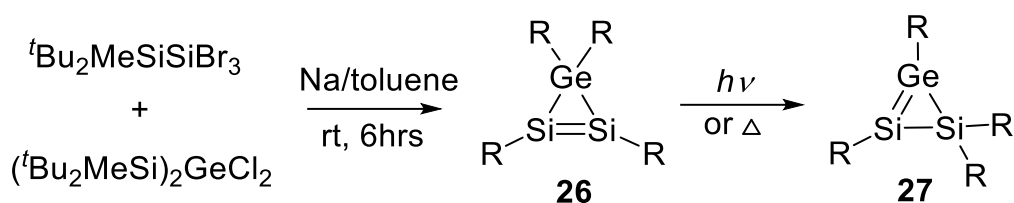


Scheme 16. Reduction of trihalosilane with KC_8 results in spiropentasiladiene **25** and cyclotrisilene **2** ($\text{R} = \text{SiMe}_2^t\text{Bu}$).⁵⁴

High stability of **25** was indicated by the melting point which up to $216\text{ }^\circ\text{C}$. The steric protection of four bulky silyl groups and a smaller strain energy (SE) of the silicon spiro-ring system,^{36,54} without doubt contribute to the stability of **25**. The longest wavelength absorption maximum of **25** in UV/vis spectrum is at 560 nm, highly red-shifted relative to that for cyclotrisilene **2** (482 nm)²³ and **3** (466 nm).²⁴

1.4.7 1-Disilagermirene and 2-Disilagermirene

The reaction of 2,2,2-tribromo-1,1-di(*tert*-butyl)-1-methyl-disilane and dichlorobis[di-*tert*-butyl(methyl)silyl]germane with excess amounts of sodium in toluene at room temperature produced a dark-red reaction mixture, which contains **26** as a major product (Scheme 17).⁵⁵ The 1-disilagermirene **26** was isolated as hexagonal ruby crystals and shows the ²⁹Si NMR chemical shift of sp²-Si at 92.2 ppm, only upfield shifted by 5.5 ppm compared with that of cyclotrisilene **3** (97.7 ppm). The geometry about the Si=Si double bond of **26** is more *trans*-bent than that in cyclotrisilene **3**, as determined by the dihedral angle ψ along R-Si=Si-R of 37.0° (**3** : ψ = 31.9°).



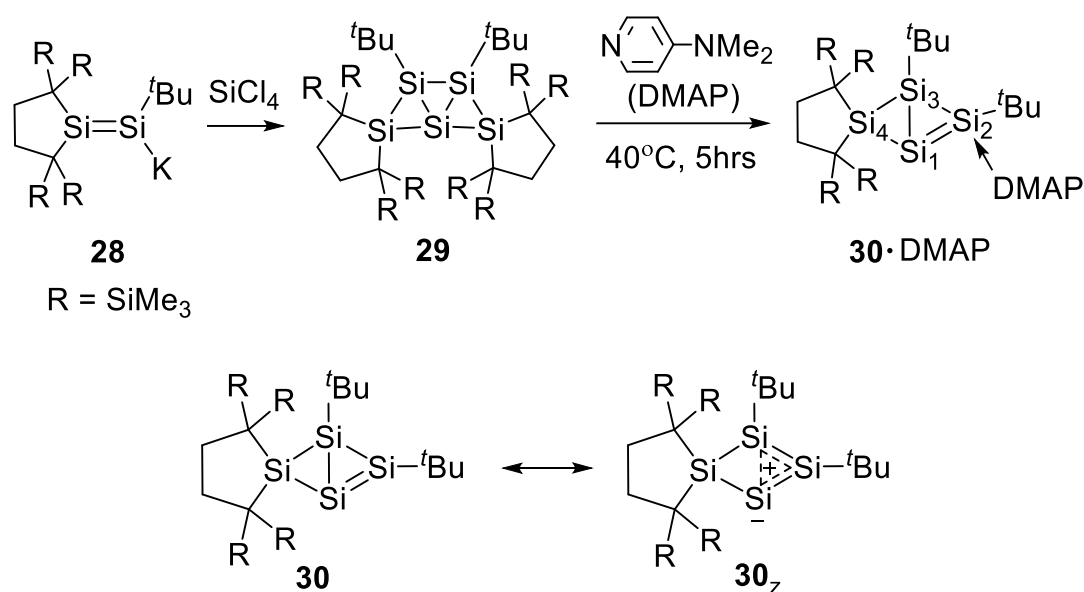
Scheme 17. Synthesis of 1-disilagermirene **26** and 2-disilagermirene **27** (R = SiMe^tBu₂).⁵⁵

Interestingly, the transformation of **26** to 2-disilagermirene **27** can be achieved via photolysis of the C₆D₆ solution of **26** with a high-pressure Hg-lamp ($\lambda > 300$ nm) or thermolysis of the solution of **26** in mesitylene at 120 °C (Scheme 17).⁵⁵ This constitutes yet another example of the ease of silyl group migration, here leading to the formation of an endocyclic Si=Ge double bond system. Disilagermirene **27** was produced quantitatively and shows extremely thermally stable with a melting point of 194-196 °C. The endocyclic double-bonded silicon atom exhibits a downfield signal at 99.3 ppm while the endocyclic saturated silicon atom has an upfield resonance at -120.1 ppm.

1.4.8 Recent Advances

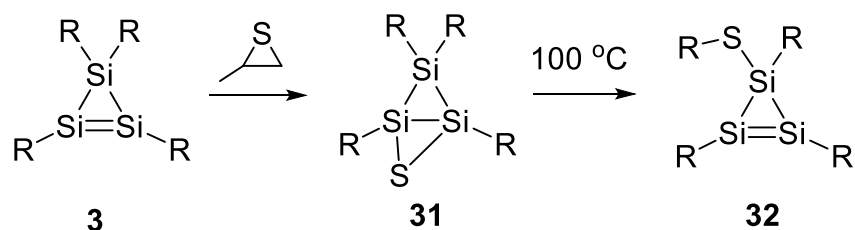
In 2014, Iwamoto and co-workers reported the thermolysis behavior of

hexaalkyltricyclo[2.1.0.0]pentasilane **29** that was prepared by the reaction of the corresponding potassium trialkyldisilene **28** with 0.5 equivalent amount of SiCl_4 . Heating **29** at 40 °C for 5 hours in the presence of 7.6 equivalents of 4-(N,N-dimethylamino)pyridine (DMAP) affords an orange solution, from which **30**·DMAP was isolated as orange crystals in 89% yield (Scheme 18).⁵⁶ **30**·DMAP exhibits three resonances in the ^{29}Si NMR at 84.5 (Si2), 13.3 (Si4) and -79.8 (Si3) ppm, however, no resonance assignable to the naked Si1 could be observed either in solution or in solid state.



Scheme 18. Synthesis of silicon analogue of bicyclo[1.1.0]but-1(2)-ene (BBE) **30**·DMAP and the canonical structure **30_z**.⁵⁶

X-ray structure analysis of **30**·DMAP shows the Si1-Si2 and Si2-Si3 bond length is 2.2906 and 2.2556 Å, respectively, which are between the typical range of Si-Si single bond length (ca. 2.36 Å)⁵⁷ and Si=Si double bond length (2.118-2.289 Å),^{15f,22} indicating a significant double-bond character in both Si1-Si2 and Si2-Si3 bond. Indeed, a theoretical study indicates that the zwitterionic structure **30_z** (Scheme 18) is the main existence which involves a tetrasilahomocyclopropenylium cation and a silyl anion rather than a bicyclic structure with a localized highly strained double bond.



Scheme 19. Synthesis of cyclotrisilene **32** with heteroatom substituent ($R = \text{SiMe}^t\text{Bu}_2$).⁵⁸⁻⁵⁹

The [1+2] cycloaddition reaction of cyclotrisilene **3** with propylene sulfide affording thiatrisilabicyclo[1.1.0]butane **31** was reported by Sekiguchi in 2008.⁵⁸ Almost seven years later in 2015, Lee and Sekiguchi *et al.* found thermolysis of **31** in toluene solution at 100 °C cleanly produces the cyclotrisilene **32**, featuring a ($t\text{Bu}_2\text{MeSi-S}$)-substituent at the skeletal $\text{sp}^3\text{-Si}$ atom and thus representing the first cyclotrisilene with a heteroatom substituent (Scheme 19).⁵⁹ The ^{29}Si NMR chemical shift of the tricoordinate Si atoms of **32** is observed at 137.1 ppm.

1.5 UV/vis Spectroscopy

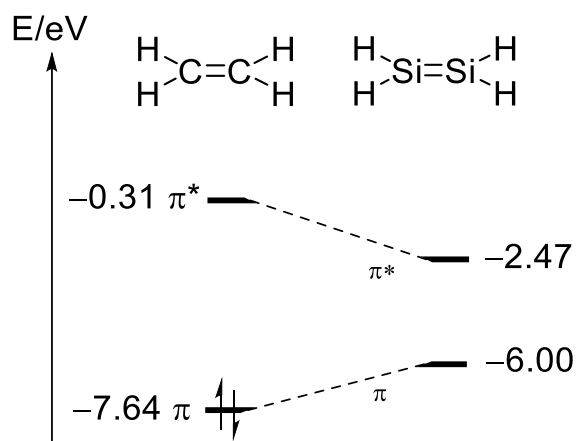


Figure 5. Frontier orbitals and their energy levels of ethylene and disilene at the B3LYP/6-311++G(2d,p)//B3LYP/6-31G(d) level of theory.^{15f}

Compounds with Si=Si double bond are colored, in marked contrast to their carbon congeners, which are colorless in most cases. The differences in frontier orbital splitting of disilene and ethylene provide a good explanation for the highly variable color of currently isolated disilenes. As shown in Figure 5, calculations performed by

Kira and co-workers demonstrate the HOMO-LUMO splitting energy in ethylene ($\Delta E = 7.33$ eV) is almost twice as much as the parent disilene ($\Delta E = 3.53$ eV).^{15f}

Generally, the π - π^* absorption maxima of cyclic disilenes (λ_{\max} 391 to 482 nm) are observed at significantly longer wavelengths than those of corresponding acyclic-disilenes (λ_{\max} 420 to 517 nm).^{15f} However, the intensely blue ($t\text{-Bu}_2\text{MeSi}$)₂Si=Si(SiMe $t\text{-Bu}_2$)₂ with its absorption maxima at λ_{\max} 612 nm is an exception, which originates from the severe twisting of the Si=Si double bond ($\tau = 54.5^\circ$).⁶⁰ In comparison, the longest wavelength absorption of the corresponding cyclotrisilene **3** is strongly blue-shifted to λ_{\max} 466 nm as the incorporation into the three-membered rings precludes any significant twisting the double bond.²⁴ Table 2 shows the λ_{\max} of selected cyclotrisilenes.

Table 2. λ_{\max} of selected cyclotrisilenes. a) in hexane, nm; b) L mol⁻¹ cm⁻¹

	2	3	6	9	13	18	24
λ_{\max}^a	482	466	468	472	457	391	413
$(\epsilon)^b$	(2640)	(440)	(2200)	(500)	(2060)	(4400)	(4912)

Cyclotrisilenes with silyl substituents in general have a λ_{\max} at 460-480 nm,²³⁻²⁴ while **24** with peraryl substituents shows a more blue-shifted longest absorption wavelength at λ_{\max} 413.⁵² Cyclotrisilene **13** with mixed silyl and alkyl substituents appear a little shorter λ_{\max} (457 nm) than these of persilyl-substituted cyclotrisilenes.⁴² The bicyclic **18** with a rigid dialkyl-backbone shows the shortest λ_{\max} (391 nm) among currently isolated cyclotrisilenes.⁴⁹

1.6 ²⁹Si NMR Spectroscopy

Despite the relative low natural abundance of ²⁹Si (the only NMR active silicon nucleus 4.67%),¹ ²⁹Si NMR is a useful diagnostic tool for recognizing silicon with different coordination environments and electronics states, particularly in the cases of low valent silicon compounds. The ²⁹Si NMR shifts of unsaturated silicon atoms in

cyclotrisilenes are remarkably upfield shifted compared with that of acyclic disilenes. For instance, the resonances of the unsaturated ^{29}Si nuclei of persilyl-substituted cyclotrisilene **2** and **3** located at δ 81.9, 99.8 and 97.7 ppm, respectively,²³⁻²⁴ while disilene ($t\text{Bu}_2\text{MeSi}$)₂Si=Si(SiMe t Bu₂)₂ shows ^{29}Si NMR of sp^2 hybridized silicon atom at δ 155.5 ppm.⁶⁰ Table 3 shows the ^{29}Si NMR chemical shifts of selected cyclotrisilenes. The peraryl-substituted cyclotrisilenes **21** and **24** shows signals of the unsaturated silicon atom at δ 58.6, 37.3 and 42.5 ppm,⁵² ca.10 ppm upfield shifted in comparison to that of the symmetric tetraaryl disilenes, in which the ^{29}Si NMR shifts were found between δ 53 and 72 ppm.^{15f}

Table 3. ^{29}Si NMR chemical shifts of selected cyclotrisilenes. a) in d_6 -benzene, ppm

	2	3	6	9	13	21	24
$\text{sp}^2 \delta^{29}\text{Si}^a$	81.9, 99.8	97.7	147.1	97.4	122.8	58.6, 37.3	42.5
$\text{sp}^3 \delta^{29}\text{Si}^a$	-117.2	-127.3	-85.4	-115.7	-71.7	-15.3	-23.2

^{29}Si NMR shifts of disilenes show a clear-cut dependency on the substitution pattern on each of the sp^2 hybridized silicon atom.^{61 - 62} For instance, homoleptic silyl-substituted disilenes (δ 131-156 ppm) are downfield shifted by ca. 90 ppm compared with that of aryl-substituted disilenes (δ 53-72 ppm).^{15f,22} As shown in Table 3, the substitution pattern also affects the ^{29}Si NMR of cyclotrisilenes, represented by signals of sp^2 hybridized silicon atoms of **21** and **24** being ca. 50 ppm upfield shifted in comparison to that of **2** and **3**, being up to 80 ppm with respect to that of **13**. Figure 6 shows the three ^{29}Si chemical shift tensors that were determined by solid state NMR spectroscopy.⁶³ Significant deshielding along one principal axis occurs to various disilenes. According to West and co-workers' study, the large deshielding ^{29}Si NMR signals of disilenes with silyl substituents is rationalized by the significant paramagnetic contribution along the axis δ_{11} .⁶¹ For tetrasilyl disilenes this extreme deshielding in δ_{11} can be related to the low $\sigma-\pi^*$ transition energy resulted from the higher-lying σ orbital levels of Si=Si double bonds, which is ascribed to the

contribution of electropositive silyl substituents.⁶¹

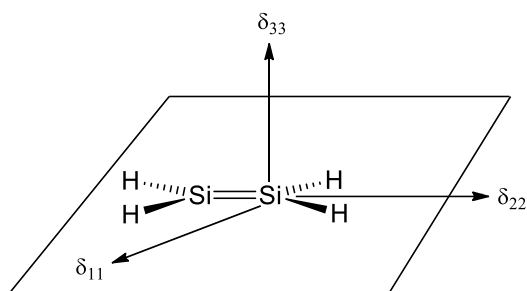
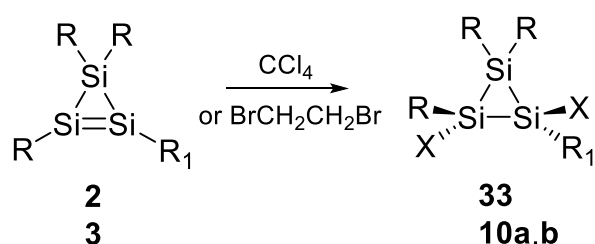


Figure 6. Approximate orientation of the principal shielding tensor components in disilenes.⁶¹,^{Error! Bookmark not defined.}

1.7 Reactions of Stable Cyclotrisilenes

1.7.1 Halogen Abstraction

After the successful synthesis of cyclotrisilene **2** and **3**, their reactions with halogenated compounds were studied. Similarly to the acyclic disilenes which undergo 1,2-addition reaction with halogens and hydrogen halides,²² cyclotrisilene **2** reacts immediately with CCl_4 even at $-70\text{ }^\circ\text{C}$ resulting quantitatively in *trans*-1,2-dichlorocyclotrisilane **33** (Scheme 20).²³ As matter of fact 1,2-dichloro- and dibromo cyclotrisilane **10a** and **10b** as discussed in 1.4.2 was also prepared via reaction of cyclotrisilene **3** with CCl_4 and $\text{BrCH}_2\text{CH}_2\text{Br}$, respectively.⁴⁰

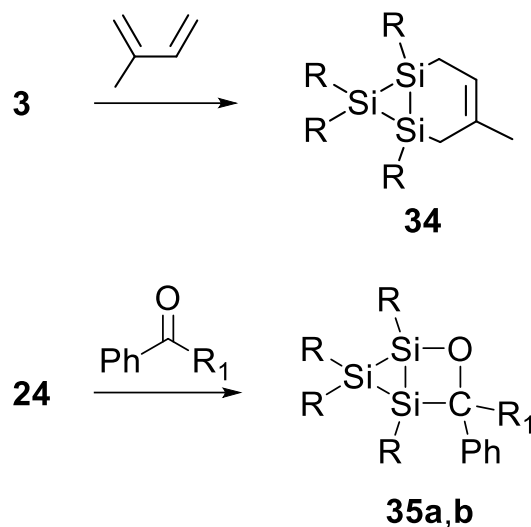


Scheme 20. Reaction of cyclotrisilene **2**, **3** with CCl_4 and $\text{BrCH}_2\text{CH}_2\text{Br}$ (**2**: $\text{R} = \text{SiMe}_2^t\text{Bu}$, $\text{R}_1 = \text{SiR}_3$; **33**: $\text{X} = \text{Cl}$; **3**: $\text{R} = \text{R}_1 = \text{SiMe}^t\text{Bu}_2$; **10a**: $\text{X} = \text{Cl}$; **10b**: $\text{X} = \text{Br}$).^{23,40}

1.7.2 Cycloaddition

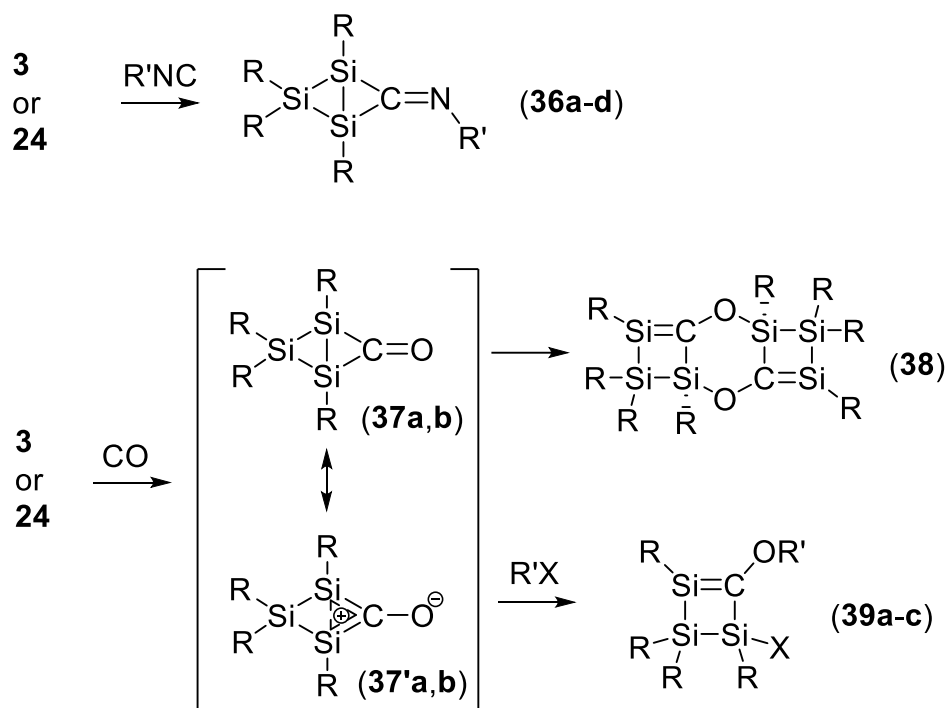
The first cycloaddition of a cyclotrisilene was reported by Sekiguchi *et al.* with the [4+2] reaction of persilyl-substituted **3** with 2-methyl-1,3-butadiene (Scheme 21).

Although this reaction proceeds under rather severe conditions (toluene, 100°C, 36 h) it leads to the formation of bicyclic adduct **34** in 82% yield.⁶⁴



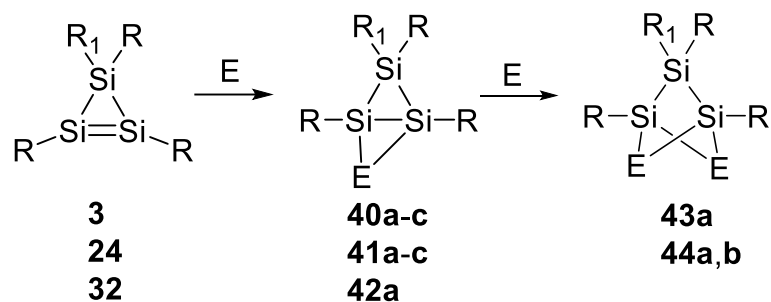
Scheme 21. Reactions of cyclotrisilene **3** and **24** with 1,3-butadiene and ketone affording cycloaddition adduct **34** and **35a,b** (**34**: R = SiMe^tBu₂; **35a**: R = Tip, R₁ = H; **35b**: R = Tip, R₁ = H).^{64,68}

In the case of acyclic disilenes in general, one of the most investigated Si=Si reactivities is that with carbonyl species (typically affording disiloxetanes).¹⁵ As the only reaction of cyclotrisilenes with a C-O species, a [1+2] cycloaddition with carbon monoxide itself was reported (Scheme 22).⁶⁵ In case of heteronuclear heavier cyclopropenes, the reaction of 1-disilagermirene **26** with benzaldehyde affords the [2+2] cycloaddition product,⁶⁶ the same species gives rise to a 1,2-OH addition product with the enolizable ketone, acetophenone.⁶⁷ In 2018, we reported the reaction of cyclotrisilene **26** with aldehydes and benzophenone, both of which proceed smoothly at mild condition and result exclusively in the cycloaddition product **35a** and **35b**, respectively (Scheme 21). The reaction procedures as well as the detailed discussion of the product structure have been published in *Angew. Chem. Int. Ed.* **2018**, 57, 2445-2449⁶⁸ and a brief introduction is also given in 3.1.



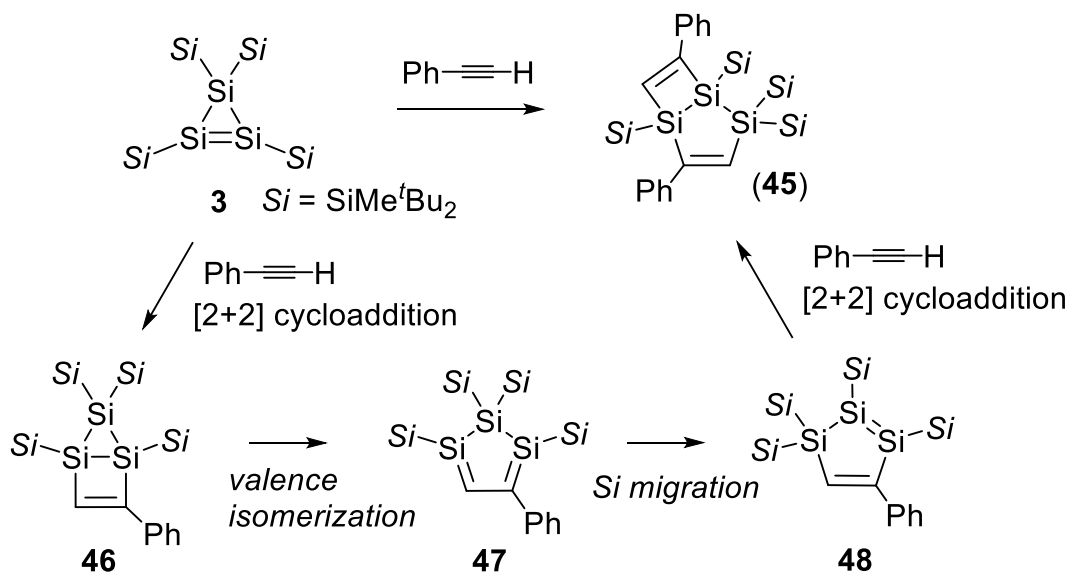
Scheme 22. Reactions of cyclotrisilene **3** and **24** with isocyanides and carbon monoxide (**36a**: R = SiMe^tBu₂, R' = cyclohexyl; **36b**: R = SiMe^tBu₂, R' = Xyl; **36c**: R = Tip, R' = ^tBu; **36d**: R = Tip, R' = Xyl; **37/37'a**: R = SiMe^tBu₂; **37/37'b**: R = Tip; **38**: R = Tip; **39a**: R = SiMe^tBu₂, R' = H, X = OH; **39b**: R = SiMe^tBu₂, R' = H, X = OMe; **39c**: R = Tip, R' = TMS, X = OTf).^{65,69}

Cyclotrisilene **3** (peraryl) and **24** (persilyl) were also reported to undergo cycloaddition reaction with alkyl and aryl isocyanides under ambient conditions with the formation of bicyclic adduct **36a-d** (Scheme 22).⁶⁹ Interestingly, exposure of a benzene solution of either **3** and **24** to 1 atm of CO at room temperature appears to result in a similar [1+2] cycloaddition product **37a,b** initially, which due to its polar oxyallyl nature rapidly dimerizes to the tricyclic Brook-type bis(silene) **38** in the case of **24**, while in the case of **3** the cyclic silenol **39a** is formed as the final product by reaction with trace water.⁶⁵ The postulated mechanism was further confirmed by reaction of **3** and **24** in the presence of MeOH or trimethylsilyl trifluoromethanesulfonate (TMSOTf), resulting in cyclic silenol **39b,c**, respectively.⁶⁵



Scheme 23. Reactions of cyclotrisilene **3**, **24** and **32** with chalcogen elements yielding **40/41a-c**, and **42a**, followed by formation of **43a** and **44a,b** (**40**, **43**: R = R₁ = SiMe^tBu₂, **41**, **44**: R = R₁ = Tip; **42**: R₁ = SR, R = SiMe^tBu₂; **a**: E = S; **b**: E = Se; **c**: E = Te).^{59,70,71}

Reaction of **3** with sulfur, selenium and tellurium was firstly reported by Sekiguchi *et al.* yielding bicyclo[1.1.0]trisilabutane derivative **40a-c**, individually,⁷⁰ among which the bridging Si–Si single bond can add a further equivalent of sulfur resulting in bicyclo[1.1.1]pentane derivative **43a** (Scheme 23).^{70b} In the case of peraryl-substituted cyclotrisilene **24** and as a result of this PhD thesis, its reactivity towards chalcogen elements was reported in 2018 affording **41a-c**. In particular, due to the smaller steric congestion in **41** than **40**, besides the dithia species **44a**, 2,4-diselena-1,3,5-trisilabicyclo[1.1.1]pentane **44b** could also be obtained. Preparative and analytical data as well as a detailed discussion of products **41a-c** and **44a,b** has been published in *Z. Anorg. Allg. Chem.* DOI 10.1002/zaac.201800182⁷¹ and a brief introduction is also given in 3.4. Moreover, cyclotrisilene **32** was also reported to react with one equivalent of sulfur resulting in bicyclic adduct **42a**.⁵⁹



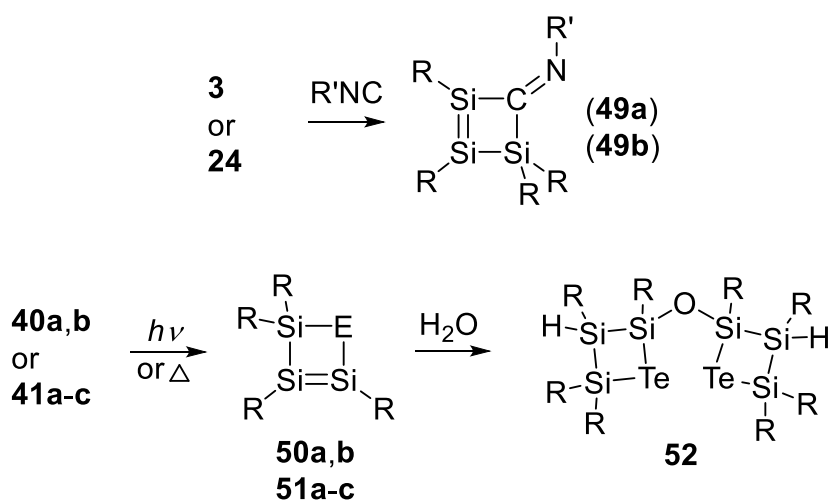
Scheme 24. Reaction of cyclotrisilene **3** with phenylacetylene yields **45**.⁷²

Cycloaddition of cyclotrisilene with alkynes was suggested by Sekiguchi *et al.* as key step of the reaction of **3** with an excess of phenylacetylene at room temperature resulting in 1,2,5-trisilabicyclo[3.2.0]hepta-3,6-diene derivative **45** as final product (Scheme 24).⁷² The reaction with deuterium-labelled cyclotrisilene with phenylacetylene under identical conditions indicates that the reaction proceeds as follows: the phenylacetylene undergoes [2+2] cycloaddition to the Si=Si double bond to form the bicyclic adduct **46**, which isomerizes to the 1,2,3-trisilacyclopenta-3,5-diene derivative **47** with a conjugated Si=C–C=Si system followed by the migration of a silyl substituent. The resulting 1,2,3-trisilacyclopenta-2,4-diene derivative **48** reacts further with another phenylacetylene molecule *via* [2+2] cycloaddition forming the final product.⁷²

1.7.3 Si–Si single bond insertion

Reaction of cyclotrisilene **3** with xylyl isocyanide at 25 °C affords the ring-expanded iminotrisilacyclobutene **49a** arising from insertion into one of the Si–Si single bond of **3** in 48% yield (Scheme 25).⁶⁹ Similarly, **49b** is formed via the reaction of **24** with *tert*-butyl isocyanide at 60 °C. However, when the reaction is performed at –94 °C,

only bicyclic adduct **36c** (Scheme 22) is observed. Samples of isolated **36c** only transform to **49b** very slowly over several days at room temperature, which is clear-cut evidence that the bicyclic adducts **36** are formed under kinetic control, while iminotrisilacyclobutenes **49** are obtained as thermodynamic product. On this basis it was speculated that the kinetic [1+2] cycloaddition be reversible, although a competing intramolecular isomerization pathway cannot be excluded.



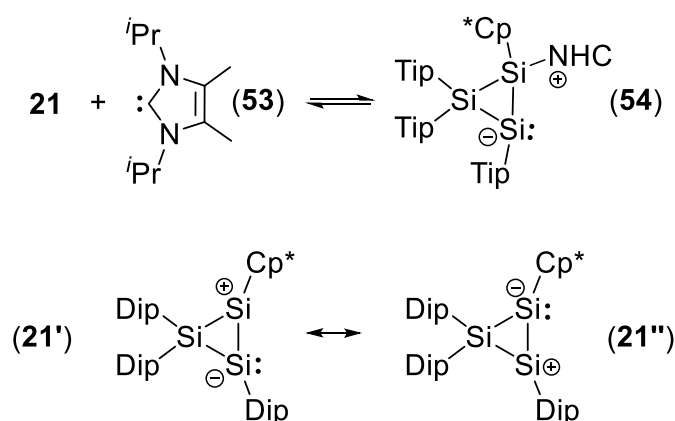
Scheme 25. σ -insertion of Si-Si single bond of cyclotrisilene results in ring-expanded products **49-51** (**49a**: R = SiMe^tBu₂, R' = Xyl; **49b**: R = Tip, R' = ^tBu; **50**: R = SiMe^tBu₂; **51**, **52**: R = Tip; **a**: E = S, **b**: E = Se, **c**: E = Te).^{69,70a,71}

With the synthesis of chalcogen-bicyclo[1.1.0]trisilabutane derivatives **40** (Scheme 23), Sekiguchi *et al.* also reported the photochemical isomerization of **40a,b** to the heavier cyclobutenes **50a,b**, respectively (Scheme 25).^{70a} In the very recent report published as one of the results of this PhD thesis regarding the reactivity of **24** towards chalcogens, chalcogenatrisilacyclobutenes **51a-c** are described as thermal rearrangement products from the corresponding bicyclobutenes. Formation of **51a-c** is supported by multinuclear NMR data and the isolation of the hydrolysis product **52**. Details of this process are also discussed in *Z. Anorg. Allg. Chem.* **2018**, DOI 10.1002/zaac.201800182.⁷¹ A brief introduction is provided in section 3.4.

1.7.4 Miscellaneous Reactions

1.7.4.1 Base coordination

By treatment of cyclotrisilene **21** with one equivalent of N-heterocyclic carbene (NHC) **53**, the 1:1 adduct **54**, with the carbenic carbon atom attached at the Cp*-substituted silicon atom, is formed (Scheme 26).⁵² Calculations of the model system of **21'** suggest a reverse polarization of the Si=Si double bond according to resonance structure **21''** (Scheme 26), in which the weak π donation approximates a η^3 coordination mode and apparently stabilizes a partial positive charge at the Si atom bonded to Cp*. The reversibility of Lewis base coordination is confirmed by variable-temperature NMR studies which shows at 223 K only the appearance of signals of adduct **54**, which co-exist at room temperature with **21** in comparable concentrations.

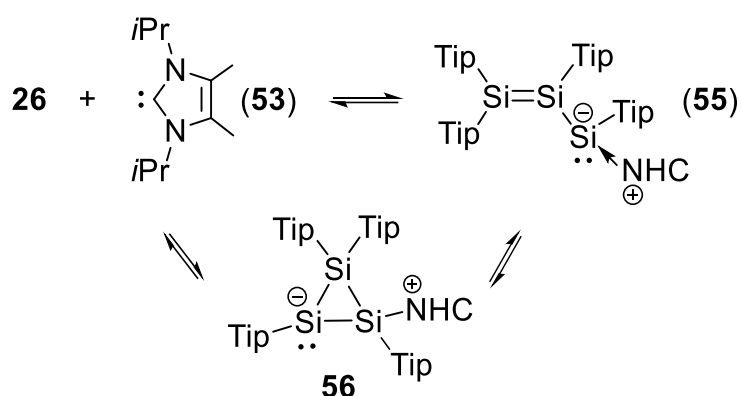


Scheme 26. Reaction of **21** with N-heterocyclic carbene yields **54**.⁵²

1.7.4.2 Ring-opening

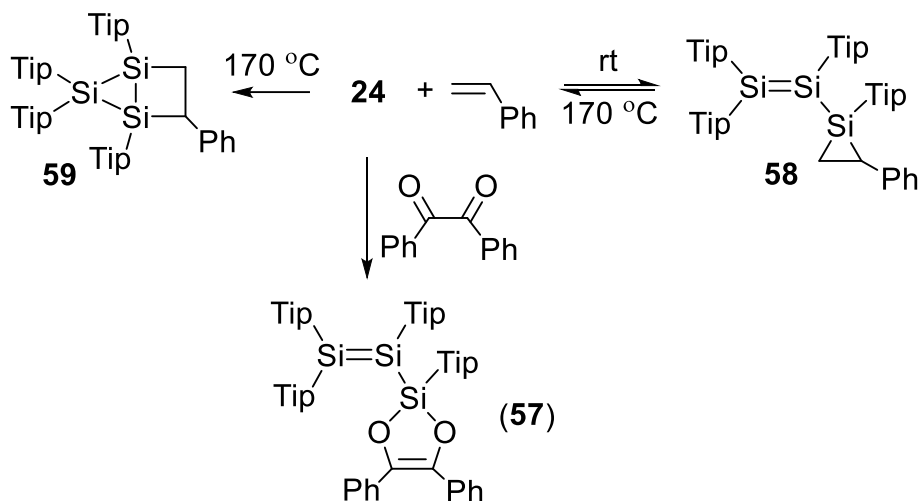
The first example of ring-opening reaction of cyclotrisilene was reported in 2013 by Scheschkewitz *et al.* by treatment of peraryl-substituted cyclotrisilene **24** with N-heterocyclic carbene **53** affording the base-stabilized disilyl silylene **55** (Scheme 27), the silicon version of vinyl carbene.⁷³ Disilyl silylene **55** was isolated as dark-green crystals in acceptable yield (23%) by crystallization from hydrocarbon

solvents at $-20\text{ }^{\circ}\text{C}$. Time-dependent DFT calculations showed that the longest wavelength UV/vis absorption band of **55** at λ_{max} 568 nm resulting from the HOMO \rightarrow LUMO transition. Formation of **55** was proposed to proceed *via* the cyclic cyclotrisilene-NHC adduct **56** on the basis of the ^{29}Si NMR spectrum at 210 K, which exhibits three signals at δ -45.6 , -95.3 and -126.8 ppm, being very similar to that of the Cp*-cyclotrisilene NHC complex **54** (δ -61.5 , -85.6 and -85.9 ppm).⁵²



Scheme 27. Reaction of **26** with N-heterocyclic carbene **53** yields ring-opening product **55**.⁷³

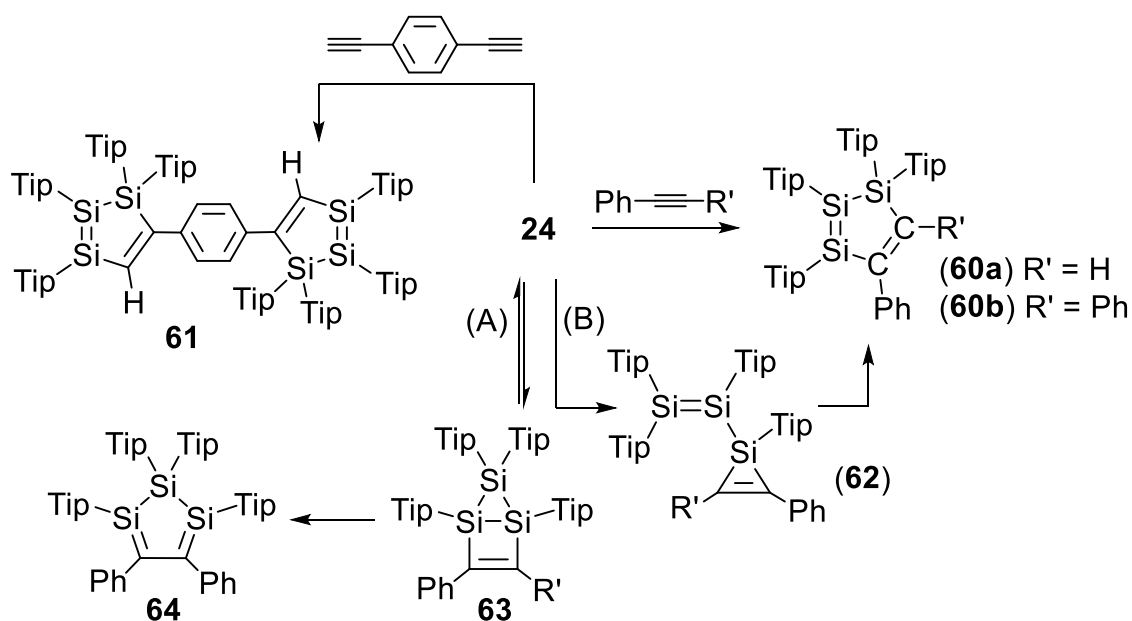
The first irreversible disilyl silylene-like reactivity of a cyclotrisilene was reported very recently as a major result of the work described in this thesis. Reaction of **24** with benzil and styrene at room temperature produces exclusively the ring-opening product **57** and **58**, respectively (Scheme 28). Interestingly, after the disilyl silacyclopropane derivative **55** was heated at $170\text{ }^{\circ}\text{C}$ for twenty minutes housane **59** formed as the major product. A repeat experiment performed at the same temperature in vacuum leads to recovery of starting material **24** in $\sim 80\%$ spectroscopic yield, indicating housane **59** formed *via* [2+2] cycloaddition of cyclotrisilene with styrene as the thermodynamic product instead of an intramolecular rearrangement of **58**. Experimental details and discussion of results has also been published in *Angew. Chem. Int. Ed.* **2018**, *57*, 2445-2449 and a brief introduction is given in 3.1.⁶⁸



Scheme 28. Reaction of **24** with benzil and styrene affords ring-opening product **57-58** and cycloaddition product **59**.⁶⁸

1.7.4.3 Synthesis of 1,2,3-trisilacyclopentadiene derivatives

Unlike the reaction of phenylacetylene with persilylated cyclotrisilene **3** that yields trisilabicyclo[3.2.0]-hepta-3,6-diene derivative **45** (Scheme 24),⁷² its reaction with peraryl cyclotrisilene **24** affords the 1,2,3-trisilapenta-2,4-diene **60a** (Scheme 29).



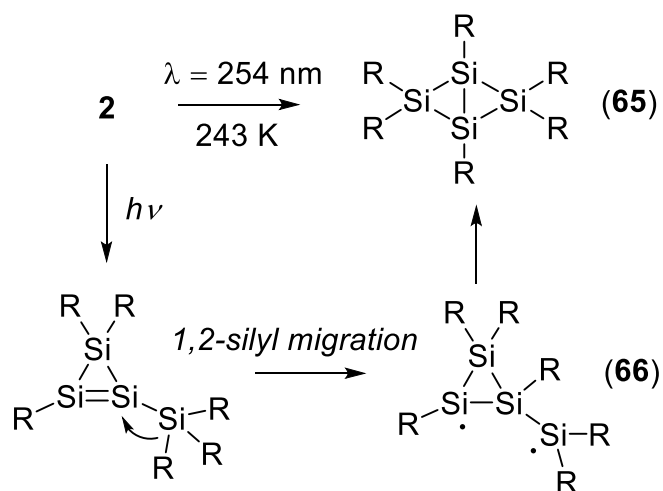
Scheme 29. Synthesize 1,2,3-trisilacyclopenta-2,4-diene derivative **60-61** via reaction of **24** with alkyne and the proposed reaction mechanism.

While **3** reportedly does not react with diphenylacetylene, the reaction of **24** with

diphenylacetylene proceeds smoothly at room temperature resulting in **60b** in acceptable yield. Moreover, the combination of **24** with 1,4-diethynylbenzene generates with **61** a phenylene-bridged 1,2,3-trisilapentadiene derivative for the first time. All three compounds show a significant red-shifted longest wavelength band in the UV/vis spectra each (λ_{\max} 493 for **60a**, 495 for **60b**, 495 nm for **61**) in comparison to cyclotrisilene **24** itself (λ_{\max} 413 nm).

In the proposed mechanistic scenario, the ring-opening intermediate **62** plays a more important role than the [2+2] cycloaddition housane **63** (Scheme 29). The ^{29}Si NMR spectrum of the reaction mixture of **24** with diphenylacetylene unambiguously exhibits a signal at -118.5 ppm, which is characteristic for three-membered silirene rings.⁷⁴ Experimental details and discussion of results has been published in *Chem. Commun.*, **2018**, 54, 8399-8402. DOI: [10.1039/C8CC03297A](https://doi.org/10.1039/C8CC03297A) and a brief introduction is given in 3.3.

1.7.4.4 Photochemical Isomerization



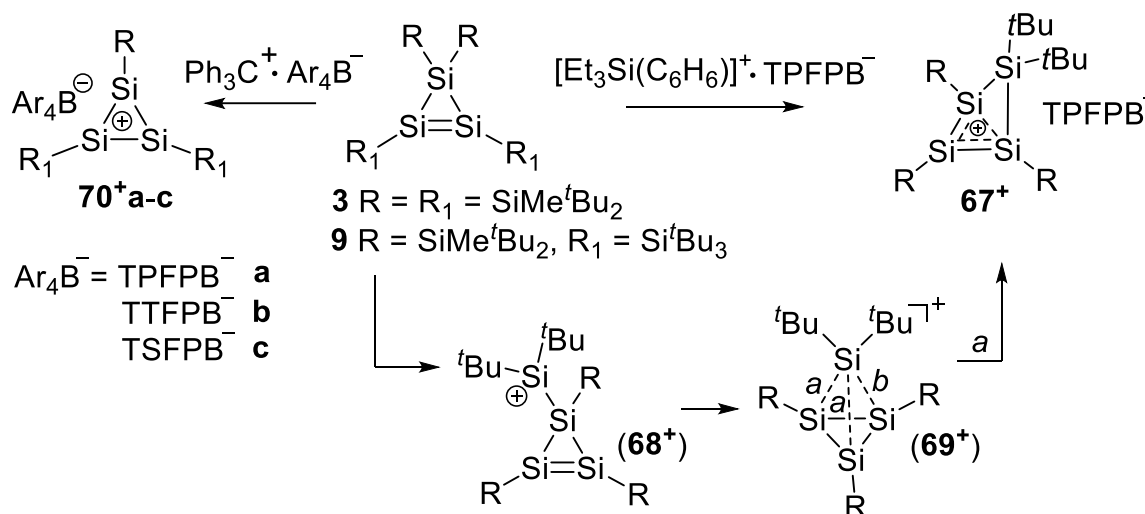
Scheme 30. Photochemical isomerization of cyclotrisilene **2** to tetrasilabicyclo[1.1.0]butane derivative **65** ($\text{R} = \text{SiMe}_2^t\text{Bu}$).⁷⁵

Cyclotrisilene **2** was reported to undergo photochemical isomerization to the corresponding tetrasilabicyclo[1.1.0]butane derivative **65** in 90% yield upon irradiation with UV light of λ 254 nm at 243 K (Scheme 30).⁷⁵ Formation of **65** was rationalized

by the generation of an intermediate 1,3-silyl biradical **66** via 1,2-migration of the trialkylsilyl group followed by intramolecular radical combination.

1.7.4.5 Synthesis of cyclotetra- and cyclotrisilylenylium ion

The silyl substituents in cyclotrisilene **3** make it a possible precursor for a cyclotrisilylenylium ion, a sila-aromatic system. The attempted oxidative removal of one $t\text{Bu}_2\text{MeSi}$ group, however, by reaction of **3** with trityl tetraarylborate failed. Instead the cyclotetrasilylenylium ion **67⁺** was obtained by reaction of **3** with $[\text{Et}_3\text{Si}(\text{benzene})]^+\text{TPFPB}^-$ (Scheme 31).⁷⁶

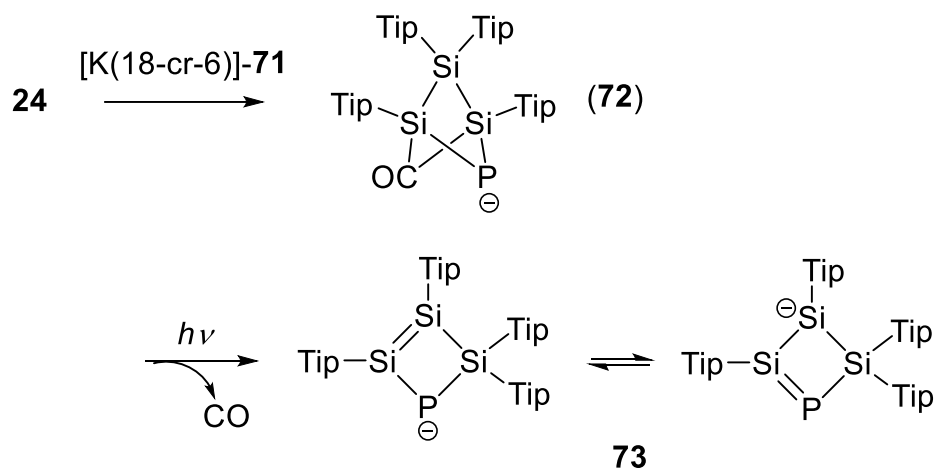


Scheme 31. Synthesize cyclotetra- and cyclotrisilylenylium ion **67⁺**, **70⁺** by oxidative removal of substituent of cyclotrisilene **3** and **9**, respectively (TFPFB: $(\text{C}_6\text{F}_5)_4\text{B}$; TTFPB: $(\text{C}_6\text{F}_4)_4\text{B}$; TSFPB: $([4-(t\text{BuMe}_2\text{Si})\text{C}_6\text{F}_4]_4\text{B})$).^{39,76}

A mechanistic investigation using deuterium-labeled cyclotrisilene indicates that the methyl group of one of the silyl substituents at the saturated ring silicon is initially abstracted by $[\text{Et}_3\text{Si}(\text{benzene})]^+$. The intermediately formed silyl cation **68⁺** then isomerizes via the plausible transition state **69⁺** to the final product. Finally, the cyclotrisilylenylium ion **70⁺** was synthesized by reaction of the slightly modified cyclotrisilene **9**, containing the extremely bulky Si^tBu_3 groups at the $\text{Si}=\text{Si}$ double bond, with trityl tetraarylborate (Scheme 31).³⁹

1.7.4.6 Phosphide delivery to a cyclotrisilene

The direct incorporation of a phosphide anion into an unsaturated ring system was realized by reaction of cyclotrisilene **24** with potassium salt of 2-phosphaethynolate anion **71** ([K(18-crown-6)]-**71**).⁷⁷



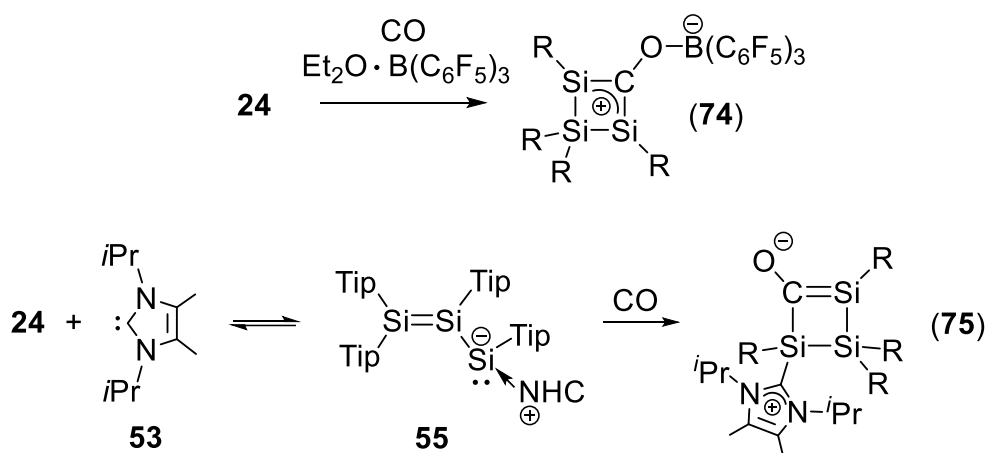
Scheme 32. Reaction of **24** with 2-phosphaethynolate anion **71** yields **72** followed by photolysis to **73**.⁷⁸

The initial product was isolated as bright-orange crystals and confirmed by X-ray crystal structure analysis as anionic $[P(CO)Si_3(Tip)_4]^-$ **72** (Scheme 32).⁷⁸ The decarbonylation of **72** occurs upon photolysis of the mixture of [K(18-crown-6)]-**71** and **24** in toluene, affording [K(18-crown-6)]-**73**, a heavier congener of the cyclobutene anion, that was isolated as blue-green crystals showing the longest absorption wavelength band at λ_{max} 594 nm.

1.7.4.7 Synthesis of Donor-Acceptor Adduct of 1,3-Disila-2-oxyallyl Zwitterion

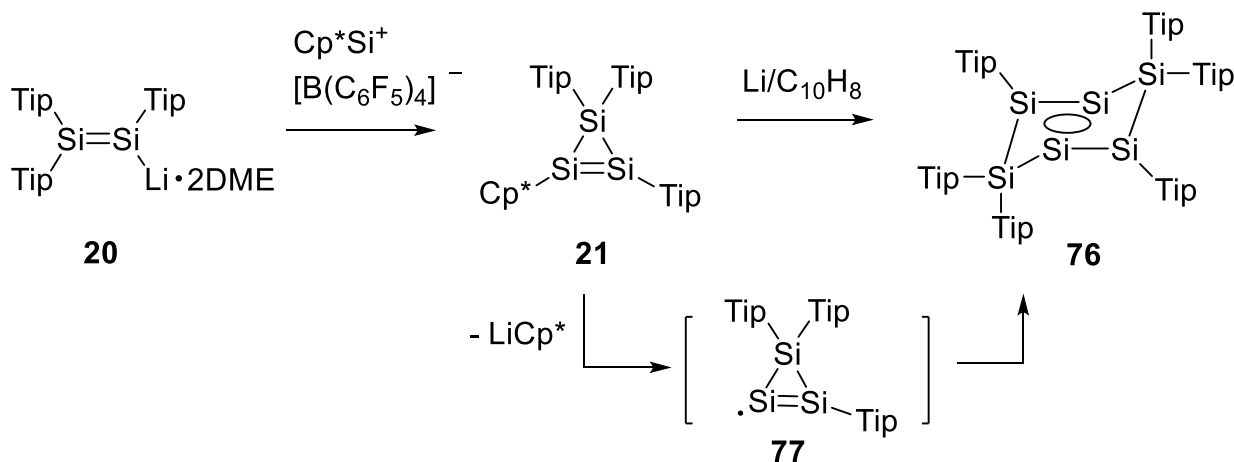
Reaction of cyclotrisilene **24** with carbon monoxide (1 atm) was also performed in the presence of one equivalent amount of $Et_2O \cdot B(C_6F_5)_3$, leading to the formation a 1,3-disila-2-oxyallyl-borate adduct **74** (Scheme 33).⁷⁹ The presence of cyclic π system in **74** is suggested by both Wiberg bond index (0.2986) and out-of-plane zz tensor components of the calculated nucleus independent chemical shifts (NICS) at the center of gravity of the Si-C-Si plane in **74**. Similarly, exposure of the mixture of **24**

with N-heterocyclic carbene (NHC) to one atmosphere of CO leads to the formation of silenolate-type species **75**.⁷⁹



Scheme 33. Synthesize Donor-Acceptor adduct of 1,3-disila-2-oxallyl zwitterion **74** and **75**.⁷⁹

1.7.4.8 Cyclotrisilene as stoichiometric silicon source



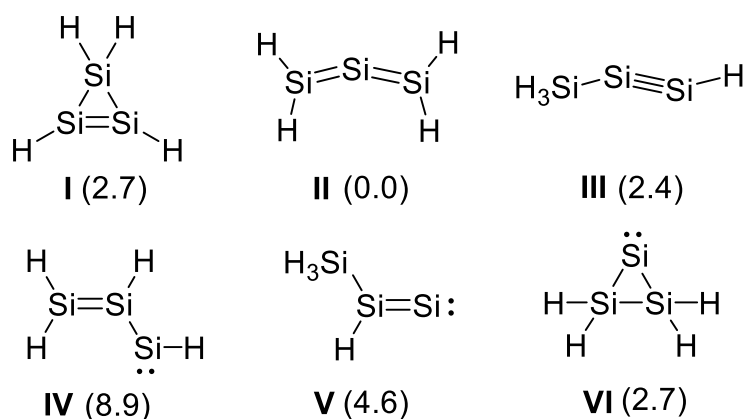
Scheme 34. Alternative synthetic route to hexasilabenzene **76** by the reaction of disilenide **20** with Cp^*Si^+ cation via cyclotrisilene **21**.⁸⁰

The synthesis of dismutational hexasilabenzene isomer **76** was initially achieved through dehalogenation of trichlorocyclotrisilane by Scheschkewitz *et al.*¹⁹ In 2012, an alternative preparative route to **76** was afforded by a collaborative work of the groups of Scheschkewitz and Jutzi. Acting as a stoichiometric source of silicon, the reaction of Cp^*Si^+ with disilenide **20** initially yields cyclotrisilene **21**, in which the Cp^* ligand

can be cleaved in a one electron reduction and the presumably occurring transient cyclotrisilylenyl radical **77** dimerizes to afford siliconoid **76**.⁸⁰

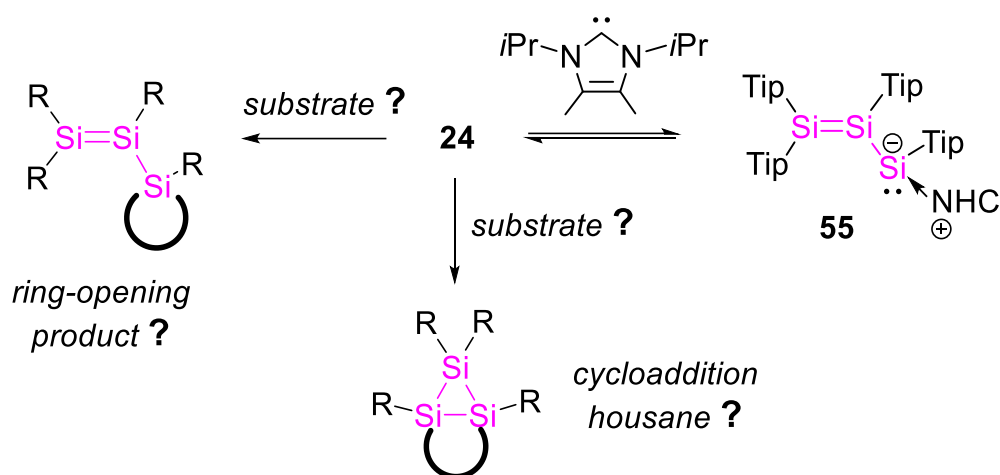
2 Aims and Scope

On the potential-energy surface of Si_3H_4 , six electron-precise isomers were located as minima (**I-VI**, Scheme 35),⁸¹ of which the persila species **I-III** were isolated as stable derivatives with bulky substituents in the early 21st by the groups of Kira,²³ Sekiguchi²⁴ and Wiberg⁵⁰. Conversely, no stable derivatives of the silylene-type isomers **IV** and **VI** have been reported until recently. NHC adducts of representatives of **IV**, **V** and **VI** were isolated by taking advantage of the stabilizing effect of Lewis base coordination.⁸²⁻⁸³



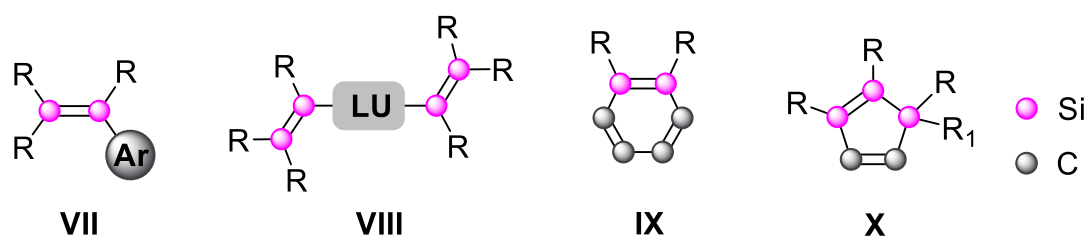
Scheme 35. Relative energies (kcal/mol) of singlet Si_3H_4 .⁸¹

The first stable derivative of disilyl silylene **IV** – the silicon version of vinyl carbene – is formed in the equilibrium reaction of peraryl-substituted cyclotrisilene **24** with an N-heterocyclic carbene (NHC) (Scheme 36).⁷³ Apart from that, no ring-opening reactivity of cyclotrisilene **24** has so far been reported. Therefore investigation into the ring-opening reaction of cyclotrisilene was a central focus of this work.



Scheme 36. Synthesis of disilyl silylene derivative **55** and possible reaction yields ring-opening and cycloaddition products.⁷³

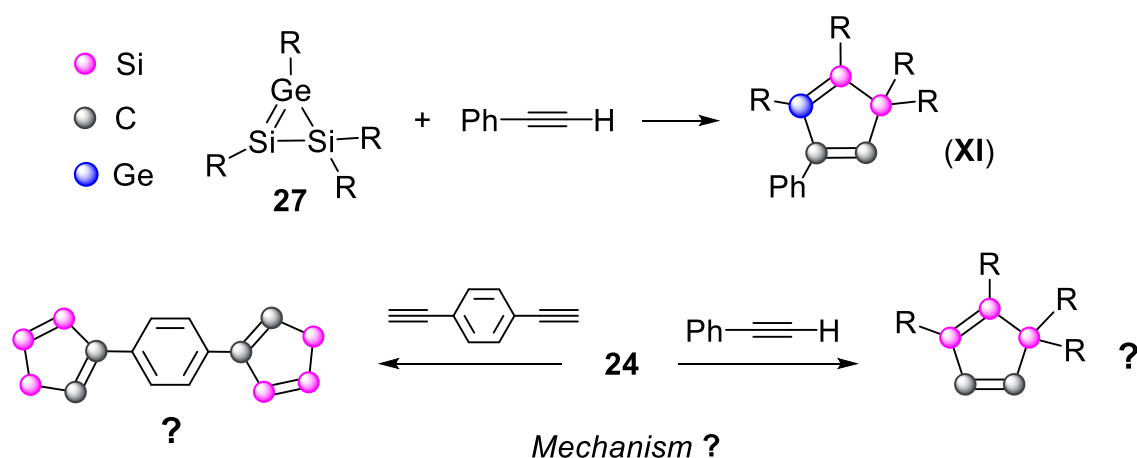
The second major objective of this work was the synthesis of cyclic conjugated Si=Si-C=C systems. Acyclic conjugated Si=Si-C=C system of the type **VII** and **VIII** were obtained at the beginning of this decade, for instance, disilenes with phenyl substituents that show elongation of Si=Si double bond due to conjugation with aromatic linking unit (Scheme 37).⁸⁴⁻⁸⁵ In contrast, cyclic conjugated Si=Si-C=C systems are relatively rare. 1,2-Disilabenzenes of type **IX** are accessible by reaction of disilynes RSi≡SiR with acetylenes.⁸⁶ The only example of Si₃-cyclopentadiene derivative of type **X** had been obtained by reaction of a 1,2,3-trisilabicyclo[1.1.0]butane derivative with an excess of hex-3-yne at elevated temperature.⁸⁷



Scheme 37. Generic examples of conjugated Si=Si-C=C systems (Ar = aromatic unit, LU = linking unit).⁸⁴⁻⁸⁷

In view of Sekiguchi's synthesis of a Si₂Ge-cyclopentadiene derivative **XI** with cyclic Si=Ge-C=C system from **27** and phenylacetylene (Scheme 38),⁸⁸ the intermediacy

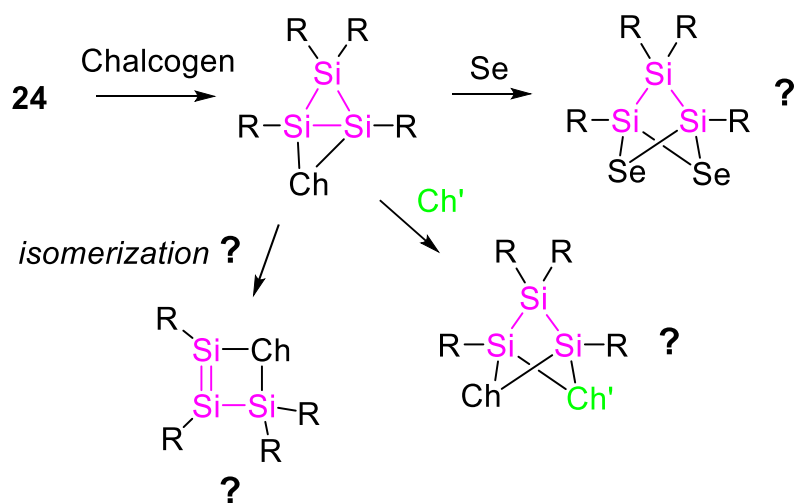
of a transient cyclotrisilene during the formation of **XI** seems plausible. We therefore considered employing cyclotrisilene **24** in reactions with acetylene and 1,4-diethynyl benzene with the purpose to synthesize trisilacyclopentadiene derivatives of type **X** with cyclic conjugated Si=Si-C=C system and moreover, cross-conjugated bridging of two of Si₃C₂ unit by a *para*-phenylene linker (Scheme 38). Considering the higher migration tendency of silyl compared to aryl group, mechanistic investigations are also of importance in this work.



Scheme 38. Synthesis of cyclic Ge=Si-C=C system and the possible reactions of cyclotrisilene **24** with acetylene and 1,4-diethynylbenzene (Ar = aromatic unit, LU = linking unit).⁸⁸

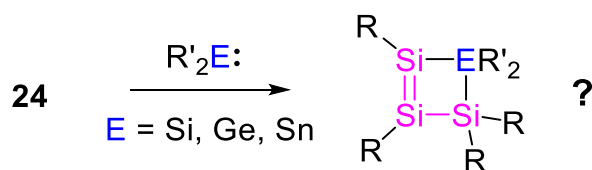
Thirdly, this thesis deals with the reactivity of peraryl-substituted cyclotrisilene **24** towards chalcogens. Inspired by Sekiguchi's synthesis of chalcogena-bicyclo[1.1.0]butane and disulfur-bicyclo[1.1.1]pentane derivatives,⁷⁰ the main task of this work was to explore whether **24** would not only be able to expand the range of known chalcogena- bicyclo[1.1.0]butane and bicyclo[1.1.1]pentane systems (here with aryl substituents), but also transform to corresponding chalcogena-trisilacyclobutene system under appropriate conditions (Scheme 39). Moreover, the anticipated propensity of bridging the Si-Si single bond of the bicyclobutane systems for homolytic cleavage encouraged us to study the possibility of synthesizing bicyclo[1.1.1]pentane derivatives with mixed-chalcogen elements by

reaction with another equivalent of a second chalcogen element.



Scheme 39. Possible reactions of cyclotrisilene **24** with chalcogen elements (R = Tip, Ch, Ch' = S, Se, Te).

Finally, considering the limited reports of cyclic disilenes with mixed Group 14 elements, we therefore sought an alternative method – usage of cyclotrisilene as a σ -insertion precursor – by reaction of **24** with Group 14 divalent species. Basing on the previous reactions of cyclotrisilene with isocyanides, it is reasonable to propose the insertion of divalent E (E = Si, Ge, Sn) atoms into the ring Si–Si single bond would yield targeted cyclic disilenes composed of different Group 14 elements.

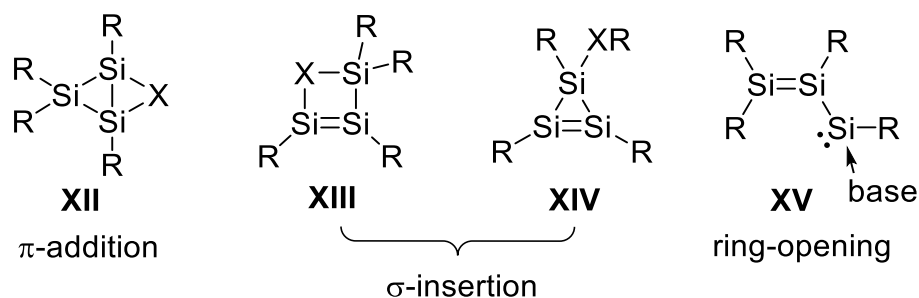


Scheme 40. Possible reactions of cyclotrisilene **24** with divalent Group 14 species (R = Tip).

3 Results and Discussion

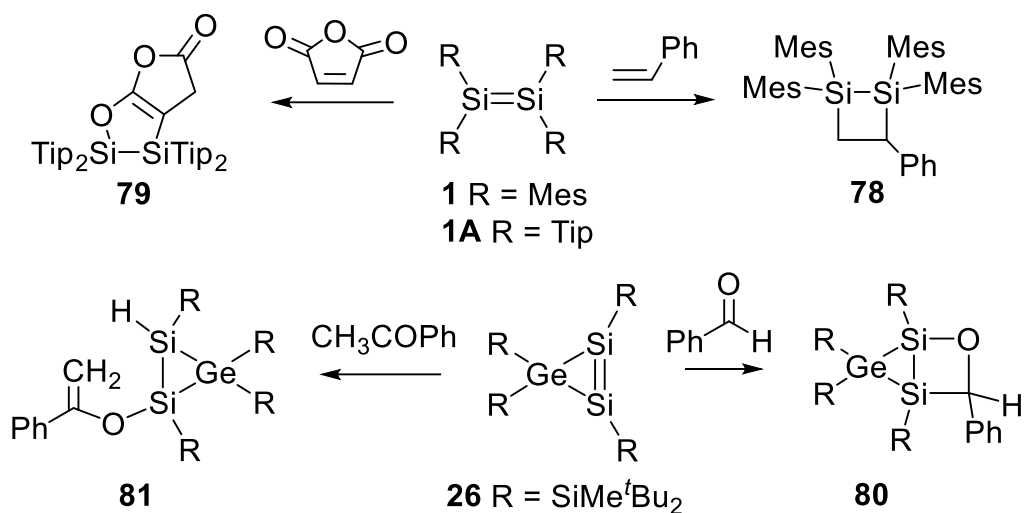
3.1 Disileny Silylene like Reactivity of Cyclotrisilene

As introduced in Chapter 1.7 *Reactions of Stable Cyclotrisilenes* two main generic reaction pathways can be differentiated for these strained, unsaturated silacycles: (1) The π -addition to the Si=Si double bond leading to 1,2-addition or cycloaddition products such as **XII** (Scheme 41) represented by bicyclic products **36**, **40** and (2) the σ -insertion into one of the endocyclic Si–Si single bonds, effectively resulting in ring expansion products of type **XIII**. Trisilacyclobutenes **49** and **50** are typical representatives of this reaction course. A third reaction pathway is much less frequently observed, described as (3) the formal insertion into an exocyclic σ -bond of one of the substituents yields **XIV** (formation of **32** provides an example). The reversible ring-opening reaction of cyclotrisilene to give adduct of type **XV** sets an example for a fourth pathway, which was only recently reported by our group (equilibrium reaction of aryl-substituted cyclotrisilene **24** with an N-heterocyclic carbene).⁷³



Scheme 41. Generic products of cyclotrisilenes reactions.

As the relatively small HOMO-LUMO energy split of disilenes renders them susceptible to oxidative additions,²² one of the general reactivities of disilenes involves (oxidative) cycloaddition of the Si=Si double bond with multiple bonds. For instance, reaction of tetramesityldisilene **1** with styrene affords the [2+2] cycloadduct **78**⁸⁹ and disilene **1A** reacts with maleic anhydride through formal [2+3] addition accompanied by hydrogen shift to give **79** (Scheme 42).⁹⁰

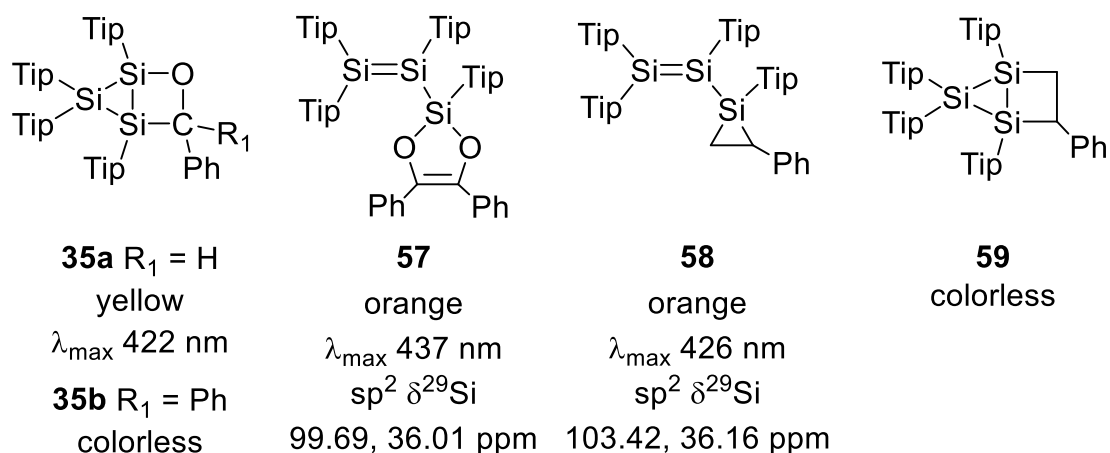


Scheme 42. Representatives of reactions of disilene with alkene and carbonyl compound.^{72,89,90}

In the case of cyclotrisilenes, however, only limited examples involving cycloaddition of the endocyclic Si=Si double bond with multiply bonded systems have been reported during last decades. Cyclotrisilene **3** was reported to react under rather severe conditions with 2-methyl-1,3-butadiene resulting in [2+2] cycloaddition product **34** (Scheme 21).⁶⁴ Another example reported by Sekiguchi *et al.* involves the reaction of endocyclic Si=Si double bond of Si₂Ge-cyclotrimetallene **26** with aldehydes yielding bicyclo[2.1.0]pentane derivative **80** while the reaction with enolizable ketone affords 1,2-OH addition product **81** (Scheme 42).⁷² Considering the well-studied ring-opening process in the cases of carbon-based cyclopropenes – e. g. the field of ring-opening polymerization (ROP)⁹¹ – it was motivating that apart for the equilibrium formation of **XV** no further ring-opening reactivity of cyclotrisilene has been reported yet. We were therefore keen to find the preparative manifestation of such disilanyl silylene reactivity of cyclotrisilenes.

In this publication, reactions of cyclotrisilene **24** with ketones and styrene have been investigated in detail. While reaction of cyclotrisilene **24** with benzaldehyde and benzophenone results in the [2+2] cycloaddition product **35a** and **35b**, respectively, reaction with benzil and styrene at room temperature affords the ring-opening product **57** and **58**. Interestingly, reaction of **24** with styrene at 170 °C also generates [2+2]

cyclic adduct **59** in substantial yield (Scheme 43). This process is realized by heating solid **58** at 170 °C in a sealed Schlenk tube. When the procedure is performed in vacuum, regenerated starting material cyclotrisilene **24** can be detected in ca. 80% yield by measuring ¹H NMR of the reaction mixture.



Scheme 43. Cycloadduct **35**, **59** and ring-opening product **57-58**.

DFT calculations at the dispersion-corrected M062X/def2-SVP level of theory reveal **58** to be about 16.8 kcal/mol higher in ΔG_{298} than **59** and this difference is only slightly lowered at 443 K with $\Delta\Delta G_{443} = 14.6$ kcal/mol. The experimental observations and computational results support a mechanistic scenario in which the kinetic product of [1+2] addition **58** re-dissociates to give free styrene and the transient disilyl silylene, which rapidly isomerize to cyclotrisilene **24** even at elevated temperature. Under thermodynamic control, [2+2] cycloaddition of **24** with styrene affords housane **59**. Gibb's enthalpies also show dissociation of **58** to free disilyl silylene is thermodynamically significantly more feasible ($\Delta\Delta G_{298} = +5.7$ kcal/mol vs. $\Delta\Delta G_{443} = +21.4$ kcal/mol).

Products **35a,b** and **57-59** are isolated as pure colorless to orange crystals from hydrocarbon solvents in 50%-60% yield and fully characterized by multinuclear NMR spectroscopy, X-ray single crystal structure analysis, UV/vis absorption spectrum and elemental analysis. The UV/vis absorption spectrum of **57** and **58** shows the longest wavelength absorption at λ_{\max} 437 and 426 nm, respectively, due to the π - π^* transition.

In the ^{29}Si NMR spectrum saturated housane **35a,b** and **59** exhibit signals of the bridgehead silicon atoms at relatively high-field (δ 7.87, -65.83 ppm for **35a**, -1.66, -67.14 ppm for **35b**, 9.28, -84.22 for **59**), while the three-coordinated silicon atoms of **57** and **58** show signals at δ 99.69, 36.01 and 103.42, 36.16 ppm, respectively. Bond lengths and angles as well as the Si=Si double bond *trans*-bent and torsion angle are also discussed in detail.

Results of the described studies have been published in the *Angewandte Chemie International Edition* and *Angewandte Chemie*.

H. Zhao, K. Leszczyńska, L. Klemmer, V. Huch, M. Zimmer and D. Scheschkewitz, Disilynyl Silylene Reactivity of a Cyclotrisilene, *Angew. Chem. Int. Ed.* **2018**, *57*, 2445-2449. [DOI:10.1002/anie.201711833](https://doi.org/10.1002/anie.201711833). *Angew. Chem.* **2018**, *130*, 2470-2474. [DOI:10.1002/ange.201711833](https://doi.org/10.1002/ange.201711833).

All people mentioned as authors made a range of effort to the publication of this paper: H. Zhao performed all experiments and the characterization of all products. Manuscript and supporting information of this publication was drafted by her. Substantial conception of study was suggested by K. Leszczyńska. L. Klemmer performed the DFT calculations. V. Huch contributed to the crystallographic data collection and refinement. M. Zimmer engaged in the VT-NMR as well as solid state NMR data collections. D. Scheschkewitz has given critical revision of the manuscript and he is the supervisor of the research. An authorship statement signed by all co-authors including more detailed contributions of each co-author is also provided.

Silylenes

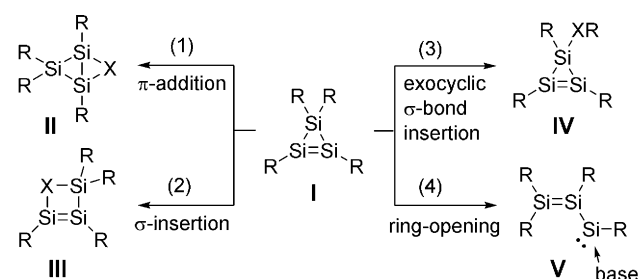
International Edition: DOI: 10.1002/anie.201711833
German Edition: DOI: 10.1002/ange.201711833

Disilyl Silylene Reactivity of a Cyclotrisilene

Hui Zhao, Kinga Leszczyńska, Lukas Klemmer, Volker Huch, Michael Zimmer, and David Scheschkewitz*

Abstract: The highly reactive silicon congeners of cyclopropene, cyclotrisilenes ($c\text{-Si}_3\text{R}_4$), typically undergo either π -addition to the Si=Si double bond or σ -insertion into the Si–Si single bond. In contrast, treatment of $c\text{-Si}_3\text{Tip}_4$ (Tip = 2,4,6- i -Pr $_3$ C $_6$ H $_2$) with styrene and benzil results in ring opening of the three-membered ring to formally yield the [1+2]- and [1+4] cycloaddition product of the isomeric disilyl silylene to the C=C bond and the 1,2-diketone π system, respectively. At elevated temperature, styrene is released from the [1+2]-addition product leading to the thermodynamically favored housane species after [2+2] cycloaddition of styrene and $c\text{-Si}_3\text{Tip}_4$.

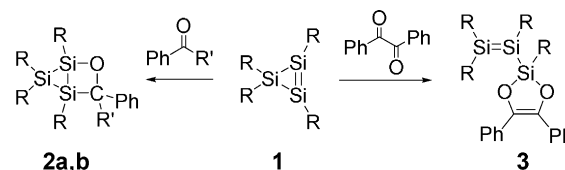
The heavier congeners of cyclopropenes ($c\text{-C}_3\text{R}_4$), namely cyclotrisilene ($c\text{-Si}_3\text{H}_4$), continue to attract interest from theory^[1] and experiment alike owing to their unique structure and reactivity. A significant number of stable cyclotrisilenes **I** have been isolated taking advantage of kinetic stabilization by sterically demanding silyl and aryl substituents.^[2] The extensive investigations into the reactivity of strained, unsaturated silacycles revealed two main generic reaction pathways (Scheme 1): 1) The π -addition to the Si=Si double bond



Scheme 1. Generic reactivity pathways of cyclotrisilenes **I**.

leading to products of type **II**^[3,4] and 2) the σ -insertion into one of the endocyclic Si–Si single bonds effectively resulting in ring expansion products of type **III**.^[4] In addition, a few reactions under (Scheme 1, 3) formal insertion into an exocyclic σ bond of one of the substituents have been reported,^[2e,5] for example, the insertion of sulfur into one of the

bonds to the silyl substituents.^[5] Ring-opening reactions of cyclotrisilenes were notably absent, although well-studied in the cases of carbon-based cyclopropenes and even applied for the synthesis of polymers.^[6] Recently, we reported the first example of (Scheme 1 4) the reversible ring-opening of a cyclotrisilene: the equilibrium reaction of aryl-substituted cyclotrisilene with an N-heterocyclic carbene (NHC).^[7] Disilyl silylenes, such as the resulting NHC-coordinated example **V** (Scheme 1), have also been proposed as transient intermediates.^[1a,2f] Clear-cut preparative manifestations of disilyl silylene reactivity of cyclotrisilenes, however, remain elusive. We now report the reactions of homoleptic cyclotrisilene $c\text{-Si}_3\text{Tip}_4$ (**1**, Tip = 2,4,6- i -Pr $_3$ C $_6$ H $_2$, Scheme 2) with substrates containing C=C or C=O double bond(s) that allow for the detection and—in two cases—even isolation and full characterization of the assumed kinetic product of disilyl silylene-like reactivity of **1**.



Scheme 2. Reactions of cyclotrisilene **1** with benzaldehyde, benzophenone, and benzil to give housanes **2a,b** and disilyl-substituted 2,5-dioxasilol **3** (R' = H (**2a**), Ph (**2b**); R = Tip = 2,4,6- i -Pr $_3$ C $_6$ H $_2$).

One of the most investigated Si=Si reactivities in general is the [2+2] cycloaddition of carbonyl species to afford disiloxetanes.^[8] In the case of cyclotrimetallenes of heavier Group 14 elements, however, just a limited number of reactions with carbonyl compounds is known.^[3,9] As the only example in the case of cyclotrisilenes, a [1+2] cycloaddition of carbon monoxide itself was reported.^[3b] While the reaction of a 1-disilagermirene with benzaldehyde affords the [2+2] cycloaddition product,^[3a] the same species gives rise to a 1,2-OH addition product with the enolizable acetophenone.^[9] Building on the divergent reactivity of cyclotrisilenes towards isonitriles ([1+2] cycloaddition leading to the kinetic and σ insertion to the thermodynamic product),^[3b] we investigated the behavior of **1** towards carbonyl compounds with a view to possible disilyl silylene-like reactivity.

Treatment of **1** with one equivalent of benzaldehyde or benzophenone in benzene at room temperature, however, leads to rapid conversion into the [2+2] cycloaddition products, housane derivatives **2a,b** (Scheme 2). Three sharp ^{29}Si NMR signals each (**2a**: $\delta = 43.87, 7.87, \text{ and } -65.83$ ppm; **2b**: $\delta = 27.61, -1.66, \text{ and } -67.14$ ppm) are comparable to those of the aforementioned imino trisilabicyclo[1.1.0]butane

[*] M. Sc. H. Zhao, Dr. K. Leszczyńska, M. Sc. L. Klemmer, Dr. V. Huch, Dr. M. Zimmer, Prof. Dr. D. Scheschkewitz
Krupp-Lehrstuhl für Allgemeine und Anorganische Chemie
Universität des Saarlandes
Campus, C4.1, 66123 Saarbrücken (Germany)
E-mail: scheschkewitz@mx.uni-saarland.de

Supporting information and the ORCID identification number(s) for the author(s) of this article can be found under:
<https://doi.org/10.1002/anie.201711833>.

($\delta = 45.0, 27.9, \text{ and } -78.7 \text{ ppm}$).^[3b] On the basis of $^1\text{H}/^{29}\text{Si}$ HMBC spectrum, the two downfield ^{29}Si NMR signals are assigned to the bridgehead silicon atoms, while the upfield signal is due to the SiTip_2 bridge. In the ^1H NMR spectrum of **2a**, the benzylic hydrogen atom gives rise to a singlet at $\delta = 6.34 \text{ ppm}$, very similar to that of *trans*-disilagermabicyclo[2.1.0]pentane ($\delta 6.01 \text{ ppm}$).^[3a] Both, **2a** and **2b** show diagnostic ^{13}C NMR resonances (**2a**: $\delta = 77.38$; **2b**: $\delta = 92.31 \text{ ppm}$) in the typical range for the ring carbon atoms in disilaoxetanes.^[3a]

Housanes **2a,b**, were isolated as single crystals in acceptable yields (**2a**: 60%, yellow blocks, m.p. $> 200^\circ\text{C}$; **2b**: 55%, colorless blocks, m.p. $> 200^\circ\text{C}$). The solid-state structures of **2a,b** were confirmed by X-ray crystallography (**2a**: Figure 1,

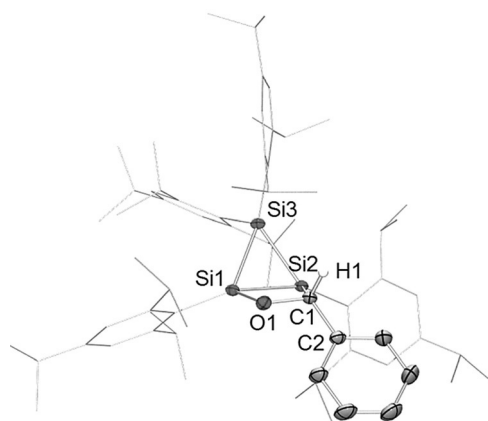


Figure 1. Molecular structure of **2a** in the solid state. Hydrogen atoms are omitted for clarity (thermal ellipsoids set at 50% probability). Selected bond lengths [Å] and angles [°]: Si1–Si2 2.347(6), Si2–Si3 2.333(6), Si1–Si3 2.364(7), Si1–O1 1.675(1), Si2–C1 1.975(2), C1–O1 1.453(2), C1–C2 1.505(2), C1–H1 0.964(2); Si1–Si3–Si2 59.95(2), Si3–Si1–O1 109.14(5), Si3–Si2–C1 98.99(5), Si1–O1–C1 104.76(8), Si2–C1–O1 102.85(9), C2–C1–H1 106.40(1).

2b: see Supporting Information).^[10] Housanes **2a,b** display a three- and four-membered ring fused skeleton with the angle between the two planes being $115.9(4)^\circ$ in **2a** and $113.4(1)^\circ$ in **2b**, which is slightly larger than that of the *trans*-disilagermabicyclo[2.1.0]pentane (107.8°),^[3a] but significantly smaller than the dihedral angle in imino-1,2,3-trisila-bicyclo[1.1.0]butane (134.2°).^[3b] The Si–Si bond lengths in the three-membered rings of **2a,b** (**2a**: 2.333(6), 2.347(6), and 2.364(7) Å, **2b**: 2.338(2), 2.349(3), and 2.403(3) Å) are within the typical range for Si–Si single bonds.

As the [2+2] cycloaddition of an isolated C=O moiety prevails over the targeted [1+2] cycloaddition with the postulated transient disilyl silylene **6** (see Scheme 4), we speculated that the [1+4] cycloaddition of the silylene moiety with a 1,2-diketone might be sufficiently favored compared to any reaction of the Si=Si fragment. Reactions of isolated silylenes with 1,2-diketones were previously reported to give dioxasilole derivatives.^[11] Indeed, an equimolar mixture of benzil and **1** dissolved in C_6D_6 or toluene afforded an intensely bright red solution almost instantly, as opposed to the pale yellow to colorless reaction mixtures of **2a,b**. Three

new signals in ^{29}Si NMR spectrum at $\delta = 99.69, 36.01, \text{ and } 14.40 \text{ ppm}$ served as first indication for the formation of 1,3,2-dioxasilole **3** with an exocyclic Si=Si double bond and thus the desired disilyl silylene reactivity of cyclotrisilene **1**. The product **3** was isolated as an orange powder in acceptable yield (60%). In the ^{29}Si NMR, the two signals at low field are assigned to the formally sp^2 hybridized silicon atoms. The signal at $\delta = 14.40 \text{ ppm}$ corresponds to the tetracoordinate silicon atom of the dioxasilole ring. As typical for disilylenes, the UV/Vis spectrum of **3** in hexane shows a longest wavelength absorption at $\lambda_{\text{max}} = 437 \text{ nm}$ ($\epsilon = 14950 \text{ M}^{-1} \text{ cm}^{-1}$), which is assigned to the $\pi\text{--}\pi^*$ transition.^[8f]

Crystals of **3** suitable for X-ray crystallography were obtained from hexane solution (Figure 2).^[10] The Si=Si double

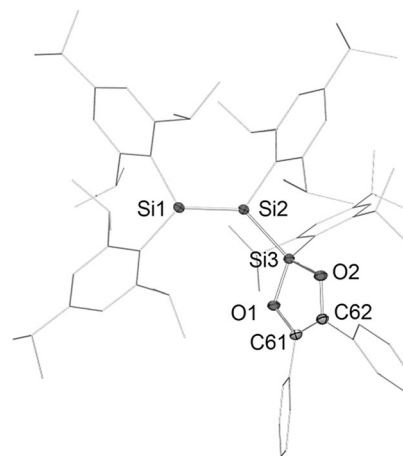


Figure 2. Molecular structure of disilyl-substituted 2,5-dioxasilole **3-C₆H₁₄** in the solid state. Co-crystallized C_6H_{14} and hydrogen atoms are omitted for clarity (thermal ellipsoids set at 50% probability). Selected bond lengths [Å] and angles [°]: Si1–Si2 2.179(4), Si1–Si3 2.333(4), Si3–O1 1.679(8), Si3–O2 1.679(8), C61–O1 1.396(1), C62–O2 1.393(1), C61–C62 1.345(2); Si2–Si1–Si3 136.78(2), Si1–Si3–O1 122.40(3), O1–Si3–O2 94.17(4), Si3–O1–C61 109.06(6), O1–C61–C62 113.59(9).

bond length of 2.179(4) Å is within the typical range (2.138–2.289 Å).^[12] The twisted Si=Si double bond (twist angle $\tau = 23.5(4)^\circ$) is only moderately *trans*-bent ($\theta = 12.4(3)^\circ$ at SiTip_2 , $6.7(2)^\circ$ at $\text{Si}(\text{Tip})\text{Si}$). The dioxasilole ring of **3** exhibits an envelope conformation with an angle of $6.3(4)^\circ$ between the planes of O1–C61–C62–O2 and O1–Si3–O2, slightly more than in the reported 1,3,2-dioxasilole (3.3°).^[11g] The two phenyl groups twist from the dioxasilole ring by interplane angles of $39.9(4)^\circ$ and $37.3(4)^\circ$.

It is well-established that polar substrates facilitate the [2+2] cycloaddition to Si=Si bonds.^[13] As the lower polarity of the C=O bonds in benzil might contribute to the prevalence of the [1+4] cycloaddition pathway, we extrapolated that a reaction of cyclotrisilene **1** with the inherently less-polar C=C bond of alkenes might also result in disilyl silylene reactivity. While a *cis/trans* isomeric mixture of stilbene (1,2-diphenyl ethene) does not react with **1** even at elevated temperatures, presumably a result of steric hindrance, the treatment of cyclotrisilene **1** with one equivalent of styrene (phenyl ethene) at room temperature results in the uniform

appearance of three new signals in the ^{29}Si NMR spectrum at $\delta = 103.42, 36.16,$ and -94.15 ppm (Scheme 3). As in case of **3**, the two downfield signals are diagnostic of an acyclic Si=Si unit. The signal upfield falls well within the typical region for the endocyclic silicon atom of three-membered C_2Si rings: for instance, siliranes obtained by the reaction of an acyclic iminosilylsilylene and a silylsilylene with ethylene were reported to show resonances at $\delta = -100.90$ and -80.76 ppm, respectively.^[14] With the help of a DEPT-135 spectrum (Figures S14,S15), the ^{13}C NMR signal at $\delta = 10.84$ ppm is assigned to the CH_2 moiety in the three-membered ring of **4**, while the phenyl substituted ring carbon gives rise to a signal at $\delta = 23.59$ ppm. As in the case of **3**, the longest wavelength absorption in the UV/Vis spectrum of **4** at $\lambda_{\text{max}} = 426$ nm ($\epsilon = 17430 \text{ M}^{-1} \text{ cm}^{-1}$) confirms the presence of an acyclic Si=Si unit as it is almost identical to that of a previously reported chlorosilyl disilene ($\lambda_{\text{max}} = 427$ nm).^[15]

After workup, disilyl-substituted silirane **4** is isolated in 54% yield (m.p. 168–170°C) as an orange powder. Orange blocks suitable for X-ray structure analysis were obtained at -20°C from toluene solution. The molecular structure of **4** in the solid state confirmed the connectivity deduced from the spectroscopic data (Figure 3).^[10] The Si=Si double bond of

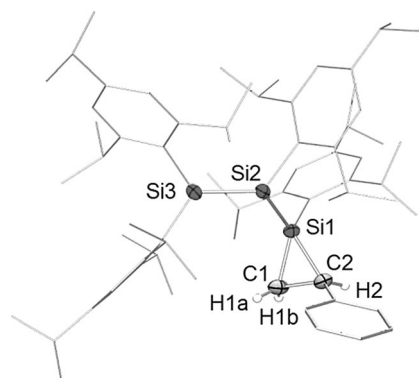
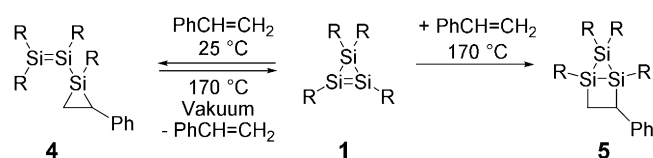


Figure 3. Molecular structure of disilyl-substituted silirane **4** in the solid state. Hydrogen atoms are omitted for clarity (thermal ellipsoids set at 50% probability). Selected bond lengths [Å] and angles [°]: Si1–Si2 2.300(1), Si2–Si3 2.180(1), C1–C2 1.533(4), Si1–C1 1.844(3), Si1–C2 1.890(2); Si1–Si2–Si3 125.37(4), C1–Si1–C2 48.44(1), Si1–C2–C1 64.21(2).

2.180(1) Å displays moderate twisting and *trans*-bending (twist angle $\tau = 17.9(9)^\circ$, *trans*-bent angle $\theta = 13.2(7)^\circ$ at SiTip_2 , $18.4(6)^\circ$ at $\text{Si}(\text{Tip})\text{Si}$). The Si1–Si2 distance of 2.300(1) Å is rather short for the typical Si–Si single bond suggesting a certain degree of hyperconjugation^[16] with the adjacent Si=Si unit.

Given that the steric requirements of styrene and benzaldehyde are fairly comparable, we considered the possibility of isomerization of the disilyl-substituted silirane **4** to a saturated housane structure akin to **2a,b**. Indeed, heating of solid **4** slightly above the melting point for 20 min under argon atmosphere affords trisilabicyclo[2.1.0]pentane **5** (Scheme 3) in 32% yield after crystallization from hexane.



Scheme 3. Synthesis of disilyl-substituted silirane **4** (kinetic product) and its conversion into housane **5** (thermodynamic product; $\text{R} = \text{Tip} = 2,4,6\text{-iPr}_3\text{C}_6\text{H}_2$).

Colorless single crystals suitable for X-ray diffraction analysis (Figure 4) were obtained from hexane at 5°C confirming the

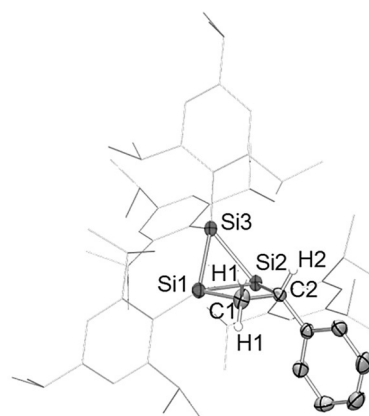


Figure 4. Molecular structure of housane **5** in the solid state. Hydrogen atoms are omitted for clarity (thermal ellipsoids set at 50% probability). Selected bond lengths [Å] and angles [°]: Si1–Si2 2.392(2), Si1–Si3 2.311(2), Si2–Si3 2.371(1), Si1–C1 1.905(4), Si2–C2 1.916(4), C1–C2 1.546(7), C1–H1 1.05(4), 0.92(5), C2–H2 0.97(3); Si3–Si1–Si2 60.54(5), Si1–Si3–Si2 61.41(5); C1–Si1–Si2 75.38(2), Si1–C1–C2 106.0(3), Si2–C2–C1 99.6(3).

constitution of a housane structure.^[10] The angle between the mean planes of the three- and four-membered rings is $119.0(9)^\circ$, which is slightly larger than that in **2a,b** (**2a**: $115.9(4)^\circ$; **2b**: $113.4(1)^\circ$). The Si–Si single bond lengths vary between 2.311(2) Å and 2.392(2) Å. Curiously, in the ^{29}Si NMR spectrum of **5** in C_6D_6 solution at 25°C only one signal at $\delta = 14.28$ ppm is observed, while in the solid state CP-MAS ^{29}Si NMR revealed the expected three signals at $\delta = 14.72, 8.39,$ and -88.75 ppm. Similarly, the ^{29}Si NMR spectrum in solution at -40°C displays three signals at $\delta = 13.19, 9.28,$ and -84.22 ppm, which coalesce in a rather undefined manner upon warming to room temperature. These findings suggest that the two signals at $\delta = 9.28$ and -84.22 ppm arise from an unknown dynamic process. Despite the high probability that the upfield signal at $\delta = -84.22$ ppm belongs to the SiTip_2 moiety on grounds of similarity with **2a**, we confirmed the assignment by calculating the NMR shifts at the M06-2X/def2TZVPP level of theory. The results ($\delta^{29}\text{Si}_{\text{calcd}} = -79.04$ (SiTip_2), 29.43 (SiCPh), 20.90 (SiCH_2) ppm) are in qualitative agreement with the experiments. We tentatively explain the peculiar NMR behavior with hindered rotation at the two more congested silicon atoms.

Finally, we pondered the question whether the formation of **5** proceeds 1) as an intramolecular isomerization or 2) through the dissociation of styrene from the kinetic product **4**. A few reversible [1+2] cycloadditions involving silylenes and ethylene have indeed been reported, for example, the reaction of ethylene with a phosphonium silaylide^[17] and with acyclic silylenes.^[14b,18] Melting of **4** was therefore repeated under dynamic vacuum to remove any liberated styrene rapidly. The melt residue of **4** after having been kept in vacuum at 170°C for two minutes showed the characteristic ²⁹Si NMR signals of cyclotrisilene **1** at $\delta = 42.82$, -22.98 ppm. From the ¹H NMR spectrum the yield of regenerated **1** was estimated to about 78% (Figures S15, S16), accompanied by small quantities of π -addition product **5** and other by-products.

On this basis, we propose the following mechanistic scenario for the formation of **5**: the kinetic product of [1+2] addition **4** re-dissociates to give free styrene and the transient disilylenyl silylene **6**, which should rapidly isomerize to cyclotrisilene **1** even at elevated temperature. Under thermodynamic control, [2+2] cycloaddition of **1** with styrene affords housane **5** (Scheme 4). DFT calculations at the dispersion-

6 to give [1+4] and [1+2] addition products **3** and **4**, respectively, which represent the first examples of disilylenyl silylene reactivity of any cyclotrisilene. Under thermodynamic control, however, **1** and styrene react through the usual [2+2] cycloaddition pattern to give the housane product **5**. Thermolysis of **4** under vacuum strongly supports the dissociative nature of the transformation to **5**.

Acknowledgements

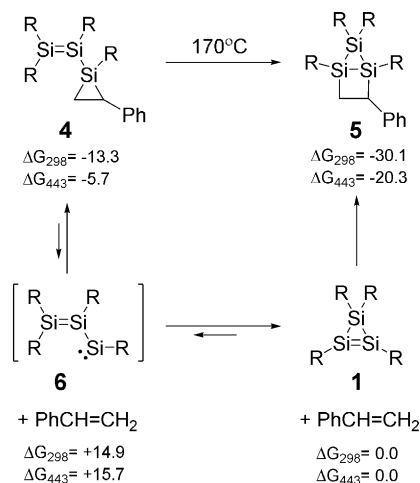
Support by Saarland University, the China Scholarship Council (Fellowship H.Z.), and COST Action CM1302 (Smart Inorganic Polymers) is gratefully acknowledged.

Conflict of interest

The authors declare no conflict of interest.

Keywords: cycloaddition · Group 14 elements · low-valent species · ring-opening · silicon

How to cite: *Angew. Chem. Int. Ed.* **2018**, *57*, 2445–2449
Angew. Chem. **2018**, *130*, 2470–2474



Scheme 4. Mechanism proposed for the formation of housane **5** from the kinetic product disilylenyl-substituted silirane **4** (R = Tip = 2,4,6-*i*-Pr₃C₆H₂; Gibb's enthalpies at the M062X/def2-SVP level of theory are given in kcal mol⁻¹).

corrected M062X/def2-SVP level of theory indeed reveal **4** to be about 16.8 kcal mol⁻¹ higher in ΔG_{298} than **5** (Scheme 4). While this difference is only slightly lowered at 443 K, dissociation of **4** to free disilylenyl silylene **6** is thermodynamically significantly more feasible ($\Delta\Delta G_{298}^{\ddagger} = +28.2$ kcal mol⁻¹ vs. $\Delta\Delta G_{443}^{\ddagger} = +21.4$ kcal mol⁻¹). According to Hammond's postulate,^[19] the kinetics of an equilibrium between **1** and **4** under these conditions ($\Delta\Delta G_{443}^{\ddagger} = +5.7$ kcal mol⁻¹) can be approximated by the energy of the transient intermediate **6**.

In conclusion, with species with one isolated carbonyl group cyclotrisilene **1** undergoes formal [2+2] cycloaddition to give housanes **2a,b**. In contrast, the reaction with less-polar double bonds of benzil and styrene at room temperature likely proceeds via ring-opening to transient disilylenyl silylene

- [1] a) M. Kosa, M. Karni, Y. Apeloig, *J. Chem. Theory Comput.* **2006**, *2*, 956–964; b) B. Pintér, A. Olasz, K. Petrov, T. Veszprémi, *Organometallics* **2007**, *26*, 3677–3683.
- [2] a) T. Iwamoto, C. Kabuto, M. Kira, *J. Am. Chem. Soc.* **1999**, *121*, 886–887; b) T. Iwamoto, M. Tamura, C. Kabuto, M. Kira, *Science* **2000**, *290*, 504–506; c) M. Ichinohe, T. Matsuno, A. Sekiguchi, *Angew. Chem. Int. Ed.* **1999**, *38*, 2194–2196; *Angew. Chem.* **1999**, *111*, 2331–2333; d) K. Uchiyama, S. Nagendran, S. Ishida, T. Iwamoto, M. Kira, *J. Am. Chem. Soc.* **2007**, *129*, 10638–10639; e) V. Y. Lee, H. Yasuda, A. Sekiguchi, *J. Am. Chem. Soc.* **2007**, *129*, 2436–2437; f) K. Leszczyńska, K. Abersfelder, A. Mix, B. Neumann, H. G. Stammler, M. J. Cowley, P. Jutzi, D. Scheschkewitz, *Angew. Chem. Int. Ed.* **2012**, *51*, 6785–6788; *Angew. Chem.* **2012**, *124*, 6891–6895; g) A. Tsurusaki, J. Kamiyama, S. Kyushin, *J. Am. Chem. Soc.* **2014**, *136*, 12896–12898.
- [3] a) V. Y. Lee, M. Ichinohe, A. Sekiguchi, *Chem. Lett.* **2001**, *30*, 728–729; b) M. J. Cowley, Y. Ohmori, V. Huch, M. Ichinohe, A. Sekiguchi, D. Scheschkewitz, *Angew. Chem. Int. Ed.* **2013**, *52*, 13247–13250; *Angew. Chem.* **2013**, *125*, 13489–13492.
- [4] a) V. Y. Lee, S. Miyazaki, H. Yasuda, A. Sekiguchi, *J. Am. Chem. Soc.* **2008**, *130*, 2758–2759; b) Y. Ohmori, M. Ichinohe, A. Sekiguchi, M. J. Cowley, V. Huch, D. Scheschkewitz, *Organometallics* **2013**, *32*, 1591–1594.
- [5] V. Y. Lee, O. A. Gapurenko, S. Miyazaki, A. Sekiguchi, R. M. Minyaev, V. I. Minkin, H. Gornitzka, *Angew. Chem. Int. Ed.* **2015**, *54*, 14118–14122; *Angew. Chem.* **2015**, *127*, 14324–14328.
- [6] R. Singh, C. Czekelius, R. R. Schrock, *Macromolecules* **2006**, *39*, 1316–1317.
- [7] M. J. Cowley, V. Huch, H. S. Rzepa, D. Scheschkewitz, *Nat. Chem.* **2013**, *5*, 876–879.
- [8] Recent Reviews (Si=Si): a) C. Präsang, D. Scheschkewitz, *Chem. Soc. Rev.* **2016**, *45*, 900–921; b) T. Iwamoto, S. Ishida, *Struct. Bonding (Berlin)* **2014**, *156*, 125–202; c) D. Scheschkewitz, *Chem. Lett.* **2011**, *40*, 2–11; d) V. Y. Lee, A. Sekiguchi, J. Escudé, H. Ranaivonjatovo, *Chem. Lett.* **2010**, *39*, 312–318; e) D. Scheschkewitz, *Chem. Eur. J.* **2009**, *15*, 2476–2485; f) M. Kira, T. Iwamoto, *Adv. Organomet. Chem.* **2006**, *54*, 73–148.

- [9] V. Y. Lee, M. Ichinohe, A. Sekiguchi, *Chem. Commun.* **2001**, 2146–2147.
- [10] CCDC 1586039 (**2a**), 1586040 (**2b**), 1586041 (**3**), 1586042 (**4**), 1586043 (**5**) contain the supplementary crystallographic data for this paper. These data can be obtained free of charge from The Cambridge Crystallographic Data Centre.
- [11] Examples see: a) I. Masayuki, A. Wataru, *J. Chem. Soc. Chem. Commun.* **1979**, 655–656; b) J. Heinicke, B. Gehrhus, *J. Organomet. Chem.* **1992**, 423, 13–21; c) H. G. Stammler, B. Neumann, A. Moehrke, E. A. Bunte, D. Eikenberg, P. Jutzi, *Organometallics* **1996**, 15, 1930–1934; d) B. Gehrhus, P. B. Hitchcock, M. F. Lappert, *Organometallics* **1997**, 16, 4861–4864; e) S. Meinel, J. Heinicke, *J. Organomet. Chem.* **1998**, 561, 121–129; f) R. Azhakar, R. S. Ghadwal, H. W. Roesky, J. Hey, D. Stalke, *Organometallics* **2011**, 30, 3853–3858; g) S. Ishida, K. Uchida, T. Iwamoto, *Heteroat. Chem.* **2014**, 25, 348–353.
- [12] P. P. Power, *Chem. Rev.* **1999**, 99, 3463–3503.
- [13] a) S. Boomgaarden, W. Saak, M. Weidenbruch, *Organometallics* **2001**, 20, 2451; b) I. Bejan, D. Güclü, S. Inoue, M. Ichinohe, A. Sekiguchi, D. Scheschkewitz, *Angew. Chem. Int. Ed.* **2007**, 46, 3349–3352; *Angew. Chem.* **2007**, 119, 3413–3416; c) K. K. Milnes, L. C. Pavelka, K. M. Baines, *Chem. Soc. Rev.* **2016**, 45, 1019–1035.
- [14] a) D. Wendel, W. Eisenreich, C. Jandl, A. Poethig, B. Rieger, *Organometallics* **2016**, 35, 1–4; b) D. Wendel, A. Porzelt, F. A. D. Herz, D. Sarkar, C. Jandl, S. Inoue, B. Rieger, *J. Am. Chem. Soc.* **2017**, 139, 8134–8137.
- [15] K. Abersfelder, D. Scheschkewitz, *J. Am. Chem. Soc.* **2008**, 130, 4114–4121.
- [16] a) U. Weidner, A. Schweig, *J. Organomet. Chem.* **1972**, 39, 261–266; b) T. J. Barton, P. Boudjouk, *Silicon-Based Polymer Science* **1989**, 224, 3–46; c) M. Driess, R. Janoschek, *J. Mol. Struct.* **1994**, 313, 129–139; d) S. Inoue, M. Ichinohe, A. Sekiguchi, *J. Am. Chem. Soc.* **2008**, 130, 6078–6079; e) I. V. Alabugin, K. M. Gilmore, P. W. Peterson, *Wiley Interdiscip. Rev.: Comput. Mol. Sci.* **2011**, 1, 109–141.
- [17] R. Rodriguez, D. Gau, T. Kato, N. S. Merceron, A. D. Cózar, F. P. Cossío, A. Baceiredo, *Angew. Chem. Int. Ed.* **2011**, 50, 10414–10416; *Angew. Chem.* **2011**, 123, 10598–10600.
- [18] F. Lips, J. C. Fettinger, A. Mansikkamäki, H. M. Tuononen, P. P. Power, *J. Am. Chem. Soc.* **2014**, 136, 634–637.
- [19] Endothermic reactions proceed via a product-like transition state: G. S. Hammond, *J. Am. Chem. Soc.* **1955**, 77, 334–338.

Manuscript received: November 17, 2017

Revised manuscript received: January 4, 2018

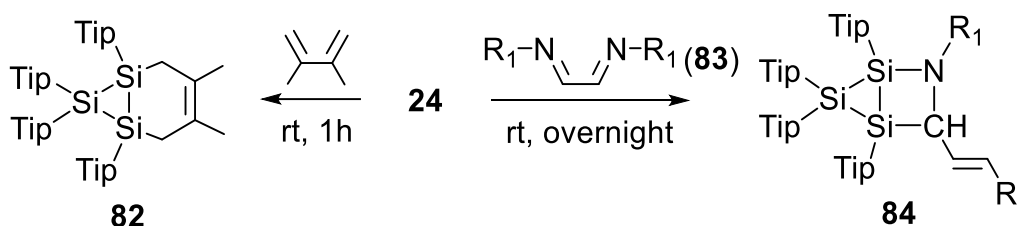
Accepted manuscript online: January 5, 2018

Version of record online: February 8, 2018

3.2 Supplementary Results

3.2.1 [2+2] and [2+4] Cycloaddition

In contrast to the reaction of cyclotrisilene **3** with 2-methyl-1,3-butadiene, which needs severe condition to produce [2+4] cyclic adduct **34**,⁶⁴ the reaction between **24** and 2,3-dimethyl-1,3-butadiene proceeds smoothly even at room temperature with the complete consumption of the starting materials in one hour. New signal appear in the ²⁹Si NMR spectrum at -46.6 ppm. After workup pale-yellow crystals of **82** are isolated in 80% yield from toluene solution (Scheme 44). Based on the 2D ¹H/²⁹Si correlation spectrum, the signal at -46.6 ppm can be assigned to the SiTip₂ unit, however, absence of signals of bridgehead silicon atoms could probably be due to signal broadening by a dynamic process related to the hindered rotation of the Tip group at SiTip₂ unit. Similar ²⁹Si NMR behavior is also observed in other cycloaddition adducts such as **41** and **59**.



Scheme 44. [2+4]/[2+2] cycloaddition of **24** with 1,3-butadiene and diimine yields adduct **82** and **84**, respectively (R₁ = Dip).

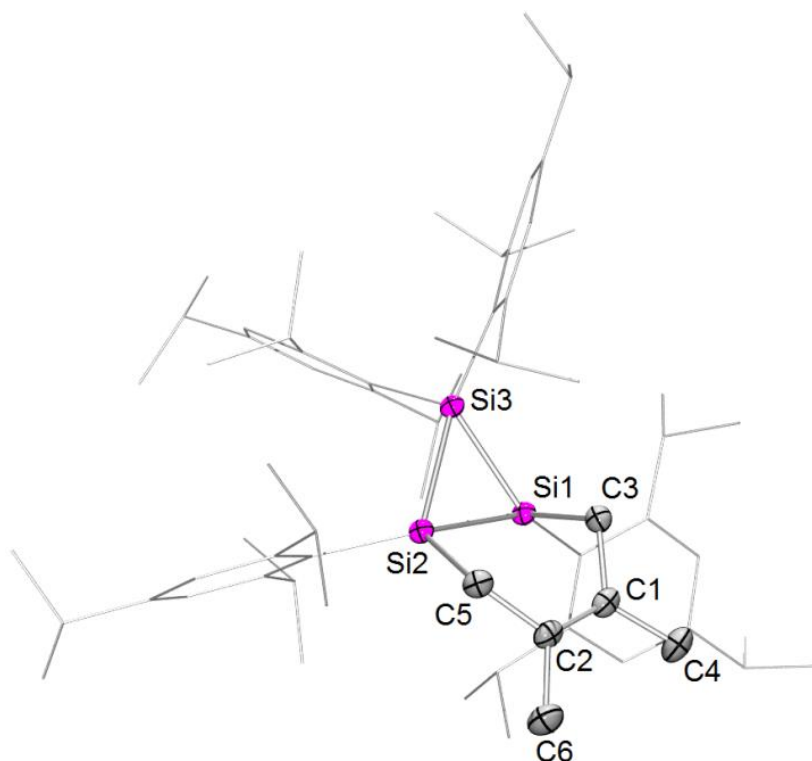


Figure 7. Molecular structure of **82**·C₇H₈ in solid state. Hydrogen atoms the co-crystallized toluene molecule are omitted for clarity. Thermal ellipsoid at 50%. Selected bond lengths [Å] and angles [°]: Si1-Si2 2.384(9), Si1-Si3 2.311(9), Si2-Si3 2.435(9), Si1-C3 1.914(2), Si2-C5 1.932(2), C1-C3 1.503(3), C2-C5 1.510(3), C1-C2 1.333(3); Si3-Si1-Si2 62.4(3), Si1-Si2-Si3 57.3(2), Si2-Si3-Si1 60.2(3), Si1-C3-C1 109.0(2), C3-C1-C4 115.6(2), C5-C2-C6 115.0(3).

X-ray single crystal structure analysis confirmed the constitution of **82** as a [2+4] bicyclic adduct composed of three- and six-membered rings (Figure 7), in which the Si-Si bond lengths (2.311(9) to 2.435(9) Å) lie within the normal Si-Si single bond range⁹² and the C1-C2 bond length 1.333(3) Å being in accordance with the typical range of C=C double bond length.⁹³ The bond distortion along C5-Si2-Si1-C3 being $\psi = 23.5(1)^\circ$. Interestingly, the two Tip groups attached to the bridgehead silicon atoms are unequally distorted with respect to the vector of Si1-Si2 with a distortion angle $\varphi_{\text{Si1}} = 75.0(3)^\circ$ and $\varphi_{\text{Si2}} = 66.2(4)^\circ$.

Since the reactivity of cyclotrisilene towards ketone and benzil indicates less polarized reagent might promote the ring-opening process,⁶⁸ the reaction of cyclotrisilene with diimine was also attractive. Indeed, after **24** and one equivalent of diimine **83** were mixed and dissolved in C₆D₆ at room temperature, ¹H NMR spectrum

showed signals of starting materials decreased slowly and disappeared completely over the course of one day. The appearance of new signals at 42.6, 17.3, -62.2 ppm in a ratio of 1:1:1 suggested the formation of a bicyclic housane derivative. Indeed, the housane derivative **84** is preparatively obtained as yellow crystals from a repeat reaction in benzene and workup of the reaction mixture (crystallization from a hydrocarbon solvent). UV/vis spectroscopy showed the longest absorption wavelength at λ_{max} 353 nm (ϵ 8376 L mol⁻¹ cm⁻¹).

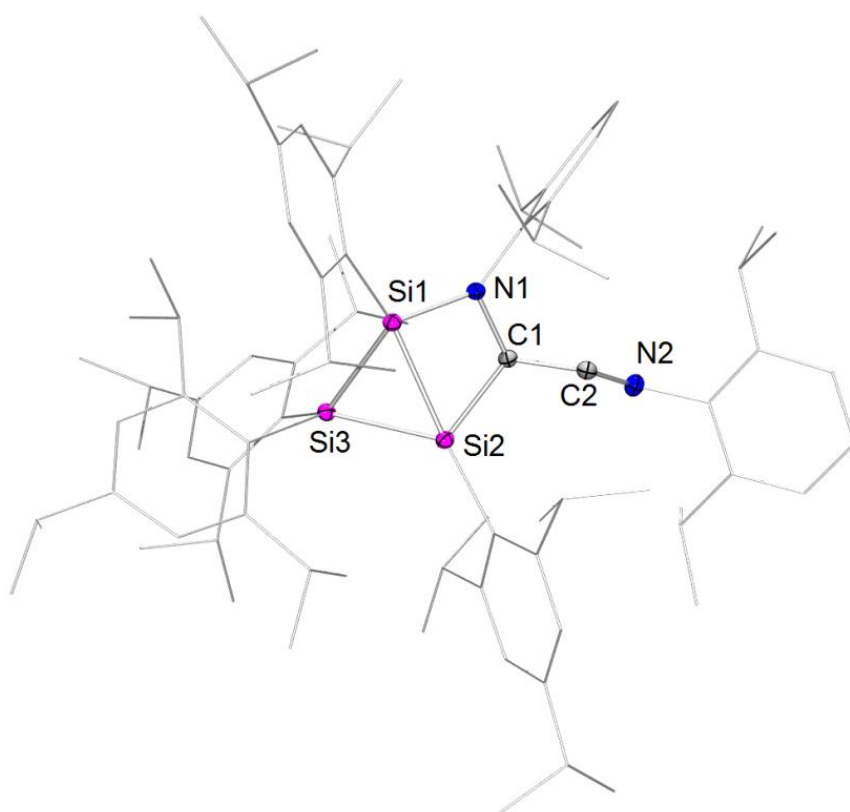


Figure 8. Molecular structure of **84** in solid state. Hydrogen atoms are omitted for clarity. Thermal ellipsoid at 30%. Selected bond lengths [Å] and angles [°]: Si1-Si2 2.389(0), Si2-Si3 2.316(1), Si1-Si3 2.428(1), Si1-N1 1.744(0), Si2-C1 1.992(0), C1-N1 1.495(0), C1-C2 1.488(0), C2-N2 1.265(0); Si3-Si1-N1 115.0(2), Si3-Si2-C1 105.4(2), N1-C1-C2 111.9(2), C1-C2-N2 121.9(3).

X-ray crystal structure analysis revealed the fused three- and four-membered ring structure of **84** (Figure 8), wherein the four-membered ring is not planar with a deviation of N atom from the plane Si1-Si2-C1 being 0.218 Å. The angle between the plane of Si1-Si2-Si3 and Si1-Si2-C1 is 120.1° and the distortion angle of the two Tip

groups attached to the bridgehead silicon atoms with respect to the vector of Si1-Si2 is $\varphi_{\text{Si1}} 84.3(5)^\circ$ and $\varphi_{\text{Si2}} 75.6(3)^\circ$. The ^{13}C NMR spectrum of **84** exhibits signals of C1 and C2 at δ 68.5 and 168.2 ppm, respectively. According to the 2D $^1\text{H}/^{13}\text{C}$ HMQC spectrum, the signal of the proton attached to C1 of the four-membered ring is observed at δ 6.17 ppm as a doublet (Figure 9). The signal at δ -62.2 ppm in the ^{29}Si NMR spectrum is assigned to SiTip_2 unit while other relative downfield signals at δ 42.6 and 17.3 ppm are attributed to SiTipCH and SiTipN , respectively.

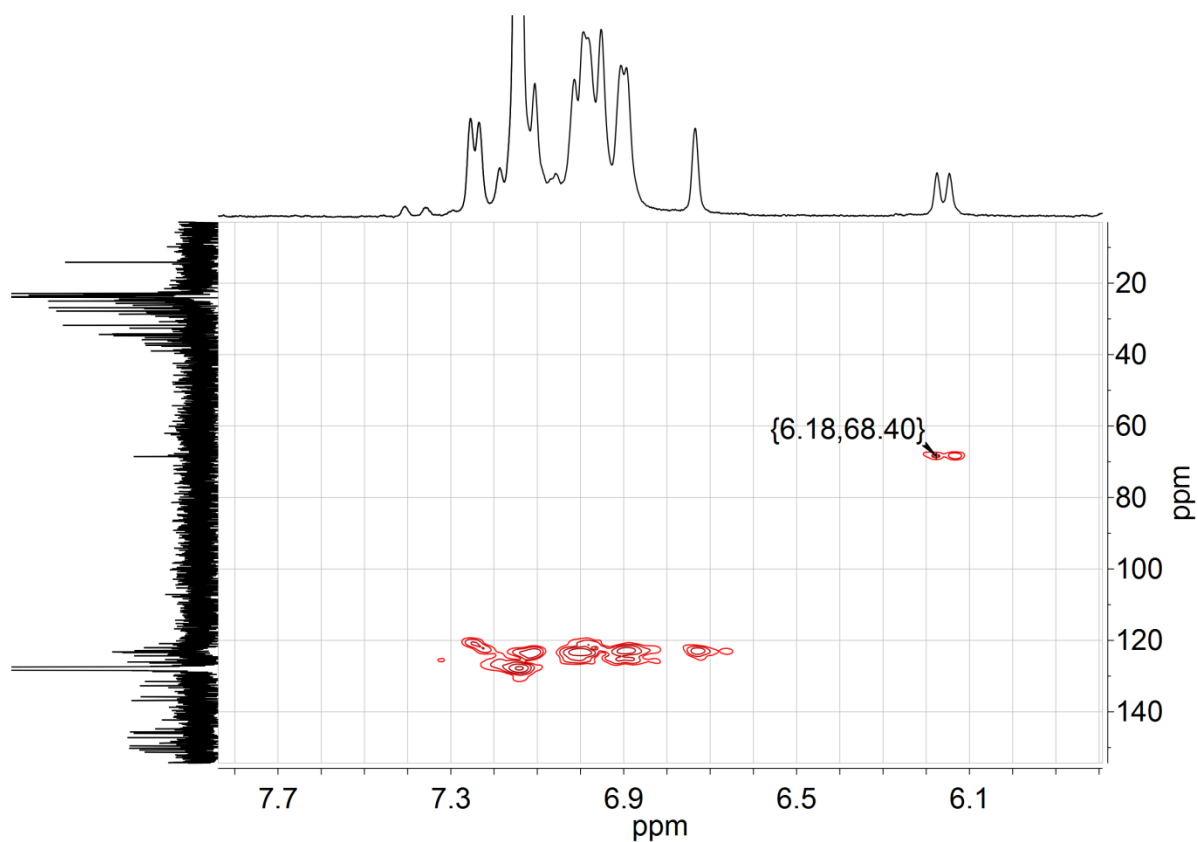
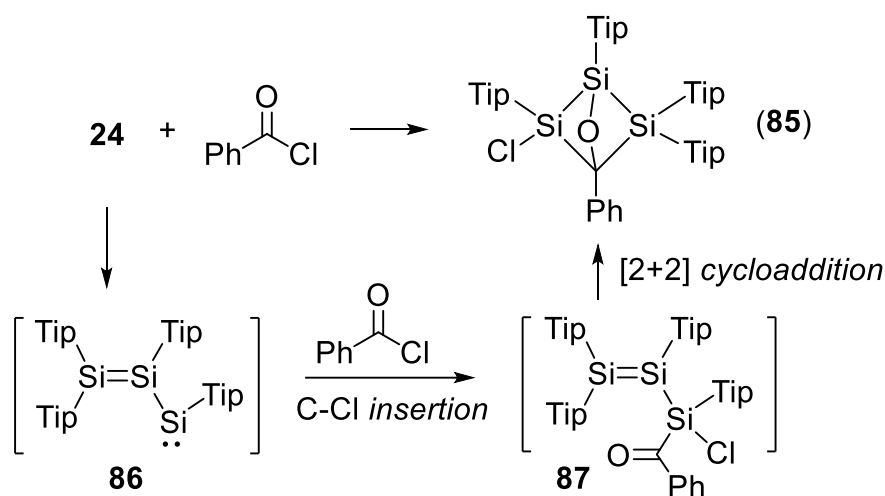


Figure 9. 2D $^1\text{H}/^{13}\text{C}$ HMQC spectrum (C_6D_6 , 300 K) of **84**.

3.2.2 Reaction of cyclotrisilene with benzoyl chloride

The reaction of **24** with benzoyl chloride proceeds smoothly at $-80\text{ }^{\circ}\text{C}$, even faster than the reaction of it with ketones which are typically complete within two hours at room temperature. When benzoyl chloride was introduced via microsyringe into the solution of **24** in toluene, an immediate reaction is indicated by the color change from orange to brown. The reaction mixture was stirred at $-80\text{ }^{\circ}\text{C}$ for 15 minutes until no further color change was observed. After removal of toluene and addition of hexane, the resulting colored solution was kept at room temperature. Pure colorless crystals suitable for X-ray crystal structure analysis deposited and were isolated by solvent decantation in 65% yield. X-ray structure analysis confirmed the constitution of **85** as a trisilabicyclo[1.1.1]pentane composed of silicon and oxygen as bridging atoms (Scheme 45).



Scheme 45. Reaction of **24** with benzoyl chloride yields **85**.

The formation of **85** could readily be explained through the ring-opening to disilylenyl silylene **86** triggered by the polarized benzoyl chloride, which then rapidly reacts with **86** in a C-Cl insertion manner to afford disilylenyl acylsilylene **87** followed by formal [2+2] cycloaddition of Si=Si and C=O double bond (Scheme 45). Insertion of the C-Cl bond of acyl chlorides into dialkyl- silylene and stannylene resulting in corresponding acylsilylene and acylstannane was previously reported by Kira *et al.*⁹⁴⁻⁹⁵ The

intramolecular isomerization of acyl disilene to silene was also reported by Scheschkewitz *et al.*⁹⁶

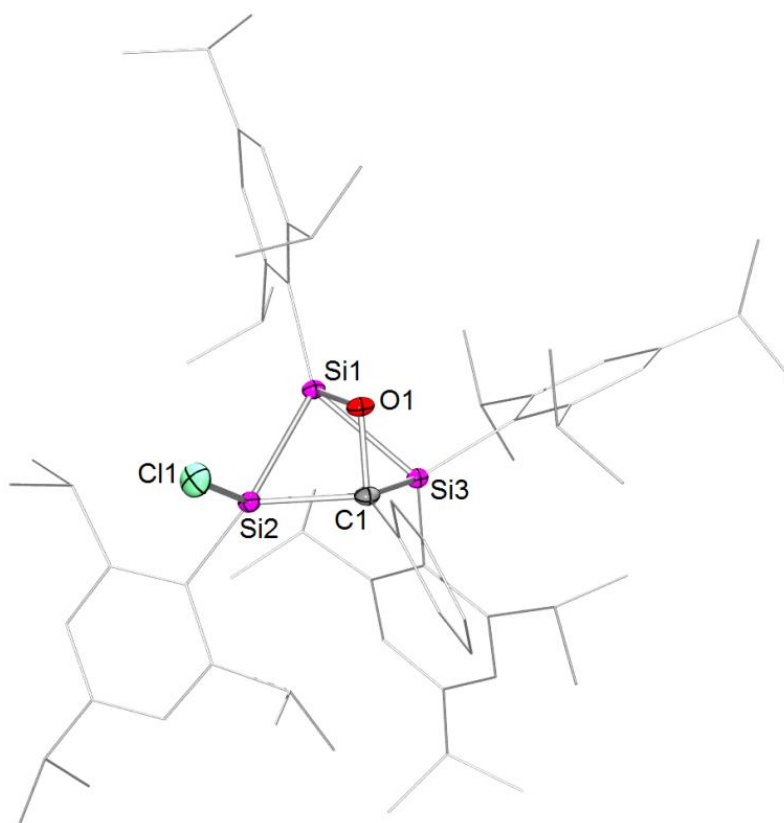


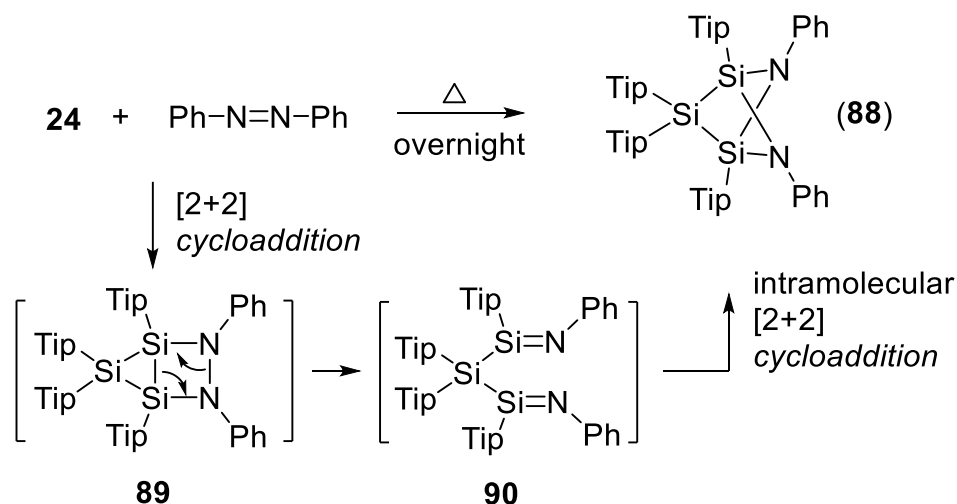
Figure 10. Molecular structure of **85**·C₆H₁₄ in solid state. Hydrogen atoms and the co-crystallized hexane molecule are omitted for clarity. Thermal ellipsoid at 50%. Selected bond lengths [Å] and angles [°]: Si1-Si2 2.344(7), Si1-Si3 2.370(7), Si2-C1 2.003(2), Si3-C1 1.971(2), Si2-Cl1 2.085(7), Si1-O1 1.725(1), C1-O1 1.499(2); Si1-O1-C1 94.0(9), Si2-Si1-Si3 84.2(2), Si2-Si1-O1 74.8(4), O1-C1-Si3 92.1(1).

²⁹Si NMR spectrum of **85** displays three signals at δ 39.3, 15.1 and -6.2 ppm, of which the upfield signal at δ -6.2 ppm is attributed to *SiTip*₂ and the relative downfield signals at δ 39.3 and 15.1 ppm are assigned to *SiTip*_O and *SiTip*_C, respectively. In the molecular structure of **85** (Figure 10), both Si2-Cl1 vector and the bridging oxygen atom point backwards from the plane of Si1-Si2-C1. The interplanar angles of the plane Si1-O1-C1 with respect to the planes of Si1-Si2-C1 and Si1-Si3-C1 are identical with 118.4(9)°. All Si-Si and Si-C bond lengths in the skeleton of **85** fall within the normal single bond length range. The phenyl group is distorted from the plane of Si1-O1-C1 with the angle of $\varphi_{C1} = 22.4(2)^\circ$, the corresponding angle of the opposite

Tip group is $\varphi_{\text{Si1}} = 15.2(2)^\circ$.

3.2.3 Reaction with azobenzene

The reactivity of $c\text{-Si}_3\text{Tip}_4$ towards azobenzene was also examined. After **24** and azobenzene were mixed and dissolved in C_6D_6 , a ^1H NMR spectrum showed a very slow consumption of the starting materials with full conversion after three days. New signals appeared in the ^{29}Si NMR spectrum at δ 37.66 and -24.23 ppm with a ratio of 1:2. In order to promote the reaction to some extent in a repeat reaction on a preparative scale, the mixture was dissolved in toluene and heated to 60°C . Indeed, ^1H NMR spectrum showed complete disappearance of starting materials after heating the mixture to that temperature overnight. Work-up of the reaction mixture resulted in the isolation of **88** as pale-yellow crystals in 70% yield (Scheme 46). Single crystals suitable for X-ray structure analysis were obtained by recrystallization from hexane at 0°C .



Scheme 46. Reaction of **24** with azobenzene results in **88**.

Instead of the anticipated [2+2] cycloaddition product – a trisila[1.1.0]butane derivative – X-ray crystal structure analysis reveals the constitution of **88** as a diaza-trisila[1.1.1]pentane (Figure 11), probably formed through cycloaddition of Si=Si and N=N double bonds to afford **89** followed by consecutive cleavage of the bridging

Si-Si and N-N single bond, resulting in the intermediate **90** that undergoes intramolecular cycloaddition to yield **88** as final product. Skeletal Si1-Si2 2.420(5) Å and Si2-Si3 2.436(5) Å bond lengths are within the typical range of Si-Si single bonds. The distance between N1 and N2 is at 2.370(2) Å much larger than the typical N-N single bond length (ca. 1.45 Å), unambiguously confirming the complete cleavage of the N-N bond.

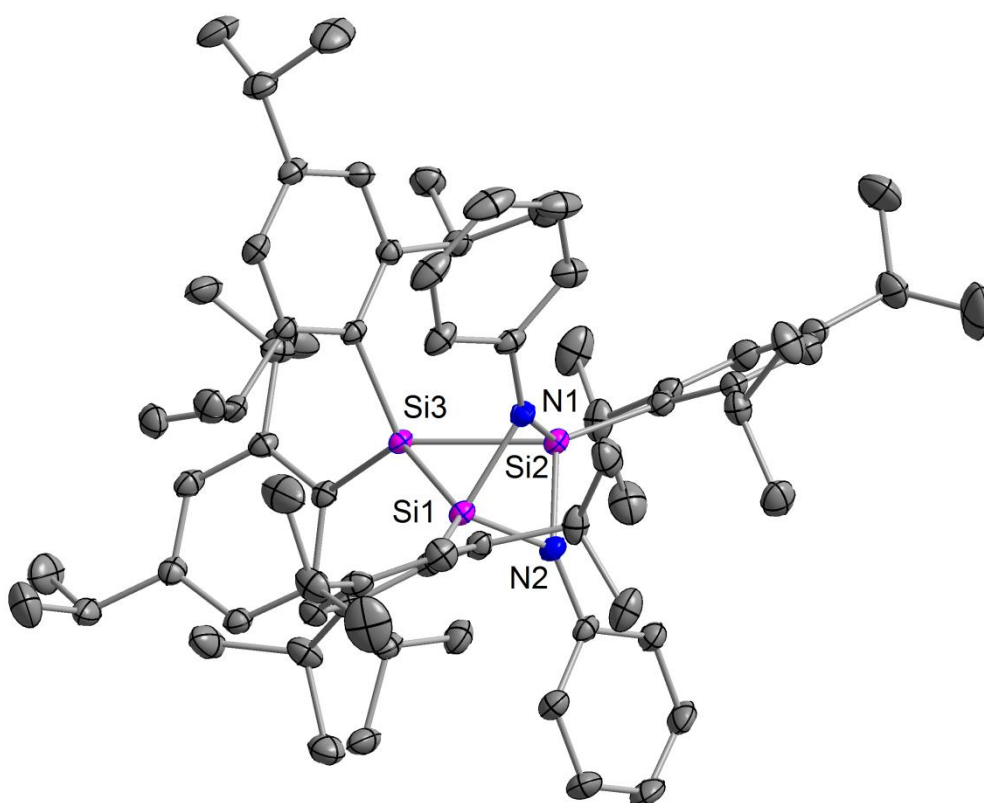


Figure 11. Molecular structure of **88**·C₅H₁₂ in solid state. Hydrogen atoms and the co-crystallized pentane molecule are omitted for clarity. Thermal ellipsoid at 50%. Selected bond lengths [Å] and angles [°]: Si1-Si3 2.420(5), Si2-Si3 2.436(5), Si1-N1 1.797(1), Si2-N1 1.782(1), Si2-N2 1.769(1), Si1-N2 1.773(1); Si1-Si3-Si2 59.2(2), Si3-Si1-N2 91.8(4), Si3-Si2-N2 91.4(4), Si1-N2-Si2 85.2(5), Si1-N1-Si2 84.1(5).

The ²⁹Si NMR signal at δ 37.66 ppm is attributed to the *S*Tip₂ unit, while the other at δ -24.23 ppm is due to the *S*Tip moiety. It is worth mentioning that the reactions of azobenzene with low-valent group 14 species, such as West's disilene,⁹⁷ alkyne analogues ArE≡EAr (E = Ge, Sn),⁹⁸ amidinate-stabilized silylsilylene,⁹⁹ in no case

resulted in the complete cleavage of the N=N double bond. Selected ^{29}Si NMR chemical shifts, structure parameters as well as physical properties of **82-88** are given in Table 4.

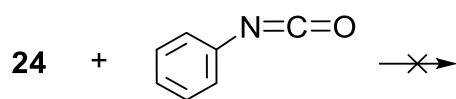
Table 4. Selected ^{29}Si NMR shifts, structure parameters as well as physical properties of **82-88**. a) ring Si-Si single bond length; b) in d_6 -benzene; c) in solid state.

	82	84	85	88
Si-Si [Å] ^a	2.384(9), 2.311(9), 2.435(9)	2.389(0), 2.316(1), 2.428(1)	2.344(7), 2.370(7)	2.420(5), 2.436(5)
$\delta^{29}\text{Si}$, ppm	2.85, -33.2, -48.23 ^c , -46.6 ^b	42.61, 17.27, -62.19 ^b	39.3, 15.1, -6.2 ^b	37.66, -24.23 ^b
color	pale yellow	yellow	colorless	pale yellow
mp. °C	175-78	> 200	139-42	> 200

3.2.4 Attempt reaction of cyclotrisilene with phenyl isocyanate

Since both cyclotrisilene **3** and **24** turned out to be highly reactive towards isocyanides⁶⁹ and, as discussed in 3.2.1 and 3.2.3, **24** also reacts with ketones, imines as well as azobenzene, we were curious about the reactivity of cyclotrisilene **24** towards isocyanate in order to gather a first idea about the selectivity of the two possible cycloadditions to the C=O and C=N moieties. Therefore phenyl isocyanate was introduced into the solution of **24** in C_6D_6 at room temperature. However, ^1H NMR spectrum of the reaction mixture showed that even after one day large amount of starting material remains. After the reaction mixture was kept at room temperature over two days, ^{29}Si NMR still showed signals of the starting material of substantial intensity. Two further sets of signals appeared at δ 33.7, 9.7, -15.1 ppm and -30.1, -15.1 and -86.8 ppm (Figure 12). Attempts to improve conversion or separate the two products by crystallization failed: either the prolongation of reaction time or increasing the reaction temperature only resulted in the increased intensity of

unidentified signals in ^{29}Si NMR spectrum.



Scheme 47. Cyclotrisilene **24** is inert towards phenyl isocyanate.

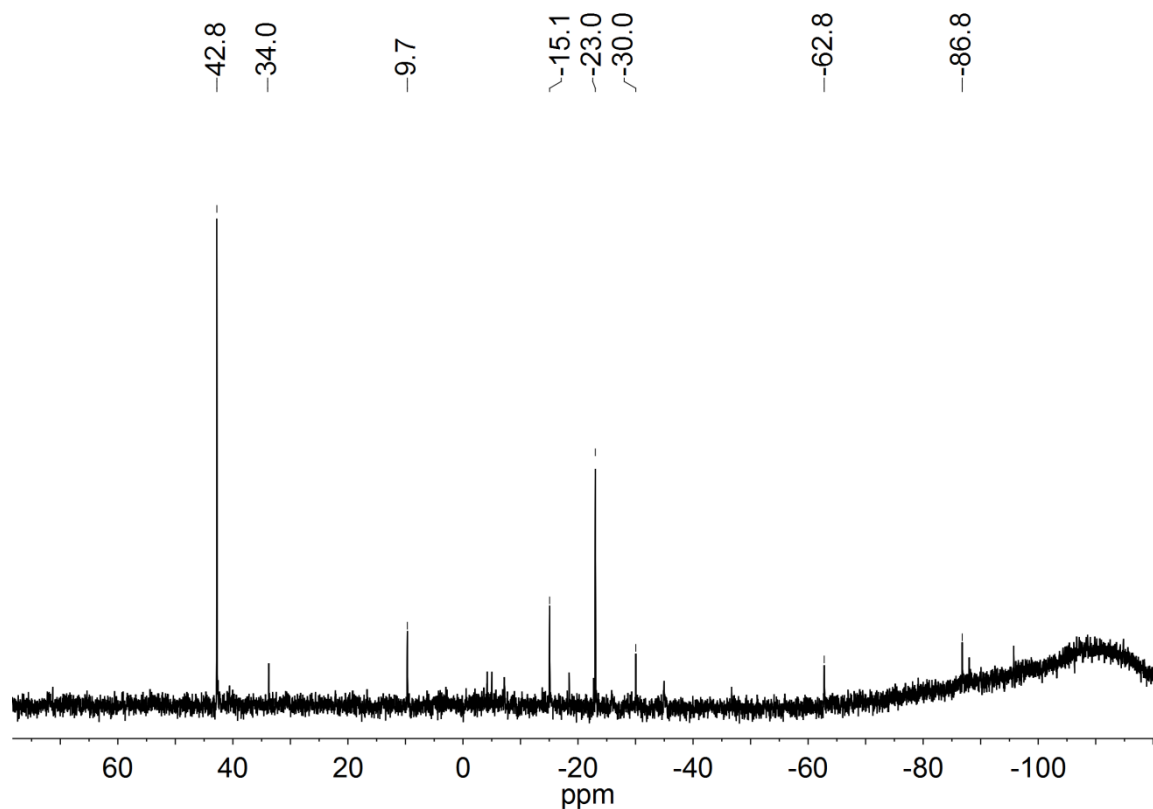


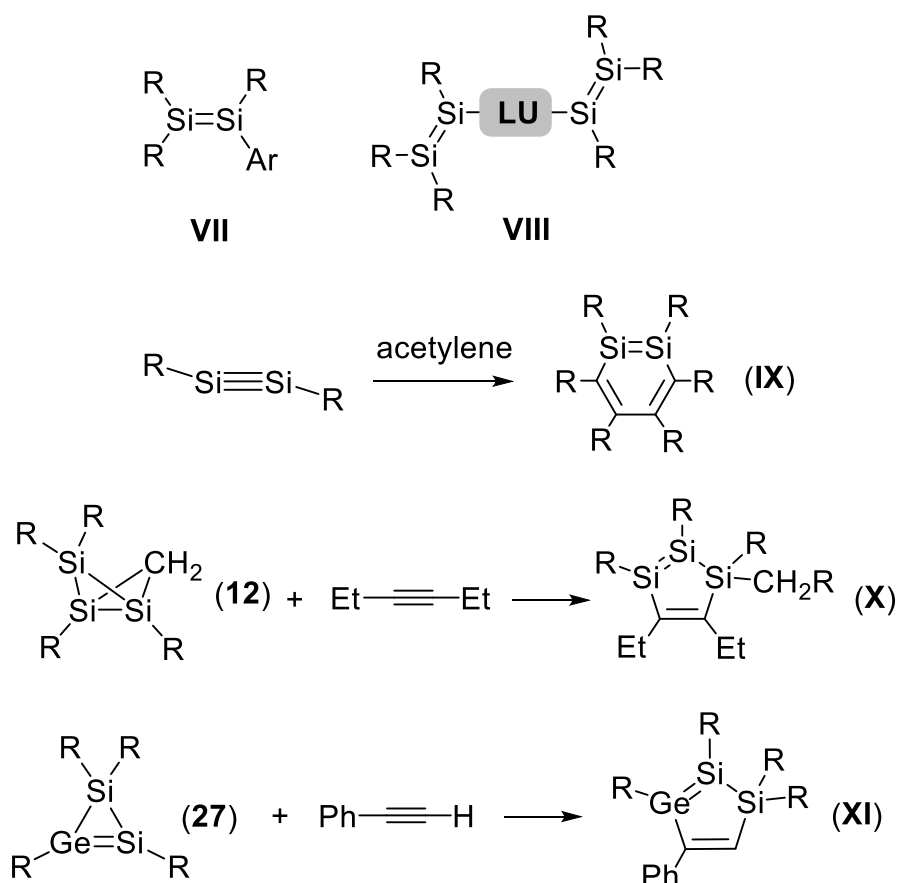
Figure 12. ^{29}Si NMR spectrum (59.6 MHz, 300 K, C_6D_6) of the reaction mixture of **24** with phenyl isocyanate.

3.3 Phenylene-Bridged

Cross-conjugated

1,2,3-Trisilacyclopentadienes

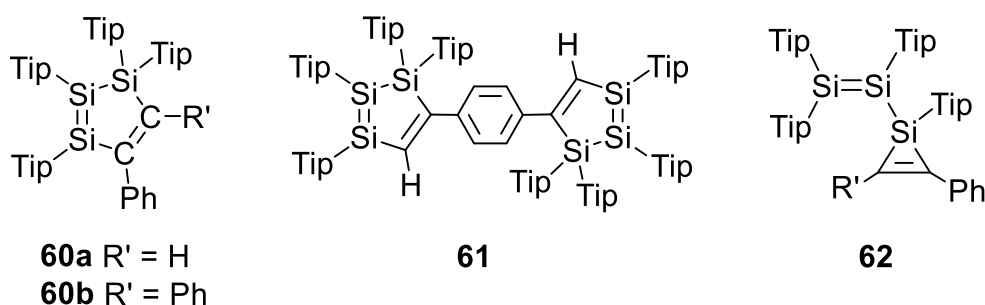
Incorporation of Si=Si double bonds into carbon-based systems has gradually moved into focus due to the markedly different chemical and physical properties of Si=Si and C=C bonds and the unique optical properties of heavier π -conjugated systems. Due to the limited synthetic options for the generation of Si=Si double bonds, disilenes of the type **VII** (Scheme 48) were only obtained at the beginning of this decade.⁸⁴ Even the incorporation of a single unhindered phenyl group as in **VII** typically result in an appreciable red-shift of the longest wavelength UV/vis absorption.^{84b,c} Electronic communication between two Si=Si moieties as in type **VIII** is effectively mediated by various aromatic linking unit, for instance, anthracenyl-bridged tetrasiladiene shows near-IR emission in the solid state.⁸⁵ Phenylene-bridged tetrasiladiene were also employed as precursors for σ,π -conjugated polymers.¹⁰⁰ In contrast, cyclic conjugated Si=Si-C=C systems are relatively rare. The 1,2-disilabenzene of type **IX** (Scheme 48), which benefit from their aromaticity, are typically accessible by reaction of disilynes $\text{RSi}\equiv\text{SiR}$ with acetylenes.⁸⁶ A formally antiaromatic benzodisilacyclobutadiene reported by Iwamoto *et al.* was also shown to be stable very recently.¹⁰¹ One of the examples of Si₃-cyclopentadiene derivative of type **X** was obtained by reaction of a 1,2,3-trisilabicyclo[1.1.0]butane derivative with an excess of hex-3-yne at elevated temperature.⁸⁷ In view of Sekiguchi's synthesis of Si₂Ge-cyclopentadiene derivative **XI** with cyclic Si-Si=Ge-C=C system from a Si₂Ge-cyclotrimetallene and phenylacetylene,⁸⁸ the intermediacy of a transient cyclotrisilene during the formation of **XI** seems plausible. Therefore we considered employing cyclotrisilene **24** under similar reaction conditions.



Scheme 48. Generic examples of molecule with conjugated Si=Si-C=C systems (LU = linking units).

Cyclotrisilene **24** was reacted with phenylacetylene, diphenylacetylene, resulting in the 1,2,3-trisilacyclopentadiene **60a,b**, respectively. The first cross-conjugated bridging of two of the Si₃C₂ cycles by a *para*-phenylene linker **61** was also achieved by reaction of **24** with 1,4-diethynyl benzene (Scheme 49). Derivatives **60-61** were fully characterized by multinuclear NMR spectroscopy, UV/vis absorption spectrum, X-ray single crystal structure analysis and elemental analysis. All three compounds show typical ²⁹Si chemical shift of the three-coordinated silicon atom at δ 111.0, 34.3 for **60a**, 106.8, 43.2 for **60b**, 109.7, 33.0 ppm for **61**. The signals of the four-coordinated silicon atoms are upfield shifted at **60a**: δ -26.8 ppm; **60b**, -19.9 ppm; **61**: -27.0 ppm. Based on the 2D ¹H/¹³C spectra, the ¹³C signals of the endocyclic C=C units are identified at δ 145.49, 160.73 ppm for **60a** and δ 146.84, 160.21 ppm for **61**. The molecular structure of **60a** and **61** were discussed in detail. In

both cases the Si1=Si2 double bond is less twisted (torsion angle $\tau = 37.2(3)^\circ$ in **60a**, $30.0(2)^\circ$ in **61**) than that of **X** (59.4°). In contrast to their carbon congeners and cyclopentadiene derivatives of Group 14 elements which have almost planar five-membered ring framework, the five-membered Si₃C₂ ring of **60a** displays an envelope conformation with a folding angle of $21.8(1)^\circ$. While the trisilacyclopentadiene moieties of **61** are close to planarity with a folding angle of only $3.2(6)^\circ$. The *para*-phenylene linker in **61** is distorted from co-planarity with the two five-membered rings by a dihedral angle of $43.1(8)^\circ$.



Scheme 49. 1,2,3-Trisilacyclopentadiene derivatives **60**, **61** and ring-opening intermediate **62**

Density functional theory (DFT) calculations at the B3LYP/6-311G(d,p) level of theory show the HOMOs of **60a,b** are delocalized across the unsaturated cyclic backbone with dominant π contributions by the Si=Si moieties and less pronounced C=C components. The LUMOs correspond to antibonding π -type orbitals with expectedly larger contributions by the carbon ring atoms. In the case of **61**, the interaction between the two 1,2,3-trisilacyclopentadiene units leads to a near-degenerate HOMO and HOMO-1 and slightly split LUMO and LUMO+1. Noticeable contributions by the *para*-phenylene spacers are observed as well. TD-DFT calculations reveal the longest absorption wavelength band of **60a** ($\lambda_{\max} = 493$ nm) and **60b** ($\lambda_{\max} = 495$ nm) mainly originates from the HOMO→LUMO transition, while the presence of no less than four transitions of comparable oscillator strength is probably responsible for the broadening of the experimental longest wavelength band of **61** ($\lambda_{\max} = 495$ nm). When compared with the cyclotrisilene starting material **24** ($\lambda_{\max} = 413$ nm), however, the

longest wavelength bands are bathochromically shifted by a significant margin of $\Delta\lambda \cong 80$ nm. This contrasts with **IVa** ($\lambda_{\max} = 493$ nm) for which the red-shift compared to the silyl-substituted cyclotrisilene precursor is much smaller ($\lambda_{\max} = 466$ nm).

A mechanistic investigation by room temperature and variable-temperature NMR allows proposing two distinct reaction pathways during the reaction of cyclotrisilene **24** with alkynes: (A) [2+2] cycloaddition followed by the intramolecular valence isomerization and (B) initial ring-opening to disilynyl silirenes followed by isomerization (Scheme 29). Due to the sterically more demanding substitution pattern in the case of diphenylacetylene, the ring-opening intermediate **62** (Scheme 49) could be detected even at room temperature with signals at δ 99.6, 43.0 and -118.5 ppm. Predicted ^{29}Si NMR shifts of **62** (calc. δ 133.23, 78.87 and -119.22 ppm) at the M06-2X(D3)/def2-TZVPP level of theory also support the postulated intermediate.

Results of the described studies have been published in the *Chemical Communications – Royal Society of Chemistry*.

Hui Zhao, Lukas Klemmer, Michael J. Cowley, Moumita Majumdar, Volker Huch, Michael Zimmer and David Scheschkewitz, Phenylene-bridged cross-conjugated 1,2,3-trisilacyclopentadienes, *Chem. Commun.*, **2018**, *54*, 8399-8402.
[DOI: 10.1039/C8CC03297A](https://doi.org/10.1039/C8CC03297A).

All people mentioned as authors made a range of effort to the publication of this paper: all experiments and the characterization of products were performed by Hui Zhao, basing on the preliminary results obtained by Michael J. Cowley and Moumita Majumdar during their post-doc period. Manuscript and supporting information of this publication was drafted by Hui Zhao. Lucas Klemmer and Hui Zhao performed the DFT calculations. Volker Huch contributed to the crystallographic data collection and refinement. Michael Zimmer made an effort to collect the VT-NMR data. David Scheschkewitz has given critical revision of the manuscript and he is the supervisor of the research. An authorship statement signed by all co-authors including more

detailed contributions of each co-author is also provided.



Cite this: *Chem. Commun.*, 2018, 54, 8399

Received 23rd April 2018,
Accepted 22nd June 2018

DOI: 10.1039/c8cc03297a

rsc.li/chemcomm

Phenylene-bridged cross-conjugated 1,2,3-trisilacyclopentadienes†

Hui Zhao,[†] Lukas Klemmer,[†] Michael J. Cowley,[‡] Moumita Majumdar,[§] Volker Huch, Michael Zimmer and David Scheschkewitz^{*,†}

1,2,3-Trisilacyclopentadienes are obtained from the reactions of cyclotrisilene $c\text{-Si}_3\text{R}_4$ ($\text{R} = \text{iPr}_3\text{C}_6\text{H}_2$) with phenyl and diphenyl acetylene, respectively. With 1,4-diethynyl benzene the cross-conjugated bridging of two of the Si_3C_2 cycles by a *para*-phenylene linker is achieved. UV/vis spectroscopy indicates a small but significant effect of cross-conjugation, which is confirmed by TD-DFT calculations. The formation mechanism of the 1,2,3-trisilacyclopentadienes is elucidated by VT NMR.

Since the first disilene was isolated by West, Michl and Fink in 1981,¹ research on species with $\text{Si}=\text{Si}$ double bonds has enormously developed.² More recently, the incorporation of $\text{Si}=\text{Si}$ bonds into carbon π -electron systems has moved into focus due to the small HOMO–LUMO gap of disilenes.^{2g} Even a single phenyl group as in **I** (Chart 1) typically results in an appreciable red-shift of the longest wavelength UV/vis absorption.³ Electronic communication between two $\text{Si}=\text{Si}$ moieties as in **II** is effectively mediated by various aromatic linking units.^{3,4} Tetrasiladienes **II** not only show interesting

photophysical properties,⁴ but were also employed as precursors for σ,π -conjugated polymers.⁵

In contrast, cyclic conjugated $\text{Si}=\text{Si}-\text{C}=\text{C}$ systems are relatively rare. 1,2-Disilabenzenes of type **III**, accessible by reaction of disilynes $\text{RSi}\equiv\text{SiR}$ with acetylenes, benefit from their aromaticity,^{6a,b} although a formally antiaromatic benzodisilacyclobutadiene was shown to be stable very recently.^{6c} Reaction of a 1,2,3-trisilabicyclo[1.1.0]butane derivative with an excess of hex-3-yne at elevated temperature unexpectedly afforded a Si_3 -cyclopentadiene derivative of type **IVa**.⁷ In view of Sekiguchi's synthesis of Si_2Ge -cyclopentadiene derivative **IVb** with cyclic $\text{Si}-\text{Si}=\text{Ge}-\text{C}=\text{C}$ system from a Si_2Ge -cyclotrimetallene and phenylacetylene,⁸ the intermediacy of a transient cyclotrisilene during the formation of **IVa** seems plausible. We therefore considered to employ cyclotrisilene **1**⁹ (Scheme 1, $\text{R} = 2,4,6\text{-iPr}_3\text{C}_6\text{H}_2$) under similar conditions. Due to its ring strain and the highly reactive $\text{Si}=\text{Si}$ bond, **1** exhibits a versatile reactivity towards various substrates.¹⁰ In the present study, we were particularly intrigued by the prospect of accessing hitherto unknown bridged species.

Indeed, treatment of cyclotrisilene **1** with one equivalent of either phenylacetylene or diphenylacetylene at ambient temperature affords the 1,2,3-trisilacyclopentadienes **2a,b** (Scheme 1), isolated from hydrocarbons as bright-red crystals in 55–60% yield. Under similar conditions, two equivalents of **1** and 1,4-diethynylbenzene, gave *para*-phenylene-bridged **3** as purple crystals in 52% yield (Scheme 1).

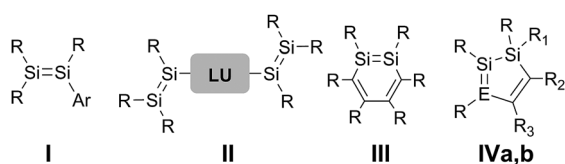


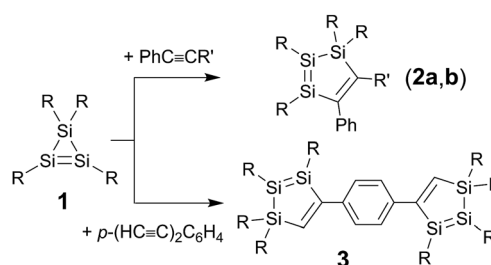
Chart 1 Generic examples **I–IVa** of molecule with conjugated $\text{Si}=\text{Si}-\text{C}=\text{C}$ system (LU = linking units; **IVa**: $\text{E} = \text{Si}$, $\text{R} = \text{SiMe}^t\text{Bu}_2$, $\text{R}_1 = \text{CH}_2\text{R}$, $\text{R}_2 = \text{R}_3 = \text{Et}$; **IVb**: $\text{E} = \text{Ge}$, $\text{R} = \text{R}_1 = \text{SiMe}^t\text{Bu}_2$, $\text{R}_2 = \text{H}$, $\text{R}_3 = \text{Ph}$).

Krupp-Chair of General and Inorganic Chemistry, Saarland University, 66123, Saarbrücken, Germany. E-mail: scheschkewitz@mx.uni-saarland.de

† Electronic supplementary information (ESI) available: Plots of NMR, optical spectra, details on X-ray structures and computations. CCDC 1835094 (**2a**), 1835095 (**2b**) and 1835096 (**3**). For ESI and crystallographic data in CIF or other electronic format see DOI: 10.1039/c8cc03297a

‡ Current address: School of Chemistry, University of Edinburgh, Edinburgh, EH9 3JJ UK.

§ Current address: Department of Chemistry, Indian Institute of Science, Education and Research (IISER), Pune-411008, India.



Scheme 1 Synthesis of **2–3** ($\text{R} = 2,4,6\text{-iPr}_3\text{C}_6\text{H}_2$; **2a**: $\text{R}' = \text{H}$, **2b**: $\text{R}' = \text{Ph}$).

In all cases, the ^{29}Si NMR shows three signals in a ratio of 1:1:1. The two downfield signals (**2a**: δ 111.0, 34.3 ppm; **2b**: 106.8, 43.2 ppm; **3**: 109.7, 33.0 ppm) are diagnostic of the Si=Si unit. The more pronounced shielding of the Si=Si nuclei in comparison to those of **IVa** (δ 166.4, 95.6 ppm)⁷ is a well-known effect of aryl vs. silyl substitution. Conversely, the signals of the saturated ring silicon atoms (**2a**: δ -26.8 ppm; **2b**, -19.9 ppm; **3**: -27.0 ppm) are shifted downfield in comparison to that of **IVb** (δ -45.6 ppm).^{8a} The 2D $^1\text{H}/^{13}\text{C}$ spectra of **2a** and **3** (ESI \dagger), allowed for the identification of the ^{13}C signals of the endocyclic C=C units at δ 145.49, 160.73 ppm for **2a** and δ 146.84, 160.21 ppm for **3**.

Single crystals of **2a,b** and **3** were investigated by X-ray diffraction (Fig. 1). \ddagger All datasets suffer from weak diffraction at higher 2θ angles, probably due to severe disorder of the *tert*-propyl substituents. The structural models of **2a** and **3** are still of sufficient quality for a discussion of bonding parameters. In both cases the Si1=Si2 double bond is less twisted (torsion angle $\tau = 37.2(3)^\circ$ in **2a**, $30.0(2)^\circ$ in **3**) in comparison to that of **IVa** (59.4°),⁷ indicating less steric repulsion between aryl substituents than between the bulky silyl groups of **IVa**. The five-membered Si₃C₂ ring of **2a** displays an envelope conformation with a folding angle between the mean planes of Si1-C2-C1-Si3 and Si1-Si2-Si3 of $21.8(1)^\circ$. This is in contrast to not only their carbon congeners,¹¹ but also most reported cyclopentadiene derivatives of Group 14 elements with their almost planar five-membered ring framework.^{7,8} While a similar deviation from planarity is also apparent in **2b** (ESI \dagger), the trisilacyclopentadiene

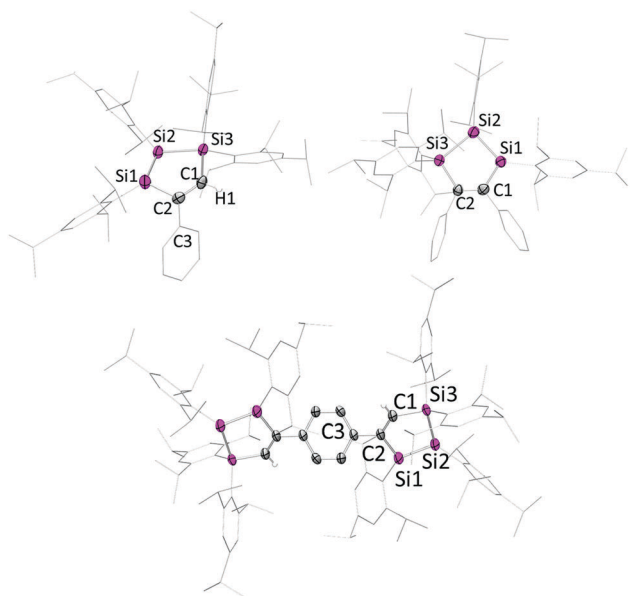


Fig. 1 Molecular structure of **2a** (top left) **2b** (top right) and **3**-C₅H₁₂ (bottom). Thermal ellipsoids at 50%. Hydrogen atoms, disorder of isopropyl groups and solvent molecules are omitted for clarity. Selected bond lengths (Å) and angles ($^\circ$): **2a** Si1–Si2 2.188(2), Si2–Si3 2.365(2), Si3–C1 1.884(5), Si1–C2 1.880(5), C1–C2 1.364(6), C2–C3 1.489(6); Si1–Si2–Si3 92.1(7), Si2–Si3–C1 96.9(2), C2–Si1–Si2 104.5(2); **3** Si1–Si2 2.150(2), Si2–Si3 2.336(2), C1–C2 1.341(4), Si1–C2 1.868(3), Si3–C1 1.878(3), C2–C3 1.480(4); Si1–Si2–Si3 94.1(6), Si2–Si3–C1 97.6(1); Si2–Si1–C2 105.5(9).

moieties of **3** are close to planarity with a folding angle of only $3.2(6)^\circ$, identical to that of **IVa** (3.2°).⁷ The *para*-phenylene linker in **3** is distorted from co-planarity with the five-membered rings by $43.1(8)^\circ$.

The 1,2,3-trisilacyclopentadienes **2a,b** and **3** show two bands in the UV/vis spectra each (λ_{abs} 493, 375 nm for **2a**; λ_{abs} 495, 356 nm for **2b**; λ_{abs} 495, 386 nm for **3**). While a pronounced red-shift with increasing conjugation path length is discernible for the lower wavelength absorption, the band at longest wavelength is almost invariant except for a certain broadening in the case of **3**. When compared with the cyclotrisilene starting material **1** ($\lambda_{\text{max}} = 413$ nm),⁹ however, the longest wavelength bands (Fig. 2, λ_{max} : **2a** 493 nm, **2b** 495 nm, **3** 495 nm) are bathochromically shifted by a significant margin of $\Delta\lambda \cong 80$ nm. This is in contrast to **IVa** ($\lambda_{\text{max}} = 493$ nm),⁷ for which the red-shift of 27 nm compared to the silyl-substituted cyclotrisilene precursor is much smaller.¹²

In order to gain more insight into the π conjugation features of **2a,b** and **3**, density functional theory (DFT) calculations at the B3LYP/6-311G(d,p) level of theory¹³ were performed. The optimized structures (calc. $d_{\text{Si=Si}}$ 2.187 in **2a**, 2.173 Å in **3**; $d_{\text{C=C}}$ 1.354 in **2a**, 1.361 Å in **3**) are in good agreement with the experimental data (Fig. 1). The HOMOs of **2a,b** (**2a**: Fig. 3, for **2b** see ESI \dagger) are delocalized across the unsaturated cyclic backbone with dominant π contributions by the Si=Si moieties and less pronounced C=C components. The LUMOs correspond to antibonding π orbitals with expectedly larger contributions by the carbon ring atoms. In the case of **3**, the interaction between the two 1,2,3-trisilacyclopentadiene units leads to a near-degenerate HOMO and HOMO-1 (0.0013 eV) and slightly split LUMO and LUMO+1 (0.0067 eV, Fig. 3c–f). Although primarily located at one of the five-membered rings, there are noticeable contributions by the *para*-phenylene spacer as well. Time-dependent DFT (TD-DFT) calculations reproduce the trends of the experimental UV/vis spectra of **2a,b** reasonably well even though the calculated longest wavelength absorption is a little overestimated in both cases (calc. $\lambda_{\text{max}} = 508$ nm for

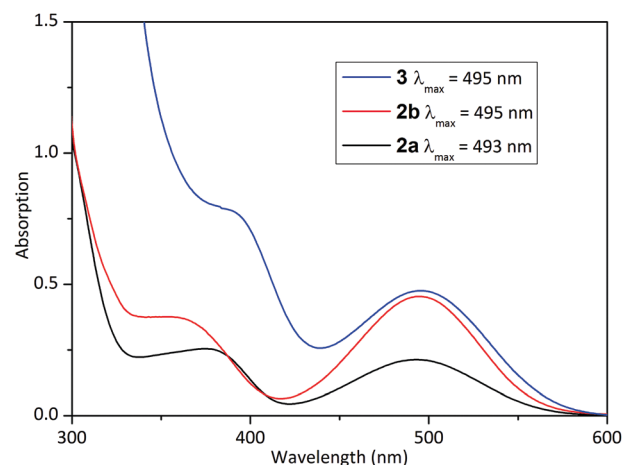


Fig. 2 UV/vis absorption spectra of **2a** (black), **2b** (red) and **3** (blue) in hexane (0.0008 M) at 25 $^\circ\text{C}$.

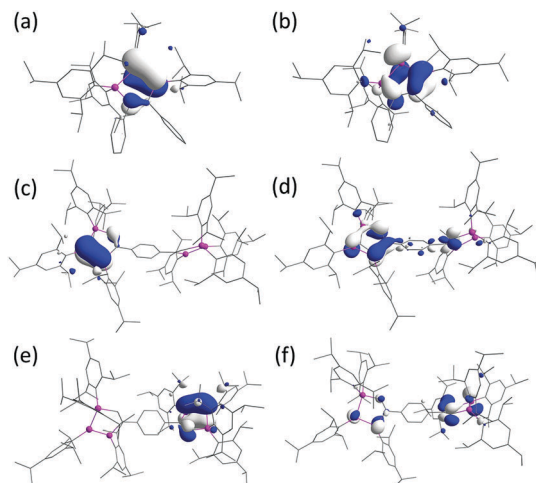
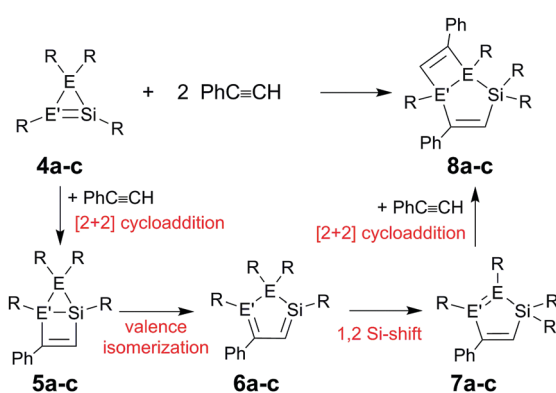


Fig. 3 HOMOs (a, **2a**; c, e, HOMO and HOMO–1 of **3**) and LUMOs (b, **2a**; d, f, LUMO and LUMO+1 of **3**) at the B3LYP/6-311G(d,p) level of theory (isosurface = 0.04 a.u.).

2a, 519 nm for **2b**). In contrast, the calculated lowest energy band of **3** (calc. λ_{\max} = 543) differs substantially from the experimental value by a red-shift of $\Delta\lambda$ = 48 nm. The presence of no less than four transitions of comparable oscillator strength (HOMO \rightarrow LUMO 543, HOMO–1 \rightarrow LUMO 530, HOMO \rightarrow LUMO+1 481, HOMO–1 \rightarrow LUMO+1 478 nm) is probably responsible for the broadening of the experimental longest wavelength band of **3**, prohibiting its accurate read-out (for the second longest wavelength absorptions see ESI[†] Tables S4–S6).

For the reactions of silyl-substituted Si₂Ge- and Si₃-cyclo-trimetalenes **4a–c** with phenylacetylene, an initial [2+2] cycloaddition to give the intermediate housane derivatives **5a–c** was proposed by Sekiguchi *et al.* (Scheme 2).^{8a,b,14} Valence isomerization to trimetalla-cyclopentadienes **6a–c** with an E'=C bond and silyl migration would give the corresponding E'=E isomers **7a–c**, which in turn could react with excess phenyl acetylene to yield **8a–c**. Although **5b** had been detected by NMR spectroscopy and isomers **7b,c** were even isolated, in

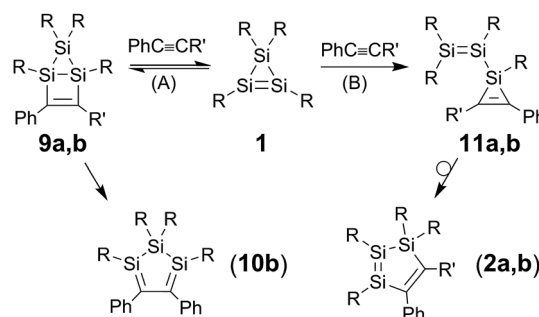


Scheme 2 Formation mechanism of heavier cyclopentadienes as proposed by Sekiguchi *et al.*^{8,14} (R = ^tBu₂MeSi, **a**: E=E'=Si; **b**: E=Ge, E'=Si; **c**: E=Si, E'=Ge).

the case of **4a** none of the intermediates were confirmed experimentally. Moreover, neither reaction of **4b** with diphenylacetylene nor with styrene was observed.^{8b} In marked contrast to **4b**, cyclotrisilene **1** reacts smoothly with styrene^{10a} and – as we show here – with diphenylacetylene under mild conditions. In order to clarify the mechanistic differences between cyclotrisilenes **1** and **4a–c** regarding the reaction with alkynes, the reaction of **1** with phenylacetylene was monitored by ²⁹Si NMR at variable temperature.

At 216 K, three high-field signals in the typical range for cyclotrisilanes¹⁵ start appearing at δ –23.4, –60.0 and –73.5 ppm. Two of these signals are similar to the bridgehead silicon signals of intermediate **5b** (–65.0, –84.1 ppm) in line with the mechanism proposed by Sekiguchi.^{8a,b} At 236 K the signals of **2a** (δ 111.9, 34.3, –26.8 ppm) start growing in until at 276 K only signals of **2a** and residual cyclotrisilene **1** remain (see ESI[†]). Conversely, a mixture of **1** and one equivalent of diphenylacetylene reveals three ²⁹Si NMR signals at δ 99.6, 43.0 and –118.5 ppm after 20 minutes at ambient temperature. The two downfield signals at δ 99.6 and 43.0 ppm are attributed to an Si=Si unit different from that of **2b**, while the upfield signal at δ –118.5 ppm is characteristic for a three-membered silirene ring.¹⁶ We thus propose disilanyl silirene **11b** as initial product, similar to the recently reported isolated intermediate from the reaction of **1** with styrene.^{10a} Predicted ²⁹Si NMR shifts of **11b** (calc. δ 133.23, 78.87 and –119.22) at the M06-2X(D3)/def2-TZVPP level of theory support the postulated intermediate (the chemical shifts of low coordinate silicon atoms are routinely overestimated by DFT methods). As the reaction proceeds, signals of **2b** (δ 106.8, 43.2, –19.9 ppm) grow in at the expense of those of **11b**. In addition, a minor product with signals at δ 61.8, 4.2 and –13.8 ppm is observed in the final reaction mixture (see ESI[†]).

Considering the higher migration tendency of silyl compared to aryl groups,¹⁷ we propose that unlike in the case of **4a**, two distinct reaction pathways are active during the reaction of cyclotrisilene **1** with alkynes: (A) a [2+2] cycloaddition yields housanes of type **9** followed in case of **9b** by the intramolecular valence isomerization to **10b** and (B) initial ring-opening to disilanyl silirenes **11** (Scheme 3). In the case of phenylacetylene, the reaction pathway of type A prevails at 216 K with reversible formation of the [2+2] product, housane **9a** (Scheme 3). The principal possibility of reversible reaction of Si=Si double bond



Scheme 3 Proposed mechanism of formation of **2a,b** with side product **10b** (R = Tip = *i*Pr₃C₆H₂; **a**: R' = H, **b**: R' = Ph).

has been reported recently.^{10f,18} With increasing temperature, ring-opening to disilanyl silirene **11a** is proposed to occur although in this case it could not be detected, presumably due to rapid rearrangement to the final product **2a**. Due to the sterically more demanding substitution pattern in the case of diphenylacetylene, the intermediate **11b** isomerizes to **2b** in a sufficiently slow manner allowing detection even at room temperature. The minor signals at δ 61.8 and -13.8 ppm in a ratio of 2 : 1 are tentatively assigned to cyclic bis(silene) **10b**, which would plausibly result from valence isomerization by cleavage of the Si–Si bridge in **9b** (Scheme 3). The calculated ²⁹Si NMR chemical shifts of the optimized structure of **10b** support the assignment: the signal of the tetracoordinate *S*Tip₂ unit at $\delta_{\text{calc.}}$ -9.8 ppm shows a good agreement with the experiment, while those of the tricoordinate Si atoms ($\delta_{\text{calc.}}$ 91.5 and 99.1 ppm) are once again overestimated.

In summary, we have prepared 1,2,3-trisilacyclopentadienes (**2a,b**) and – for the first time – a bridged bis(1,2,3-trisilacyclopentadiene) (**3**). The UV-vis data and DFT calculations prove π -conjugation across the five-membered cyclic framework. Unlike in case of Sekiguchi's **4a**, the housane product of type **9** does not seem to be an intermediate towards **2a,b** and **3**. Instead, ring-opening to disilanyl silirenes **11** precedes the isomerization to 1,2,3-trisilacyclopentadienes.

Financial support by China Scholarship Council ([2014]3026, doctoral scholarship H. Z.), Saarland University and COST Action CM1302 (Smart Inorganic Polymers) is gratefully acknowledged.

Conflicts of interest

There are no conflicts to declare.

Notes and references

† Crystal data for **2a**: C₆₈H₉₈Si₃, *M* = 999.73, monoclinic, *a* = 19.538(1), *b* = 14.015(9), *c* = 24.330(1) Å, β = 108.596(1)°, *V* = 6315(7) Å³, *T* = 182 K, space group = *P*2₁/*n*, *Z* = 4, $\rho_{\text{calc.}}$ = 1.052 g cm⁻³. The final *R* factor was 0.0835 (*R*_w = 0.2255 for all data) for 43 839 reflections with *I* > 2 σ (*I*) GOF = 0.976. CCDC 1835094. **3**: C₁₃₀H₁₉₀Si₆, C₅H₁₂ *M* = 1993.49, monoclinic, *a* = 40.86(3), *b* = 14.207(9), *c* = 24.479(2) Å, β = 96.47(3)°, *V* = 13 542(2) Å³, *T* = 224 K, space group = *C*2/*c*, *Z* = 4, $\rho_{\text{calc.}}$ = 0.978 g cm⁻³. The final *R* factor was 0.0819 (*R*_w = 0.2478 for all data) for 59 910 reflections with *I* > 2 σ (*I*) GOF = 1.738. CCDC 1835096. Diffraction data were collected on a Bruker APEX-II CCD Diffractometer employing graphite-monochromatized Mo-K α radiation (λ = 0.71070 Å). The structure was solved by the direct method and refined by the full-matrix least-squares method using SHELXL-2014/6 program.¹⁹

1 R. West, J. M. Fink and J. Michl, *Science*, 1981, **214**, 1343.

2 Recent reviews (Si=Si): (a) A. Rammo and D. Scheschkewitz, *Chem. – Eur. J.*, 2018, **24**, 1; (b) A. Baceiredo and T. Kato, *Organosilicon Compd.*, 2017, 533; (c) C. Präsang and D. Scheschkewitz, *Chem. Soc. Rev.*, 2016, **45**, 900; (d) T. Iwamoto and S. Ishida, *Struct. Bonding*, 2014, **156**, 125; (e) D. Scheschkewitz, *Chem. Lett.*, 2011, **40**, 2; (f) D. Scheschkewitz, *Chem. – Eur. J.*, 2009, **15**, 2476; (g) M. Kira and T. Iwamoto, *Adv. Organomet. Chem.*, 2006, **54**, 73.

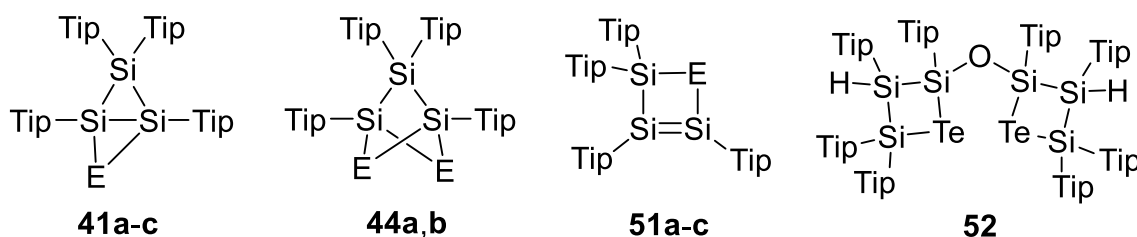
3 (a) A. Fukazawa, Y. Li, S. Yamaguchi, H. Tsuji and K. Tamao, *J. Am. Chem. Soc.*, 2007, **129**, 14165; (b) I. Bejan and D. Scheschkewitz, *Angew. Chem.,*

Int. Ed., 2007, **46**, 5783; (c) J. Jeck, I. Bejan, A. J. P. White, D. Nied, F. Breher and D. Scheschkewitz, *J. Am. Chem. Soc.*, 2010, **132**, 17306.

- 4 (a) L. Li, T. Matsuo, D. Hashizume, H. Fueno, K. Tanaka and K. Tamao, *J. Am. Chem. Soc.*, 2015, **137**, 15026; (b) M. Kobayashi, T. Matsuo and K. Tamao, *J. Am. Chem. Soc.*, 2010, **132**, 15162; (c) N. M. Obeid, L. Klemmer, D. Maus, M. Zimmer, J. Jeck, I. Bejan, A. J. P. White, V. Huch, G. Jung and D. Scheschkewitz, *Dalton Trans.*, 2017, **46**, 8839.
- 5 M. Majumdar, I. Bejan, V. Huch, A. J. P. White, G. R. Whittel, A. Schäfer, I. Manners and D. Scheschkewitz, *Chem. – Eur. J.*, 2014, **20**, 9225.
- 6 (a) R. Kinjo, M. Ichinohe, A. Sekiguchi, N. Takagi, M. Sumimoto and S. Nagase, *J. Am. Chem. Soc.*, 2007, **129**, 7766; (b) J. S. Han, T. Sasamori, Y. Mizuhata and N. Tokitoh, *Dalton Trans.*, 2010, **39**, 9238; (c) S. Ishida, Y. Misawa, S. Sugawara and T. Iwamoto, *Angew. Chem., Int. Ed.*, 2017, **56**, 13829.
- 7 H. Yasusa, V. Y. Lee and A. Sekiguchi, *J. Am. Chem. Soc.*, 2009, **131**, 6352.
- 8 (a) V. Y. Lee, M. Ichinohe and A. Sekiguchi, *J. Am. Chem. Soc.*, 2000, **122**, 12604; (b) V. Y. Lee, M. Ichinohe and A. Sekiguchi, *J. Organomet. Chem.*, 2001, **636**, 41; (c) V. Y. Lee, R. Kato, S. Aoki and A. Sekiguchi, *Russ. Chem. Bull.*, 2011, **60**, 2434.
- 9 K. Leszczyńska, K. Abersfelder, A. Mix, B. Neumann, H. G. Stammer, M. J. Cowley, P. Jutzi and D. Scheschkewitz, *Angew. Chem., Int. Ed.*, 2012, **51**, 6785.
- 10 (a) H. Zhao, K. Leszczyńska, L. Klemmer, V. Huch, M. Zimmer and D. Scheschkewitz, *Angew. Chem., Int. Ed.*, 2018, **57**, 2445 (*Angew. Chem.*, 2018, **130**, 2470); (b) T. P. Robinson, M. J. Cowley, D. Scheschkewitz and J. M. Goicoechea, *Angew. Chem., Int. Ed.*, 2015, **54**, 683; (c) M. J. Cowley, V. Huch and D. Scheschkewitz, *Chem. – Eur. J.*, 2014, **20**, 9221; (d) M. J. Cowley, V. Huch, H. S. Rzepa and D. Scheschkewitz, *Nat. Chem.*, 2013, **5**, 876; (e) M. J. Cowley, Y. Ohmori, V. Huch, M. Ichinohe, A. Sekiguchi and D. Scheschkewitz, *Angew. Chem., Int. Ed.*, 2013, **52**, 13247; (f) Y. Ohmori, M. Ichinohe, A. Sekiguchi, M. J. Cowley, V. Huch and D. Scheschkewitz, *Organometallics*, 2013, **32**, 1591.
- 11 (a) G. Liebling and R. E. Marsh, *Acta Crystallogr.*, 1965, **19**, 202; (b) C. H. Chang and S. H. Bauer, *J. Phys. Chem.*, 1971, **75**, 1685; (c) T. Haumann, J. B. Buchholz and R. Böse, *J. Mol. Struct.*, 1996, **374**, 299; (d) C. Benda, W. Klein and T. F. Fässler, *Z. Kristallogr. – New Cryst. Struct.*, 2017, **232**, 511.
- 12 M. Ichinohe, T. Matsuno and A. Sekiguchi, *Angew. Chem., Int. Ed.*, 1999, **38**, 2194.
- 13 (a) W. J. Hehre, R. Ditchfield and J. A. Pople, *J. Chem. Phys.*, 1972, **56**, 2257; (b) R. Krishnan, J. S. Binkley, R. Seeger and J. A. Pople, *J. Chem. Phys.*, 1980, **72**, 650; (c) A. D. McLean and G. S. Chandler, *J. Chem. Phys.*, 1980, **72**, 5639.
- 14 M. Ichinohe, T. Matsuno and A. Sekiguchi, *Chem. Commun.*, 2001, 183.
- 15 (a) M. Weidenbruch, *Chem. Rev.*, 1995, **95**, 1479; (b) V. Y. Lee, T. Matsuno, M. Ichinohe and A. Sekiguchi, *Heteroat. Chem.*, 2001, **12**, 223; (c) R. Fischer, T. Konopa, J. Baumgartner and C. Marschner, *Organometallics*, 2004, **23**, 1899; (d) K. Abersfelder and D. Scheschkewitz, *J. Am. Chem. Soc.*, 2008, **130**, 4114; (e) K. Abersfelder and D. Scheschkewitz, *Pure Appl. Chem.*, 2010, **82**, 595.
- 16 (a) K. Hatano, N. Tokitoh, N. Takagi, and S. Nagase, *J. Am. Chem. Soc.*, 2000, **122**, 4829; (b) J. Ohshita, H. Ohnishi, A. Naka, N. Senba, J. Ikada, A. Kunai, H. Kobayashi and M. Ishikawa, *Organometallics*, 2006, **25**, 3955; (c) S. Yao, C. Wüllen, X. Y. Sun and M. Driess, *Angew. Chem., Int. Ed.*, 2008, **47**, 3250; (d) S. Ishida, T. Iwamoto and M. Kira, *Heteroat. Chem.*, 2010, **22**, 432; (e) M. Ishikawa, A. Naka and J. Ohshita, *Asian J. Org. Chem.*, 2015, **4**, 1192.
- 17 (a) S. Nagase and T. Kudo, *J. Chem. Soc., Chem. Commun.*, 1984, 1392; (b) S. Ishida, T. Iwamoto and M. Kira, *Organometallics*, 2009, **28**, 919.
- 18 M. Majumdar, V. Huch, I. Bejan, A. Meltzer and D. Scheschkewitz, *Angew. Chem., Int. Ed.*, 2013, **52**, 3516.
- 19 G. M. Sheldrick, *SHELXL-2014/6*, University of Göttingen, Germany, 2017.

3.4 Reactivity of peraryl Cyclotrisilene towards Chalcogens

Compared with bicyclo[1.1.10]butane derivatives composed of Si or Si/C atoms,¹⁰² those comprising chalcogen heteroatoms are rare. Sekiguchi *et al.* obtained the so far only bicyclo[1.1.0]butane species with both silicon and chalcogen in the scaffold (**40a-c**, Scheme 23) by treatment of a silyl-substituted cyclotrisilene **3** with sulfur, selenium and tellurium.⁷⁰ Notably, the sulfur and selenium derivatives **40a,b** were transformed into the corresponding cyclobutene isomers (**50a,b**, Scheme 25) upon UV irradiation.^{70a} The successful synthesis of peraryl-substituted cyclotrisilene **24** as well as its highly versatile reactivity in terms of π -addition to the Si=Si double bond, σ -insertion to an endocyclic Si-Si single bond and ring-opening under formation of acyclic disilene derivatives discovered in recent years (see Chapter 1.7), prompted us to investigate the effect of the peraryl substitution on the reactivity of **24** towards chalcogens.



Scheme 50. Products resulting from reaction of **24** with chalcogen element (a: E = S, b: E = Se, c: E = Te).

In this vane, **24** was treated with elemental sulfur, selenium and tellurium, individually, affording 2-chalcogena-1,3,4-trisilabicyclo[1.1.0]butanes **41a-c** (**Scheme 50**). The monochalcogenation products **41a-c** was isolated as air-sensitive yellow to orange crystals from hydrocarbon solvents in acceptable yields (45% to 55%). Pure 2-thia-1,3,4-trisilabicyclo[1.1.0]butane (**41a**) could only be obtained by reaction of **24** with one equivalent of propylene sulfide as stoichiometric source of sulfur to suppress the addition of a second equivalent of sulfur. Indeed, the intrinsic ring strain of the bicyclo[1.1.0]butane skeletons of **41a** and **41b** allows for the insertion of a second

equivalent of the same chalcogen into bridging Si–Si single bond with formation of 2,4-dichalcogena-1,3,5-trisilabicyclo[1.1.1]-pentanes (**44a** and **44b**, Scheme 50). Both bicyclo[1.1.1]pentanes **44a,b** were isolated as air-stable colorless crystals. Constitutions of **41** and **44** were confirmed by X-ray crystal structure analysis.

41a-c show three signals in ^{29}Si CP-MAS NMR spectrum at δ 3.0, –44.4, and –59.2 ppm (**41a**), 0.61, –54.3, and –68.9 ppm (**41b**), 1.1, –85.9, and –98.0 ppm (**41c**), in a ratio of 1:1:1, of which the two relatively upfield signals are attributed to *SiTip* moieties. DFT calculation at the BP86(D3)/def2-SVP level of theory reveals the non-equivalence silicon chemical shift of *SiTip* originates from the near orthogonality of the rotationally hindered *Tip* group at one of the bridgehead silicon atoms, which allows for considerable in-phase interaction. The more pronounced paramagnetic contribution to the chemical shift tensor results in the deshielding of *Si2a* relative to *Si1*. In contrast to the silyl-substituted Si_3E -bicyclo[1.1.0]butanes **40a-c**, which show the expected two ^{29}Si NMR signals in a 1:2 ratio for the bridging and bridgehead silicon atoms, the ^{29}Si NMR spectra of **41a-c** in C_6D_6 at room temperature exhibit just a single signal at relatively low field (δ 3.17 (**41a**), –1.63 (**41b**), –1.24 (**41c**) ppm). The non-equivalence of the two *SiTip* moieties is also confirmed by variable-temperature ^{29}Si NMR, wherein three ^{29}Si NMR signals of equal intensity appear at 233 K at δ 1.86, –43.0, and –58.27 ppm for **41a**, –2.67, –54.9, and –68.9 ppm for **41b**, –2.10, –87.4, and –98.7 ppm for **41c**. With rising temperature, the latter two signals are gradually broadened and disappear in the noise at approximately 263 K.

After heating of the solution of **41a-c** in a nmr tube to 60 °C for 1 h, characteristic signals for tricoordinate silicon atoms appeared in the ^{29}Si NMR spectrum at δ 128.2, 19.4 ppm for **51a**, 127.7, 21.7, and –8.9 ppm for **51b**, 103.4, 35.6 and –30.0 ppm for **51c**, suggesting the formation of chalcogena-trisilacyclobutenes **51** as the thermodynamically favoured isomer. Attempts to isolate **51a-c** by crystallization from different solvents such as hexane, toluene and thf failed. Deliberate quenching of the reaction mixture containing **51c** with a small amount of water added by microsyringe,

however, resulted in the product **52** of two fold OH-addition, which was obtained from toluene as colourless crystals in 30% yield (Scheme 50).

Results of the described studies have been published in the *Zeitschrift für Anorganische und Allgemeine Chemie – Wiley online Library*.

Hui Zhao, Lukas Klemmer, Michael J. Cowley, Volker Huch, Michael Zimmer and David Scheschkewitz, Reactivity of a Peraryl Cyclotrisilene (*c*-Si₃R₄) Toward Chalcogens, *Z. Anorg. Allg. Chem.* **2018**, DOI: [10.1002/zaac.201800182](https://doi.org/10.1002/zaac.201800182)

All people mentioned as authors made a range of effort to the publication of this paper: all experiments and the characterization of products were performed by H. Zhao. M. J. Cowley obtained the preliminary results regarding the synthesis of Si₃Se-bicyclo[1.1.0]butane **41b**. H. Zhao drafted the manuscript and supporting information of this publication. L. Klemmer performed the DFT calculations. V. Huch contributed to the crystallographic data collection and refinement. M. Zimmer made an effort to collect the VT-NMR and solid state NMR data. D. Scheschkewitz has given critical revision of the manuscript and he is the supervisor of the research. An authorship statement signed by all co-authors including more detailed contributions of each co-author is also provided.

Reactivity of a Peraryl Cyclotrisilene ($c\text{-Si}_3\text{R}_4$) Toward Chalcogens

Hui Zhao,^[a] Lukas Klemmer,^[a] Michael J. Cowley,^[a,b] Volker Huch,^[a] and Michael Zimmer,^[a] David Scheschkewitz*^[a]

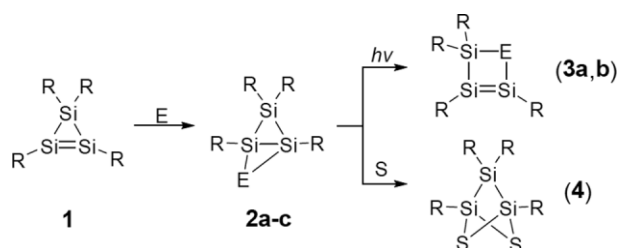
Dedicated to Prof. Alexander Filippou on the Occasion of his 60th Birthday

Abstract. Reactions of the peraryl-substituted cyclotrisilene **5** ($c\text{-Si}_3\text{R}_4$, $R = \text{Tip} = i\text{Pr}_3\text{C}_6\text{H}_2$) with chalcogens initially result in Si=Si double bond π -addition products, 2-chalcogena-1,3,4-trisilabicyclo[1.1.0]butanes **6a–6c**. Treatment with an excess of sulfur or selenium leads to the insertion of a second equivalent into the bridging Si-Si single bond of **6a** and **6b** and thus affords 2,4-dichalcogena-1,3,5-trisilabicyclo[1.1.1]pentanes **7a** and **7b**. In the solid state as well as at low temperature in solution, the monoaddition products **6a–6c**

show three signals in ^{29}Si CP-MAS NMR spectroscopy. The rapid degenerate exchange of the differing aryl group conformations at the bridging silicon atoms leads to coalescence (and thus disappearance) of two of these signals in C_6D_6 at elevated temperature. Thermal isomerization of **6a–6c** to 2-chalcogena-1,3,4-trisilacyclobutenes **8a–8c** is suggested by NMR spectroscopic data and supported by the isolation of the hydrolysis product of **8c**.

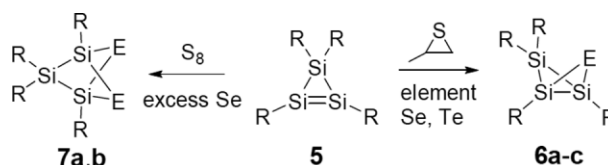
Introduction

The chemistry of the heavier Group 14 elements is strongly influenced by the interplay of their thermodynamic preference for single bonds vs. the (predominantly) kinetic effect of steric bulk.^[1] By the careful choice of substituents, unsaturated species with heavier double bonds can be favored over saturated cyclic isomers or vice versa; occasionally both even co-exist in equilibrium.^[2] Silabicyclo[1.1.0]butanes ($\text{Si}_n\text{C}_{(4-n)}\text{R}_6$; $n = 1$ to 4)^[3] are attractive in this regard as the number of isomers for $E_4\text{R}_6$ species is in general still manageable. The facile interconversion of $\text{B}_2\text{P}_2\text{R}_6$, for instance, allowed for a detailed picture of the relevant potential energy surface through the synthesis of stable representatives.^[4] In comparison to the abundant bicyclo[1.1.0]butane derivatives composed of Si or Si/C atoms,^[3] those comprising chalcogen heteroatoms are rare, although Si–Si single and double bonds are well-known to oxidatively add chalcogens under mild conditions.^[5,6] Indeed, Sekiguchi et al. obtained the so far the only bicyclo[1.1.0]butane species with both silicon and chalcogen in the scaffold (**2a–2c**, Scheme 1) by treatment of a silyl-substituted cyclotrisilene **1** ($c\text{-Si}_3\text{R}_4$, $R = \text{SiMe}/\text{Bu}_2$)^[7] with sulfur, selenium, and tellurium.^[8] Notably, the sulfur and selenium derivatives **2a** and **2b** were transformed into the corresponding cyclobutene isomers **3a** and **3b** upon UV irradiation (Scheme 1).^[8a]



Scheme 1. Sekiguchi's synthesis of chalcogen-containing bicyclo[1.1.0]butanes **2a–2c** and isomerization to cyclobutene derivatives **3a** and **3b** ($R = \text{SiMe}/\text{Bu}_2$; **a**: $E = \text{S}$; **b**: $E = \text{Se}$; **c**: $E = \text{Te}$).^[8]

In 2012, we reported the first peraryl-substituted cyclotrisilene **5** ($c\text{-Si}_3\text{R}_4$, $R = \text{Tip} = i\text{Pr}_3\text{C}_6\text{H}_2$, Scheme 2),^[9] which displays a highly versatile reactivity in terms of π addition to the Si=Si double bond,^[10] σ insertion to an endocyclic Si–Si single bond,^[11] and ring-opening with formation of acyclic disilene derivatives.^[12] The reaction of cyclotrisilene **5** with acetylenes to yield 1,2,3-trisilacyclopentadienes was shown to be particularly susceptible to the nature of the substituents.^[13] We were thus curious about the effect of the peraryl substitution on the reactivity of **5** towards chalcogens.



Scheme 2. Synthesis of **6a–6c** and **7a**, **7b**. ($R = \text{Tip} = i\text{Pr}_3\text{C}_6\text{H}_2$; **a** $E = \text{S}$, **b** $E = \text{Se}$, **c** $E = \text{Te}$; reaction conditions: **6a** toluene, -20°C to room temperature; **6b** thf, room temperature; **6c** thf, 40°C ; **7a**, **7b** thf, 25°C).

* Prof. Dr. D. Scheschkewitz
E-Mail: scheschkewitz@mx.uni-saarland.de

[a] Krupp-Lehrstuhl für Allgemeine und Anorganische Chemie
Universität des Saarlandes
Campus, C4.1
66123 Saarbrücken, Germany

[b] New address: School of Chemistry
University of Edinburgh
Edinburgh, EH9 3JJ, UK

Supporting information for this article is available on the WWW under <http://dx.doi.org/10.1002/zaac.201800182> or from the author.

Results and Discussion

Synthesis

The reactions of peraryl cyclotrisilene **5** with an equimolar ratio of either elemental sulfur, selenium or tellurium expectedly afford 2-chalcogena-1,3,4-trisilabicyclo[1.1.0]butanes **6a–6c** (Scheme 2).

Unlike previously reported for the silyl-substituted derivatives,^[8] pure 2-thia-1,3,4-trisilabicyclo[1.1.0]butane (**6a**) could only be obtained by reaction of cyclotrisilene **5** with one equivalent of propylene sulfide as stoichiometric source of sulfur. The monochalcogenation products **6a–6c** were isolated as air-sensitive yellow to orange crystals from hydrocarbon solvents in acceptable yields (45% to 55%).

The intrinsic ring strain of the bicyclo[1.1.0]butane skeletons of **6a** and **6b** allows for the insertion of a second equivalent of the same chalcogen into bridging Si–Si single bond with formation of 2,4-dichalcogena-1,3,5-trisilabicyclo[1.1.1]pentanes (**7a** and **7b**, Scheme 2). In case of Sekiguchi's silyl-substituted derivatives only the 2,4-dithia-1,3,5-trisilabicyclo[1.1.1]pentane (**4**) had been obtained, presumably due to more pronounced steric encumbrance of **1** in comparison to **5** (Scheme 1).^[8] Both bicyclo[1.1.1]pentanes **7a**, **7b** were isolated as air-stable colorless crystals. Treatment of cyclotrisilene **5** with an excess amount of elemental tellurium failed to achieve the insertion of a second tellurium atom even at elevated temperature, probably due to the large size of tellurium center in **6c**. Attempts to synthesize mixed derivatives of type **7** with two different chalcogen atoms remained inconclusive.

Spectroscopy

The yellow to orange color of **6a–6c** mainly originates from the longest wavelength absorptions (**6a**: $\lambda_{\max} = 404$ nm, $\epsilon = 1487$ L·cm⁻¹·mol⁻¹; **6b**: $\lambda_{\max} = 408$ nm, $\epsilon = 1773$ L·cm⁻¹·mol⁻¹; **6c**: $\lambda_{\max} = 408$ nm, $\epsilon = 1355$ L·cm⁻¹·mol⁻¹), which are similar to those of silyl-substituted Si₃S- and Si₃Se-bicyclo[1.1.0]butanes **2a** (394 nm) and **2b** (403 nm). Conversely, the λ_{\max} of **6c** is blue-shifted by no less than $\Delta\lambda = 55$ nm with respect to that of Si₃Te-bicyclo[1.1.0]butane **2c** ($\lambda_{\max} = 463$ nm).^[8b]

Interestingly, in contrast to the silyl-substituted Si₃E-bicyclo[1.1.0]butanes **2a–2c**, which show the expected two ²⁹Si NMR signals in a 1:2 ratio for the bridging and bridgehead silicon atoms,^[8] the ²⁹Si NMR spectra of **6a–6c** in C₆D₆ at room temperature consist of just a single signal at relatively low field [$\delta = 3.17$ (**6a**), -1.63 (**6b**), -1.24 (**6c**) ppm]. A dynamic process equilibrating all three silicon atoms seemed unlikely on the basis of the low propensity for migration of silicon-bonded aryl groups.^[14] Indeed, the NMR spectra of **6a–6c** in the solid state suggested that apparently only two of the ring atoms are involved in a dynamic process.

Figure 1a shows the representative ²⁹Si CP-MAS NMR spectrum of **6b** with three signals at $\delta = 0.61$, -54.3 , and -68.9 ppm in a ratio of 1:1:1. Similar signals were also observed in the ²⁹Si CP-MAS NMR spectra of **6a** ($\delta = 3.0$, -44.4 , and -59.2 ppm) and **6c** ($\delta = 1.1$, -85.9 , and -98.0 ppm). The most downfield shifted signals of each spectrum agree reason-

ably well with those of the single signals in the corresponding solution spectra at room temperature and are therefore as expected not involved in the exchange reaction. The non-equivalence of the two SiTip moieties is confirmed by variable-temperature ²⁹Si NMR of **6b**. At 233 K in [D₈]toluene, three ²⁹Si NMR signals of equal intensity appear at $\delta = -2.67$, -54.9 , and -68.9 ppm (Figure 1b), very similar to those of **6b** in the solid state. Analogous ²⁹Si NMR behavior occurs in the cases of **6a** and **6c** with three signals each (**6a**: $\delta = 1.86$, -43.0 , and -58.27 ppm; **6c**: $\delta = -2.10$, -87.4 , and -98.7 ppm) at 233 K (Figure S29, Supporting Information). On the basis of a 2D ¹H/²⁹Si correlation spectrum, the low-field signals of **6a–6c** are assigned to the SiTip₂ unit and the two high-field signals to the bridgehead SiTip. With rising temperature, the latter signals are gradually broadened and disappear in the noise at approximately 263 K (Figure 1b).

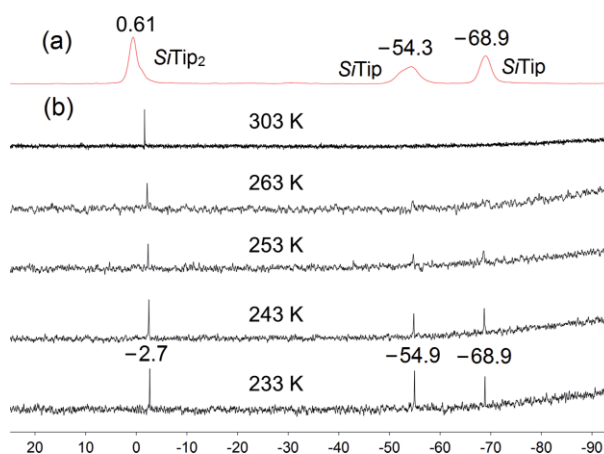


Figure 1. (a) ²⁹Si CP-MAS NMR of **6b** at 303 K; (b) variable-temperature ²⁹Si NMR of **6b** in [D₈]toluene.

In contrast, the ²⁹Si NMR spectra of the disulfur and diselenium species **7a** and **7b** show as expected two signals in a ratio of 1:2 at $\delta = 35.37$, -9.18 ppm for **7a** and $\delta = 37.16$, -31.62 ppm for **7b**. The assignment of signals was therefore straightforward on the basis of relative intensities. The release of ring strain in comparison to **6a** and **6b** explains the relative downfield shift of the ²⁹Si NMR signals as previously reported for **4** ($\delta = 69.8$, -4.1 ppm) versus **2a** ($\delta = -22.0$, -119.9 ppm)^[8] as well as for monochalcogen versus dichalcogen addition product of disilenes.^[6] Selected spectroscopic and crystal data of **6a–6c** and **7a**, **7b** are summarized in Table 1.

Table 1. Selected bond lengths /Å and spectroscopic data of **6a–6c** and **7a**, **7b**.

	Si1–Si2 ^{a)}	$\delta = ^{29}\text{Si}$ /ppm (25 °C, C ₆ D ₆)	$\delta = ^{29}\text{Si}$ /ppm (in the solid)	λ_{\max} /nm
6a	2.275(1)	3.17	3.0, -44.4 , -59.2	404
6b	2.302(8)	-1.63	0.61, -54.3 , -68.9	408
6c	–	-1.24	1.1, -85.9 , -98.0	408
7a	2.548(4)	35.37, -9.18	– ^{b)}	–
7b	2.655(1)	37.16, -31.62	– ^{b)}	–

a) Bond length between bridgehead silicon atoms. b) ²⁹Si CP-MAS of **7a** and **7b** were not measured due to solution spectra being consistent with expectations.

Solid State Structures

Single crystals of **6a–6c** were obtained from hexane at room temperature. Unlike the Si_3E -bicyclo[1.1.0]butanes **2a–2c**, which adopt an orthorhombic crystal system,^[8a,b] **6a–6c** crystallize in the triclinic $P\bar{1}$ space group. In all cases, pronounced positional disorder of almost the entire asymmetric unit needed to be addressed by refinement as split models between two alternative orientations of the molecule in a 4:1 ratio (Figure 2). Refinement proceeded smoothly for both **6a** and **6b** so that the bonding parameters can be discussed with confidence. Figure 2a shows the molecular structure of **6a** as an example (**6b**: Figure S40, Supporting Information).

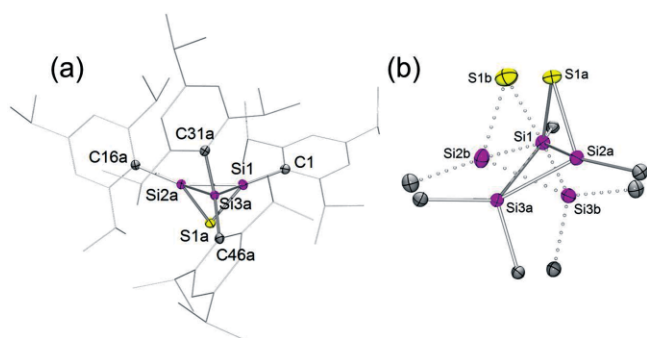


Figure 2. (a) The major position in the disordered solid-state structure of **6a**. (b) Disorder in crystals of **6a**. The dashed bond indicates the minor position. Thermal ellipsoids at 50%, hydrogen atoms are omitted for clarity. Selected bond lengths /Å and angles /°: Si1–Si1a 2.196(1), Si2a–Si1a 2.195(1), Si1–Si2a–2.275(1), Si2a–Si3a 2.339(1), Si1–Si3a 2.346(1); C16a–Si2a–Si1 151.9(9), C1–Si1–Si2a 150.2(9), C31a–Si3a–C46a 107.8(1), Si3a–Si2a–Si1a 96.3(5), Si2a–Si3a–Si1 58.1(3)

Both **6a** and **6b** are typical short-bond isomers^[15] with relatively small interplanar angle (**6a**: 122.2°, **6b**: 120.0°) between the two three-membered rings and large R –Si–Si angles [151.9(9)°, 150.2(9)° in **6a**; 150.3(5)°, 152.1(6)° in **6b**]. The remarkable short Si–Si bridge in **6a** and **6b** [Si1–Si2a: **6a** 2.275(1) Å; **6b** 2.302(8) Å] had also been observed in **2a–2c**^[8] and is characteristic for chalcogenadisiliranes in general.^[6] The differing ^{29}Si NMR chemical shifts for the SiTip moieties in low temperature experiments and the solid state are readily explained by the strongly differing torsion of the Tip substituents about the Si–C bond vector with respect to the Si_3 ring [τ_{Si1Tip} 39.2(3)° in **6a**, 40.6(2)° in **6b**; τ_{Si2aTip} 71.2(2)° in **6a**, 70.3(1)° in **6b**].

The optimized structure of **6a** and **6b** based on DFT calculations at the BP86(D3)/def2-SVP level of theory nicely reproduced the differing dihedral distortion at the bridgehead silicon atoms (calcd. τ_{Si1Tip} 41.2° in **6a**, 41.4° in **6b**; τ_{Si2aTip} 72.8° in **6a**, 73.7° in **6b**). The ^{29}Si NMR chemical shifts of **6a** predicted at the M06–2X(D3)/def2-TZVPP level of theory [$\delta^{29}\text{Si}_{\text{calc}}$ 0.9 (SiTip_2), –39.4 (Si2aTip), –54.4 (SiTip) ppm] are in good agreement with the experiment and allow for an assignment of the more deshielded ^{29}Si NMR signal to the silicon atom with the more twisted Tip group. Indeed, a contour plot (**6a**: Figure 3, **6b**: Figure S44, Supporting Information) shows the

LUMO to be predominantly located at the Si2aTip moiety. Therefore, the non-equivalence silicon chemical shift of SiTip unit below 263 K in solution and in solid state is proposed to originate from the near orthogonality of the rotationally hindered Tip group at Si2a, which allows for considerable in-phase interaction of π orbitals at C16a with the σ^* orbital at Si2a. As the LUMO is largely determining the paramagnetic contribution to the chemical shift tensor the deshielding of Si2a relative to Si1 is plausible.^[16] The non-reappearance of an averaged signal even at 303 K, however, suggests a more complicated interplay of more than one dynamic equilibrium, possibly related to the equally hindered rotation of the Tip groups at Si3.

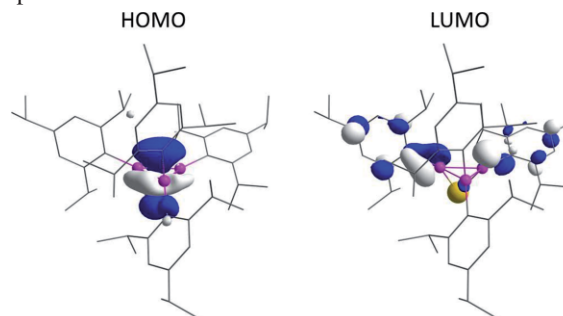


Figure 3. Contour plots of HOMO and LUMO of **6a** at the BP86(D3)/def2-SVP level of theory (isosurface = 0.05 a.u.).

The Si_3E_2 -trisilabicyclo[1.1.1]pentanes **7a**, **7b** (Figure 4) crystallize in the monoclinic $P2_1/c$ space group. The skeletal Si–Si bond lengths of **7a** and **7b** [2.372(4), 2.353(4) Å for **7a**; 2.368(0), 2.375(1) Å for **7b**] fall within the normal range of Si–Si single bonds.^[17] Similarly, the Si– E bond lengths of **7a** and **7b** [**7a**: $E = \text{S}$, 2.164(1) to 2.198(1); **7b**: $E = \text{Se}$, 2.309(6) to 2.339(7) Å] differ only insignificantly from those of **6a** [2.159(1) Å] and **6b** [2.330(7) Å] or **2a–2c**^[8] and other chalcogenadisiliranes.^[6a–6g]

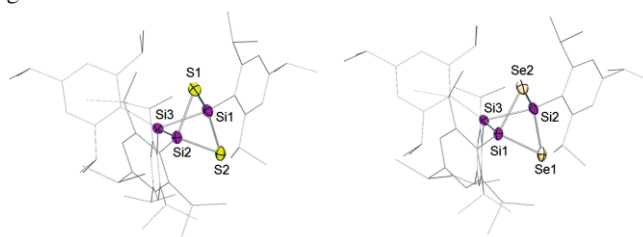


Figure 4. Molecular structure of **7a** (right) and **7b** (left). Thermal ellipsoids at 50%, hydrogen atoms are omitted for clarity. Selected bond lengths /Å and angles /°: **7a**: Si1–Si3 2.351(1), Si2–Si3 2.371(1), Si1–Si1 2.167(1), Si2–Si1 2.187(1), Si1–S2 2.198(1), Si2–S2 2.164(1); Si1–Si3–Si2 65.4(2), Si3–Si2–S2 91.4(3), Si3–Si1–S2 91.1(4), Si2–Si1–Si1 71.7(3), Si1–S2–Si2 71.5(3). **7b**: Si3–Si1 2.375(8), Si3–Si2 2.368(9), Si1–Se1 2.309(6), Si2–Se1 2.339(7), Si1–Se2 2.335(7), Si2–Se2 2.314(6); Si1–Si3–Si2 68.1(3), Si3–Si2–Se1 91.2(3), Si2–Se1–Si1 69.7(2), Se1–Si1–Si3 91.8(2), Si3–Si1–Se2 90.4(3), Se1–Si2–Se2 90.6(2), Si1–Se2–Si2 69.6(2).

Thermal Isomerization of **6c** to Tellura-Trisilacyclobutene **8**

Thermal isomerization between tetrasilabicyclo[1.1.0]butane and tetrasilacyclobutene had initially been observed by

Kira et al.^[3d] Transformation of Si₃E-trisilabicyclo[1.1.0]butane **2a** and **2b** to corresponding trisilacyclobutene **3a** and **3b** was achieved by photochemical irradiation (Scheme 1).^[8a] Tellura-trisilacyclobutenes, however, have not been reported previously.

We anticipated that the more sterically demanding peraryl-substitution of tellurabicyclobutane **6c** might allow for its isomerization. After heating of a solution of **6c** in an NMR tube to 60 °C for 1 h, indeed three new signals appeared in the ²⁹Si NMR in a ratio of 1:1:1 at $\delta = 103.4$, 35.6 and -30.0 ppm. The two low-field signals are indicative of the presence of tricoordinate silicon atoms and thus suggest the formation of tellura-trisilacyclobutene **8c** as the thermodynamically favored isomer (Scheme 3). Very large chemical shift differences in polarized Si=Si double bonds (such as the one in **8c**) have been subject to intense theoretical scrutiny.^[18] The sulfur and selenium derivatives **6a** and **6b** are similarly transformed into new species upon heating to 60 °C with diagnostic signals in the ²⁹Si NMR spectrum ($\delta = 128.2$, 19.4 and -12.2 ppm for **8a**; 127.7, 21.7, and -8.9 ppm for **8b**, Figures S31–33, Supporting Information). Attempts to isolate **8a–8c** by crystallization from different solvents such as hexane, toluene and thf failed. After deliberate quenching of the reaction mixture containing **8c** with a small amount of water added by microsyringe, however, the hydrolyzed dimer **9** was obtained from toluene as colorless crystals in 30% yield (Scheme 3).



Scheme 3. Isomerization of **6c** to tellura-trisilacyclobutene **8c** and subsequent hydrolysis product **9**.

Single crystal X-ray structure analysis confirmed the constitution of **9** as disiloxane-bridged Si₃Te cycles (Figure 5), in which the Si–Si single bond lengths are within the normal range from 2.380(8) to 2.401(8) Å.^[17] The Si–Te bond lengths are between 2.540(6) and 2.562(6) Å, highly comparable with that in 2-tellura-1,3,4-trisilabicyclo[1.1.0]butane (**2c**) (2.551 and 2.572 Å).^[18b] The four-membered rings of Si₁–Si₂–Si₃–Te₁ are almost planar with small folding angles of the tellurium atoms regarding the adjacent Si₃ planes [Te₁–Si₁–Si₃ versus Si₁–Si₂–Si₃ 5.3(2)°/ Te₂–Si₄–Si₆ versus Si₄–Si₅–Si₆ 9.0(2)°]. In the ¹H NMR of **9** the Si–H signal is detected at $\delta = 6.52$ ppm as a singlet with ²⁹Si satellites (¹J_{Si–H} = 143 Hz). The ²⁹Si NMR shows three signals at $\delta -2.22$, -28.87 , and -45.36 ppm. On the basis of the 2D ¹H/²⁹Si HMBC spectrum (Figure S25, Supporting Information), the signal at -28.87 ppm is attributed to SiH, whereas the signals at $\delta -45.36$ and -2.22 ppm are due to the SiTip₂ and SiOTip moieties, respectively.

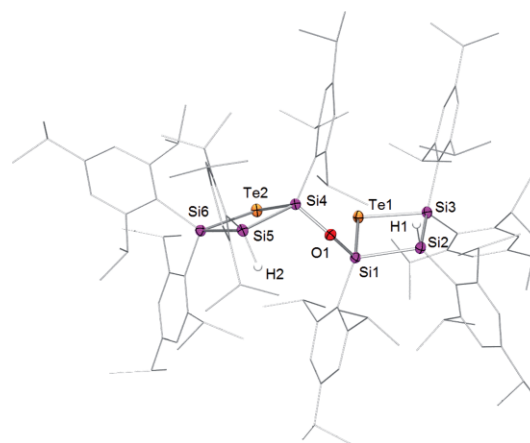


Figure 5. Molecular structure of **9**·C₇H₈. Thermal ellipsoids at 50% hydrogen atoms and co-crystallized C₇H₈ molecule are omitted for clarity. Selected bond lengths /Å and angles /°: Si₁–Si₂ 2.380(8), Si₂–Si₃ 2.401(8), Si₄–Si₅ 2.380(8), Si₅–Si₆ 2.394(8), Si₂–H₁ 1.37(2), Si₅–H₂ 1.38(2), Si₁–O₁ 1.656(2), Si₄–O₁ 1.657(2), Si₃–Te₁ 2.555(6), Si₁–Te₁ 2.540(6), Si₄–Te₂ 2.547(6), Si₆–Te₂ 2.562(6); Si₄–O₁–Si₁ 143.5(9), Si₁–Te₁–Si₃ 87.7(2), Si₄–Te₂–Si₆ 88.5(2).

Conclusions

We reported the synthesis of peraryl-substituted 2-chalcogen-1,3,4-trisila-bicyclo[1.1.0]butanes **6a–6c** and 2,4-dichalcogen-1,3,5-trisilabicyclo[1.1.1]pentanes **7a** and **7b** via reactions of cyclotrisilene **5** with chalcogens. In comparison to the previously reported silyl-substituted **2a–2c**, **6a–6c** show peculiar dynamics in solution NMR studies related to the conformation of the aryl substituents. Thermal isomerization of **6c** to 2-tellurium-1,3,4-trisilacyclobutene (**8c**) is confirmed by the isolation of the hydrolysis product **9**.

Experimental Section

General All manipulations were carried out in a protective atmosphere of argon applying standard Schlenk techniques or in a glovebox. Solvents were distilled over sodium/benzophenone in an argon atmosphere. C₆D₆ and [D₈]toluene were dried with potassium and distilled in an argon atmosphere before use. 1,1,2,3-Tetra(2,4,6-triisopropylphenyl)trisilacyclopropene (cyclotrisilene **5**) was prepared according to the published procedure.^[9] All other chemicals were obtained commercially and used as supplied. NMR spectra in solution were recorded with a Bruker Avance III 300 MHz spectrometer. ¹H and ¹³C NMR spectra were referenced to residual signals of the deuterated solvent; ²⁹Si was referenced to external SiMe₄. Solid-state ²⁹Si CP-MAS NMR spectra were recorded with a Bruker AV400 WB spectrometer at 79.5 MHz with a 13 KHz spinning rate. UV/Vis spectra were acquired with a Perkin-Elmer Lambda 35 spectrometer using quartz cells with a path length of 0.1 cm. Melting points were determined in an argon atmosphere in a sealed NMR tube. Elemental analysis was performed with a Leco CHN-900 analyzer.

Crystallographic data (excluding structure factors) for the structures in this paper have been deposited with the Cambridge Crystallographic Data Centre, CCDC, 12 Union Road, Cambridge CB21EZ, UK. Copies of the data can be obtained free of charge on quoting the depository numbers CCDC-1840604 (**6a**), CCDC-1840606 (**6b**), CCDC-

1840605 (**7a**), CCDC-1840607 (**7b**), and CCDC-1840608 (**9**) (Fax: +44-1223-336-033; E-Mail: deposit@ccdc.cam.ac.uk, http://www.ccdc.cam.ac.uk).

Synthesis of 6a: Cyclotrisilene **5** (300 mg, 0.334 mmol) was dissolved in 10 mL toluene and the resulting solution cooled to -20°C . Propylene sulfide (27 μL , 0.334 mmol) was introduced via micro syringe, upon which the color of the reaction mixture changed from orange to yellow within 2 min. Stirring was maintained for 1 h while warming to room temperature. After removal of volatiles in vacuo, the resulting light yellow residue was dissolved in 2 mL hexane. Cubic yellow crystals of **6a** formed over 5 h and were isolated by solvent decantation (170 mg, yield: 55%, m.p. 165–168 $^{\circ}\text{C}$, dec.). $^1\text{H NMR}$ (300.13 MHz, C_6D_6 , 300 K): $\delta = 7.31, 7.30$ (br., 1 H, Tip-CH); 7.15 (overlapped with solvent, 4 H, Tip-CH); 7.00, 6.99 (br., 1 H, Tip-CH); 6.95 (br., 2 H, Tip-CH); 4.89–4.81, (m, 1 H, *iPr*-CH); 3.93 (br., 3 H, *iPr*-CH); 3.72 (br., 3 H, *iPr*-CH); 3.19–3.11 (m, 1 H, *iPr*-CH); 2.75–2.70 (m, 4 H, *iPr*-CH); 1.74 (br., 6 H, *iPr*-CH₃); 1.41 (br., 12 H, *iPr*-CH₃); 1.22 (br., 9 H, *iPr*-CH₃); 1.19, 1.18, 1.17, 1.15, 1.13 (each br, together 30 H, *iPr*-CH₃); 1.06 (br., 9 H, *iPr*-CH₃); 0.80 (br., 6 H, *iPr*-CH₃) ppm. $^{13}\text{C}\{^1\text{H}\}$ NMR (75.47 MHz, C_6D_6 , 300 K): $\delta = 155.97, 154.90, 153.78, 152.18, 150.37, 150.11$ (Tip-C); 136.88, 133.05, 126.40, 122.20, 121.87, 121.64 (Tip-CH); 37.44, 36.10, 36.00, 34.58, 34.42, 31.79 (*iPr*-CH); 25.77, 25.48, 23.96, 23.87, 23.77, 23.68, 22.87 (*iPr*-CH₃) ppm. $^{29}\text{Si}\{^1\text{H}\}$ NMR (59.6 MHz, C_6D_6 , 300 K): $\delta = 3.17$ (*SiTip*₂) ppm. $^{29}\text{Si}\{^1\text{H}\}$ CP-MAS (79.5 MHz, 300 K): $\delta = 3.0$ (*SiTip*₂), -44.4 (*SiTip*), -59.2 (*SiTip*) ppm. UV/Vis (hexane) λ_{max} (ϵ): 404 nm (1487 $\text{M}^{-1}\text{cm}^{-1}$). $\text{C}_{60}\text{H}_{92}\text{Si}_3\text{Se}$: calcd. C 77.51; H 9.97%; found: C 76.25; H 9.90%.

Synthesis of 6b: A suspension of cyclotrisilene **5** (500 mg, 0.557 mmol) and selenium powder (44 mg, 0.557 mmol) in 6 mL thf was stirred at room temperature overnight. Removal of the solvent in vacuo resulted in a yellow residue, which was extracted with hexane (2 \times 5 mL) and filtered. The filtrate was concentrated to ca. 3 mL from which yellow crystals of **6b** were obtained at room temperature overnight and isolated by solvent decantation (233 mg, yield: 45%, m.p. 163–166 $^{\circ}\text{C}$, dec.). $^1\text{H NMR}$ (300.13 MHz, C_6D_6 , 300 K): $\delta = 7.31$ (br., 1 H, Tip-CH); 7.13 (overlapped with solvent, 4 H, Tip-CH); 6.99 (br., 1 H, Tip-CH); 6.94 (br., 2 H, Tip-H); 4.91–4.82 (m, 1 H, *iPr*-CH); 3.92 (br., 6 H, *iPr*-CH); 3.18–3.10 (m, 1 H, *iPr*-CH); 2.74–2.70 (m, 4 H, *iPr*-CH); 1.73 (br., 6 H, *iPr*-CH₃); 1.41 (br., 21 H, *iPr*-CH₃); 1.18 (s, 3 H, *iPr*-CH₃); 1.16, 1.15, 1.13 (each br, 24 H, *iPr*-CH₃); 1.02 (br., 12 H, *iPr*-CH₃); 0.69 (br., 6 H, *iPr*-CH₃) ppm. $^{13}\text{C}\{^1\text{H}\}$ NMR (75.47 MHz, C_6D_6 , 300 K): $\delta = 156.12, 155.18, 153.71, 152.06, 150.41, 150.23$ (Tip-C); 138.28, 132.66 (Tip-CH); 126.06, 122.36, 122.02, 121.84, 121.72 (Tip-CH); 36.86, 36.25, 36.10, 34.56, 34.10 (*iPr*-CH); 24.93, 24.28, 23.94, 23.85, 23.77, 23.62, 22.87 (*iPr*-CH₃) ppm. $^{29}\text{Si}\{^1\text{H}\}$ NMR (59.6 MHz, C_6D_6 , 300 K): $\delta = -1.64$ (*SiTip*₂) ppm. $^{29}\text{Si}\{^1\text{H}\}$ CP-MAS (79.5 MHz, 300 K): $\delta = 0.61$ (*SiTip*₂), -54.3 (*SiTip*), -68.9 (*SiTip*) ppm. UV/Vis (hexane) λ_{max} (ϵ): 352 nm (1951 $\text{M}^{-1}\text{cm}^{-1}$), 408 nm (1773 $\text{M}^{-1}\text{cm}^{-1}$). $\text{C}_{60}\text{H}_{92}\text{Si}_3\text{Se}$: calcd. C 73.79; H, 9.50%; found: C 72.84; H, 9.24%.

Synthesis of 6c: Cyclotrisilene **5** (500 mg, 0.557 mmol) and 1.2 equivalents of tellurium powder (85.4 mg, 0.669 mmol) were mixed in a Schlenk tube. After addition of 10 mL of thf, the reaction mixture was stirred at 40°C for 8 h. Removal of thf in vacuo resulted in an orange solid that was extracted with hexane (2 \times 5 mL) and filtered. The filtrate was concentrated to ca. 2 mL and stored at room temperature. Orange crystals of **6c** were obtained over 2 d and isolated by solvent decantation (280 mg, yield: 50%, m.p. 165–170 $^{\circ}\text{C}$, dec.). $^1\text{H NMR}$ (300.13 MHz, C_6D_6 , 300 K): $\delta = 7.30$ (br., 1 H, Tip-CH); 7.16 (br., overlap with solvent, 3 H, Tip-CH); 7.10 (br., 2 H, Tip-CH); 6.99 (br.,

1 H, Tip-CH); 6.96 (br., 1 H, Tip-CH); 4.96 (m, 1 H, *iPr*-CH); 4.23 (br., 3 H, *iPr*-CH); 3.80 (br., 3 H, *iPr*-CH); 3.16, 3.14 (m, 1 H, *iPr*-CH); 2.76–2.65 (m, 4 H, *iPr*-CH); 1.70 (br., 6 H, *iPr*-CH₃); 1.48, 1.39 (each br, 18 H, *iPr*-CH₃); 1.17, 1.16, 1.14, 1.13 (each br, 27 H, *iPr*-CH₃); 0.94 (br., 21 H, *iPr*-CH₃) ppm. $^{13}\text{C}\{^1\text{H}\}$ NMR (75.47 MHz, C_6D_6 , 300 K): $\delta = 157.80, 156.13, 155.52, 154.48, 153.62, 151.78, 150.41, 150.37, 141.29$ (Tip-CH); 132.82 (Tip-CH); 122.62, 122.36, 122.09, 121.73 (Tip-CH); 38.13, 37.00, 36.37, 36.21, 34.57, 34.51, 34.37, 34.27, 31.79 (*iPr*-CH); 26.51, 25.13, 24.36, 24.22, 23.92, 23.81, 23.80, 23.78, 23.54, 22.88 (*iPr*-CH₃) ppm. $^{29}\text{Si}\{^1\text{H}\}$ NMR (59.6 MHz, C_6D_6 , 300 K): $\delta = -1.24$ (*SiTip*₂) ppm. $^{29}\text{Si}\{^1\text{H}\}$ CP-MAS (79.5 MHz, 300 K): $\delta = 1.1$ (*SiTip*₂), -85.9 (*SiTip*), -98.0 (*SiTip*) ppm. UV/Vis (hexane) λ_{max} (ϵ): 408 nm (1355 $\text{M}^{-1}\text{cm}^{-1}$). $\text{C}_{60}\text{H}_{92}\text{Si}_3\text{Te}$: calcd. C 70.92; H, 9.04%; found: C 69.68; H, 8.72%.

Synthesis of 7a: Cyclotrisilene **5** (400 mg, 0.446 mmol) and one equivalent of S_8 (114 mg, 0.446 mmol) were mixed and dissolved in 10 mL thf. A color change from orange to pale-yellow occurred after the reaction mixture was stirred at room temperature for 1 h. The solvent was removed in vacuo and the resulting pale-yellow residue extracted with hexane (2 \times 5 mL) and filtered. The filtrate was concentrated to ca. 3 mL and stored at room temperature. Colorless crystals of **7a** formed over 2 h and were isolated by solvent decantation (231 mg, yield: 54%, m.p. 217–220 $^{\circ}\text{C}$). $^1\text{H NMR}$ (300.13 MHz, C_6D_6 , 300 K): $\delta = 7.26$ (br., 2 H, Tip-H); 7.07 (br., 4 H, Tip-H); 6.92 (br., 2 H, Tip-H); 4.27–4.22 (m, 3 H, *iPr*-CH); 3.49–3.44 (m, 3 H, *iPr*-CH); 2.78–2.66 (m, 6 H, *iPr*-CH); 1.88 (d, $J_{\text{H,H}} = 6.4$ Hz, 6 H, *iPr*-CH₃); 1.48 (d, $J_{\text{H,H}} = 6.6$ Hz, 9 H, *iPr*-CH₃); 1.40 (br., 6 H, *iPr*-CH₃); 1.21, 1.19 (each d, 18 H, *iPr*-CH₃); 1.13 (d, $J_{\text{H,H}} = 6.9$ Hz, 18 H, *iPr*-CH₃); 0.98 (d, $J_{\text{H,H}} = 6.7$ Hz, 6 H, *iPr*-CH₃); 0.47 (d, $J_{\text{H,H}} = 6.7$ Hz, 6 H, *iPr*-CH₃) ppm. $^{13}\text{C}\{^1\text{H}\}$ NMR (75.47 MHz, C_6D_6 , 300 K): $\delta = 156.96, 153.65, 153.20, 152.27, 151.81, 150.00$ (Tip-C); 135.04 (Tip-CH); 124.46, 123.04, 122.48, 122.07 (Tip-CH); 37.99, 35.31, 34.50, 34.38 (*iPr*-CH); 28.06, 24.77, 24.74, 24.12, 24.04, 23.83, 23.73, 23.61, 22.97 (*iPr*-CH₃) ppm. $^{29}\text{Si}\{^1\text{H}\}$ NMR (59.6 MHz, C_6D_6 , 300 K): $\delta = 35.37$ (*SiTip*₂), -9.18 (*SiTip*) ppm. $\text{C}_{60}\text{H}_{92}\text{Si}_3\text{S}_2$: calcd. C 74.93; H, 9.64%; found: C 73.15; H, 9.44%.

Synthesis of 7b: Cyclotrisilene **5** (300 mg, 0.33 mmol) and excess amount of selenium powder (156 mg, 1.98 mmol) were mixed and dispersed in 6 mL thf. After the reaction mixture was stirred at room temperature overnight, thf was removed in vacuo, and the resulting residue was extracted with hexane (2 \times 5 mL) and filtered. The filtrate was concentrated to ca. 3 mL, colorless crystals of **7b** were obtained at room temperature overnight and isolated by solvent decantation (174 mg, yield: 50%). $^1\text{H NMR}$ (300.13 MHz, C_6D_6 , 300 K): $\delta = 7.26$ (s, 2 H, Tip-CH); 7.06 (br., 4 H, Tip-CH); 6.91 (s, 2 H, Tip-CH); 4.42–4.34 (m, 2 H, *iPr*-CH); 4.03 (br., 2 H, *iPr*-CH); 3.62 (br., 2 H, *iPr*-CH); 3.47–3.40 (m, 2 H, *iPr*-CH); 2.78–2.62 (m, 4 H, *iPr*-CH); 1.86 (d, $J_{\text{H,H}} = 6.2$ Hz, 6 H, *iPr*-CH₃); 1.48 (d, $J_{\text{H,H}} = 6.3$ Hz, 12 H, *iPr*-CH₃); 1.21, 1.19, 1.17 (each d, 18 H, *iPr*-CH₃); 1.13 (br., 6 H, *iPr*-CH₃); 1.11 (br., 6 H, *iPr*-CH₃); 0.92 (d, $J_{\text{H,H}} = 6.6$ Hz, 6 H, *iPr*-CH₃); 0.69 (br., 6 H, *iPr*-CH₃); 0.41 (d, $J_{\text{H,H}} = 6.5$ Hz, 6 H, *iPr*-CH₃) ppm. $^{13}\text{C}\{^1\text{H}\}$ NMR (75.47 MHz, C_6D_6 , 300 K): $\delta = 153.39, 153.17, 151.99, 149.95$ (Tip-C); 136.11 (Tip-CH); 123.26, 122.73, 122.18 (Tip-CH); 37.66, 35.58, 35.14, 34.49, 31.79, 29.30, 27.75 (*iPr*-CH); 24.79, 24.27, 24.01, 23.81, 23.72, 23.60, 22.87 (*iPr*-CH₃) ppm. $^{29}\text{Si}\{^1\text{H}\}$ NMR (59.6 MHz, C_6D_6 , 300 K): $\delta = 37.16$ (*SiTip*₂), -31.62 (*SiTip*) ppm. $\text{C}_{60}\text{H}_{92}\text{Si}_3\text{S}_2$: calcd. C 68.27; H, 8.79%; found: C 67.25; H, 8.64%.

Synthesis of 9: At room temperature **6c** (100 mg, 0.11 mmol) was dissolved in 5 mL thf and the resulting solution was heated to 60°C for 2 h in a sealed Schlenk tube. After that the solution was cooled

down to room temperature, water (20 μL) was added in 10-fold excess to the reaction mixture via micro syringe. The resulting colorless mixture was stirred for 5 min followed by removal of solvent in vacuo. The residue was extracted by addition of 5 mL toluene and filtered. The filtrate was condensed to ca. 2 mL and kept at room temperature. Colorless crystals of **9** appeared overnight, which were isolated by solvent decantation and dried in vacuo (34 mg, yield: 30%). $^1\text{H NMR}$ (300.13 MHz, C_6D_6 , 300 K): δ = 7.19 (br., 2 H, SiTip₂ Tip-CH); 7.13 (br., 2 H, SiTip₂ Tip-CH); 7.09 (br., 2 H, Tip-CH); 7.06 (br., 2 H, SiTip₂ Tip-CH); 6.96 (br., 2 H, SiTip Tip-CH); 6.88 (br., 2 H, SiTip₂ Tip-CH); 6.80 (br., 2 H, Tip-CH); 6.62 (br., 1 H, Tip-CH); 6.52 (br., 2 H, SiH); 5.70 (m, 2 H, iPr-CH); 4.99–4.92 (m, 2 H, iPr-CH); 4.17–4.13 (m, 2 H, iPr-CH); 3.90–3.82 (m, 2 H, iPr-CH), 3.52 (m, 2 H, iPr-CH); 3.18–3.12 (m, 2 H, iPr-CH); 2.84–2.68, 2.62–2.52 (m, 12 H, iPr-CH₃); 1.79 (d, $J_{\text{H,H}}$ = 6.7 Hz, 6 H, iPr-CH₃); 1.75 (d, $J_{\text{H,H}}$ = 6.7 Hz, 3 H, iPr-CH₃); 1.56 (d, $J_{\text{H,H}}$ = 6.5 Hz, 9 H, iPr-CH₃); 1.45 (d, $J_{\text{H,H}}$ = 6.5 Hz, 6 H, iPr-CH₃); 1.40, 1.38, 1.36 (each br, total 18 H, iPr-CH₃); 1.31, 1.29 (each d, 21 H, iPr-CH₃); 1.26 (d, $J_{\text{H,H}}$ = 2.8 Hz, 6 H, iPr-CH₃); 1.24 (d, $J_{\text{H,H}}$ = 6.9 Hz, 6 H, iPr-CH₃); 1.08, 1.06, 1.04, 1.02 (each d, total 24 H, iPr-CH₃); 0.73–0.70 (m, 9 H, iPr-CH₃); 0.57 (d, $J_{\text{H,H}}$ = 6.4 Hz, 6 H, iPr-CH₃); 0.44–0.40 (m, 12 H, iPr-CH₃); 0.36 (d, $J_{\text{H,H}}$ = 6.7 Hz, 6 H, iPr-CH₃); 0.27 (d, $J_{\text{H,H}}$ = 6.3 Hz, 12 H, iPr-CH₃) ppm. $^{13}\text{C}\{^1\text{H}\}$ NMR (75.47 MHz, C_6D_6 , 300 K): δ = 158.63, 155.43, 155.01, 154.83, 154.64, 154.11, 153.83, 151.82, 150.81, 150.50, 149.48, 149.28 (Tip-C); 136.50, 133.92, 131.58, 130.21, 129.15, 128.39, 125.52, 124.73, 122.96, 122.65, 122.42, 122.25, 122.05, 121.72 (Tip-CH); 39.12, 36.40, 36.23, 35.94, 34.98, 34.81, 34.27, 34.14, 33.45 (iPr-CH); 31.37, 30.91, 30.04, 29.07, 27.86, 26.68, 26.44, 25.7, 25.34, 25.27, 25.13, 24.45, 24.31, 23.78, 23.73, 23.59, 23.49, 23.13, 21.64 (iPr-CH₃) ppm. $^{29}\text{Si}\{^1\text{H}\}$ NMR (59.6 MHz, C_6D_6 , 300 K): δ = -2.22 (SiTeTip), -28.87 (SiTip), -45.36 (SiTip₂) ppm. $\text{C}_{120}\text{H}_{186}\text{OSi}_6\text{Te}_2$: calcd. C 69.68; H, 9.06%; found: C 68.37; H, 8.62%.

Supporting Information (see footnote on the first page of this article): Plots of NMR spectra (Figure S1–S33), UV/vis spectra (Figure S34–S39), molecular structure of **6b** (Figure S40), X-Ray crystallographic and computational details.

Acknowledgements

Financial support by China Scholarship Council (doctoral scholarship H.Z.), as well as by Saarland University and COST Action CM1302 (Smart Inorganic Polymers) is gratefully acknowledged.

Keywords: Subvalent compounds; Silanes; Chalcogens; Cyclo[1.1.0]butane analogues; Heavier cyclobutenes

References

- Heavier group 14 species, reviews: a) A. Rammo, D. Scheschke-witz, *Chem. Eur. J.* **2018**, *24*, 1–21; b) J. Teichmann, M. Wagner, *Chem. Commun.* **2018**, *54*, 1397–1412; c) C. Präsang, D. Scheschke-witz, *Chem. Soc. Rev.* **2016**, *45*, 900–921; d) M. Unno, *Struct. Bonding (Berlin)* **2014**, *156*, 49–84; e) G. He, O. Shynkaruk, M. W. Lui, E. Rivard, *Chem. Rev.* **2014**, *114*, 7815–7880; f) V. Y. Lee, A. Sekiguchi, J. Escudié, H. Ranaivonjatovo, *Chem. Lett.* **2010**, *39*, 312–318.
- a) A. Jana, I. Omlor, V. Huch, H. S. Rzepa, D. Scheschke-witz, *Angew. Chem. Int. Ed.* **2014**, *53*, 9953–9956; *Angew. Chem.* **2014**, *126*, 10112–10116; b) A. Jana, V. Huch, H. S. Rzepa, D. Scheschke-witz, *Angew. Chem. Int. Ed.* **2015**, *54*, 289–292; *Angew. Chem.* **2015**, *127*, 291–295; c) A. Jana, V. Huch, H. S. Rzepa, D. Scheschke-witz, *Organometallics* **2015**, *34*, 2130–2133.
- a) S. Masamune, Y. Kabe, S. Collins, *J. Am. Chem. Soc.* **1985**, *107*, 5552–5553; b) R. Jones, D. J. Williams, Y. Kabe, S. Masamune, *Angew. Chem. Int. Ed. Engl.* **1986**, *25*, 173–174; c) P. v. R. Schleyer, A. F. Sax, J. Kalcher, R. Janoschek, *Angew. Chem. Int. Ed. Engl.* **1987**, *26*, 364–366; d) M. Kira, T. Iwamoto, C. Kabuto, *J. Am. Chem. Soc.* **1996**, *118*, 10303–10304; e) T. Iwamoto, D. Z. Yin, C. Kabuto, M. Kira, *J. Am. Chem. Soc.* **2001**, *123*, 12730–12731; f) N. Wiberg, H. Auer, S. Wagner, K. Polborn, G. Kramer, *J. Organomet. Chem.* **2001**, *619*, 110–131; g) K. U. Ohshima, T. Iwamoto, M. Kira, *Organometallics* **2008**, *27*, 320–323.
- a) D. Scheschke-witz, H. Amii, H. Gornitzka, W. W. Schoeller, D. Bourissou, G. Bertrand, *Science* **2002**, *295*, 1880–1881; b) D. Scheschke-witz, H. Amii, H. Gornitzka, W. W. Schoeller, D. Bourissou, G. Bertrand, *Angew. Chem.* **2004**, *116*, 595–597; c) A. Rodriguez, R. A. Olsen, N. Ghaderi, D. Scheschke-witz, F. S. Tham, L. J. Mueller, G. Bertrand, *Angew. Chem.* **2004**, *116*, 4988–4991.
- Addition to Si–Si: a) M. Weidenbruch, A. Schäfer, R. Rankers, *J. Organomet. Chem.* **1980**, *195*, 171–184; b) E. Hengge, H. G. Schuster, *J. Organomet. Chem.* **1982**, *231*, 17–20; c) D. Seyferth, E. W. Goldman, J. Escudie, *J. Organomet. Chem.* **1984**, *260–278*, 337–352; d) C. W. Carlson, R. West, *Organometallics* **1983**, *2*, 1798–1801; e) B. Wrackmeyer, E. V. Klimkina, W. Milius, *Z. Anorg. Allg. Chem.* **2012**, *638*, 1080–1092; f) M. Unno, *Phosphorus Sulfur Sulfur* **2011**, *186*, 1259–1262.
- Addition to Si=Si: a) M. J. Michalczyk, R. West, J. Michl, *J. Chem. Soc., Chem. Commun.* **1984**, 1525–1526; b) R. West, D. J. De Young, K. J. Haller, *J. Am. Chem. Soc.* **1985**, *107*, 4942–4946; c) J. E. Mangette, D. R. Powell, R. West, *Organometallics* **1995**, *14*, 3551–3557; d) A. Yuasa, T. Sasamori, Y. Hosoi, Y. Furukawa, N. Tokitoh, *Bull. Chem. Soc. Jpn.* **2009**, *82*, 793–805; e) R. P.-K. Tan, G. R. Gillette, D. R. Powell, R. West, *Organometallics* **1991**, *10*, 546–551; f) S. Khan, R. Michel, D. Koley, H. W. Roesky, D. Stalke, *Inorg. Chem.* **2011**, *50*, 10878–10883; g) C. Mohapatra, K. C. Mondal, P. P. Samuel, H. Keil, B. Niepötter, R. Herbst-Irmer, D. Stalke, S. Dutta, D. Koley, H. W. Roesky, *Chem. Eur. J.* **2015**, *21*, 12572–12576; h) Y. C. Chan, B. X. Leong, Y. Li, M. C. Yang, Y. Li, M. D. Su, C. W. So, *Angew. Chem. Int. Ed.* **2017**, *56*, 11561–11569.
- M. Ichinohe, T. Matsuno, A. Sekiguchi, *Angew. Chem. Int. Ed.* **1999**, *38*, 2194–2196.
- a) V. Y. Lee, S. Miyazaki, H. Yasuda, A. Sekiguchi, *J. Am. Chem. Soc.* **2008**, *130*, 2758–2759; b) V. Y. Lee, S. Miyazaki, H. Yasuda, A. Sekiguchi, *Phosphorus Sulfur Sulfur* **2011**, *186*, 1346–1350; c) V. Y. Lee, O. A. Gapurenko, S. Miyazaki, A. Sekiguchi, R. M. Minyaev, V. I. Minkin, H. Gornitzka, *Angew. Chem. Int. Ed.* **2015**, *54*, 1–6.
- K. Leszczyńska, K. Abersfelder, A. Mix, B. Neumann, H. G. Stammner, M. J. Cowley, P. Putzi, D. Scheschke-witz, *Angew. Chem. Int. Ed.* **2012**, *51*, 6785–6788.
- M. J. Cowley, Y. Ohmori, V. Huch, M. Ichinohe, A. Sekiguchi, D. Scheschke-witz, *Angew. Chem. Int. Ed.* **2013**, *52*, 13247–13250.
- Y. Ohmori, M. Ichinohe, A. Sekiguchi, M. J. Cowley, V. Huch, D. Scheschke-witz, *Organometallics* **2013**, *32*, 1591–1594.
- a) M. J. Cowley, V. Huch, H. S. Rzepa, D. Scheschke-witz, *Nat. Chem.* **2013**, *5*, 876–879; b) H. Zhao, K. Leszczyńska, L. Klemmer, V. Huch, M. Zimmer, D. Scheschke-witz, *Angew. Chem. Int. Ed.* **2018**, *57*, 2445–2449.
- a) H. Zhao, M. J. Cowley, M. Majumdar, V. Huch, M. Zimmer, D. Scheschke-witz, submitted; b) M. Ichinohe, T. Matsuno, A. Sekiguchi, *Chem. Commun.* **2001**, 183–184.
- a) S. Nagase, T. Kudo, *J. Chem. Soc., Chem. Commun.* **1984**, 1392–1394; b) S. Ishida, T. Iwamoto, M. Kira, *Organometallics* **2009**, *28*, 919–921.
- a) W. W. Schöller, T. Dabisch, T. Busch, *Inorg. Chem.* **1987**, *26*, 4383–4389; b) J. A. Boat, M. S. Gordon, *Organometallics* **1996**,

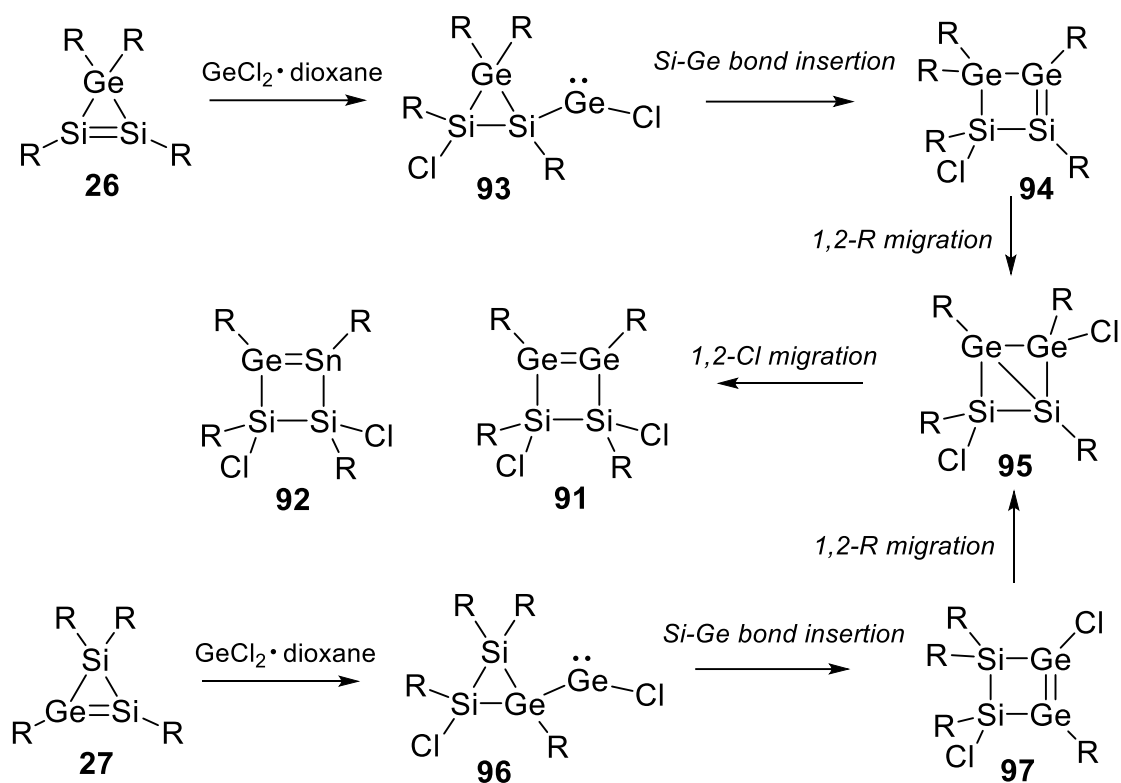
- 15, 2118–2124; c) R. Koch, T. Bruhn, M. Weidenbruch, *J. Mol. Struct.* **2004**, 680, 91–97.
- [16] σ – π interaction between Si–Si and aromatic rings: a) R. Gleiter, W. Schäfer, G. Krennrich, H. Sakurai, *J. Am. Chem. Soc.* **1988**, 110, 4117–4120; b) A. Sekiguchi, T. Yatabe, C. Kabuto, H. Sakurai, *Angew. Chem. Int. Ed. Engl.* **1989**, 28, 757–758.
- [17] a) P. P. Power, *Chem. Rev.* **1999**, 99, 3463–3503; b) M. Kira, T. Iwamoto, *Adv. Organomet. Chem.* **2006**, 54, 73–148.
- [18] D. Auer, C. Strohmann, A. V. Arbuznikov, M. Kaupp, *Organometallics* **2003**, 22, 2442–2449.

Received: May 2, 2018

Published online: June 26, 2018

3.5 Supplementary Results: Reactivity of Cyclotrisilene towards Divalent Species of Group 14 Elements

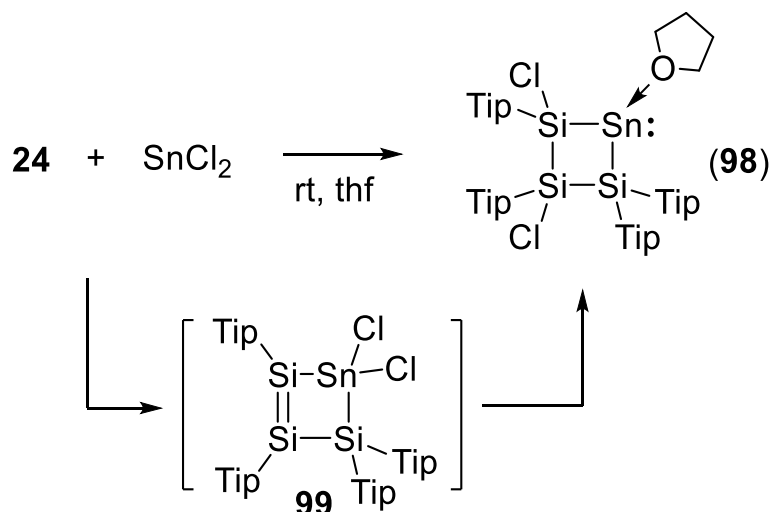
In 2003, Sekiguchi *et al.* reported a rather unusual type of reaction of the 1-disilagermirene **26** and 2-disilagermirene **27** with GeCl_2 -dioxane, which gave fast and effective access to disiladigermetene **91** as a new unsaturated four-membered ring system consisting of Ge=Ge double bond (Scheme 51).¹⁰³ Formation of **91** was proposed to proceed through GeCl_2 -dioxane oxidative addition across the Si=Si double bond to produce chlorogermylene **93** (**96** in the case of **27**). The resulting **93** (**96**) then would quickly undergo intramolecular insertion into the Si–Ge bond to form compound **94** (**97**) with a Si=Ge (Ge=Ge) bond. The latter then could possibly rearrange to bicyclo[1.1.0]butane derivative **95** followed by 1,2-Cl migration to form the final **91**. The general applicability of this protocol was demonstrated by the reaction of both **26** and **27** with SnCl_2 -dioxane, which quantitatively produced the same product **92** (Scheme 51). In our previous research these heavy dichlorocarbene analogues were used as well as a source of germanium and tin to synthesize the germanium- and tin-substituted dismutational isomer of benzene analogues $\text{E}_2\text{Si}_4\text{R}_4$ (E = Ge, Sn).¹⁰⁴ With the knowledge of reactivity of cyclotrisilene **24** towards a wide range of reagents as discussed in the chapter 1.7 and 3.1-0, we were therefore inspired to investigate its reactivity towards these divalent species of Group 14 elements.



Scheme 51. Reaction of 1-disilagermirene **26** and 2-disilagermirene **27** with $\text{GeCl}_2/\text{SnCl}_2 \cdot \text{dioxane}$ yields **91** and **92**, respectively, and the proposed mechanism.¹⁰³

3.5.1 Reactions of **24** with SnCl_2

A solution of cyclotrisilene **24** was introduced *via* cannula to the colorless suspension of SnCl_2 in thf at room temperature. Color of the mixture turned green immediately after the first several drops of cyclotrisilene had been added. After complete addition the reaction mixture gradually turned dark-brown. Yellow crystals of **98** are obtained by crystallization at 5 °C accompanied by precipitated particles of elemental Sn (Scheme 52). The green color at the very beginning of the reaction could hint towards an initial σ -bond insertion intermediate **99**, from which the final product **98** could be derived by a twofold migration of chlorine atoms from the tin center to the unsaturated $\text{Si}=\text{Si}$ moiety.



Scheme 52. Reaction of **24** with SnCl_2 results in **98**.

In the ^1H NMR spectrum of **98**, the resonances of the coordinated thf molecule are detected at δ 3.51, 3.47 and 1.62 ppm as broad signals. Due to the low stability of **98** in both deuterated- thf and benzene (complex signals appeared in ^{29}Si NMR spectrum after **98** was dissolved in these solvents over 30 minutes), ^{29}Si CP-MAS was measured in order to obtain reliable data of the chemical shifts of **98** regarding its integrity in solution. As shown in Figure 13, three signals appear in the solid state NMR spectrum at δ 36.6, 19.1 and 16.5 ppm, of which the latter signal at δ 15.6 ppm is slightly broad in comparison to another two singlet signals. Needle-shaped yellow crystals of **98** suitable for X-ray single crystal structure analysis were obtained by careful crystallization from thf at 0 °C, and isolated by solvent decantation in 40% yield. UV/vis spectroscopy recorded on a light-yellow tetrahydrofuran solution shows a clear maximum at λ 271 nm mainly resulting from the aryl substituents absorption and a weak shoulder at λ 450 nm (see: 9.2.2 UV/vis Spectra and Determination of ϵ for **98**). The molecular structure of **98** in the solid state is shown in Figure 14.

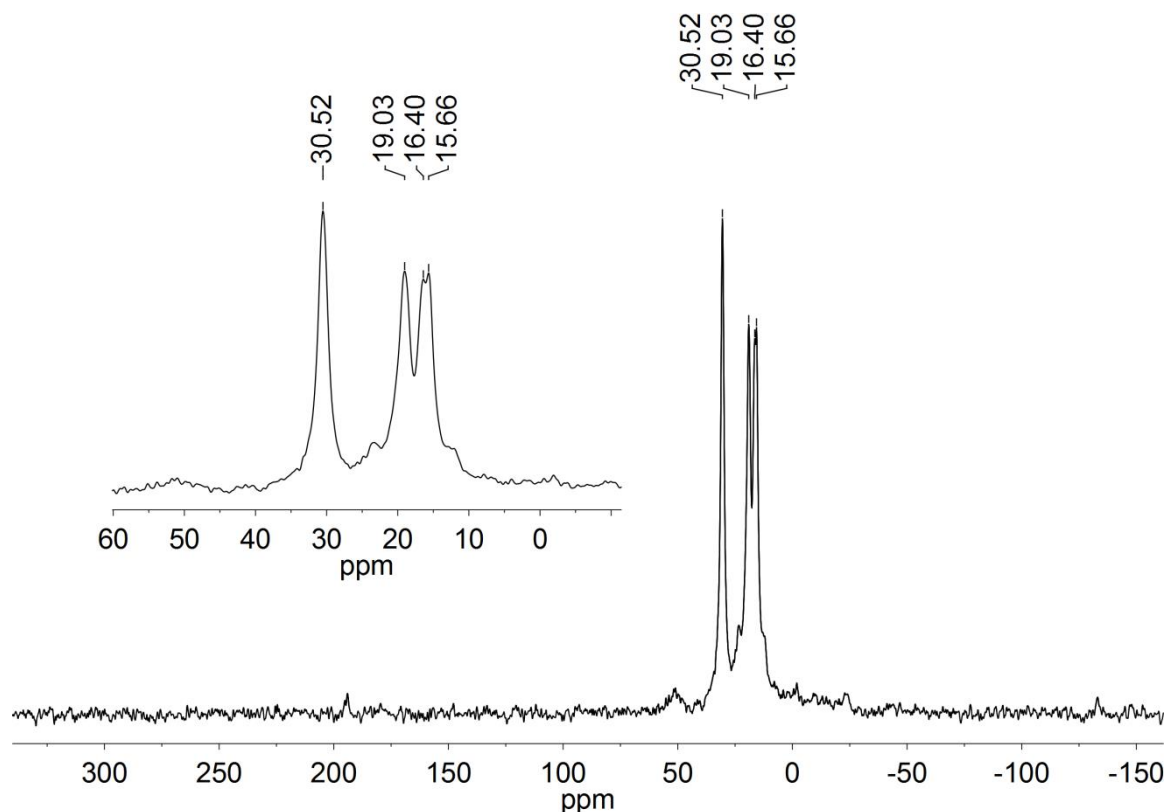


Figure 13. ^{29}Si CP-MAS NMR spectrum (79.5 MHz, 300 K) of **98**.

X-ray structure analysis confirms the cyclic four-membered constitution, wherein the two chlorine atoms are in *trans*-configuration with angles of Cl1-Si1-Si2 at $112.5(1)^\circ$ and Cl2-Si2-Si1 at $80.6(9)^\circ$. The Si-Si bond lengths (Si1-Si2 2.371(2) Å, Si2-Si3 2.412(3) Å) are within the normal range of Si-Si single bond lengths. The Si-Sn bond lengths (Sn1-Si3 2.719(3) Å, Si1-Sn1 2.701(3) Å) are slightly longer than that in the cyclic disilylated stannylene phosphane adduct (2.648 and 2.653 Å) reported by Marschner and Müller *et al.*¹⁰⁵ and even longer than that of 1-stannacyclopentasilane (2.620 and 2.594 Å).¹⁰⁶ Nonetheless, the Sn1-O1 bond length (2.372(3) Å) is significantly longer than that of the Sn-P bond (Sn-P 2.608 Å) of the stannylene phosphane adduct.¹⁰⁵ The Sn1 is significantly pyramidal with sum of the bonding angles at 276.5° (Figure 14). The four-membered skeleton of **98** exhibits a folding constitution with a derivation of Sn1 from the plane of Si1-Si2-Si3 being 1.317 Å.

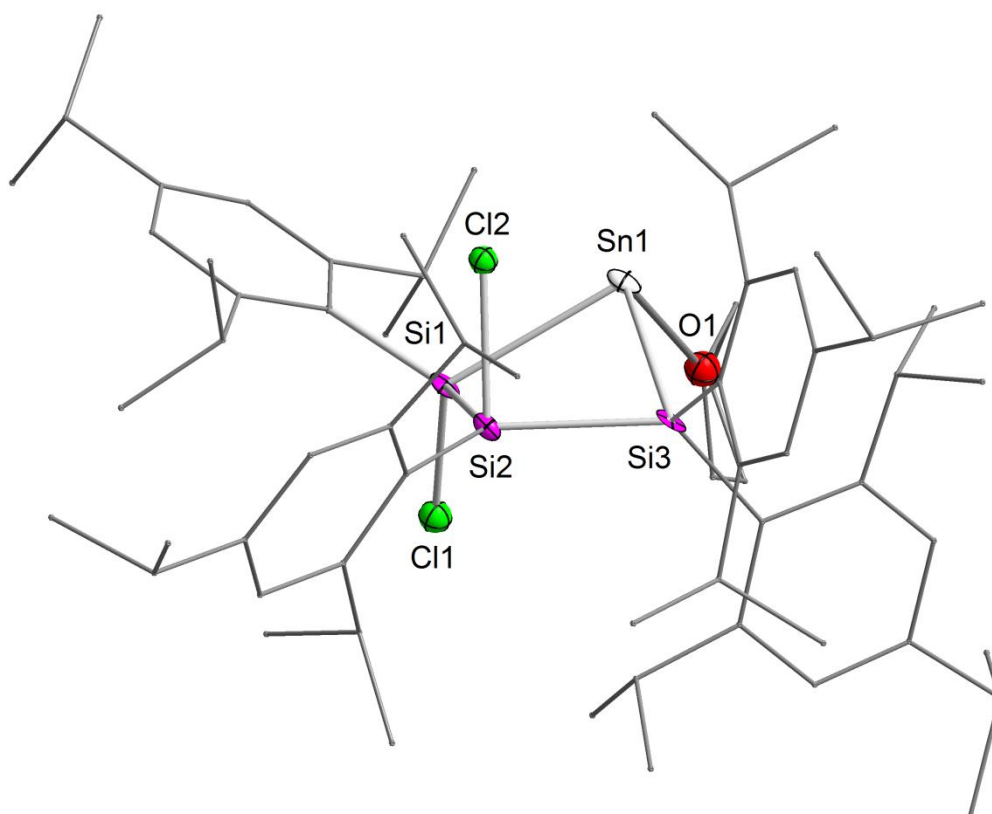
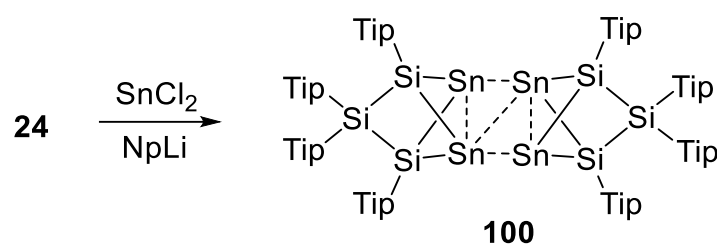


Figure 14. Molecular structure of **98** in solid state. Thermal ellipsoid at 50%. Selected bond lengths [Å] and angles [°]: Si1-Si2 2.371(2), Si2-Si3 2.410(3), Sn1-Si3 2.720(3), Si1-Sn1 2.700(3), Sn1-O1 2.371(3), Si1-Cl1 2.105(4), Si2-Cl2 2.177(2); Cl1-Si1-Si2 112.5(1), Cl2-Si2-Si1 80.6(9), Si1-Sn1-Si3 82.7(9), Sn1-Si1-Si2 84.0(2), Si1-Si2-Si3 97.0(9), Sn1-Si3-Si2 82.8(2), Si1-Sn1-O1 96.6(1), O1-Sn1-Si3 97.2(1).

3.5.2 Reduction of **98** with NpLi

The two chlorine atoms in **98** was supposed to originate from SnCl₂ which undergoes σ -insertion with cyclotrisilene **24** followed by chlorine migration to Si=Si double bond resulting simultaneously in the stannylene stabilized with donor solvent thf. Therefore we sought to remove the chlorine atoms with reduce reagent in order to reproduce the Si=Si double bond in the four-membered ring and further obtain a targeted cyclic disilyl stannylene. Considering the low stability of **98** in thf the procedure was performed without isolating it. Therefore after cyclotrisilene **24** had been added to the suspension of SnCl₂ in thf and stirred the reaction mixture for 30 minutes, the brown mixture was cooled down to -30 °C and newly prepared naphthalene lithium

suspension was introduced. The color gradually changed and finally an opaque green mixture resulted, which was brought to room temperature with stirring overnight. Removal of thf in vacuum resulted in a green residue, which showed the complete disappearance of the starting material by ^1H and ^{29}Si NMR spectra. NMR spectroscopy, however, does not provide any useful information in identifying the product due to the multitude of signals (Figure 15). The green residue was dissolved in hexane from which green blocks of **100** formed after storing at room temperature for one month.



Scheme 53. Reduce the mixture of **24** and SnCl_2 with NpLi affording Si/Sn cluster **100** in a non-stoichiometric manner.

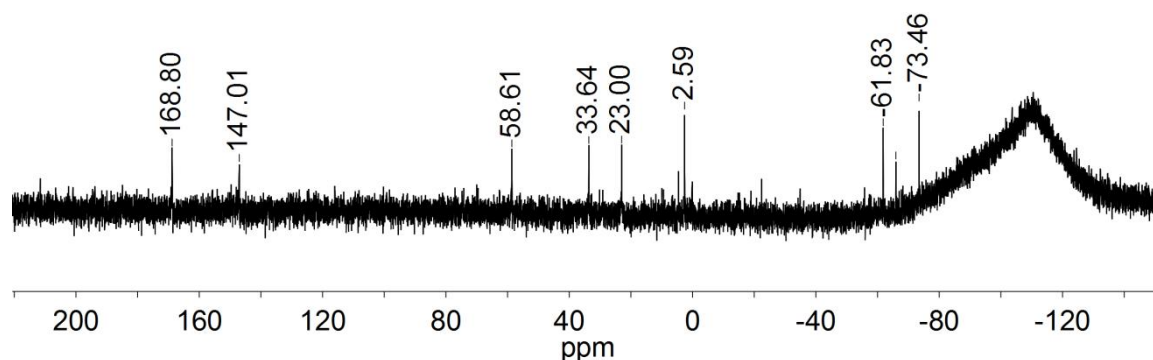


Figure 15. ^{29}Si NMR spectrum (79.5 MHz, C_6D_6 , 300 K) of the reaction mixture of **24** with SnCl_2 and NpLi .

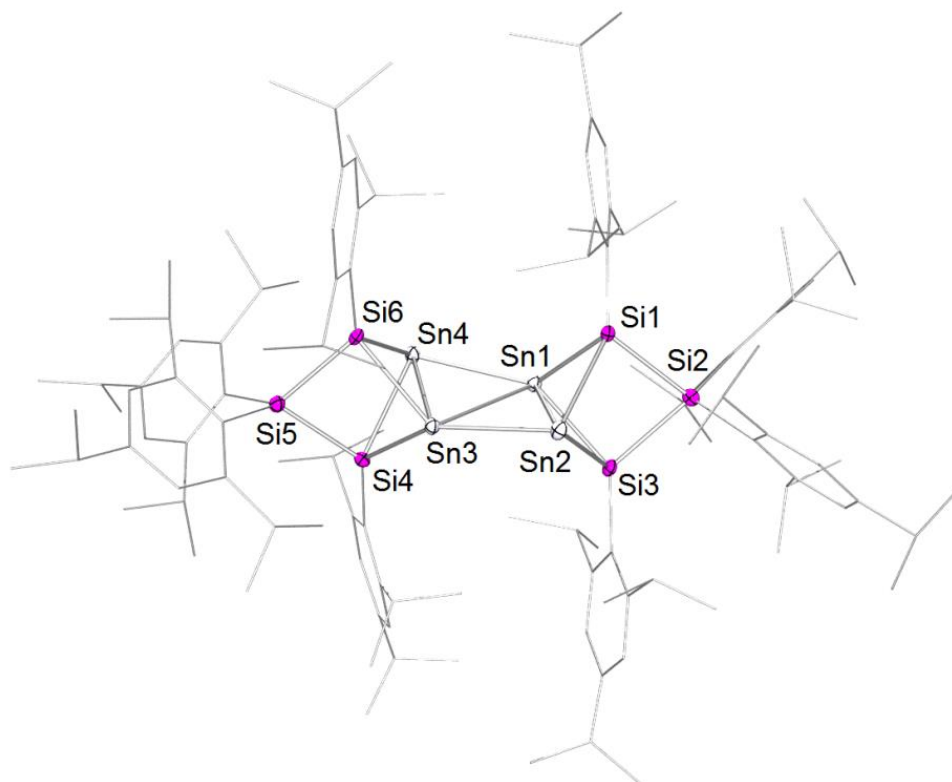


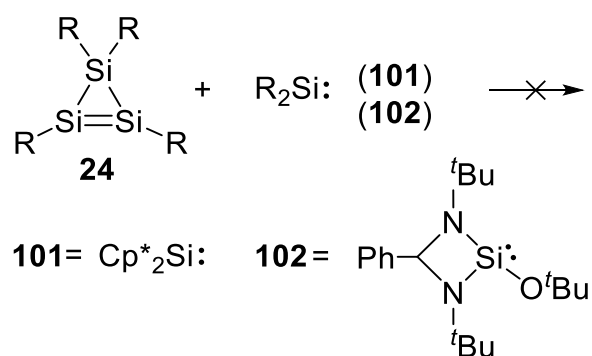
Figure 16. Molecular structure of **100** in solid state. Thermal ellipsoid at 50%. Selected bond lengths [Å] and angles [°]: Si1-Si2 2.418(2), Si2-Si3 2.382(2), Si1-Sn1 2.573(2), Si1-Sn2 2.668(2), Si3-Sn1 2.568(2), Si3-Sn2 2.710(2), Si5-Si6 2.389(2), Si5-Si4 2.384(2), Si6-Sn4 2.680(2), Si6-Sn3 2.581(2), Si4-Sn4 2.705(2), Si4-Sn3 2.561(2), Sn4-Sn1 2.905(3), Sn4-Sn3 3.163(2), Sn3-Sn2 2.915(3), Sn1-Sn2 3.152(3), Sn3-Sn1 3.094(2); Si6-Si5-Si4 81.5(6), Si1-Si2-Si3 81.5(6), Sn1-Sn4-Sn3 61.1(4), Sn4-Sn1-Sn2 117.8(5).

X-ray crystal structure analysis revealed the constitution of these green crystals to be a Si_6Sn_4 cluster with four-coordinate silicon atoms and four three-coordinate tin atoms (Scheme 53, Figure 16). In the molecular skeleton all Si-Si bond lengths (from 2.382 (2) to 2.418(2) Å) lie within the normal Si-Si single bond length range, most of the Si-Sn bond lengths (2.568(2) to 2.680(2) Å) are also comparable with the Si-Sn single bond lengths of 1-stannacyclopentasilane (2.620 and 2.594 Å)¹⁰⁶ and the tin-substituted dismutational isomer of benzene analogues $\text{Sn}_2\text{Si}_4\text{Tip}_4$ (2.602 to 2.657 Å).¹⁰⁴ The distances between the three-coordinate tin atoms Sn1-Sn2 and Sn3-Sn4 are 3.152(3) Å and 3.163(2) Å, respectively, and thus 0.042 Å longer than that of $\text{Sn}_2\text{Si}_4\text{Tip}_4$ (3.110 Å).¹⁰⁴ The other Sn-Sn distances are Sn4-Sn1 2.905(3), Sn3-Sn2

2.915(3), Sn3-Sn1 3.094(2) Å, much longer than the distance expected from normal Sn-Sn single bond (2.81 Å). An electron map of Sn atoms in **100** could probably be clarified with the help of calculations. Therefore, for the time being, the connectivity of the central four Sn atoms was depicted as in Scheme 53 using dash bonds. However, due to the small quantity of crystals, measurement of ^{29}Si as well as ^{119}Sn NMR of **100** failed. A repeat experiment on a preparative scale failed (no crystal is obtained even after two months).

3.5.3 Attempted reactions of cyclotrisilene **24** with silylenes

Considering the high reactivity of cyclotrisilene **24** towards SnCl_2 even at room temperature, we investigated its reactivity towards the silicon analogues of carbenes – silylenes, numerous stable representatives of which have been isolated and shown to be highly reactive towards small molecules.¹³ Silylenes **101** and **102**, however, did not react with cyclotrisilene **24**, even after heating the reaction mixture to 60 °C overnight (Scheme 54). Only signals of starting material and – presumably – unidentified decomposition products of cyclotrisilene were observed in the ^1H NMR of the reaction mixture (Figure 17).



Scheme 54. Attempted reactions of **24** with silylenes **101** and **102**.

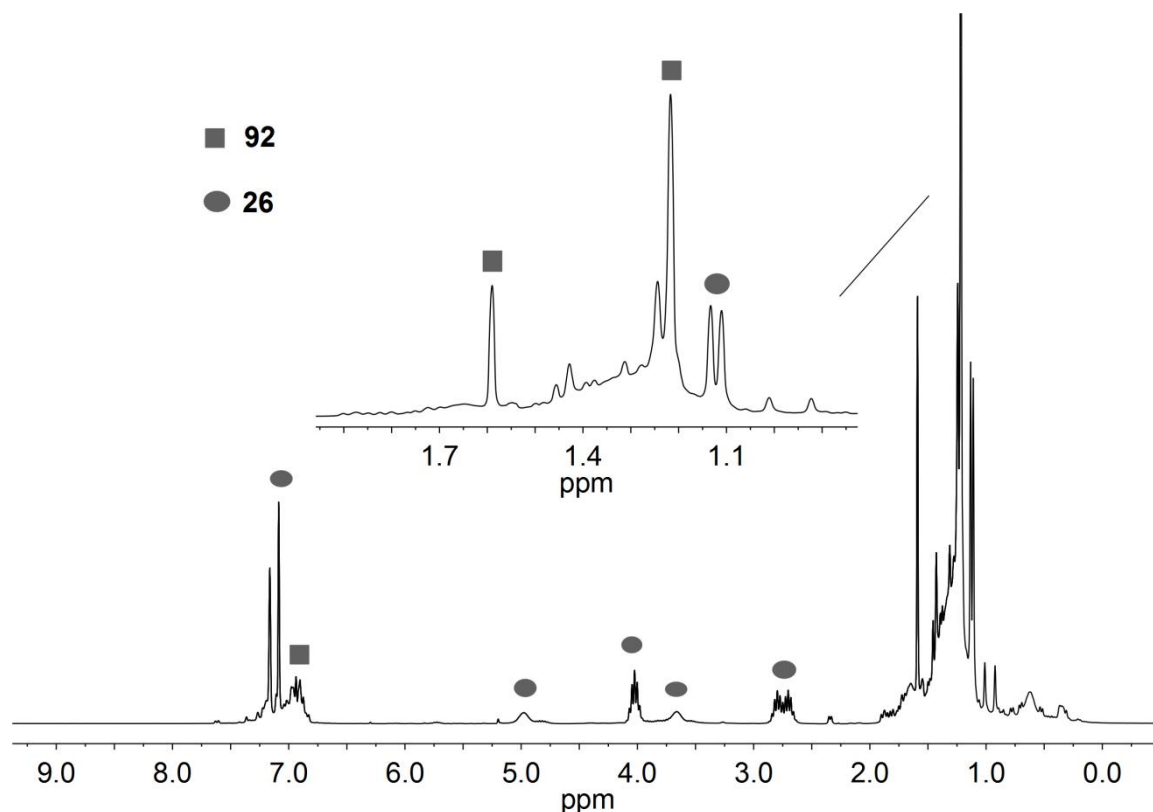


Figure 17. ^1H NMR spectrum (300.13 MHz, C_6D_6 , 300 K) of the reaction mixture of **24** with **102**.

3.5.4 Reaction of **24** with Roesky silylene

Solid cyclotrisilene **24** and one equivalent of Roesky silylene **103** were mixed in a NMR tube and dissolved in C_6D_6 at room temperature, immediately resulting in condensed deep-red solution. The reaction mixture was monitored by ^1H NMR which showed the appearance of new sets of signals after thirty minutes at room temperature. Conversion was complete after two hours at room temperature (confirmed by ^1H NMR) and at that point the ^{29}Si NMR was measured. As shown in Figure 18, apart from the signal of excess Roesky silylene at δ 14.1 ppm, another two sets of signals also appear at (i) δ 21.1, 2.7, -7.9 and -25.8 ppm (ii) δ -8.6 , -20.0 , -24.5 and -49.3 ppm as sharp singlets, indicating the formation of two products.

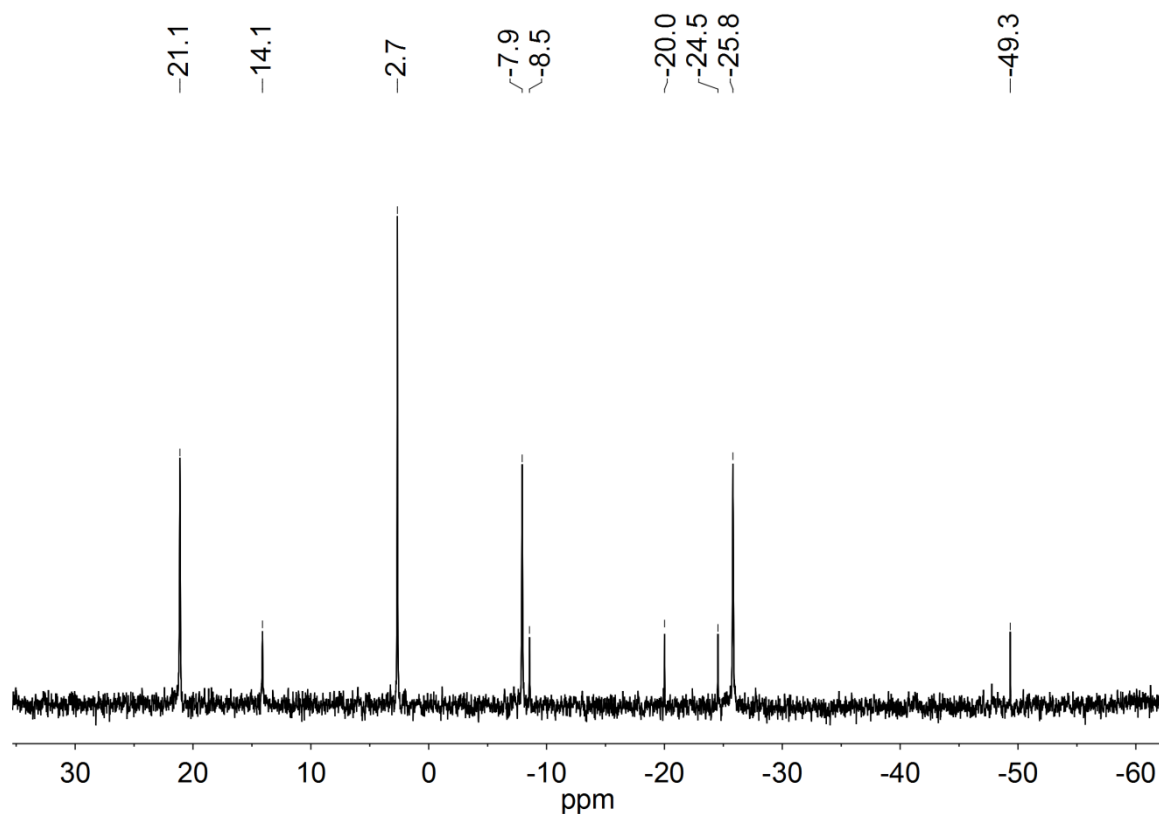
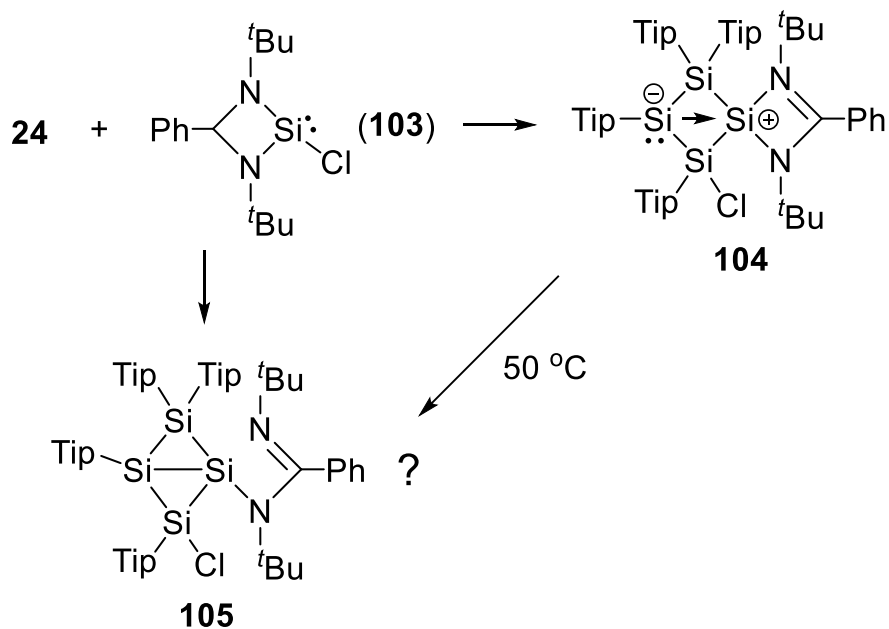


Figure 18. ^{29}Si NMR spectrum (59.6 MHz, C_6D_6 , 300 K) of the reaction mixture of **24** with **103**.



Scheme 55. Reaction of **24** with Roesky silylene **103** yields **104** and **105**.

The reaction was repeated on a preparative scale (**24**: 300 mg, **103**: 99 mg) in a Schlenk flask using toluene as solvent. After the resulting reaction mixture was stirred

at room temperature for four hours, toluene was removed in vacuum and hexane was introduced into the resulted brown residue. A bright-orange precipitate **104** formed immediately after hexane addition (Scheme 55) and was isolated by filtration. Due to the low solubility of **104** in C_6D_6 , ^{29}Si CP-MAS NMR was measured and showed signals at δ 21.9, 1.1, -10.4 and -23.5 ppm (Figure 19, up). In the UV/vis spectroscopy **104** shows obviously the longest wavelength absorption at λ_{max} 422 nm (ϵ 5820 L mol $^{-1}$ cm $^{-1}$). Crystals suitable for X-ray structure analysis formed from a condense hexane solution. The structure of **104** was confirmed to be a four-membered Si_4 ring composing of three- and four-coordinated silicon atoms (Figure 20).

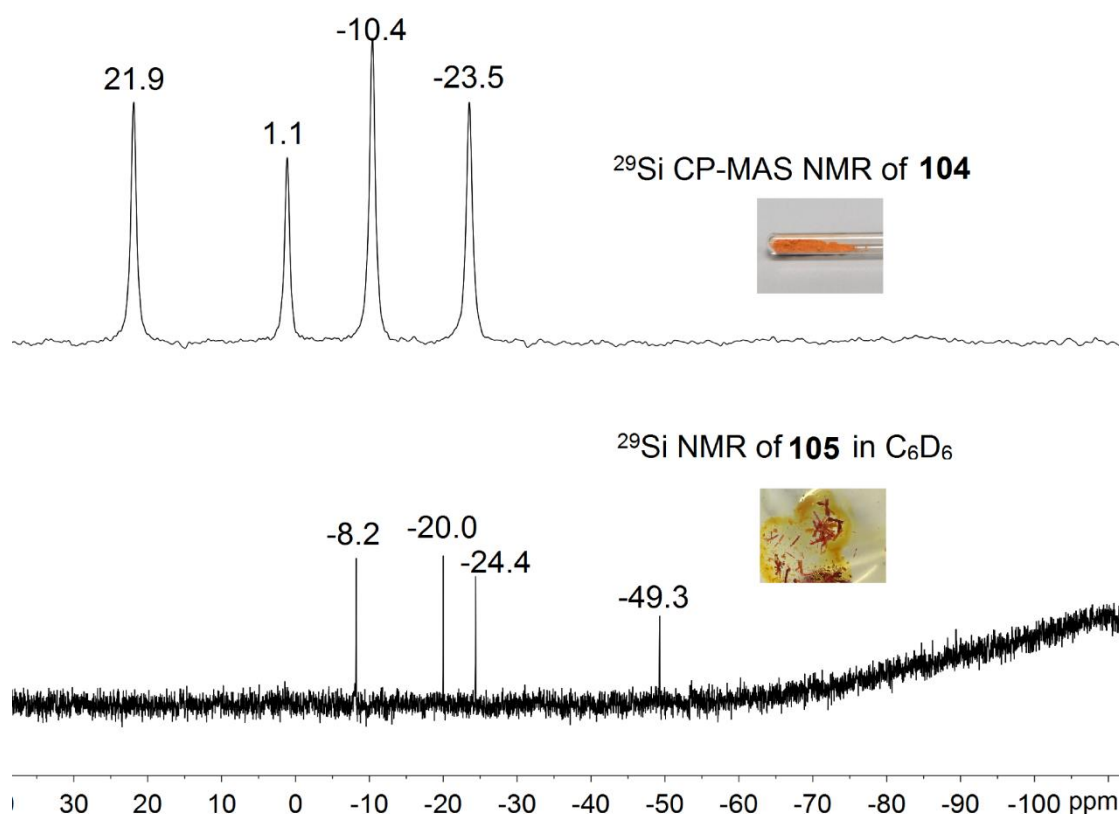


Figure 19. ^{29}Si CP-MAS NMR spectrum (79.5 MHz, 300 K) of **104** (up) and ^{29}Si NMR spectrum (59.6 MHz, C_6D_6 , 300 K) of **105** (below).

On the other hand, needle shape orange-red crystals of **105** also formed from the filtrate diluted hexane solution overnight at room temperature. ^{29}Si NMR shifts of **105** is at δ -8.2, -20.0, -24.4 and -49.3 ppm (Figure 19, below). The ^{29}Si NMR signals of

104 and **105** are identical with the two sets of signals observed in Figure 18. However, unlike **104**, in the UV/vis spectroscopy **105** shows a first clear maximum at λ 328 nm (ϵ 14350 L mol⁻¹cm⁻¹) and a shoulder absorption at λ 410 nm. Based on the similarity absorption area in comparison to that of **84** (λ_{\max} 353 nm) and the relative upfield ²⁹Si NMR signals, **105** is temporary postulated as a Si₄-bicyclo[1.1.0]butane derivative (Scheme 55).

In the molecular structure of **104** the bond length of Si2-Si3 (2.323(2) Å) and Si3-Si4 (2.370(3) Å) lie within the normal range of Si-Si single bonds, while those of Si1-Si4 (2.290(2) Å) and Si1-Si2 (2.247(4) Å) are significantly shorter. The four-membered ring is folded with a deviation of Si1 from the plane of Si2-Si3-Si4 being 1.032 Å. The distance between Si1 and Si3 is 2.770(3) Å, much shorter than the sum of the van der Waals radii of the silicon atom (4.20 Å), and comparable to the diagonal Si...Si distances (2.828 and 3.584 Å) in the charge-separated tetrasilacyclobutadiene,¹⁰⁷ and significantly shorter than the diagonal distance between the two three-coordinate silicon atoms of bicyclo[1.1.0]tetrasilatetraamide derivative (3.621 Å).¹⁰⁸ The sum of the angles about the Si1 atom is 352.6°, indicating a certain deviation from planarity of the Si1 coordination sphere.

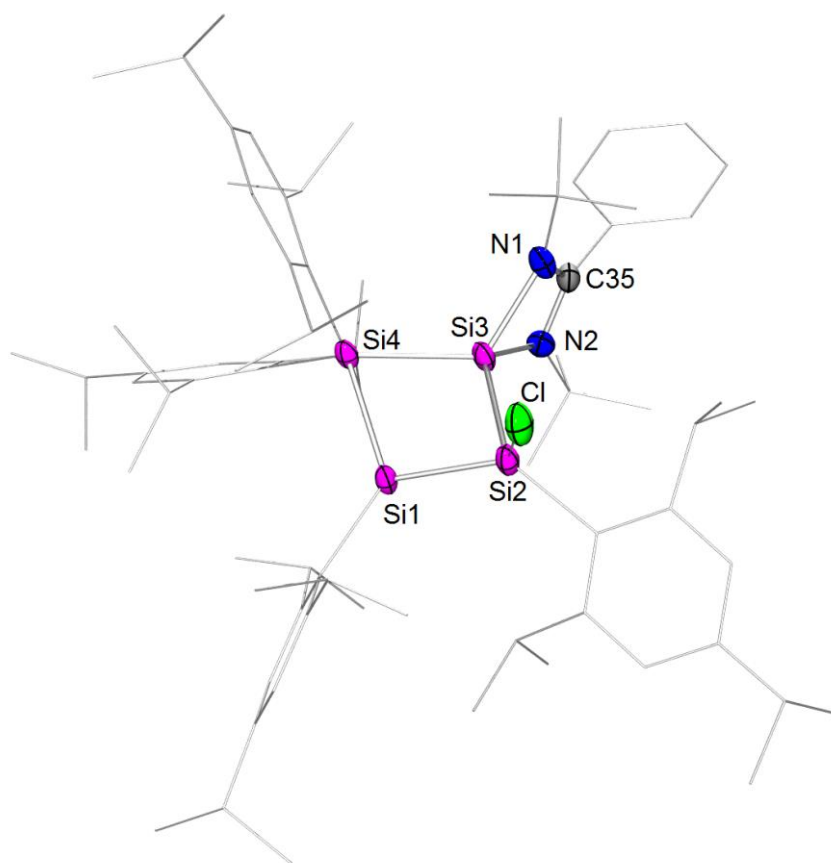


Figure 20. Molecular structure of **104** in solid state. Thermal ellipsoid at 50%. Selected bond lengths [Å] and angles [°]: Si1-Si2 2.247 (4), Si2-Si3 2.323(2), Si3-Si4 2.370(3), Si1-Si4 2.290(2), Si1-Si3 2.771(3), Si2-Cl1 2.144(3), Si3-N1 1.913(8), Si3-N2 1.864(5), N1-C35 1.316(9), N2-C35 1.327(1); Si1-Si4-Si3 72.9(8), Si4-Si3-Si2 96.5(9), Si3-Si2-Si1 74.6(9), Si2-Si1-Si4 101.0(1), N1-Si3-N2 69.4(3).

DFT calculations were performed by Dr. Diego Andrada in order to get a clear picture of the bonding situation in **104** (see: 6.1.4 *Computational Details*). Calculated geometry parameters based on the optimized structure at the BP86+D3(BJ)/def2-SVP level of theory fit well with those of the experiment ($d_{\text{Si1-Si3}}$ and $d_{\text{Si2-Si4}}$, calc. 2.700, 3.509 Å; exp. 2.771, 3.502 Å). Natural partial charge analysis at the BP86+D3(BJ)/def2-TZVPP//BP86+D3(BJ)/def2-SVP level of theory shows the value of +0.89 a. u. in Si1 and +0.31 a. u. in Si3. Wiberg bond orders analysis gives a value between Si1 and Si3 of 0.49 a.u. The distortion of the four-membered ring from planarity could thus be interpreted as a transannular donor-acceptor interaction between Si1 and Si3 (Figure 21).

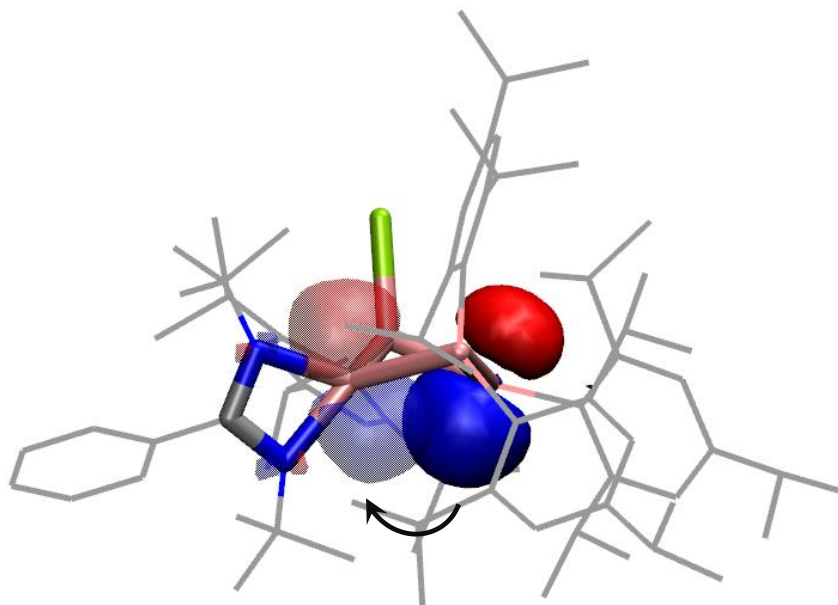


Figure 21. Stabilizing donor-acceptor interaction of **104**.

In solid state both **104** and **105** are to some extent stable towards exposure to air: remain unchanged up to 30 minutes. In contrast, after storing a solution of **104** in C_6D_6 at room temperature for two days, signals of **105** start appearing (Figure 22, red). Even at room temperature minute signals of **105** can be observed immediately after **104** is dissolved in C_6D_6 (Figure 22, black). Therefore, the solution of **104** in C_6D_6 was sealed in the NMR tube and heated to 50 °C. Indeed, signals of **105** grow substantially after overnight heating (Figure 22, green). Thus, a thermal transformation of **104** to **105** is confirmed spectroscopically, despite the fact that the identity of the latter remains obscure at this time.

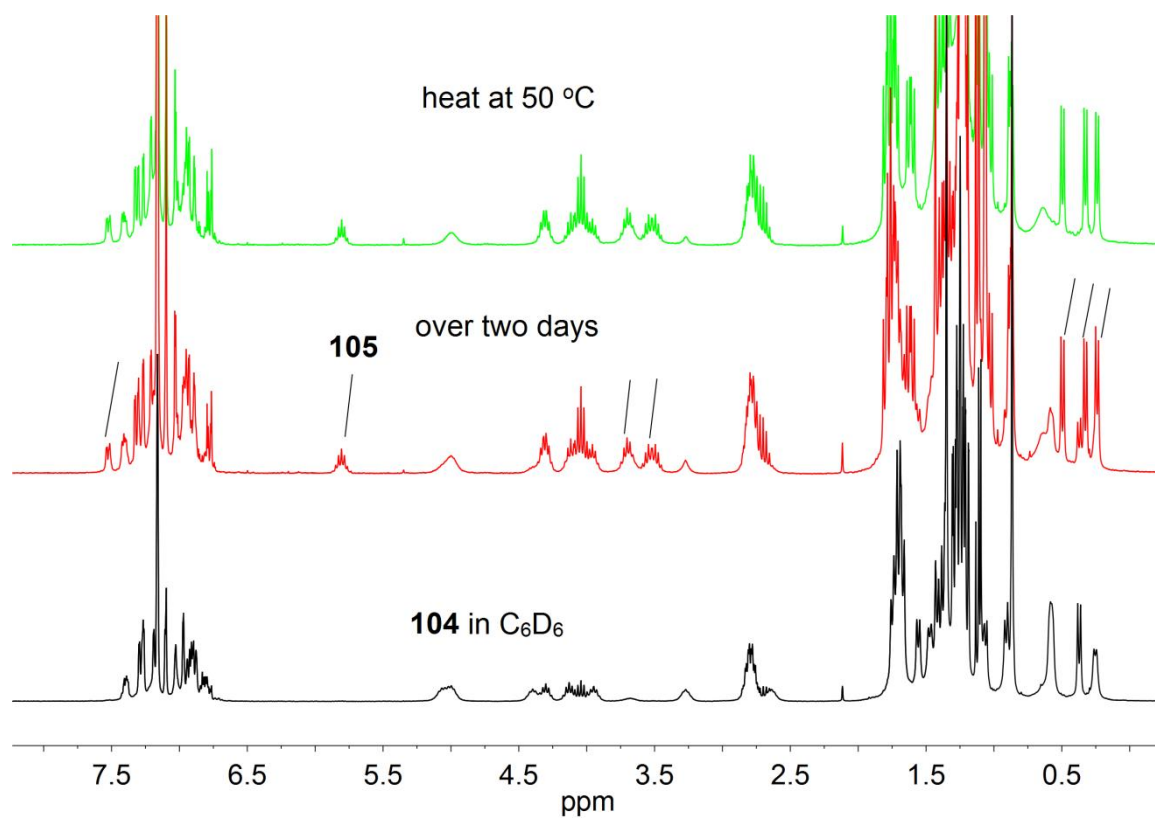


Figure 22. ^1H NMR spectrum of **104** in C_6D_6 , at 300 K (black), over two days (red) and heated at 50 °C overnight (green).

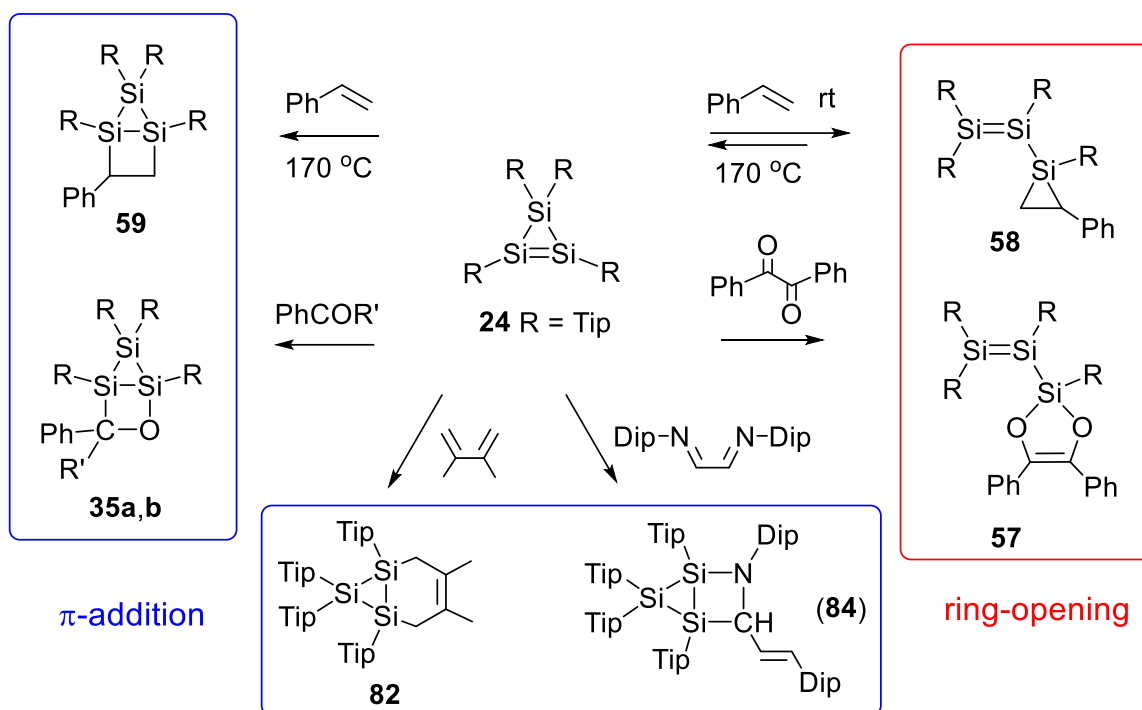
**“Probleme kann man niemals mit derselben
Denkweise lösen, durch die sie entstanden sind.”**

Albert Einstein

4 Summary

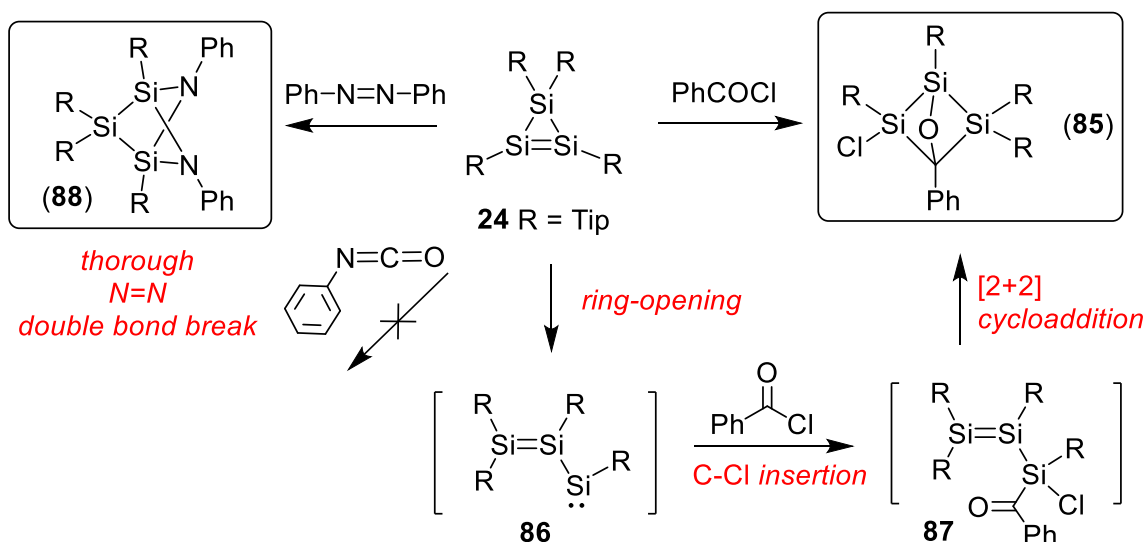
This thesis focuses mainly on cyclotrisilenes ($c\text{-Si}_3\text{R}_4$) and is organized according to the introduction of the intrinsic feature of Si=Si double bond followed by the synthesis and reactivity of cyclotrisilenes that have appeared in the scientific literature as well as the photochemical and NMR behaviour. In Particular, the latest results we have obtained in recent involving the reactivity of peraryl substituted cyclotrisilene ($c\text{-Si}_3\text{Tip}_4$) is presented.

Cyclotrisilene **24** ($c\text{-Si}_3\text{Tip}_4$), which undergoes, besides π -addition of Si=Si double bond and σ -insertion of Si–Si single bond, ring-opening reaction to a stable silicon version of vinyl carbene – disilenyl silylene – upon reaction with an N-heterocyclic carbene (NHC). Until this thesis, however, this remained the only manifestation of ring opening of cyclotrisilenes. Therefore, in this thesis the comparison reactivity of **24** towards styrene and ketones was investigated. Usual [2+4] cycloaddition occurred between cyclotrisilene **24** and 2,3-dimethyl-1,3-butadiene at room temperature yielding adduct **82** (Scheme 56). The reaction of it with benzaldehyde and benzophenone resulted in the [2+2] cycloadduct **35a** and **35b**, respectively. However, reactions of **24** with benzil and styrene at room temperature afforded the ring-opening [1+2] and [1+4] cycloaddition product **57** and **58** of the isomeric disilenyl silylene to the 1,2-diketone system and the C=C double bond, respectively. The results represent the first examples of disilenyl silylene reactivity of any cyclotrisilene. At elevated temperature starting reagent **24** and styrene were reproduced from the [1+2] addition product and reacted via usual [2+2] cycloaddition pattern yielding the thermodynamically favoured housane derivative **59**. Moreover, Si=Si double bond was also turned out to be reactive towards the C=N double bond of diimine, yielding the [2+2] cycloaddition product **84** (Scheme 56).



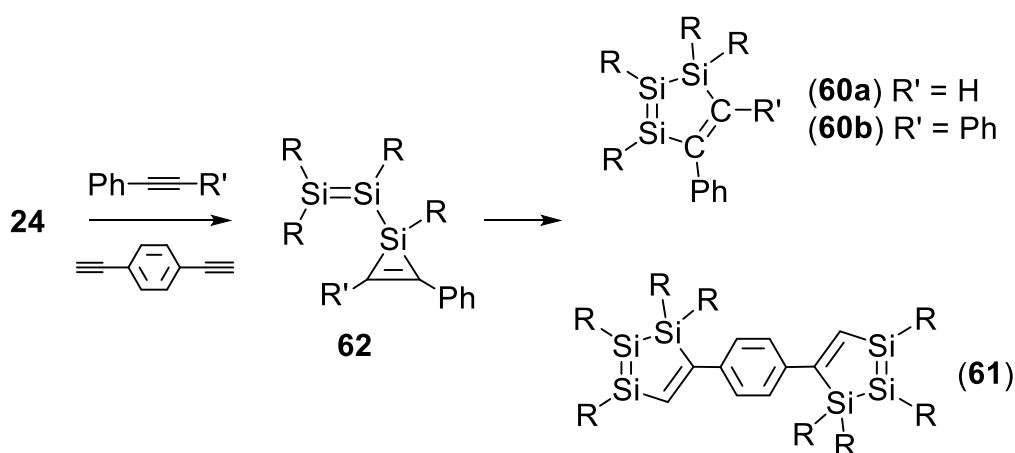
Scheme 56. Ring-opening and π -addition reactions of **24** (*c*-Si₃Tip₄).

Both **57** and **58** showed typical ²⁹Si NMR signals of Si=Si double bond, at δ 99.69, 36.01 ppm and δ 103.42, 36.16 ppm, respectively. Particularly, both **82** and **59** has a single resonance in solution ²⁹Si NMR spectrum at δ -46.6 for **82** and δ 14.28 ppm for **59**. Melting point of these π -addition housanes (> 200 °C) are higher than that of **57** (97-100 °C) and **58** (155-160 °C), in line with the less stability of Si=Si double bond than Si-Si single bond. Reactions of **24** with benzoyl chloride and azobenzene were also investigated which resulted in a bicyclo[1.1.1]pentane derivative **85** and the complete N=N double bond cleavage product **88** (Scheme 57), respectively. Ring-opening to intermediate **86** followed by C-Cl insertion to the resulting disilyenyl silylene was proposed as key step of formation of **85**, although no experiment proof was provided in this thesis.



Scheme 57. Reactions of cyclotrisilene **24** with benzoyl chloride and azobenzene.

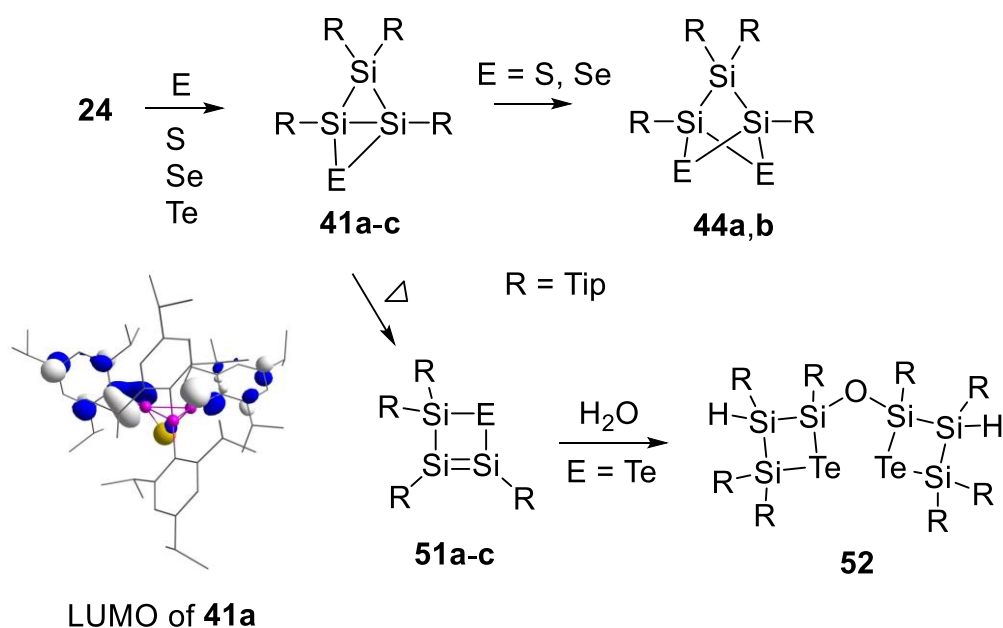
Reactions of **24** with acetylenes were investigated, affording 1,2,3-trisilacyclopentadiene **60-61**, of which **61** was the first cross-conjugated bridging of two of the Si_3C_2 cycles by a *para*-phenylene linker achieved via reaction of **24** with 1,4-diethynyl benzene (Scheme 58). In contrast to their carbon congeners and cyclopentadiene derivatives of Group 14 elements which have almost planar five-membered ring framework, five-membered Si_3C_2 ring of **60a** displays an envelope conformation with a folding angle of $21.8(1)^\circ$.



Scheme 58. Synthesis of **60-61**.

DFT calculations showed the HOMOs of **60a,b** are delocalized across the unsaturated cyclic backbone with dominant contributions by the Si=Si moieties and

less pronounced C=C components. In the case of **61**, the interaction between the two 1,2,3-trisilacyclopentadiene units leads to a near-degenerate HOMO and HOMO-1 and slightly split LUMO and LUMO+1. Noticeable contributions by the *para*-phenylene spacers were observed as well. The longest wavelength absorption bands of all three products were bathochromically shifted by a significant margin of $\Delta\lambda \cong 80$ nm compared with that of **24** (λ_{\max} 413 nm), certifying the Si=Si-C=C conjugation. Variable-temperature NMR study of in the case of reaction of **24** with diphenylacetylene discovered the initial ring-opening to disilanyl silirenes **62** (Scheme 58) that could be detected at room temperature with signals at δ 99.6, 43.0 and -118.5 ppm, was an important intermediate which isomerized to the final product **60**. Predicted ^{29}Si NMR shifts of **62** (calc. δ 133.23, 78.87 and -119.22 ppm) at the M06-2X(D3)/def2-TZVPP level of theory also support the postulated intermediate.

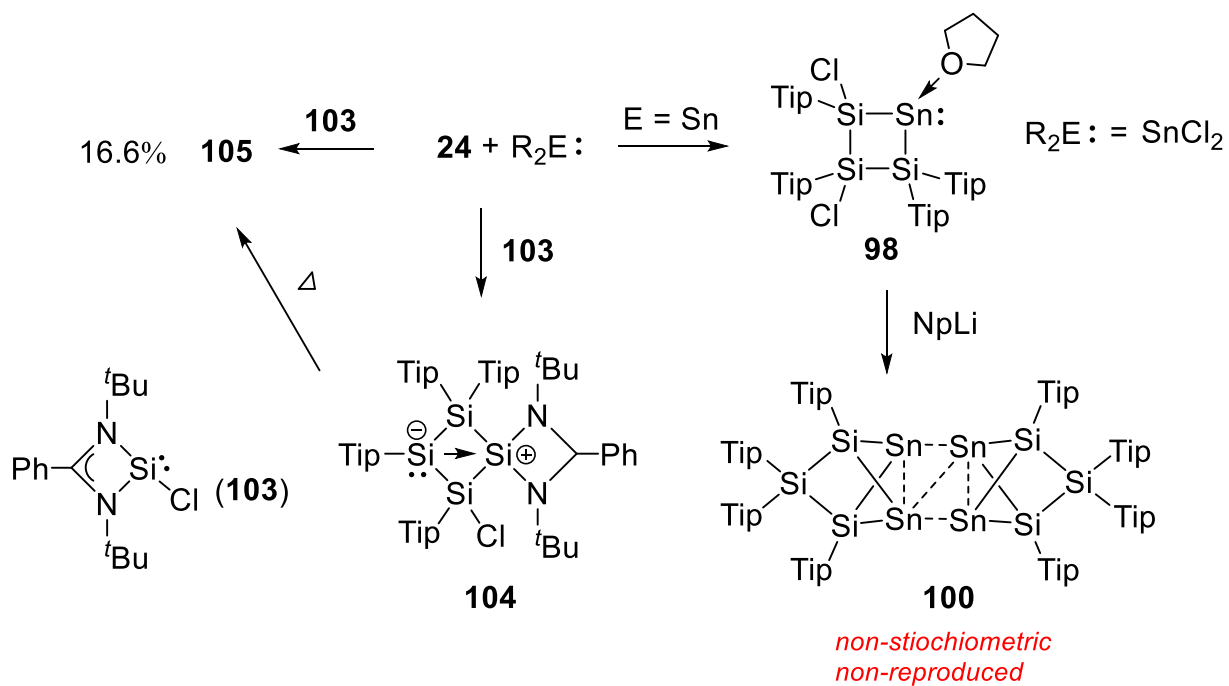


Scheme 59. Reactions of **24** with chalcogen elements.

Considering the different reactivity *c*-Si₃Tip₄ **24** exhibited from the *c*-Si₃R₄ (R = silyl), the reactions of **24** with chalcogen elements were investigated. Reaction of **24** with element S, Se and Te afforded corresponding 2-chalcogena-1,3,4-trisilabicyclo[1.1.0]butane derivatives **41a-c** (Scheme 59). An

interesting feature of these monoaddition products was that the ^{29}Si NMR in the solid state as well as at low temperature in solution of **41a-c** showed two signals for the bridgehead silicon atoms (δ -43.0, -58.27 for **41a**, -54.9, -68.9 for **41b**, -87.4, -98.7 ppm for **41c**). DFT calculations disclosed the non-equivalence silicon chemical shift of bridgehead silicon atoms originated from the near orthogonality of the rotationally hindered Tip group at one of the bridgehead silicon atoms which had a more deshielded signal (Scheme 59, LUMO of **41a**). Thermal isomerization of **41** to 2-chalcogena-1,3,4-trisilacyclobutenes **51** was suggested by NMR spectroscopic data which showed typical signals of three-coordinate silicon atoms (δ 128.2, 19.4 for **51a**, 127.7, 21.7 for **51b**, 103.4, 35.6 ppm for **51c**) and supported by the isolation of the hydrolysis product of 2-tellura-1,3,4-trisilacyclobutene **52**.

Additionally, the reaction of cyclotrisilene with Group 14 divalent species was also investigated. The reaction of **24** with SnCl_2 was proposed to undergo firstly σ -insertion of the Si-Si single bond followed by chlorine migration, yielding a tetrahydrofuran-stabilized four-membered stannylene **98** (Scheme 60). The attempt to reproduce the Si=Si double bond by reducing the reaction mixture with naphthalene lithium, however, resulted in a Si_6Sn_4 cluster **100** in a non-stoichiometric manner. Reaction of **24** with Roesky silylene **103** gave a cyclic Si_4 system **105** (Scheme 60), which was isolated as orange-red crystal and composed of three- and four-coordinate silicon atoms. An air-stable orange powder **104** was also obtained from the reaction, which was shown NMR spectroscopically to transform to **105** at elevated temperature.



Scheme 60. Reactions of **24** with $SnCl_2$ and Roesky silylene **103**.

5 Outlook

With the development of new synthesis technology and synthesis efficiency, new cyclic structures containing the main group elements are continually being discovered which add to the chemical diversity in modern inorganic chemistry, and particularly, leads to opportunities to experimentally validate theoretical predictions. Due to the novel bonding modes and the ubiquitous role of these cyclic intermediates in a wide variety of chemical transformations, reactivity investigation of these cyclic units are also becoming more and more attractive. As can be seen from this thesis, the number of elements and substituents that can be incorporated within three-membered cyclic arrangements of Group 14 elements is vast and thus resulting various reactivity profiles. As presented in this thesis, for instance, persilyl- and peraryl-substituted cyclotrisilene showed entirely different reactivity towards phenylacetylene, leading to the bicyclo[3.2.0]hepta-3,6-diene and cyclopentadiene derivative, respectively. Therefore, the synthetic strategy study can possibly afford new and efficient routes to these inorganic rings with varied substituents. This has been demonstrated through the synthesis of peraryl-substituted cyclotrisilene *c*-Si₃Tip₄, which was synthesized, instead of straightforward reducing of corresponding silanes, taking advantage of the disilenide precursor.

Specifically, the high reactivity of the weak Si=Si double bond as well as the ring strain allows for a conceptually more variable reaction behaviour than in the case of cyclic alkenes, which will likely adopt increasingly important roles in advancing small molecule activation.

“When radium was discovered, no one knew that it would prove useful in hospitals. The work was one of pure science. And this is a proof that scientific work must not be considered from the point of view of the direct usefulness of it.”

Marie Curie

6 Supplementary Experiments

6.1 General

6.1.1 Experiential Conditions

All sensitive compounds are manipulated under a protective atmosphere of argon taking advantage of standard Schlenk techniques or in a glovebox. Argon 5.0 supplied by PraxAir was used as protection gas without further purification. All glassware was cleaned prior to use in a KOH/H₂O bath, neutralized in a HCl/H₂O bath and dried in the oven at 120 °C overnight. All setups were evacuated while still hot and refilled with argon three times. The vacuum (1×10^{-3} bar) was generated by a slide vane rotary vacuum pump RZ 6 from Vacuubrand. Naphthalene was purified before use by sublimation. Silicon tetrachloride was distilled from magnesium under a protecting atmosphere of argon ahead of use. Benzophenone, benzaldehyde, styrene, benzil, benzoyl chloride, sulfur, selenium, tellurium were used as supplied.

6.1.2 Purification of Solvents

Diethyl ether (Et₂O), toluene, 1,2-dimethoxyethane (DME), tetrahydrofuran (THF), hexane and benzene as well as pentane were refluxed over sodium. Benzophenone was used as probes to identify the dry and oxygen-free condition. All solvents were distilled and stored under argon. Deuterated solvents were purchased from Sigma-Aldrich, of which deuterated benzene, toluene and thf were dried over sodium or potassium before use, distilled and stored in the glovebox. The dry solvents were transferred with cannulas of stainless steel or PTFE into the reaction flasks under a protection of argon. Deuterated solvents were transferred in the glovebox with a syringe into NMR tubes.

6.1.3 Methods of Analysis and Measurement

NMR spectra in solution were recorded on a Bruker Avance III 300 spectrometer (¹H = 300.13 MHz, ¹³C = 75.46 MHz, ²⁹Si = 59.6 MHz). Solid state NMR was recorded on a Bruker AV400 spectrometer. WB: 79.5 MHz ²⁹Si CP/MAS spectrum at 13 KHz MAS rate. All spectra were analyzed with the Topspin 3.2 suite of programs. ¹H and ¹³C NMR spectra were referenced to residual signals of the solvent (CDCl₃: H 7.26 ppm; C₆D₆: H 7.16 ppm; C 128.06 ppm; toluene-d₈: H 2.08 ppm; C 20.04 ppm;

THF-d₈: H 1.72 ppm; C 25.31 ppm). ²⁹Si was referenced to external SiMe₄. All chemical shifts are reported in parts per million (ppm). Coupling constants are reported in Hertz (Hz) and are given in the usual notation that ⁿJ_(X,Y) means a coupling of nucleus X over n bonds with nucleus Y. Coupling constants are determined by observing satellite signals next to main signal. The multiplicity and shape of the observed signals are given as s = singlet, d = doublet, t = triplet, m = multiple or convoluted signals, br. = broad signal.

UV/vis spectra of the supplementary compounds are recorded on a SHIMADZU UV-2600 spectrophotometer.

Melting points (mp.) were determined under argon in sealed NMR tubes and are uncorrected.

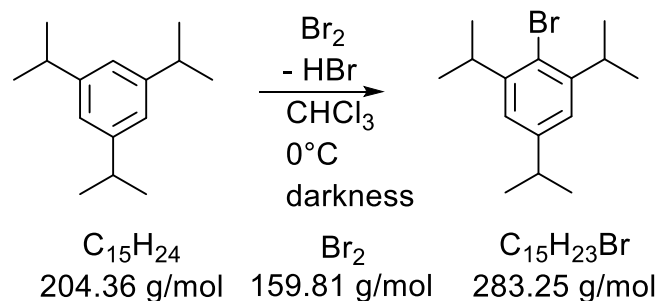
Elemental analysis was carried out using pure products with Leco CHN-900 analyzer.

6.1.4 Computational Details

Geometry optimizations of **105** were performed using the Gaussian 09 optimizer¹⁰⁹ together with TurboMole V7.0 energies and gradients.¹¹⁰ All geometry optimizations were computed using the functional BP86¹¹¹ functional with Grimme dispersion corrections D3¹¹² and the Becke-Jonson damping function¹¹³ in combination with the def2-SVP basis set.¹¹⁴ The stationary points were located with the Berny algorithm¹¹⁵ using redundant internal coordinates. Analytical Hessians were computed to determine the nature of stationary points (one and zero imaginary frequencies for transition states and minima, respectively)¹¹⁶ and to calculate unscaled zero-point energies (ZPEs) as well as thermal corrections and entropy effects using the standard statistical-mechanics relationships for an ideal gas. The atomic partial charges have been estimated with the natural bond orbital (NBO)¹¹⁷ method using NBO 5.9.¹¹⁸

6.2 Synthesis of Starting Materials

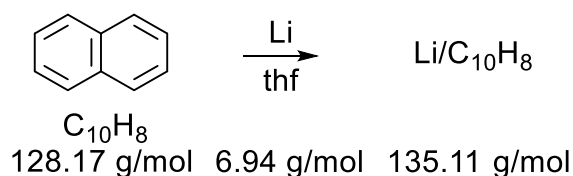
6.2.1 Synthesis of TipBr



At 0 °C, Br₂ (110.5 g, 0.69 mol, 35 mL) is introduced dropwise into a the solution of 2,4,6-triisopropylbenzene (143 g, 0.7 mol) in 700 mL CHCl₃ *via* a dropping funnel. The whole apparatus is protected from light with aluminum foil. Thus generated HBr is neutralized with isopropanol in washing bottles connected with the reaction flask (extra empty washing bottle must be set up between the isopropanol and reaction flask in order to avoid suck-back). After the addition is finished, the reaction mixture is warmed to room temperature with stirring overnight. The crude reaction mixture is neutralized by NaOH. The organic layer is separated off and washed three times with water until neutral. Drying over Na₂SO₄ for 30 min the organic layer is filtrated and concentrated by removing the CHCl₃. The remaining residue is distilled in vacuum to give TipBr as a colorless liquid (159 g, yield: 81%).

¹H NMR (300.13 MHz, CDCl₃, 300 K): δ 6.98 (s, 2H, Tip-*H*); 6.97 (s, 1H, Tip-*H*); 3.51 (m, 2H, ^{*i*}Pr-*CH*); 2.83 (m, ^{*i*}Pr-*CH*); 1.21, 1.24 (each d, *J*_{H-H} = 7 Hz, altogether 18H, ^{*i*}Pr-*CH*₃) ppm.

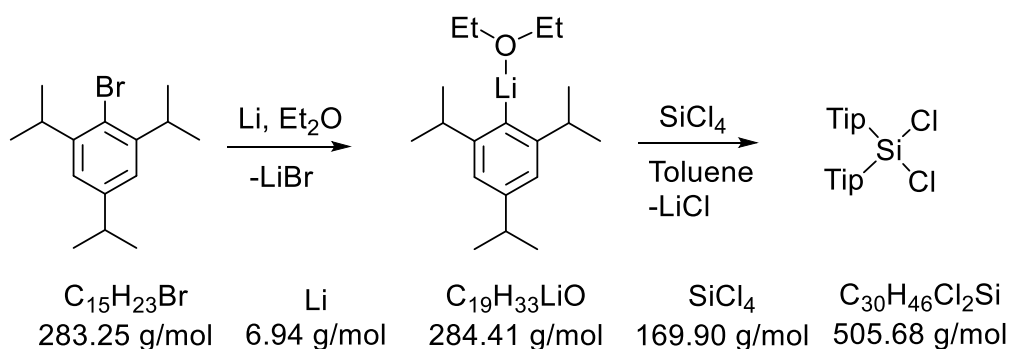
6.2.2 Preparation of Lithium Naphthalene (Li/C₁₀H₈)



Lithium granules (138 mg, 20 mmol), naphthalene (3.08 g, 24 mmol) are mixed in a 100 mL Schlenk flask with a stirring bar. 40 mL thf is introduced into the mixture via a dropping funnel in five minutes, slight heat is released at the beginning of the reaction.

Within five minutes a dark green suspension is obtained, the formed mixture is stirred at room temperature overnight. The exact concentration (ca. 0.5 mol L⁻¹) is determined by titration of a hydrolyzed aliquot with aqueous hydrochloric acid against phenolphthalein.

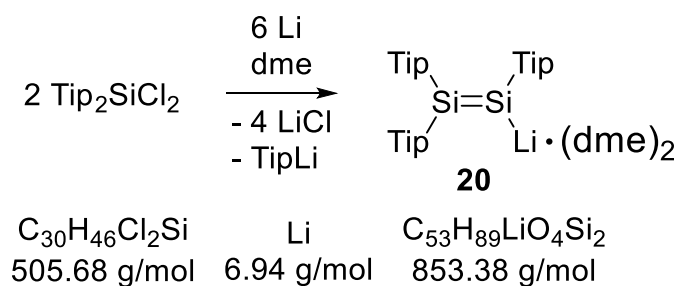
6.2.3 Synthesis of Tip₂SiCl₂



Tip₂SiCl₂ was prepared by a modified literature protocol:¹¹⁹ TipBr (156 g, 0.55 mol) is added dropwise to a suspension of 2.2 equivalent amount of Li granules (7.63 g, 1.1 mol) in 1000 mL dry Et₂O at room temperature. The resulting brown reaction mixture was stirred overnight at room temperature. Yield of TipLi can be checked by ¹H NMR spectroscopy with the hydrolyzed aliquot taken from the mixture. Remaining lithium is filtered off with a glass frit under the protection of argon and the solvent of filtrate is removed in vacuum affording crude TipLi (72%, 114 g), which is used for next step without further purification. To the resulted TipLi 1000 mL dry toluene is added and the resulting suspended solution is cooled down to 0 °C. Silicon tetrachloride (30.58 g, 0.18 mol) is added dropwise *via* a dropping funnel to the above solution and after the addition is finished the reaction mixture is stirred over two days at room temperature. For workup no protection atmosphere is needed, since the product Tip₂SiCl₂ is stable towards air and moisture for limited periods of time. All insoluble components are removed by filtration. Solvent of the filtrate is removed with a rotary evaporator. The remaining residue is dissolved in pentane (4 mL/g) and kept at -78 °C overnight. Pure block crystals of Tip₂SiCl₂ is obtained by further re-crystallization (two to three times) from pentane. Yields: 56 g, 61%.

¹H NMR (300.13 MHz, CDCl₃, 300 K): δ 6.98 (s, 4H, Tip-H); 3.66 (m, J_{H-H} = 6.8 Hz, 4H, ⁱPr-CH); 2.83 (m, J_{H-H} = 6.8 Hz, 2H, ⁱPr-CH); 1.20 (d, J_{H-H} = 6.8 Hz, 12H, ⁱPr-CH₃), 1.18 (d, J_{H-H} = 6.8 Hz, 24H, ⁱPr-CH₃) ppm.

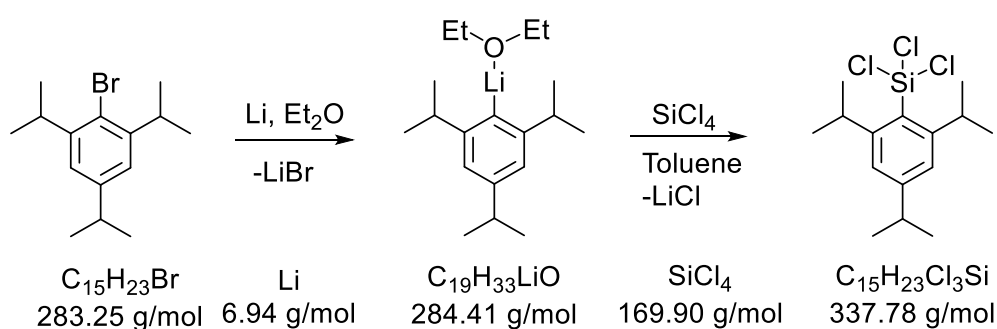
6.2.4 Synthesis of disilenide 20



Disilenide is prepared according to a published procedure.⁵⁰ At 0 °C, dry dme (200 mL) is added to the mixture of Tip₂SiCl₂ (40 g, 79 mmol) and lithium powder (2.4 g, 340 mmol). The resulting mixture is stirred at room temperature overnight to afford a deep red solution. Solvent of the formed reaction mixture is removed in vacuum. The dark-red residue is digested with 500 mL hexane and filtered off at 50 °C. The dark-red filtrate is kept at room temperature overnight from which red blocks of crude disilenide crystallize. Pure disilenide was obtained by re-crystallization from hexane in 48% yield.

¹H NMR (300.13 MHz, C₆D₆, 300 K): δ 7.13, 7.09, 7.07 (each br, 2H, Tip-H), 4.79 (m, 4H, ⁱPr-CH), 4.28 (br, 2H, ⁱPr-CH), 2.92 (s, 12H, dme-CH₃), 2.84 (s, 8H, dme-CH₂), 2.90-2.74 (br, 3H, ⁱPr-CH), 1.43, 1.41, 1.33, 1.26, 1.21, 1.20, 1.14 (each d, altogether 54H, ⁱPr-CH₃) ppm.

6.2.5 Synthesis of TipSiCl₃

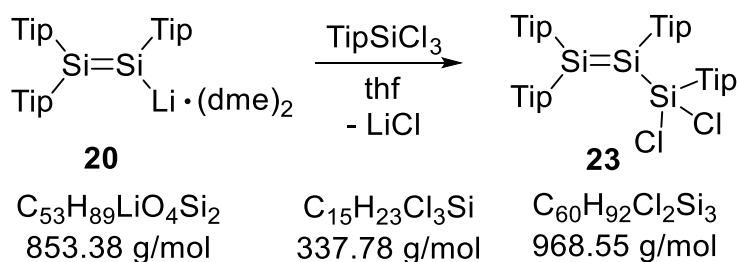


The same literature procedure referenced for Tip₂SiCl₂ is used in a modified way to prepare TipSiCl₃. At room temperature TipBr (200 g, 0.71 mol) is added dropwise to a suspension of 2.2 equivalent amount of lithium granules (10.9 g, 1.6 mol) in 1000 mL dry Et₂O. After the addition completed, the resulting mixture is stirred overnight. The yield of TipLi is checked by ¹H NMR spectroscopy with the hydrolyzed aliquot taken

from the mixture. Remaining Li is filtered off with a glass frit under the protection of argon and the solvent is removed from the filtrate in vacuum to afford crude TipLi (72%, 114 g). The product is used without further purification. To the resulting TipLi 1200 mL of dry toluene are added and the suspension is cooled to 0 °C in an ice-bath. Silicon tetrachloride (50.00 g, 0.29 mol) is added dropwise to the above solution and after the addition is finished the reaction mixture is stirred overnight. Stirring is continued for another two days to complete the reaction. Since the products is unstable towards air and moisture, all of the afterwards manipulations must carried out under argon. All insoluble components are removed by filtration. The volume of the filtrate is reduced under vacuum until a colorless solid starts precipitating. The precipitate is dissolved in 200 mL hexane and kept at -30 °C overnight. TipSiCl₃ is obtained as colorless blocks (44.16 g, 52%).

¹H NMR (300.13 MHz, C₆D₆, 300 K): δ 7.10 (s, 2H, Tip-*H*), 3.95 (m, 2H, *i*Pr-*CH*), 2.65 (m, 1H, *i*Pr-*CH*), 1.21 (d, 12H, *i*Pr-*CH*₃), 1.11 (d, 6H, *i*Pr-*CH*₃).

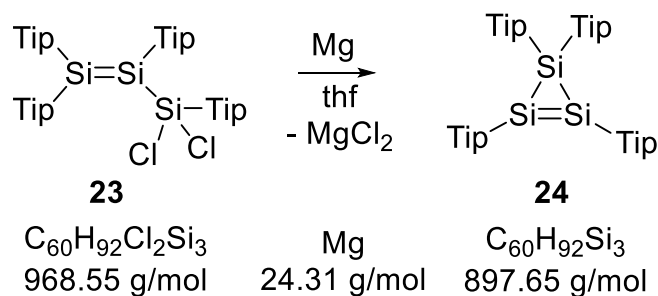
6.2.6 Synthesis of trisilaallyl chloride **23**



At -80 °C, thf (20 mL) is transferred to a mixture of disilene (5.40 g, 6.33 mmol) and TipSiCl₃ (2.14 g, 6.33 mmol). The resulted red-brown mixture is slowly brought to room temperature (ca. 30 min) and then stirred for 15 hours. All volatiles are removed in vacuum and the orange residue is dissolved in hexane (50 mL). Lithium chloride precipitates and is removed by filtration. The clear filtrate is concentrated to dryness to afford **23** as orange powder (6.07 g, 99%). Due to its very good solubility in hydrocarbon solvents crystallization is tedious, but also unnecessary as the crude product is spectroscopically pure. Therefore **23** is used for subsequent reactions without further purification.

¹H NMR (300.13 MHz, C₆D₆, 300 K): δ 7.09, 7.07, 7.01, 6.94 (s, 8H, Tip-*H*), 4.37, 4.31 (m, 4 H, *i*Pr-*CH*), 4.03 (br, 2 H, *i*Pr-*CH*), 3.59 (m, 2 H, *i*Pr-*CH*), 2.72, 2.63 (m, 4 H, *i*Pr-*CH*), 1.41, 1.22, 1.14, 1.13, 1.08, 1.07, 0.89 (d, 72 H, *i*Pr-*CH*₃) ppm.

6.2.7 Synthesis of cyclotrisilene **24**

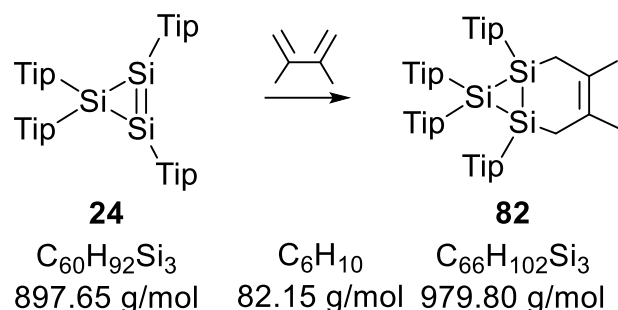


At room temperature, 100 mL of dry and degassed Et₂O are added through a septum by cannula to 20.00 g (20.6 mmol) **23** in a 250 mL Schlenk flask. The resulting red solution is transferred by cannula to another 250 mL Schlenk flask containing 0.6 g (24.7 mmol, 1.2 equiv.) magnesium powder which was activated before use. The mixture is stirred at room temperature for 30 min to 60 min to start (the reaction needs to be stirred vigorously at the beginning in order to be activated, once the reaction starts, a fine precipitate becomes apparent in solution as well as at the wall of the Schlenk flask), and then kept stirring for another 7 hours (never let the reaction mixture be stirred over 7 hours, or a further reduced byproduct α,ω -dianionic magnesium salt will be produced),⁵³ during which time it acquires a deep red color. After removal of the Et₂O in vacuum, 200 mL n-pentane are added by cannula. The solid residue is stirred for five minutes at room temperature so that the product is completely dissolved in n-pentane. Following this the Schlenk flask is connected to the reversing frit equipped with the third 250 mL round-bottom Schlenk flask. Insoluble parts are filtered off, the red filtrate is concentrated to ca. 100 mL and kept at room temperature for one day. By solvent decantation and subsequent drying in vacuum at room temperature block-shaped crystals of **24** (8.5 g, 46%) are isolated. A second crop of crystals from the mother liquid yields another 1.5 g of **24**. Total yield: 10.0 g, 54.1%.

¹H NMR (300.13 MHz, C₆D₆, 303 K): δ 7.18 (br, 2H, SiTip₂ Ar-*H*), 7.09 (s, 4H, SiTip Ar-*H*), 6.97 (br, 2H, SiTip₂ Ar-*H*), 4.98 (br sept, 2H, SiTip₂ *i*Pr-*CH*), 4.03 (sept, 4H, SiTip *i*Pr-*CH*), 3.66 (br sept, 2H, SiTip₂ *i*Pr-*CH*), 2.79 (sept, 2H, *i*Pr-*CH*), 2.69 (sept, 2H, *i*Pr-*CH*), 1.66 (br, 6H, SiTip₂ *i*Pr-*CH*₃), 1.42 (br, 6H, SiTip₂ *i*Pr-*CH*₃), 1.35 (br, 6H, SiTip *i*Pr-*CH*₃), 1.26 (br, 6H, SiTip₂ *i*Pr-*CH*₃), 1.21 (br, 6H, SiTip *i*Pr-*CH*₃), 1.22 (d, 12H, *i*Pr-*CH*₃), 1.10 (d, 12H, *i*Pr-*CH*₃), 0.62 (br, 6H, SiTip₂ *i*Pr-*CH*₃) ppm.

6.3 Reactivity of **24** towards 1,3-butadiene and imine

6.3.1 Synthesis of **82**



Cyclotrisilene **24** (300 mg, 0.334 mmol) is dissolved in 10 mL toluene at room temperature, the solution is cool down to $-30\text{ }^\circ\text{C}$ and 2,3-dimethyl-1,3-butadiene (38 μL , 1 equiv.) introduced into the solution by microsyringe. The resulting mixture is stirred overnight while warming to room temperature. The thus formed yellow reaction mixture is concentrated by reducing the solvent under vacuum to ca. 5 mL. Pale yellow sheet crystals of **82** (260 mg, yield: 80%, mp. $175\text{-}78\text{ }^\circ\text{C}$) are isolated by solvent decantation and drying in vacuum at room temperature.

^1H NMR (300.13 MHz, C_6D_6 , 300 K): δ 7.14 (overlapped with solvent, 4H, Tip-*H*), 7.10 (br. 3H, Tip-*H*), 6.78 (br. 1H, Tip-*H*), 4.63 (br. 1H, *i*Pr-*CH*), 3.60 (br. 4H, CH_2), 3.38 (br. 1H, *i*Pr-*CH*), 2.27-2.66 (m, 5H, *i*Pr-*CH*), 2.63-2.54 (m, 3H, *i*Pr-*CH*), 2.29 (br. 2H, *i*Pr-*CH*), 1.44 (br. 27H, *i*Pr- CH_3), 1.28, 1.26 (br, 9H, *i*Pr- CH_3), 1.17 (d, $J_{H-H} = 7.2\text{ Hz}$, 24H, *i*Pr- CH_3), 1.12 (d, $J_{H-H} = 6.8\text{ Hz}$, 12H, *i*Pr- CH_3), 0.44 (br. 7H, CH_3) ppm.

$^{13}\text{C}\{^1\text{H}\}$ NMR (75.47 MHz, C_6D_6 , 300 K): δ 156.3, 156.2 (Tip-*C*); 155.7 ($C=C$); 155.4 (Tip-*C*); 149.8, 149.7, 149.5 (Tip-*C*); 135.4, 134.7, 133.2, 129.2, 128.4 125.5, 123.8, 122.1, 121.9 (Tip-*CH*); 36.6 (*i*Pr-*CH*); 35.3 (CH_2); 34.4, 34.3 (*i*Pr-*CH*); 27.3, 24.9 (*i*Pr- CH_3); 23.9 (CH_3); 23.8; 23.7, 21.3 (*i*Pr- CH_3) ppm.

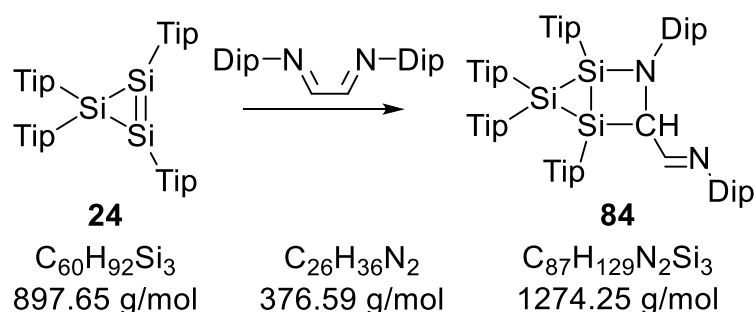
$^{13}\text{C}\{^1\text{H}\}$ CP/MAS (100.63 MHz, 300 K): δ 156.4-153.9 (m, Tip-*C*, $C=C$); 149.7-148.1 (m, Tip-*C*); 135.8, 135.3, 134.8, 131.5, 127.2 (Tip-*CH*); 122.4, 122.0, 120.6 (br., Tip-*CH*); 34.1 (br., *i*Pr-*CH*, CH_2); 27.9, 27.5, 26.4 (br., *i*Pr- CH_3); 24.8, 23.0, 21.5, 20.3 (br., CH_3 , *i*Pr- CH_3) ppm.

$^{29}\text{Si}\{^1\text{H}\}$ NMR (59.6 MHz, C_6D_6 , 300 K): δ -46.6 (*S*Tip₂) ppm.

$^{29}\text{Si}\{^1\text{H}\}$ CP/MAS (79.5 MHz, 300 K): δ 2.85 (*S*Tip), -33.21 (*S*Tip), -48.23 (*S*Tip₂) ppm.

Elemental Analysis Calc. for C₆₆H₁₀₂Si₃. C, 80.91; H, 10.49 Found: C, 79.00; H, 9.96.

6.3.2 Synthesis of **84**



Cyclotrisilene **24** (300 mg, 0.334 mmol) and diimine (125.9 mg, 0.334 mmol) are mixed in a Schlenk flask and 10 mL benzene added to the solid reagents by syringe. The resulting orange reaction mixture is stirred at room temperature for one day. The solvent is removed from the light-orange solution under vacuum resulting in a solid residue that was dissolved in 3 mL hexane. Housane **84** crystalizes as yellow blocks and is isolated by solvent decantation and drying in vacuum (298 mg, yield: 70%, mp. 220-24 °C).

¹H NMR (300.13 MHz, C₆D₆, 300 K): δ 7.96 (d, $J_{\text{H-H}} = 8.9$ Hz, 1H, HC=NDip); 7.25 (d, $J_{\text{H-H}} = 6.5$ Hz, 2H, Tip-H), 7.01 (s, 1H), 6.99 (br. 3H), 6.95 (br. 3H), 6.90 (d, $J_{\text{H-H}} = 3.5$ Hz, 4H, Tip-H), 6.73 (s, 1H), 6.17 (d, $J_{\text{H-H}} = 8.8$ Hz, 1H, HCSiTip), 4.50-4.45 (m, 1H, ⁱPr-CH), 4.30-4.26 (m, 1H, ⁱPr-CH), 4.04-3.99 (m, 1H, ⁱPr-CH), 3.76-3.74 (m, 1H, ⁱPr-CH), 3.56-3.31 (m, 5H, ⁱPr-CH), 2.85-2.74 (m, 4H, ⁱPr-CH in Dip), 2.61-2.54 (m, 3H, ⁱPr-CH), 1.84, 1.79 (each d, $J_{\text{H-H}} = 7.6$ Hz, 9H, ⁱPr-CH₃), 1.73 (d, $J_{\text{H-H}} = 7.0$ Hz, 3H, ⁱPr-CH₃), 1.59 (d, $J_{\text{H-H}} = 6.5$ Hz, 3H, ⁱPr-CH₃), 1.41 (d, $J_{\text{H-H}} = 5.3$ Hz, 6H, ⁱPr-CH₃), 1.28, 1.24, 1.20, 1.14 (each d, total 30H, $J_{\text{H-H}} = 6.5$ Hz, ⁱPr-CH₃ in Tip and Dip), 1.11, 1.06 (each d, total 24H, ⁱPr-CH₃), 0.77 (d, $J_{\text{H-H}} = 7.0$ Hz, 3H, ⁱPr-CH₃), 0.70 (d, $J_{\text{H-H}} = 6.5$ Hz, 6H, ⁱPr-CH₃), 0.15, 0.10 (each d, 12H, ⁱPr-CH₃) ppm.

¹³C{¹H} NMR (75.47 MHz, C₆D₆, 300 K): δ 168.18 (HC=NDip); 157.14, 156.56, 155.47, 155.01, 154.69, 154.38, 151.28, 150.66, 150.21, 149.53, 147.23, 146.04, 145.62, 136.82, 135.80, 132.69, 131.53 (Tip, Dip-C); 126.30, 126.04, 124.29, 123.44, 123.21, 122.86, 122.01 (Tip, Dip-CH); 68.52 (HCSiTip); 37.39, 36.84, 35.85, 35.27, 34.75, 34.38, 34.24, 32.61, 31.79 (ⁱPr-CH); 28.68, 28.35, 28.17, 27.85, 27.16, 26.89,

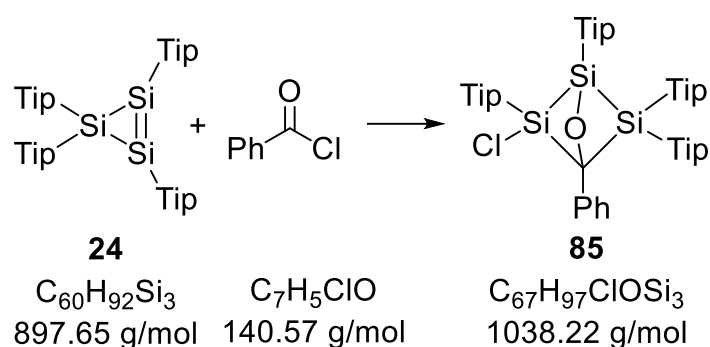
26.17, 25.64, 25.14, 25.01, 24.82, 24.43, 23.98, 23.93, 23.79, 23.69, 23.54, 23.40, 23.29, 22.88 (*i*Pr-CH₃) ppm.

²⁹Si{¹H} NMR (59.6 MHz, C₆D₆, 300 K): δ 42.61 (*S*/TipCH), 17.27 (*S*/TipN), -62.19 (SiTip₂) ppm.

UV/Vis (hexane) λ_{max}(ε) 353 nm (8367 L mol⁻¹ cm⁻¹).

Elemental Analysis Calc. for C₈₆H₁₂₈NSi₃. C, 81.96; H, 10.24, N, 1.1 Found: C, 79.72; H, 9.98; N, 1.95.

6.3.3 Synthesis of **85**



Cyclotrisilene **24** (500 mg, 0.56 mmol) is dissolved in 20 mL dry toluene at room temperature in a Schlenk flask and the resulting orange solution is cooled to -80 °C. Benzoyl chloride (64.7 μL, 0.56 mmol) is introduced into the solution by microsyringe. The resulting reaction mixture was stirred at -80 °C for 15 minutes. Removal of the solvent affords a light-orange residue which is dissolved in 10 mL hexane and then concentrated to ca. 3 mL. Colorless crystals form at room temperature (436 mg, yield: 65%, mp. 139-42 °C).

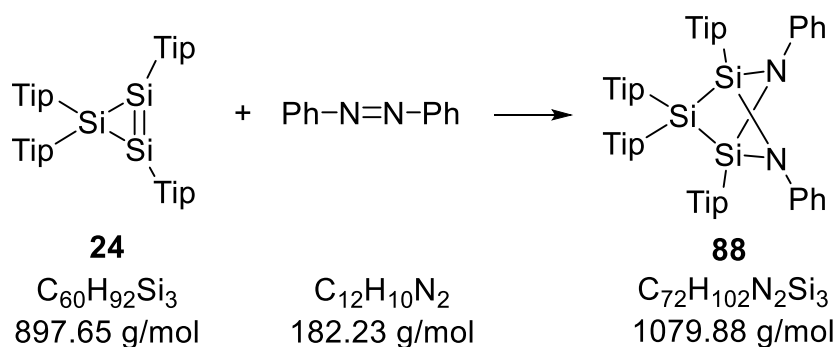
¹H NMR (300.13 MHz, C₆D₆, 300 K): δ 8.41 (br, 1H, Ph-*H*), 7.55 (br, 1H, Ph-*H*); 7.35 (br, 1H, Ph-*H*), 7.15 (overlapped with solvent, 2H, Tip-*H*), 7.10 (s, 2H, Ph-*H*), 7.08 (br, 2H, Tip-*H*), 7.03 (br, 1H, Tip-*H*), 6.99 (br, 1H, Tip-*H*), 6.85 (br, 1H, Tip-*H*), 6.74 (br, 1H, Tip-*H*), 4.14-4.08 (m, 1H, *i*Pr-*CH*), 3.91-3.74 (m, 3H, *i*Pr-*CH*), 3.50-3.43 (m, 1H, *i*Pr-*CH*), 3.34-3.17 (m, 2H, *i*Pr-*CH*), 3.09-3.05 (m, 1H, *i*Pr-*CH*), 2.68-2.61 (m, 4H, *i*Pr-*CH*), 1.53 (d, J_{H-H} = 5.8 Hz, 3H, *i*Pr-CH₃), 1.48 (d, J_{H-H} = 6.8 Hz, 9H, *i*Pr-CH₃), 1.43 (d, J_{H-H} = 6.2 Hz, 3H, *i*Pr-CH₃), 1.23 (br, 9H, *i*Pr-CH₃), 1.14, 1.13 (br, 6H, *i*Pr-CH₃), 1.12, 1.11 (br, 12H, *i*Pr-CH₃), 1.10, 1.08 (br, 9H, *i*Pr-CH₃), 0.94 (d, J_{H-H} = 6.6 Hz, 3H, *i*Pr-CH₃), 0.66, 0.64 (each d, J_{H-H} = 3.4 Hz, 6H, *i*Pr-CH₃), 0.61, 0.59 (each d, J_{H-H} = 3.5 Hz, 6H, *i*Pr-CH₃), 0.29, 0.27 (d, J_{H-H} = 6.6 Hz, 6H, *i*Pr-CH₃) ppm.

$^{13}\text{C}\{^1\text{H}\}$ NMR (75.47 MHz, C_6D_6 , 300 K): δ 157.69, 155.65, 155.05, 154.96, 154.73, 151.96, 151.87, 151.26, 149.70, 143.11 (Tip-C); 134.93, 133.51, 132.73, 131.27 (Tip-CH); 126.81, 124.98 (Ph-CH); 123.60, 123.12, 122.71, 122.55, 122.01 (Tip-CH); 121.82, 121.57 (Ph-CH); 38.19, 36.54, 36.05, 35.86, 35.72, 35.36, 35.07, 35.00, 34.47, 34.33, 34.31, 34.22, 31.79 (*i*Pr-CH); 27.84, 26.87, 26.72, 26.42, 26.23, 25.83, 25.62, 25.25, 24.66, 24.58, 24.29, 24.02, 23.85, 23.82, 23.75, 23.71, 23.65, 23.63, 22.88, 21.74 (*i*Pr-CH₃) ppm.

$^{29}\text{Si}\{^1\text{H}\}$ NMR (59.6 MHz, C_6D_6 , 300 K): δ 39.26 (S/TipO), 15.12 (S/TipC), -6.19 (S/Tip₂) ppm.

Elemental Analysis Calc. for $\text{C}_{67}\text{H}_{97}\text{ClOSi}_3$. C, 77.51; H, 9.42 Found: C, 77.40; H, 9.44.

6.3.4 Synthesis of **88**



Cyclotrisilene **24** (300 mg, 0.334 mmol) and azobenzene (61 mg, 0.334 mmol) are mixed and dissolved in 10 mL toluene. The resulting red-orange mixture is heated to 60 °C and stirred overnight at that temperature, yielding a yellow solution. Removal of toluene in vacuum results in a light-yellow powder, which is dissolved in 5 mL of hexane. The solution is kept at room temperature to afford pale yellow crystals of **88** after one day, which are isolated by solvent decantation and drying in vacuum (252 mg, yield: 70%, mp. > 200 °C).

^1H NMR (300.13 MHz, C_6D_6 , 300 K): δ 7.30 (d, $J_{\text{H-H}} = 3.9$ Hz, 4H, Tip-H), 6.88 (s, 4H, Tip-H), 6.66-6.57 (m, 8H, Ph-H), 6.45-6.40 (m, 2H, Ph-H), 4.86-4.81 (m, 2H, *i*Pr-CH), 4.26-4.22 (m, 2H, *i*Pr-CH), 3.73-3.64 (m, 4H, *i*Pr-CH), 2.80-2.64 (m, 4H, *i*Pr-CH), 1.52 (d, $J_{\text{H-H}} = 6.3$ Hz, 12H, *i*Pr-CH₃), 1.25 (d, $J_{\text{H-H}} = 6.3$ Hz, 12H, *i*Pr-CH₃), 1.21 (d, $J_{\text{H-H}} = 6.9$ Hz, 12H, *i*Pr-CH₃), 1.17 (d, $J_{\text{H-H}} = 6.9$ Hz, 12H, *i*Pr-CH₃) ppm.

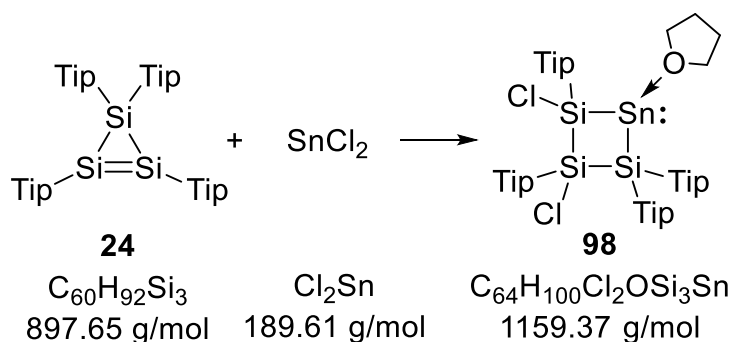
$^{13}\text{C}\{^1\text{H}\}$ NMR (75.47 MHz, C_6D_6 , 300 K): δ 160.31, 158.25, 156.10, 153.79, 149.83

(Tip-C), 146.19 (Ph-C), 136.82 (Tip-CH), 124.46, 122.39, 121.85, 121.27 (Tip-CH), 120.85, 117.67 (Ph-CH), 36.71, 36.04, 34.62, 34.35, 32.77 (*i*Pr-CH), 26.65, 26.20, 25.67, 23.93, 23.70, 22.55 (*i*Pr-CH₃) ppm.

²⁹Si{¹H} NMR (59.6 MHz, C₆D₆, 300 K): δ 37.66 (S/Tip₂), -24.23 (S/Tip) ppm.

Elemental Analysis Calc. for C₇₂H₁₀₂N₂Si₃. C, 80.08; H, 9.52 Found: C, 80.10; H, 9.72.

6.3.5 Synthesis of **98**



At -30 °C a solution of cyclotrisilene **24** (300.0 mg, 0.334 mmol) in 5 mL of thf is added by cannula to a suspension of SnCl₂ (63.3 mg, 0.334 mmol) in 8 mL thf. The suspension turns brown after the first few drops of **24** have been added. The resulting brown mixture (ca. 15 mL) is stirred for two hours while warming to room temperature, then concentrated to ca. 5 mL under vacuum and kept at -20 °C overnight. Yellow needle-shaped crystals of X-ray quality form (element Sn and brownish impurities also form during crystallization) and are isolated by solvent decantation. After removal of residual solvent **98** is isolated as powder (155 mg, yield: 40%, mp. 120 °C, dec.).

¹H NMR (300.13 MHz, thf-d₈, 300 K): δ 7.05 (br., 1H, Tip-*H*), 7.02 (br., 1H, Tip-*H*), 6.99 (br., 2H, Tip-*H*), 6.79-6.78 (br., 4H, Tip-*H*), 4.25-4.14 (m, 2H, *i*Pr-*CH*), 3.97-3.90 (m, 2H, *i*Pr-*CH*), 3.67 (m, 1H, 2H, *i*Pr-*CH*), 3.51, 3.47 (each br., 4H, C₄H₈O), 2.75-2.65 (m, 6H, 2H, *i*Pr-*CH*), 2.44-2.35 (m, 1H, 2H, *i*Pr-*CH*), 1.62 (br., 4H, C₄H₈O), 1.50 (t, 6H, *i*Pr-*CH*₃), 1.37 (d, *J*_{H-H} = 6.3 Hz, 6H, *i*Pr-*CH*₃), 1.31 (d, *J*_{H-H} = 6.9 Hz, 6H, *i*Pr-*CH*₃), 1.24 (d, *J*_{H-H} = 6.3 Hz, 6H, *i*Pr-*CH*₃), 1.12-1.07 (each br., total 32H, *i*Pr-*CH*₃), 0.95 (d, *J*_{H-H} = 6.0 Hz, 3H, *i*Pr-*CH*₃), 0.84 (d, *J*_{H-H} = 6.6 Hz, 3H, *i*Pr-*CH*₃), 0.34 (d, *J*_{H-H} = 6.9 Hz, 3H, *i*Pr-*CH*₃), 0.20 (t, 6H, *i*Pr-*CH*₃) ppm.

¹³C{¹H} CP/MAS (100.63 MHz, 300 K): δ 155.53, 154.38, 150.23, 148.30, 143.07 (Tip-C), 137.73, 134.26, 121.92 (Tip-CH), 69.61 (C₄H₈O), 38.40, 36.97, 35.78, 34.20

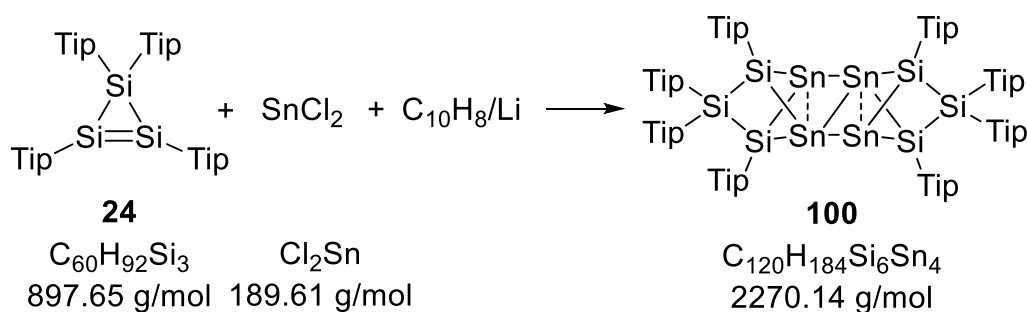
(ⁱPr-CH), 29.85 (ⁱPr-CH₃), 27.56 (C₄H₈O), 25.66, 24.79, 21.68 (ⁱPr-CH₃) ppm.

²⁹Si{¹H} CP/MAS (79.5 MHz, 300 K): δ 30.50 (s), 19.01 (s), 16.38 (br.) ppm.

UV/Vis (thf) λ(ε) 271 nm (35036 L mol⁻¹cm⁻¹), 450 nm (shoulder).

Elemental Analysis Calc. for C₆₄H₁₀₀Cl₂OSi₃Sn. C, 66.30; H, 8.69, Found: C, 65.81; H, 8.85.

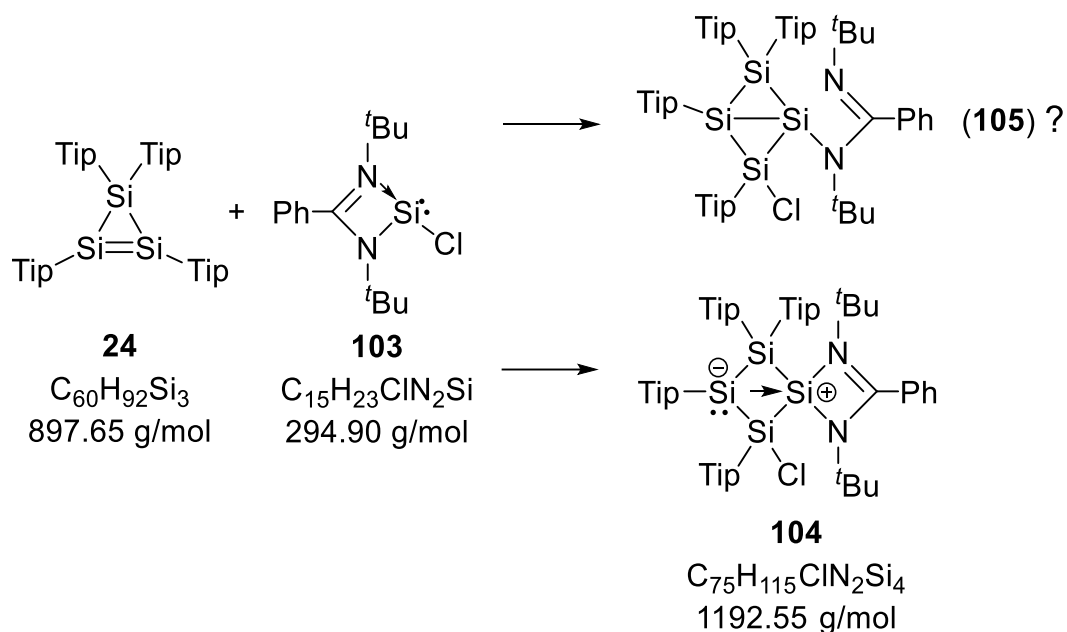
6.3.6 Synthesis of **100**



SnCl₂ (63.3 mg, 0.334 mmol) was dissolved in 5 mL thf and the resulting suspension cooled to -20 °C. A solution of cyclotrisilene **24** (300 mg, 0.334 mmol) in 8 mL thf was added to the SnCl₂ suspension by cannula at room temperature during two minutes. After the first few drops added, the color of the reaction mixture turned dark-brown. The reaction mixture was stirred at -20 °C for one hour. A newly prepared suspension of naphthalene lithium (excess) was introduced into the above brownish reaction mixture at -20 °C resulting in a greenish reaction mixture. After the greenish mixture was stirred for overnight while let it increase to room temperature, removed the solvent thf and 10mL hexane was added into the greenish residue. The filtrate hexane solution was concentrated to ~3 mL and kept still at room temperature. After one week block green crystal formed and was confirmed by X-ray single crystal analysis as product **100**.

¹H NMR (400.13 MHz, C₆D₆, 300 K): δ 7.11 (s, 4H, Tip-H), 6.97 (s, 4H, Tip-H), 6.92 (s, 4H, Tip-H), 6.75 (s, 4H, Tip-H), 4.98-4.96 (m, 3H, ⁱPr-CH), 4.39-4.36 (m, 3H, s, 4H, ⁱPr-CH), 3.48-3.45 (m, 3H, s, 4H, ⁱPr-CH), 3.16-3.13 (m, 3H, ⁱPr-CH), 2.79-2.64 (m, 12H, ⁱPr-CH), 1.80 (d, J_{H-H} = 6.2 Hz, 12H, ⁱPr-CH₃), 1.53, 1.51, 1.49 (br, 18H, ⁱPr-CH₃), 1.46 (d, J_{H-H} = 6.2 Hz, 12H, ⁱPr-CH₃), 1.32, 1.30, 1.28 (br, 30H, ⁱPr-CH₃), 1.14, 1.12, 1.11 (br, 30H, ⁱPr-CH₃), 0.56, 0.50 (each d, J_{H-H} = 6.6 Hz, 18H, ⁱPr-CH₃), 0.34 (d, J_{H-H} = 6.6 Hz, 9H, ⁱPr-CH₃), 0.30 (br, 6H, ⁱPr-CH₃), 0.13 (d, J_{H-H} = 6.6 Hz, 9H, ⁱPr-CH₃) ppm.

6.3.7 Synthesis of 104 and 105



Synthesis of 104 Cyclotrisilene **24** (300 mg, 0.334 mmol) and Roesky silylene **103** (98.5 mg, 0.334 mmol) are mixed in a 50 mL Schlenk flask in the glove box, 15 mL toluene is added to the solid mixture *via* syringe. The resulting orange solution is stirred for four hours at room temperature. 1H NMR shows two sets of signals corresponding to product **104** and **105**. Removal of the solvent in vacuum and addition of 8 mL hexane yields an orange precipitate and an orange solution. The two phases are separated by filtration via a glass frit. **104** is obtained as orange powder of high purity (103 mg) after drying of the precipitate in vacuum.

1H NMR (300.13 MHz, toluene- d_8 , 223 K): δ 7.40 (br, 1H, Ph-*H*), 7.37 (s, 1H, Tip-*H*), 7.31 (s, 2H, Tip-*H*), 7.25 (s, 2H, Tip-*H*), 7.17 (s, 2H, Tip-*H*), 7.16 (s, 1H, Tip-*H*), 7.05 (s, 1H, Tip-*H*), 6.92 (m, 2H, Ph-*H*), 6.89 (br, 1H, Ph-*H*), 6.85-6.81 (m, 1H, Ph-*H*), 5.10-5.00 (m, 2H, *i*Pr-*CH*), 4.43-4.32 (m, 2H, *i*Pr-*CH*), 4.25-4.20 (m, 1H, *i*Pr-*CH*), 4.06-4.04 (m, 1H, *i*Pr-*CH*), 3.30-3.26 (m, 1H, *i*Pr-*CH*), 2.84-2.77 (m, 4H, *i*Pr-*CH*), 2.62 (m, 1H, *i*Pr-*CH*), 1.84, 1.81, 1.79, 1.77 (each br, total 12H, *i*Pr-*CH*₃), 1.73 (d, $J_{H-H} = 6.9$ Hz, 6H, *i*Pr-*CH*₃), 1.63 (d, $J_{H-H} = 6.9$ Hz, 3H, *i*Pr-*CH*₃), 1.54 (d, $J_{H-H} = 6.9$ Hz, 3H, *i*Pr-*CH*₃), 1.47 (br, 3H, *i*Pr-*CH*₃), 1.44 (d, $J_{H-H} = 6.9$ Hz, 6H, *i*Pr-*CH*₃), 1.34 (br, 18H, *t*Bu-*CH*₃), 1.31 (br, 6H, *i*Pr-*CH*₃), 1.29 (br, 3H, *i*Pr-*CH*₃), 1.27 (d, $J = 3.3$ Hz, 3H, *i*Pr-*CH*₃), 1.24 (d, $J = 3.3$ Hz, 3H, *i*Pr-*CH*₃), 1.21 (br, 3H, *i*Pr-*CH*₃), 1.15, 1.12 (each br, 3H, *i*Pr-*CH*₃), 0.98-0.91 (br, 6H, *i*Pr-*CH*₃), 0.65 (d, $J_{H-H} = 6.1$ Hz, 6H, *i*Pr-*CH*₃), 0.44 (d, $J_{H-H} = 6.0$ Hz, 3H, *i*Pr-*CH*₃), 0.31 (d, $J_{H-H} = 6.5$ Hz, 3H, *i*Pr-*CH*₃) ppm.

$^{13}\text{C}\{^1\text{H}\}$ NMR (75.47 MHz, C_6D_6 , 300 K): δ 155.77, 153.65, 151.91, 149.76, 147.88 (d), 142.25, 140.24, 130.02, 129.07, 123.58, 123.36 (br.), 121.29, 119.95, 55.53, 54.99, 37.63, 37.02 (d), 36.88, 34.66 (d), 34.32, 32.64, 32.53, 31.32 (d), 25.09, 24.49, 24.20, 24.06, 23.98, 23.82, 23.67 ppm.

$^{13}\text{C}\{^1\text{H}\}$ CP/MAS (100.63 MHz, 300 K): δ 173.38 (Ph-C), 155.53 (d), 153.32 (d), 148.03 (d), 143.10 (d), 131.79, 129.98 (d), 127.28, 125.62, 123.82 (br), 122.91, 121.28 (br), 119.91, 55.30 (d), 37.49 (br), 34.33 (br), 32.68 (d), 30.10, 28.53, 27.49 (d), 26.02, 25.46, 25.03, 24.35, 22.89, 21.87(d) ppm.

$^{29}\text{Si}\{^1\text{H}\}$ NMR (59.6 MHz, toluene- d_8 , 223 K): δ 21.08, 0.98, -9.15 and -27.24 ppm.

$^{29}\text{Si}\{^1\text{H}\}$ CP/MAS (79.5 MHz, 300 K): δ 21.88, 1.10, -10.43 and -23.55 ppm.

UV/Vis (toluene) λ_{max} 422 nm (ϵ 5820 L mol $^{-1}$ cm $^{-1}$).

Elemental Analysis Calc. for $\text{C}_{75}\text{H}_{115}\text{ClN}_2\text{Si}_4$. C, 75.54; H, 9.72; N, 2.35, Found: C, 75.47; H, 9.65; N, 2.28.

Synthesis of 105 The above hexane solution is separated from the orange precipitate and concentrated to ca. 3 mL. Orange-red crystals of **105** appear after the hexane solution is kept at room temperature overnight. The first crop of crystals of **105** (50 mg, yield: 12.6%) are isolated by solvent decantation. Recrystallization of the mother liquid gives a second crop of crystals (16 mg). In total: 66 mg, yield: 16.6%, mp. > 200 °C.

^1H NMR (400.13 MHz, C_6D_6 , 300 K): δ 7.53-7.51 (m, 1H, Ph-H), 7.42-7.39 (m, 1H, Ph-H), 7.32 (d, 1H, Tip-H), 7.30 (d, 1H, Tip-H), 7.27 (d, 1H, Tip-H), 7.21 (d, 1H, Tip-H), 7.10 (d, 1H, Tip-H), 7.03 (d, 1H, Tip-H), 6.97-6.95 (m, 3H, Ph-H), 6.93 (d, 1H, Tip-H), 6.89 (d, 1H, Tip-H), 5.84-5.77 (m, 1H, $^i\text{Pr-CH}$), 4.35-4.26 (m, 2H, $^i\text{Pr-CH}$), 4.15-4.08 (m, 1H, $^i\text{Pr-CH}$), 3.99-3.92 (m, 1H, $^i\text{Pr-CH}$), 3.73-3.67 (m, 1H, $^i\text{Pr-CH}$), 3.58-3.46 (m, 2H, $^i\text{Pr-CH}$), 2.84-2.73 (m, 4H, $^i\text{Pr-CH}$), 1.81 (d, $J_{\text{H-H}} = 6.3$ Hz, 3H, $^i\text{Pr-CH}_3$), 1.78 (d, $J_{\text{H-H}} = 6.6$ Hz, 6H, $^i\text{Pr-CH}_3$), 1.75 (s, 1H, $^i\text{Pr-CH}_3$), 1.74 (d, $J_{\text{H-H}} = 6.2$ Hz, 6H, $^i\text{Pr-CH}_3$), 1.71 (s, 1H, $^i\text{Pr-CH}_3$), 1.64 (d, $J_{\text{H-H}} = 6.6$ Hz, 3H, $^i\text{Pr-CH}_3$), 1.60 (d, $J_{\text{H-H}} = 6.8$ Hz, 3H, $^i\text{Pr-CH}_3$), 1.40 (d, $J_{\text{H-H}} = 6.6$ Hz, 3H, $^i\text{Pr-CH}_3$), 1.34 (d, $J_{\text{H-H}} = 6.6$ Hz, 3H, $^i\text{Pr-CH}_3$), 1.26 (s, 1H, $^i\text{Pr-CH}_3$), 1.25 (d, $J_{\text{H-H}} = 1.6$ Hz, 6H, $^i\text{Pr-CH}_3$), 1.23 (br, 3H, $^i\text{Pr-CH}_3$), 1.22 (d, $J_{\text{H-H}} = 1.7$ Hz, 3H, $^i\text{Pr-CH}_3$), 1.21 (br, 3H, $^i\text{Pr-CH}_3$), 1.20 (s, 1H, $^i\text{Pr-CH}_3$), 1.19 (s, 3H, $^i\text{Pr-CH}_3$), 1.07 (br, 9H, $^t\text{Bu-CH}_3$), 1.06 (br, 9H, $^t\text{Bu-CH}_3$), 1.03 (d, $J_{\text{H-H}} = 6.6$ Hz, 3H, $^i\text{Pr-CH}_3$), 0.89, 0.87, 0.86 (each br, 9H, $^i\text{Pr-CH}_3$), 0.50 (d, $J_{\text{H-H}} = 6.5$ Hz, 3H, $^i\text{Pr-CH}_3$), 0.33 (d, $J_{\text{H-H}} = 6.3$ Hz, 3H, $^i\text{Pr-CH}_3$), 0.25 (d, $J_{\text{H-H}} = 6.5$ Hz, 3H, $^i\text{Pr-CH}_3$) ppm.

$^{13}\text{C}\{^1\text{H}\}$ NMR (100.6 MHz, C_6D_6 , 300 K): δ 172.34 (Ph-C), 155.81, 155.54, 154.66, 154.51, 154.26, 153.01, 150.46, 149.29, 149.15, 148.56, 147.99 (Tip-C), 142.26, 139.70, 137.84, 137.12 (Tip-CH); 132.73 (=CPh); 130.01, 129.89 (Ph-CH), 123.61, 123.49, 123.28, 122.15, 121.93, 121.67, 121.45, 121.32 (Tip-CH); 56.17, 54.59 (^tBu -C), 37.06, 36.40, 36.27, 35.95, 35.17, 35.08, 34.76, 34.39, 34.32, 34.11, 33.97 (^iPr -CH); 32.70, 32.36 (^tBu -CH₃), 30.72, 30.50 (^iPr -CH); 28.17, 28.03, 27.74, 27.55, 27.48, 27.22, 27.00, 26.71, 25.82, 25.55, 25.46, 24.67, 24.42, 23.93 (d), 23.81 (d) (^iPr -CH₃); 23.67 (^tBu -CH₃); 22.34 (^iPr -CH₃) ppm.

$^{29}\text{Si}\{^1\text{H}\}$ NMR (79.5 MHz, C_6D_6 , 300 K): δ -8.22, -20.01, -24.39, -49.30 ppm.

UV/Vis (hexane) λ_{max} (ϵ) 328 nm (14350 L mol⁻¹cm⁻¹), 410 nm (shoulder).

Elemental Analysis Calc. for $\text{C}_{75}\text{H}_{115}\text{ClN}_2\text{Si}_4$. C, 75.54; H, 9.72; N, 2.35, Found: C, 75.32; H, 9.74; N, 2.18.

7 References

- [1] N. N. Greenwood, A. Earnshaw, *Chemistry of the Elements*, Elsevier Science, **2011**, p. 334-335.
- [2] M. Berzelius, *The Philosophical Magazine*, **1825**, *65*, 254-267.
- [3] a) H. S-C. Deville, *Comptes rendus*, **1854**, *39*, 321-326; b) H. S-C. Deville, *Comptes rendus*, **1855**, *40*, 1034-1036.
- [4] A. Stock, *Hydrides of Boron and Silicon*, Cornell University Press, **1933**.
- [5] N. N. Greenwood, A. Earnshaw, *Chemistry of the Elements*, Elsevier Science, **2011**, p. 328-366.
- [6] E. G. Rochow, *Silicon and Silicones*; Springer: Berlin/Heidelberg, Germany, **1987**.
- [7] a) P. Jutzi, *Angew. Chem. Int. Ed.* **1975**, *14*, 232; b) L. E. Gusel'nikov, N. S. Nametkin, *Chem. Rev.* **1979**, *79*, 529-577.
- [8] K. S. Pitzer, *J. Am. Soc. Chem.* **1948**, *70*, 2140-2145.
- [9] a) R. S. Mulliken, *J. Am. Chem. Soc.* **1950**, *72*, 4493-4503; b) R. S. Mulliken, *J. Am. Chem. Soc.* **1955**, *77*, 884-887.
- [10] M. Yoshifuji, I. Shima, N. Inamoto, K. Hirotsu, T. Higuchi, *J. Am. Chem. Soc.* **1981**, *103*, 4587-4589.
- [11] R. West, M. J. Fink, J. Michl, *Science* **1981**, *214*, 1343-1344.
- [12] A. G. Brook, F. Abdesaken, B. Gutekunst, G. Gutenkunst, R. K. Kallury, *J. Chem. Soc. Chem. Comm.*, **1981**, 191-192.
- [13] a) B. Gehrhus, M. F. Lappert, *J. Organomet. Chem.* **2001**, 617-618, 209-223; b) N. J. Hill, R. West, *J. Organomet. Chem.* **2004**, *689*, 4165-4183; c) Y. Mizuhata, T. Sasamori, N. Tokitoh, *Chem. Rev.* **2009**, *109*, 3479-3511; d) H. W. Roesky, *J. Organomet. Chem.* **2013**, *730*, 57-62; e) B. Blom, D. Gallego, M. Driess, *Inorg. Chem. Front.* **2014**, *1*, 134-148.
- [14] a) C. Chatgililoglu, *Chem. Rev.* **1995**, *95*, 1229-1251; b) C. Chatgililoglu, *Organosilanes in Radical Chemistry*; John Wiley & Sons, Ltd., **2004**; c) B. Tumanskii, M. Karni, Y. Apeloig, *Chapter 6, Silicon-Centered Radicals*. In *Organosilicon Compounds: Theory and Experiment (Synthesis)*, V. Y. Lee, Eds.; Elsevier Science, **2017**.
- [15] a) C. Präsang, D. Scheschkewitz, *Chem. Soc. Rev.* **2016**, *45*, 900-921; b) T.

-
- Iwamoto, S. Ishida, *Struct. Bond.* **2014**, *156*, 125-202; c) D. Scheschkewitz, *Chem. Lett.* **2011**, *40*, 2-11; d) V. Y. Lee, A. Sekiguchi, J. Escudié, H. Ranaivonjatovo, *Chem. Lett.* **2010**, *39*, 312-318; e) D. Scheschkewitz, *Chem. Eur. J.* **2009**, *15*, 2476-2485; f) M. Kira, T. Iwamoto, *Adv. Organomet. Chem.* **2006**, *54*, 73-148.
- [16] a) S. Ishida, T. Iwamoto, C. Kabuto, M. Kira, *Nature* **2003**, *421*, 725-727; b) H. Tanaka, S. Inoue, M. Ichinohe, M. Driess, A. Sekiguchi, *Organometallics* **2011**, *30*, 3475-3478.
- [17] a) N. Wiberg, W. Niedermayer, G. Fischer, H. Nöth, M. Suter, *Eur. J. Inorg. Chem.* **2002**, *5*, 1066-1070; b) A. Sekiguchi, R. Kinjo, M. Ichinohe, *Science* **2004**, *305*, 1755-1757; c) T. Sasamori, K. Hironaka, Y. Sugiyama, N. Takagi, S. Nagase, Y. Hosoi, Y. Furukawa, N. Tokitoh, *J. Am. Soc. Chem.* **2008**, *130*, 13856-13857; d) S. Ishida, R. Sugawara, Y. Misawa, T. Iwamoto, *Angew. Chem. Int. Ed.* **2013**, *52*, 12869-12873.
- [18] Y. Wang, Y. Xie, P. Wei, R. B. King, H. F. Schaefer III, P. v. R. Schleyer, G. H. Robinson, *Science* **2008**, *321*, 1067-1071.
- [19] K. Abersfelder, A. J. P. White, H. S. Rzepa, D. Scheschkewitz, *Science* **2010**, *327*, 564-566.
- [20] S. Marutheeswaran, P. D. Pancharatna, M. M. Balakrishnarajan, *Phys. Chem. Chem. Phys.* **2014**, *16*, 11186-11190.
- [21] S. Masamune, W. Hanzawa, S. Murakami, T. Bally, J. F. *J. Am. Chem. Soc.* **1982**, *104*, 1150-1153.
- [22] R. Okazaki, R. West, *Adv. Organomet. Chem.* **1996**, *39*, 231-274.
- [23] T. Iwamoto, C. Kabuto, M. Kira, *J. Am. Chem. Soc.* **1999**, *121*, 886-887.
- [24] M. Ichinohe, T. Matsuno, A. Sekiguchi, *Angew. Chem. Int. Ed.* **1999**, *38*, 2194-2196.
- [25] a) G. J. D. Peddle, D. N. Roark, A. M. Good, S. G. McGeachin, *J. Am. Chem. Soc.* **1969**, *91*, 2807-2808; b) D. N. Roark, G. J. D. Peddle, *J. Am. Chem. Soc.* **1972**, *94*, 5837-5841.
- [26] F. L. Carter, V. L. Frampton, *Chem. Rev.* **1964**, *64*, 497-525.
- [27] M. Kira, T. Maruyama, C. Kabuto, K. Ebata, H. Sakurai, *Angew. Chem. Int. Ed.* **1994**, *33*, 1489-1491.

-
- [28] a) E. A. Carter, W. A. Goddard III, *J. Phys. Chem.* **1986**, *90*, 998-1001; b) G. Trinquier, J. P. Malrieu, *J. Am. Chem. Soc.* **1987**, *109*, 5303-5315; c) J. P. Malrieu, G. Trinquier, *J. Am. Chem. Soc.* **1989**, *111*, 5916-5921; d) G. Trinquier, *J. Am. Chem. Soc.* **1990**, *112*, 2130-2137.
- [29] a) L. B. Harding, W. A. Goddard III, *J. Chem. Phys.* 1978, *55*, 217-220; b) D. G. Leopold, K. K. Murray, W. C. Lineberger, *J. Chem. Phys.* 1984, *81*, 1048-1050.
- [30] Theoretical calculations of ΔE_{ST} in SiH₂: a) K. Balasubramanian, A. D. Mclean, *J. Chem. Phys.* **1986**, *85*, 5117-5119; b) A. F. Sax, J. Kalcher, *J. Mol. Struct.* **1992**, *253*, 287; c) T. J. Van. Huis, Y. Yamaguchi, C. D. Sherrill, H. F. Schaefer III, *J. Phys. Chem.* **1997**, *101*, 6955; d) L. V. Slipchenko, A. L. Krylov, *J. Chem. Phys.* **2002**, *117*, 4696; e) Y. Apeloig, R. Pauncz, M. Karni, R. West, W. Steiner, D. Chapman, *Organometallics* **2003**, *22*, 3250-3256.
- [31] Experimental determination of ΔE_{ST} in SiH₂: a) A. Kasden, E. Herbst, W. C. Lineberger, *J. Chem. Phys.* **1975**, *62*, 541; b) J. Berkowitz, J. P. Greene, H. Cho. B. Rušćić, *J. Chem. Phys.* **1987**, *86*, 1235-1248.
- [32] H. Jacobsen, T. Ziegler, *J. Am. Chem. Soc.* **1994**, *116*, 3667-3679.
- [33] a) K. B. Wiberg, *Angew. Chem. Int. Ed. Engl.* **1986**, *25*, 312-322; b) E. Hengge, R. Janoschek, *Chem. Rev.* **1995**, *95*, 1495-1526.
- [34] P. George, M. Trachtman, C. W. Bock, A. M. Brett, *Tetrahedron* **1976**, *32*, 317-323.
- [35] B. M. Gimarc, M. Zhao, *Coord. Chem. Rev.* **1997**, *158*, 385-412.
- [36] Y. Naruse, J. Ma, S. Inagaki, *Tetrahedron Lett.* **2001**, *42*, 6553-6556.
- [37] a) K. Fukui, S. Inagaki, *J. Am. Soc. Chem.* **1975**, *97*, 4445-4452; b) S. Inagaki, H. Fujimoto, K. Fukui, *J. Am. Soc. Chem.* **1976**, *98*, 4054-4061.
- [38] A. Tsurusaki, J. Kamiyama, S. Kyushin, *J. Am. Soc. Chem.* **2014**, *136*, 12896-12898.
- [39] M. Ichinohe, M. Igarashi, K. Sanuki, A. Sekiguchi, *J. Am. Chem. Soc.* **2005**, *127*, 9978-9979.
- [40] V. Y. Lee, T. Matsuno, M. Ichinohe, A. Sekiguchi, *Heteroat. Chem.* **2001**, *12*, 223-226.
- [41] a) S. Nagase, T. Kudo, *J. Chem. Soc., Chem. Commun.* **1984**, 1392-1394; b) S. Ishida, T. Iwamoto, M. Kira, *Organometallics* **2009**, *28*, 919-921.

-
- [42] V. Y. Lee, H. Yasuda, A. Sekiguchi, *J. Am. Chem. Soc.* **2007**, *129*, 2436-2437.
- [43] H. Tanaka, S. Inoue, M. Ichinohe, M. Driess, A. Sekiguchi, *Organometallics* **2011**, *30*, 3475-3478.
- [44] N. Wiberg, S. K. Vasisht, G. Fischer, P. Mayer, *Z. Anorg. Allg. Chem.* **2004**, *630*, 1823-1828.
- [45] Y. Murata, M. Ichinohe, A. Sekiguchi, *J. Am. Chem. Soc.* **2010**, *132*, 16768-16770.
- [46] W. E. Vaughan, *J. Am. Chem. Soc.* **1932**, *54*, 3863-3876.
- [47] J. H. Kiefer, H. C. Wei, R. D. Kern, C. H. Wu, *Int. J. Chem. Kinet.* **1985**, *17*, 225-253.
- [48] a) R. Srinivasan, *J. Am. Chem. Soc.* **1963**, *85*, 4045-4046; b) J. C. Robinson, S. A. Harris, W. Sun, N. E. Sveum, D. M. Neumark, *J. Am. Chem. Soc.* **2002**, *124*, 10211-10224.
- [49] K. Uchiyama, S. Nagendran, S. Ishida, T. Iwamoto, M. Kira, *J. Am. Chem. Soc.* **2007**, *129*, 10638-10639.
- [50] D. Scheschkewitz, *Angew. Chem. Int. Ed.* **2004**, *43*, 2965-2967.
- [51] Latest reviews: a) A. Rammo, D. Scheschkewitz, *Chem. Eur. J.* **2018**, *24*, 6866-6885; b) Y. Heider, D. Scheschkewitz, *Dalton. Trans.*, **2018**, *47*, 7104-7112.
- [52] K. Leszczynska, K. Abersfelder, A. Mix, B. Neumann, H.-G. Stammer, M. J. Cowley, P. Jutzi, D. Scheschkewitz, *Angew Chem. Int. Ed.* **2012**, *51*, 6785-6788.
- [53] K. Abersfelder, D. Güclü, D. Scheschkewitz, *Angew. Chem. Int. Ed.* **2005**, *45*, 1643-1645.
- [54] T. Iwamoto, M. Tamura, C. Kabuto, M. Kira, *Science* **2000**, *290*, 504-506.
- [55] V. Y. Lee, M. Ichinohe, A. Sekiguchi, *J. Am. Chem. Soc.* **2000**, *122*, 9034-9035.
- [56] T. Iwamoto, N. Akasaka, S. Ishida, *Nat. Commun.* **2014**, *5*, 5353-5359.
- [57] M. Kaftory, M. Kapon, M. Botoshansky, *The Chemistry of Organic Silicon Compounds* Vol. 2 (eds Z. Rappoport & Y. Apeloig) chapter 5, 188-266, John Wiley & Sons, **1998**.
- [58] V. Y. Lee, S. Miyazaki, H. Yasuda, A. Sekiguchi, *J. Am. Chem. Soc.* **2008**, *130*, 2758-2759.

-
- [59] V. Y. Lee, O. A. Gapurenko, S. Miyazaki, A. Sekiguchi, R. M. Minyaev, V. I. Minkin, H. Gornitzka, *Angew. Chem. Int. Ed.* **2015**, *54*, 1-6.
- [60] A. Sekiguchi, S. Inoue, M. Ichinohe, *J. Am. Chem. Soc.* **2004**, *126*, 9626-9629.
- [61] R. West, J. D. Cavalieri, J. J. Buffy, C. Fry, K. W. Zilm, J. C. Duchamp, M. Kira, T. Iwamoto, T. Müller, Y. Apeloig, *J. Am. Chem. Soc.* **1997**, *119*, 4972-4976.
- [62] D. Auer, C. Strohmman, A. V. Arbuznikov, M. Kaupp, *Organometallics* **2003**, *22*, 2442-2449.
- [63] R. West, J. D. Cavalieri, J. Duchamp, K. W. Zilm, *Phosphorus, Sulfur, and Silicon*, **1996**, *93-94*, 213-216.
- [64] A. Sekiguchi, V. Y. Lee, *Chem. Rev.* **2003**, *103*, 1429-1447.
- [65] M. J. Cowley, Y. Ohmori, V. Huch, M. Ichinohe, A. Sekiguchi, D. Scheschkewitz, *Angew. Chem. Int. Ed.* **2013**, *52*, 13247-13250.
- [66] V. Y. Lee, M. Ichinohe, A. Sekiguchi, *Chem. Lett.* **2001**, *30*, 728-729.
- [67] V. Y. Lee, M. Ichinohe, A. Sekiguchi, *Chem. Commun.*, **2001**, 2146-2147.
- [68] H. Zhao, K. Leszczynska, L. Klemmer, V. Huch, M. Zimmer, D. Scheschkewitz, *Angew. Chem. Int. Ed.* **2018**, *57*, 2445-2449; *Angew. Chem.* **2018**, *130*, 2470-2474.
- [69] Y. Ohmori, M. Ichinohe, A. Sekiguchi, M. J. Cowley, V. Huch, D. Scheschkewitz, *Organometallics* **2013**, *32*, 1591-1594.
- [70] a) V. Y. Lee, S. Miyazaki, H. Yasuda, A. Sekiguchi, *J. Am. Chem. Soc.* **2008**, *130*, 2758-2759; b) V. Y. Lee, S. Miyazaki, H. Yasuda, A. Sekiguchi, *Phosphorus, Sulfur, and Silicon*, **2011**, *186*, 1346-1350.
- [71] H. Zhao, L. Klemmer, M. J. Cowley, M. Zimmer, V. Huch, D. Scheschkewitz, *Z. Anorg. Allg. Chem.* 10.1002/zaac.201800182
- [72] M. Ichinohe, T. Matsuno, A. Sekiguchi, *Chem. Commun.*, **2001**, 183-184.
- [73] M. J. Cowley, V. Huch, H. S. Rzepa, D. Scheschkewitz, *Nat. Chem.* **2013**, *5*, 876-879.
- [74] a) K. Hatano, N. Tokitoh, N. Takagi, S. Nagase, *J. Am. Chem. Soc.* **2000**, *122*, 4829-4830; b) J. Ohshita, H. Ohnishi, A. Naka, N. Senba, J. Ikadai, A. Kunai, H. Kobayashi, M. Ishikawa, *Organometallics* **2006**, *25*, 3955-3962; c) S. Yao, C. Wüllen, X. Y. Sun, M. Driess, *Angew. Chem. Int. Ed.* **2008**, *47*, 3250-3253; d) S. Ishida, T. Iwamoto, M. Kira, *Heteroat. Chem.* **2010**, *22*, 432-437; e) M.

-
- Ishikawa, A. Naka, J. Ohshita, *Asian J. Org. Chem.* **2015**, *4*, 1192-1209.
- [75] T. Iwamoto, M. Tamura, C. Kabuto, M. Kira, *Organometallics* **2003**, *22*, 2342-2344.
- [76] A. Sekiguchi, T. Matsuno, M. Ichinohe, *J. Am. Chem. Soc.* **2000**, *122*, 11250-11251.
- [77] A. R. Jupp, J. M. Goicoechea, *Angew. Chem. Int. Ed.* **2013**, *52*, 10064-10067.
- [78] T. P. Robinson, M. J. Cowley, D. Scheschkewitz, J. M. Goicoechea, *Angew. Chem. Int. Ed.* **2015**, *54*, 683-686.
- [79] M. J. Cowley, V. Huch, D. Scheschkewitz, *Chem. Eur. J.* **2014**, *20*, 9221-9224.
- [80] K. Leszczynska, K. Abersfelder, M. Majumdar, B. Neumann, H. -G. Stammler, H. S. Rzepa, P. Jutzi, D. Scheschkewitz, *Chem. Commun.*, **2012**, *48*, 7820-7822.
- [81] M. Kosa, M. Karni, Y. Apeloig, *J. Chem. Theory. Comput.* **2006**, *2*, 956-964.
- [82] A. Jana, M. Majumdar, V. Huch, M. Zimmer, D. Scheschkewitz, *Dalton Trans.*, **2014**, *43*, 5175-5181.
- [83] A. Jana, I. Omlor, V. Huch, H. S. Rzepa, D. Scheschkewitz, *Angew. Chem. Int. Ed.* **2014**, *53*, 9953-9956.
- [84] a) A. Fukazawa, Y. Li, S. Yamaguchi, H. Tsuji, K. Tamao, *J. Am. Chem. Soc.* **2007**, *129*, 14164-14165; b) I. Bejan, D. Scheschkewitz, *Angew. Chem. Int. Ed.* **2007**, *46*, 5783-5786; c) J. Jeck, I. Bejan, A. J. P. White, D. Nied, F. Breher, D. Scheschkewitz, *J. Am. Chem. Soc.* **2010**, *132*, 17306-17315.
- [85] N. M. Obeid, L. Klemmer, D. Maus, M. Zimmer, J. Jeck, I. Bejan, A. J. P. White, V. Huch, G. Jung, D. Scheschkewitz, *Dalton. Trans.*, **2017**, *46*, 8839-8848.
- [86] R. Kinjo, M. Ichinohe, A. Sekiguchi, N. Takagi, M. Sumimoto, S. Nagase, *J. Am. Chem. Soc.* **2007**, *129*, 7766-7767; (b) J. S. Han, T. Sasamori, Y. Mizuhata, N. Tokitoh, *Dalton Trans.*, **2010**, *39*, 9238-9240.
- [87] H. Yasusa, V. Y. Lee, A. Sekiguchi, *J. Am. Chem. Soc.* **2009**, *131*, 6352-6353.
- [88] a) V. Y. Lee, M. Ichinohe, A. Sekiguchi, *J. Am. Chem. Soc.* **2000**, *122*, 12604-12605; b) V. Y. Lee, M. Ichinohe, A. Sekiguchi, *J. Organomet. Chem.* **2001**, *636*, 41-48; c) V. Y. Lee, R. Kato, S. Aoki, A. Sekiguchi, *Russ. Chem. Bull.* **2011**, *60*, 2434-2425.
- [89] C. E. Dixon, K. M. Baines, *Phosphorus Sulfur and Silicon* **1997**, *124-125*,

-
- 123-132.
- [90] S. Boomgaarden, W. Saak, M. Weidenbruch, *Organometallics* **2001**, *20*, 2451-2453.
- [91] R. Singh, C. Czekelius, R. R. Schrock, *Macromolecules* **2006**, *39*, 1316-1317.
- [92] P. P. Power, *Chem. Rev.* **1999**, *12*, 3463-3504.
- [93] Jerry March, *Advanced Organic Chemistry: Reactions, Mechanisms, and Structure* (3rd ed.), New York: Wiley, ISBN 0-471-85472-7.
- [94] X.-Q. Xiao, X. Liu, Q. Lu, Z. Li, G. Lai, M. Kira, *Molecules* **2016**, *21*, 1376-1385.
- [95] Q. Lu, C. Yan, X.-Q. Xiao, Z. Li, N. Wei, G. Lai, M. Kira, *Organometallics* **2017**, *36*, 3633-3637.
- [96] I. Bejan, D. Güclü, S. Inoue, M. Ichinohe, A. Sekiguchi, D. Scheschkewitz, *Angew. Chem. Int. Ed.* **2007**, *46*, 3349-3352.
- [97] A. Sakakibara, Y. Kabe, T. Shimizu, W. Ando, *J. Chem. Soc., Chem. Commun.*, **1991**, 43-44.
- [98] C. Cui, M. M. Olmstead, J. C. Fettinger, G. H. Spikes, P. P. Power, *J. Am. Chem. Soc.* **2005**, *127*, 17530-17541.
- [99] S. H. Zhang, H. X. Yeong, C. W. So, *Chem. Eur. J.* **2011**, *17*, 3490-3499.
- [100] M. Majumdar, I. Bejan, V. Huch, A. J. P. White, G. R. Whittell, A. Schäfer, I. Manners, D. Scheschkewitz, *Chem. Eur. J.* **2014**, *20*, 9225-9229.
- [101] S. Ishida, Y. Misawa, S. Sugawara, T. Iwamoto, *Angew. Chem. Int. Ed.* **2017**, *56*, 13829-13832.
- [102] a) S. Masamune, Y. Kabe, S. Collins, *J. Am. Chem. Soc.* **1985**, *107*, 5552-5553; b) R. Jones, D. J. Williams, Y. Kabe, S. Masamune, *Angew. Chem. Int. Ed. Engl.* **1986**, *25*, 173-174; c) P. v. R. Schleyer, A. F. Sax, J. Kalcher, R. Janoschek, *Angew. Chem. Int. Ed. Engl.* **1987**, *26*, 364-366; d) M. Kira, T. Iwamoto, C. Kabuto, *J. Am. Chem. Soc.* **1996**, *118*, 10303-10304; e) T. Iwamoto, D. Z. Yin, C. Kabuto, M. Kira, *J. Am. Chem. Soc.* **2001**, *123*, 12730-12731; f) N. Wiberg, H. Auer, S. Wagner, K. Polborn, G. Kramer, *J. Organomet. Chem.* **2001**, *619*, 110-131; g) K. U. Ohshima, T. Iwamoto, M. Kira, *Organometallics* **2008**, *27*, 320-323.
- [103] V. Y. Lee, K. Takanashi, M. Ichinohe, A. Sekiguchi, *J. Am. Chem. Soc.* **2003**, *125*, 6012-6013.

-
- [104] A. Jana, V. Huch, M. Repisky, R. J. F. Berger, D. Scheschkewitz, *Angew. Chem. Int. Ed.* **2014**, *53*, 3514-3518.
- [105] H. Arp, J. Baumgartner, C. Marschner, T. Müller, *J. Am. Chem. Soc.* **2011**, *133*, 5632-5635.
- [106] R. Fischer, D. Frank, W. Gaderbauer, C. Kayser, C. Mechtler, J. Baumgartner, C. Marschner, *Organometallics* **2003**, *22*, 3723-3731.
- [107] K. Suzuki, T. Matsuo, D. Hashizume, H. Fueno, K. Tanaka, K. Tamao, *Science* **2011**, *331*, 1306-1309.
- [108] J. Keuter, K. Schwedtmann, A. Hepp, K. Bergander, O. Janka, C. Doerenkamp, H. Eckert, C. Mück-Lichtenfeld, F. Lips, *Angew. Chem. Int. Ed.* **2017**, *56*, 13866-13871.
- [109] Gaussian 09, Revision C.01. Gaussian, Inc.: Wallingford CT, **2009**.
- [110] A development of University of Karlsruhe and Forschungszentrum Karlsruhe GmbH, 1989-2007; TURBOMOLE GmbH, since 2007; available from <http://www.turbomole.com>; Karlsruhe.
- [111] a) A. D. Becke, *Phys. Rev. A* **1988**, *38*, 3098-3100; b) J. P. Perdew, *Phys. Rev. B* **1986**, *33*, 8822-8824.
- [112] S. Grimme, J. Antony, S. Ehrlich, H. Krieg, *J. Chem. Phys.* **2010**, *132*, 154104-154123.
- [113] S. Grimme, S. Ehrlich, L. Goerigk, *J. Comput. Chem.* **2011**, *32*, 1456-1465.
- [114] F. Weigend, R. Ahlrichs, *Phys. Chem. Chem. Phys.* **2005**, *7*, 3297-3305.
- [115] C. Y. Peng, P. Y. Ayala, H. B. Schlegel, M. J. Frisch, *J. Comput. Chem.* **1996**, *17*, 49-56.
- [116] J. W. Mclver, A. Komornic, *J. Am. Chem. Soc.* **1972**, *94*, 2625-2633.
- [117] a) A. E. Reed, R. B. Weinstock, F. Weinhold, *J. Chem. Phys.* **1985**, *83*, 735-746; b) A. E. Reed, L. A. Curtiss, F. Weinhold, *Chem. Rev.* **1988**, *88*, 899-926.
- [118] E. D. Glendening, J. K. Badenhoop, A. E. Reed, J. E. Carpenter, J. A. Bohmann, C. M. Morales, F. Weinhold, GENNBO 5.9 ed.; Theoretical Chemistry Institute, University of Wisconsin: Madison, WI, **2009**.
- [119] K. Abersfelder, *PhD Thesis*, Imperial College London, Scheschkewitz group, **2012**.

8 Supporting Information

Selected parts of supporting information belonging to the publications presented in this thesis, including experiment procedures, UV/vis absorption spectra, DTF calculations results as well as crystal structure details are provided in this chapter.

8.1 Disilyl Silylene Reactivity of a Cyclotrisilene

Supporting information belonging to the following publication:

H. Zhao, K. Leszczyńska, L. Klemmer, V. Huch, M. Zimmer and D. Scheschkewitz, Disilyl Silylene Reactivity of a Cyclotrisilene, *Angew. Chem. Int. Ed.* **2018**, *57*, 2445-2449; *Angew. Chem.* **2018**, *130*, 2470-2474.

8.2 Phenylene-bridged 1,2,3-trisilacyclopentadienes

cross-conjugated

Supporting Information belonging to the following publication:

Hui Zhao, Lukas Klemmer, Michael J. Cowley, Moumita Majumdar, Volker Huch, Michael Zimmer and David Scheschkewitz, Phenylene-bridged cross-conjugated 1,2,3-trisilacyclopentadienes, *Chem. Commun.*, **2018**, *54*, 8399-8402.

[DOI: 10.1039/C8CC03297A](https://doi.org/10.1039/C8CC03297A)

8.3 Reactivity of a peraryl cyclotrisilene ($c\text{-Si}_3\text{R}_4$) toward chalcogens

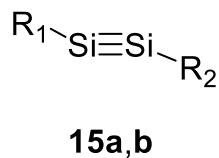
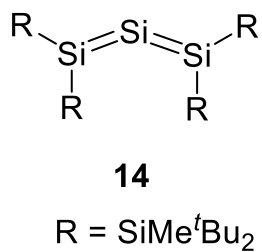
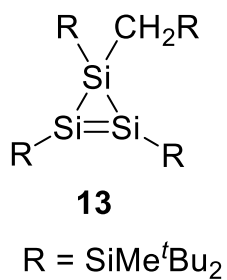
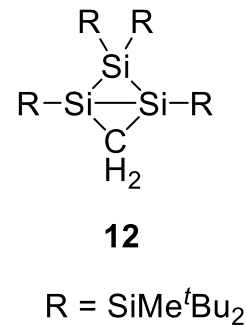
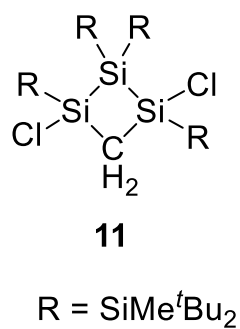
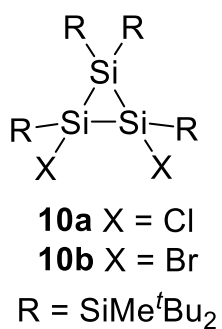
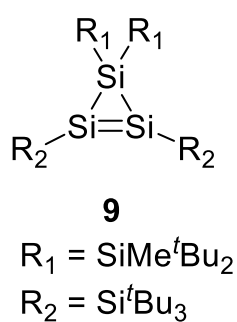
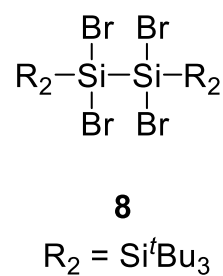
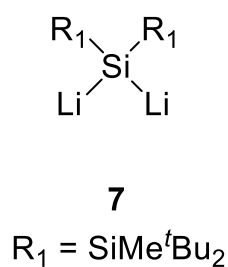
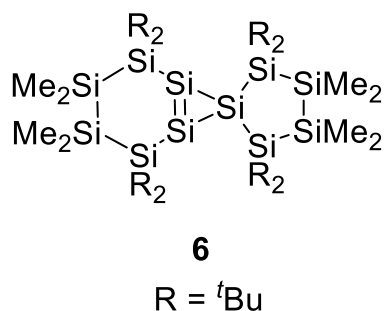
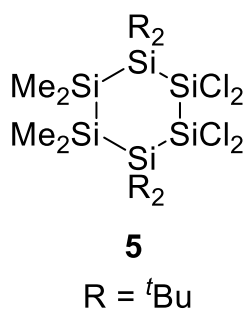
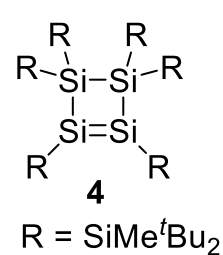
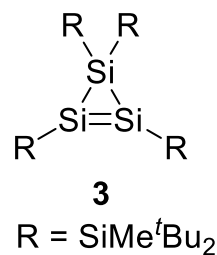
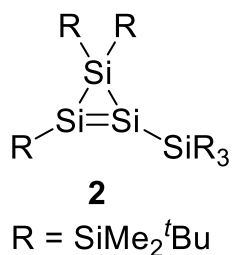
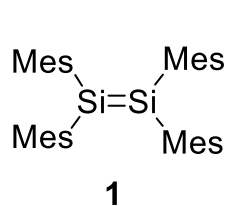
Supporting Information belonging to the following publication:

Hui Zhao, Lukas Klemmer, Michael J. Cowley, Volker Huch, Michael Zimmer and David Scheschkewitz, Reactivity of a Peraryl Cyclotrisilene ($c\text{-Si}_3\text{R}_4$) Toward Chalcogens, *Z. Anorg. Allg. Chem.* **2018**, 644, 999-1005.

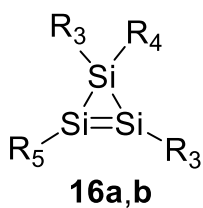
[DOI: 10.1002/zaac.201800182](https://doi.org/10.1002/zaac.201800182)

9 Appendix

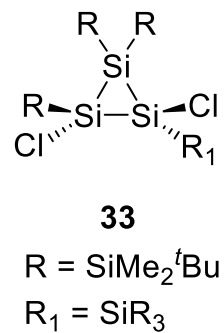
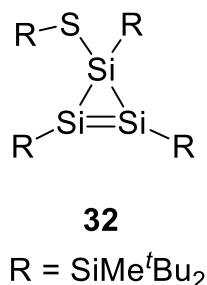
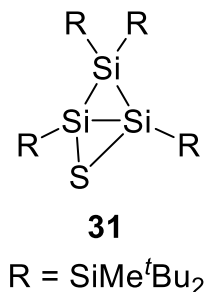
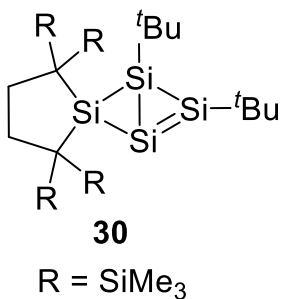
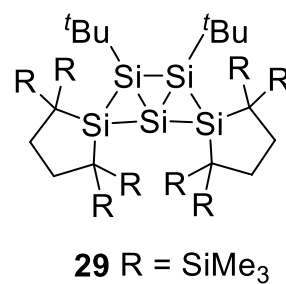
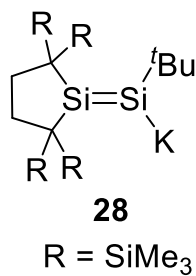
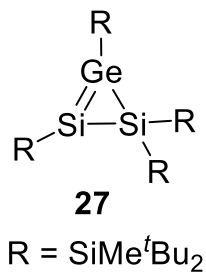
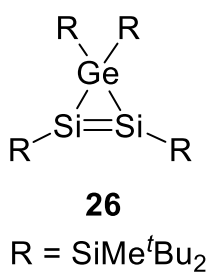
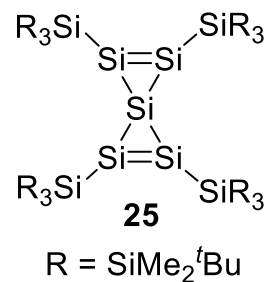
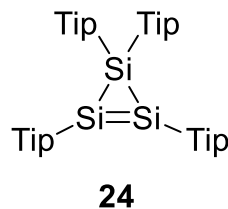
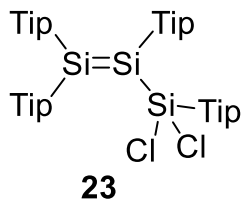
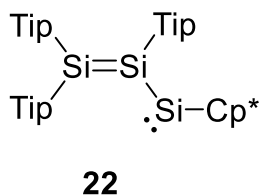
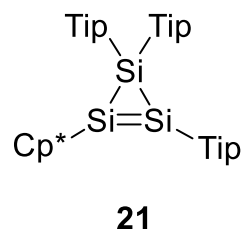
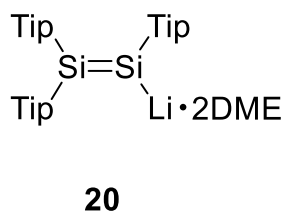
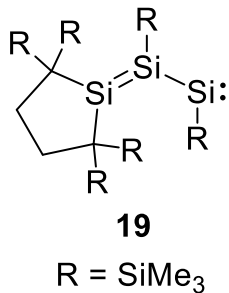
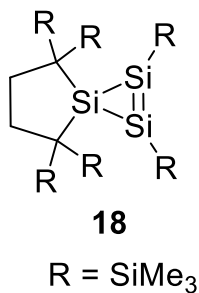
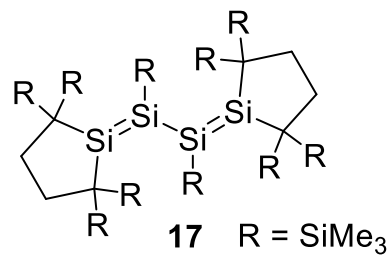
9.1 Overview of numbered compounds

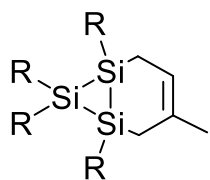


a: R₁ = R₂ = SiMe(Si^tBu₃)₂
b: R₁ = Si^tPrDsi₂
R₂ = SiNpDsi₂



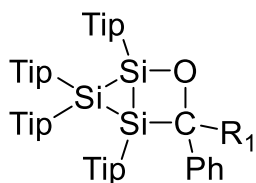
a: $R_3 = \text{Si}^t\text{Bu}_3$, $R_4 = \text{Me}$
 $R_2 = R_5 = \text{SiMe}(\text{Si}^t\text{Bu}_3)_2$
 b: $R_3 = \text{Dsi}$, $R_4 = \text{Np}$
 $R_1 = R_5 = \text{SiMe}(\text{Si}^t\text{Bu}_3)_2$





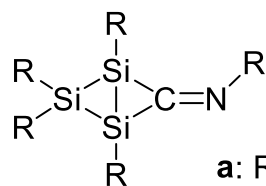
34

R = SiMe^tBu₂



35a,b

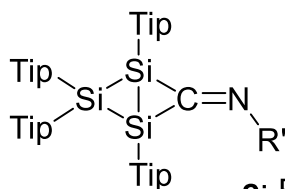
a: R1 = H
b: R1 = Ph



36a,b

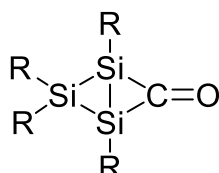
R = SiMe^tBu₂

a: R' = cyclohexyl
b: R' = Xyl

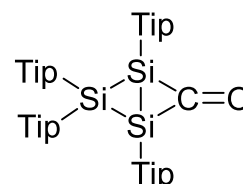


36c,d

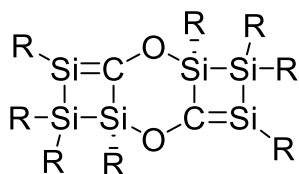
c: R' = ^tBu
d: R' = Xyl



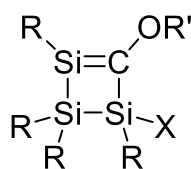
37a R = SiMe^tBu₂



37b

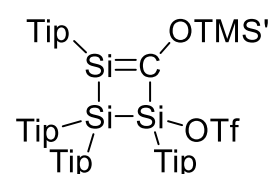


38 R = Tip

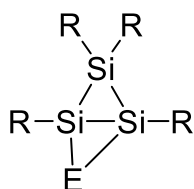


39a,b

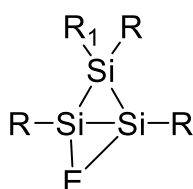
R = SiMe^tBu₂
a: R' = H, X = OH
b: R' = H, X = OMe



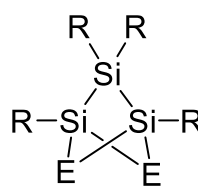
39c



40a-c R = SiMe^tBu₂
41a-c R = Tip

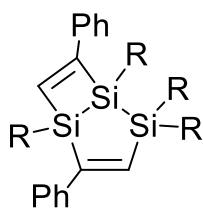


42a R = SiMe^tBu₂
R₁ = SR

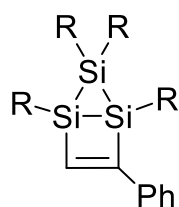


43a R = SiMe^tBu₂
44a,b R = Tip

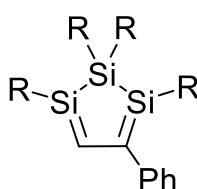
a: E = S
b: E = Se
c: E = Te



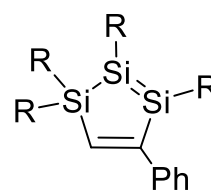
45



46

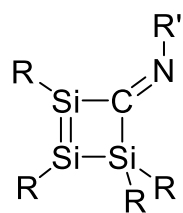


47



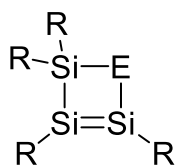
48

R = SiMe^tBu₂



49a R = SiMe^tBu₂
R' = Xyl

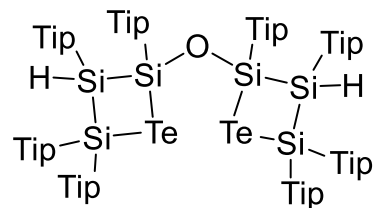
49b R = Tip, R' = ^tBu



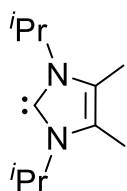
50a,b R = SiMe^tBu₂

51a-c R = Tip

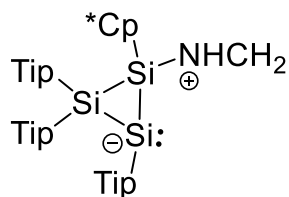
a: E = S
b: E = Se
c: E = Te



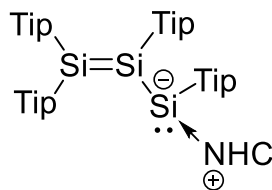
52



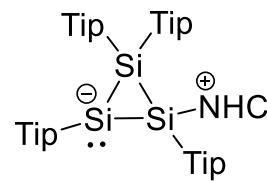
53



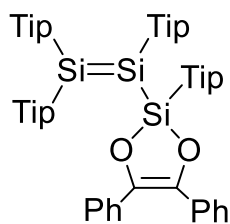
54



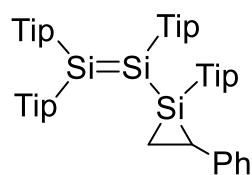
55



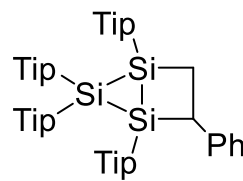
56



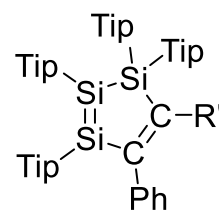
57



58

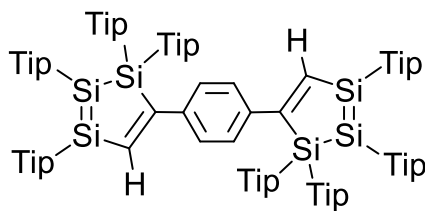


59

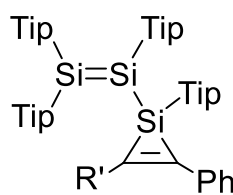


60a R' = H

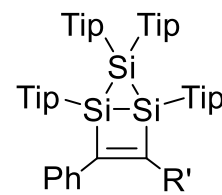
60b R' = Ph



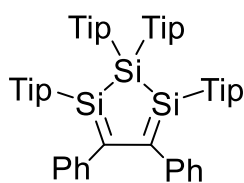
61



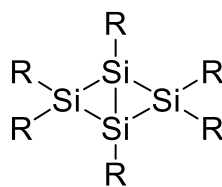
62



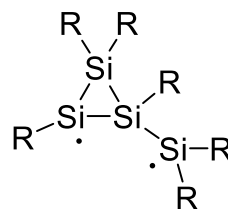
63



64

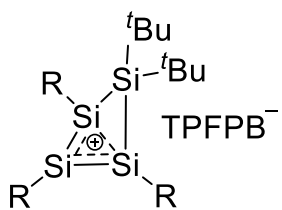


65

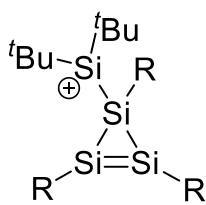
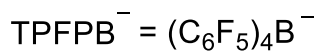


66

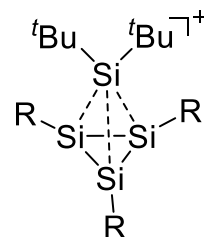
R = SiMe₂^tBu



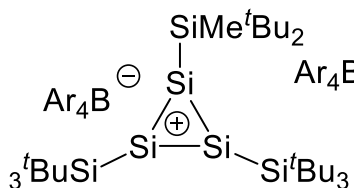
67⁺



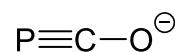
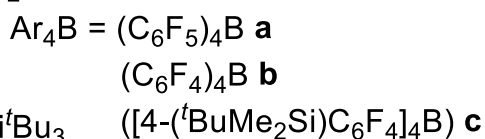
68⁺ R = SiMe^tBu₂



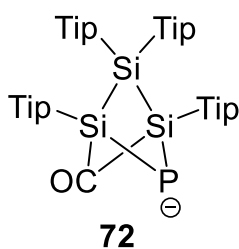
69⁺ R = SiMe^tBu₂



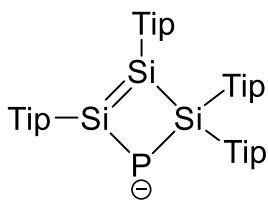
70⁺a-c



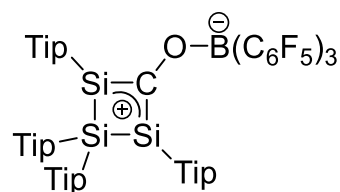
71



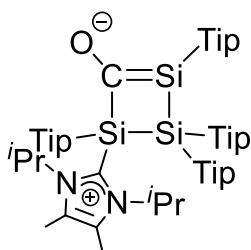
72



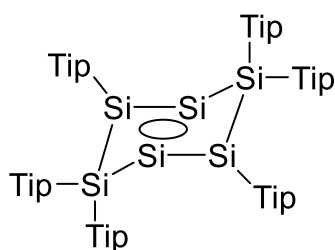
73



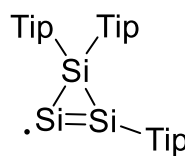
74



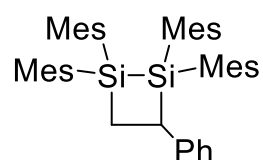
75



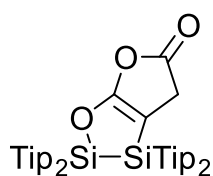
76



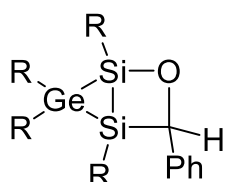
77



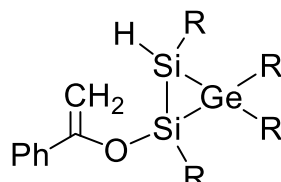
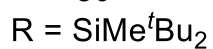
78



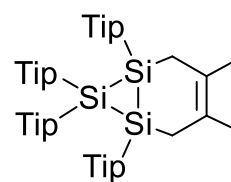
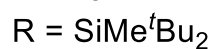
79



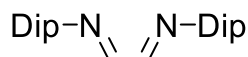
80



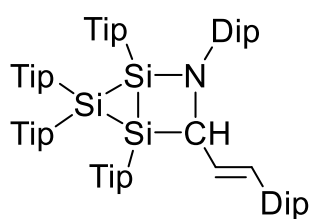
81



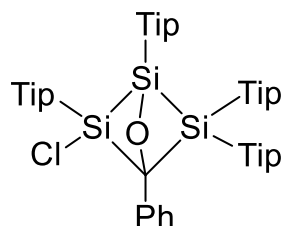
82



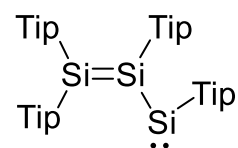
83



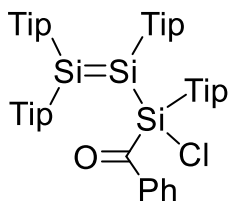
84



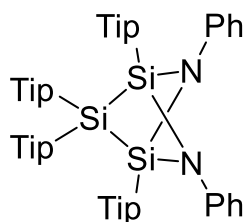
85



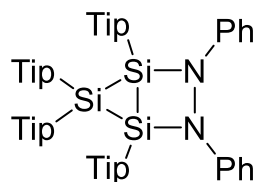
86



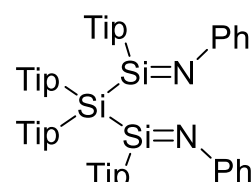
87



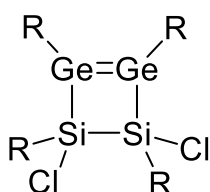
88



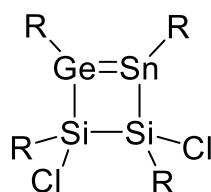
89



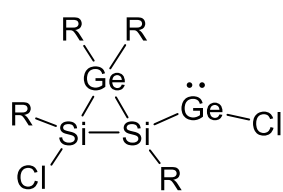
90



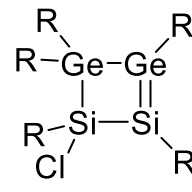
91



92

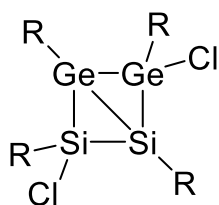


93

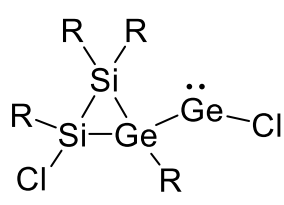


94

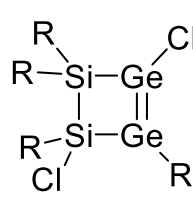
R = SiMe^tBu₂



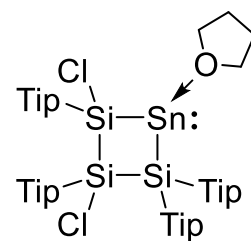
95



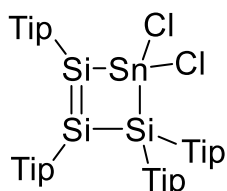
96



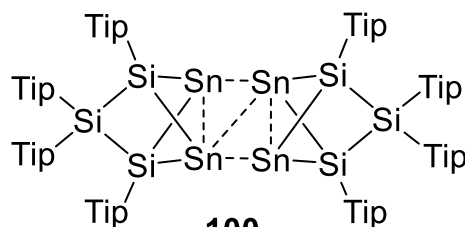
97



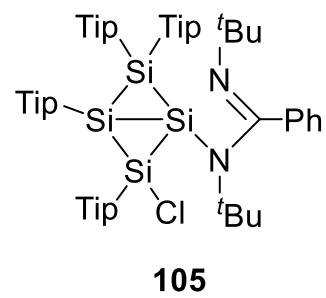
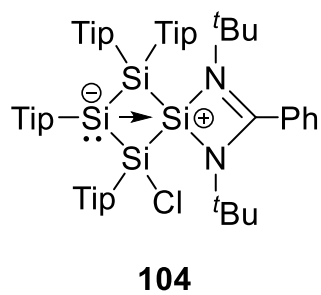
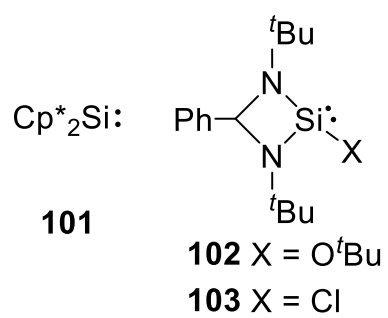
98



99



100



9.2 Absorption spectra

9.2.1 UV/vis Spectra and Determination of ϵ for **84**

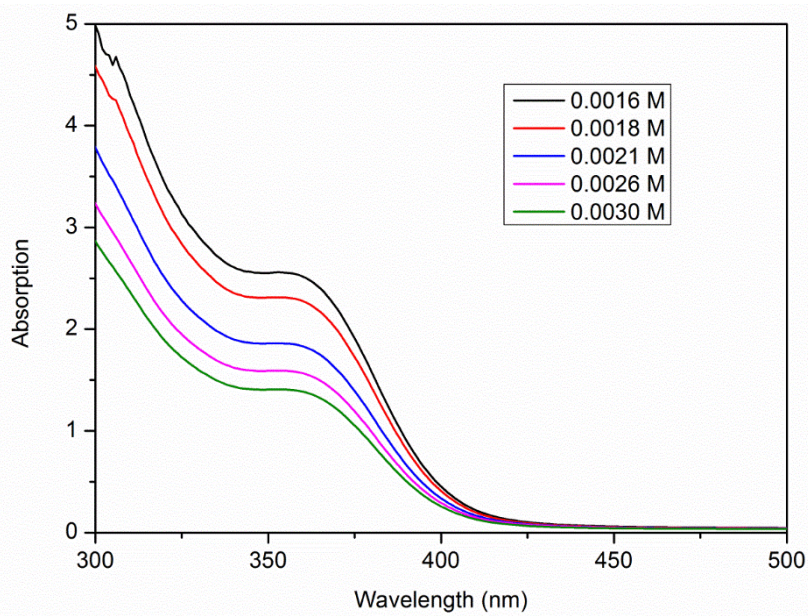


Figure 23. UV/vis spectra of **84** ($\lambda_{\text{max}} = 353 \text{ nm}$) in hexane at different concentrations ($1.6 \cdot 10^{-3} - 3.0 \cdot 10^{-3} \text{ mol L}^{-1}$).

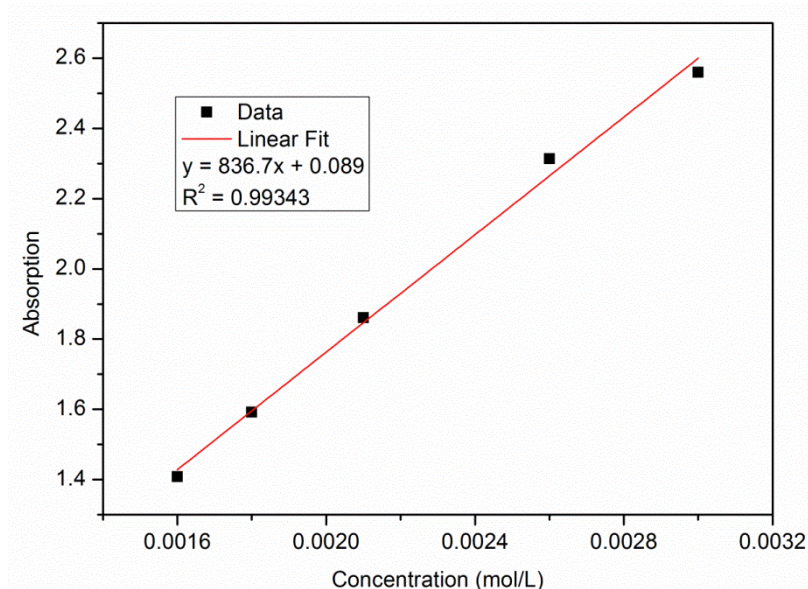


Figure 24. Determination of ϵ ($8367 \text{ L mol}^{-1}\text{cm}^{-1}$) at $\lambda = 353 \text{ nm}$ through a graphical draw of absorptions of **84** against their concentrations.

9.2.2 UV/vis Spectra and Determination of ϵ for **98**

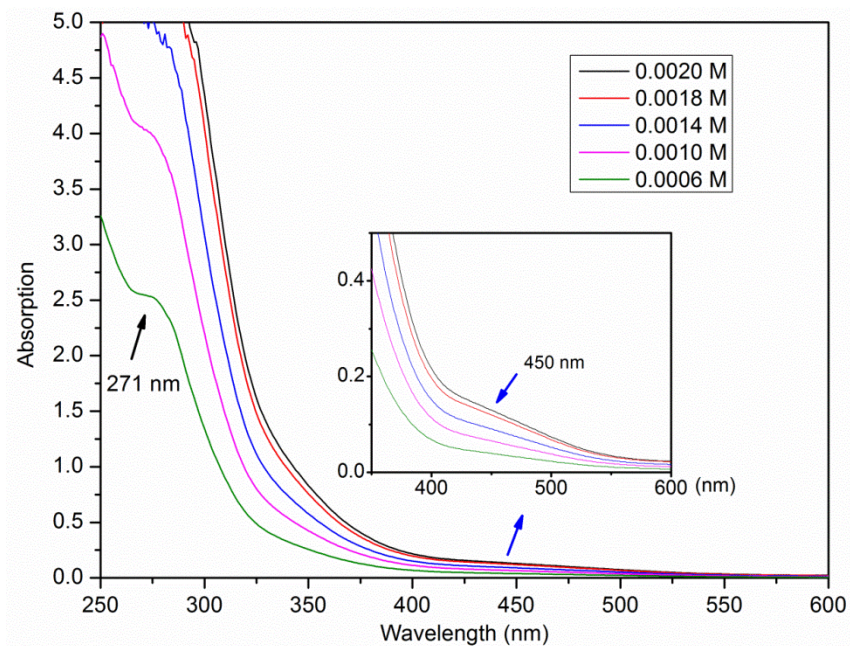


Figure 25. UV/vis spectra of **98** in thf at different concentrations ($0.6 \cdot 10^{-3} - 2.0 \cdot 10^{-3} \text{ mol L}^{-1}$). λ : 271 nm, 450 nm (shoulder).

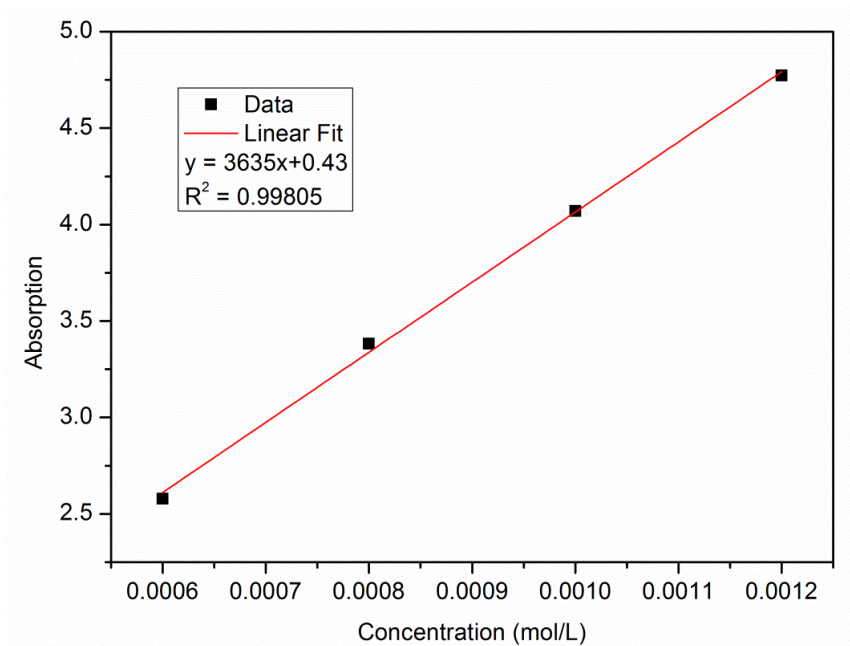


Figure 26. Determination of ϵ ($36350 \text{ L mol}^{-1} \text{ cm}^{-1}$) at $\lambda = 271 \text{ nm}$ through a graphical draw of absorptions of **98** against their concentrations.

9.2.3 UV/vis Spectra and Determination of ϵ for **104**

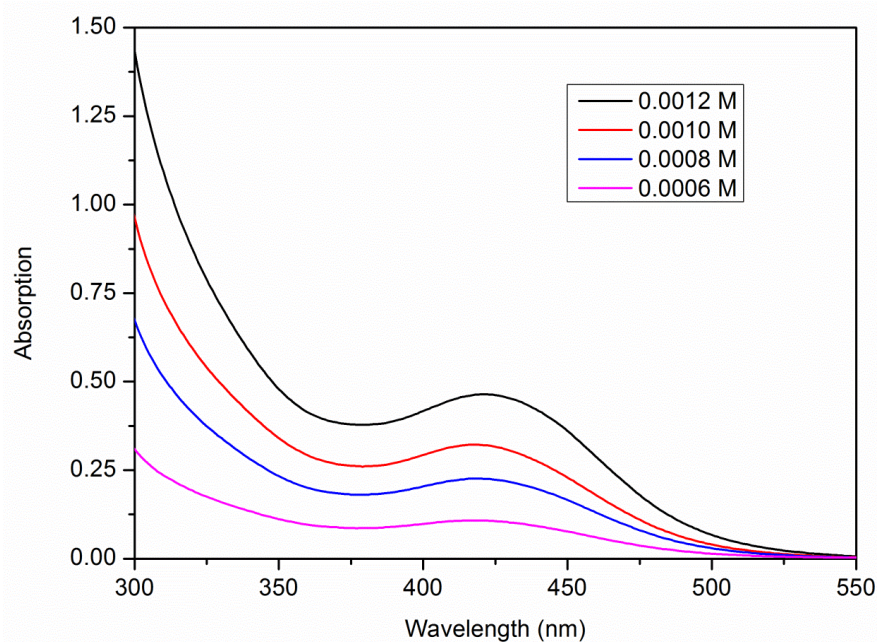


Figure 27. UV/vis spectra of **104** ($\lambda_{\text{max}} = 422 \text{ nm}$) in toluene at different concentrations ($0.6 \cdot 10^{-3} - 1.2 \cdot 10^{-3} \text{ mol L}^{-1}$).

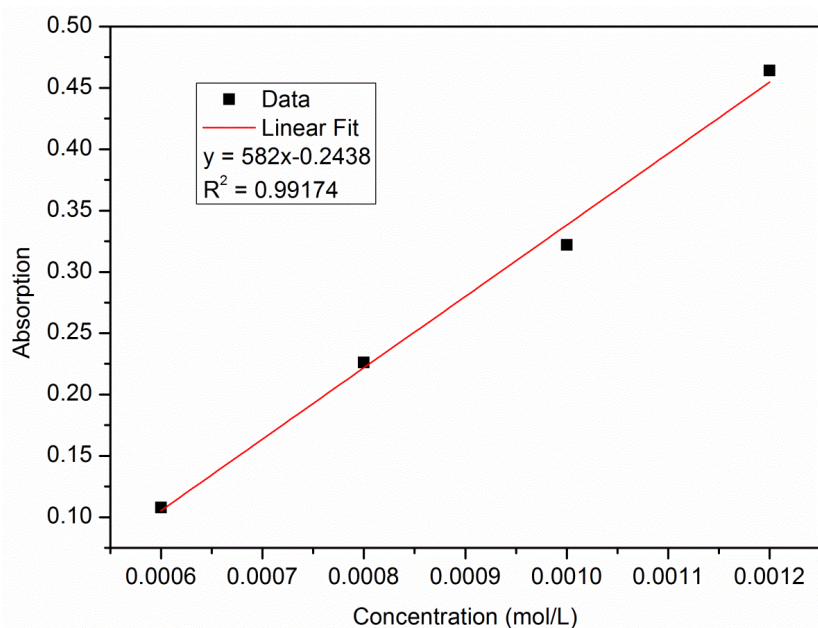


Figure 28. Determination of ϵ ($5820 \text{ L mol}^{-1}\text{cm}^{-1}$) at $\lambda = 422 \text{ nm}$ through a graphical draw of absorptions of **104** against their concentrations.

9.2.4 UV/vis Spectra and Determination of ϵ for **105**

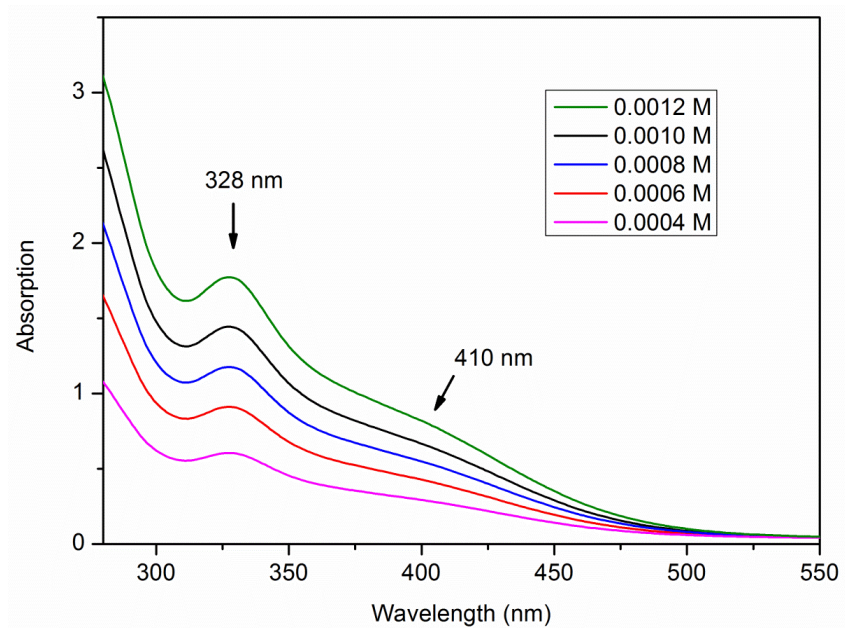


Figure 29. UV/vis spectra of **105** in hexane at different concentrations ($0.4 \cdot 10^{-3} - 1.2 \cdot 10^{-3} \text{ mol L}^{-1}$). $\lambda(\epsilon)$: 328 nm ($14350 \text{ L mol}^{-1}\text{cm}^{-1}$), 410 nm (shoulder).

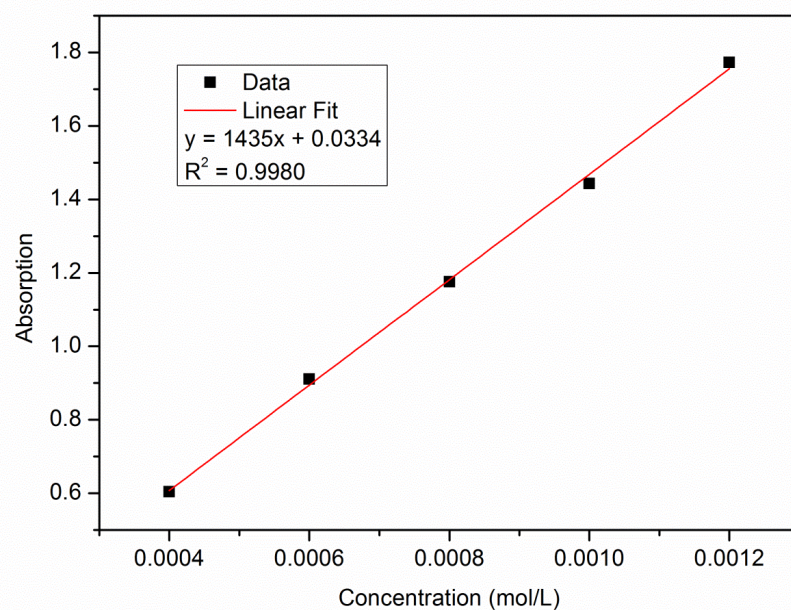
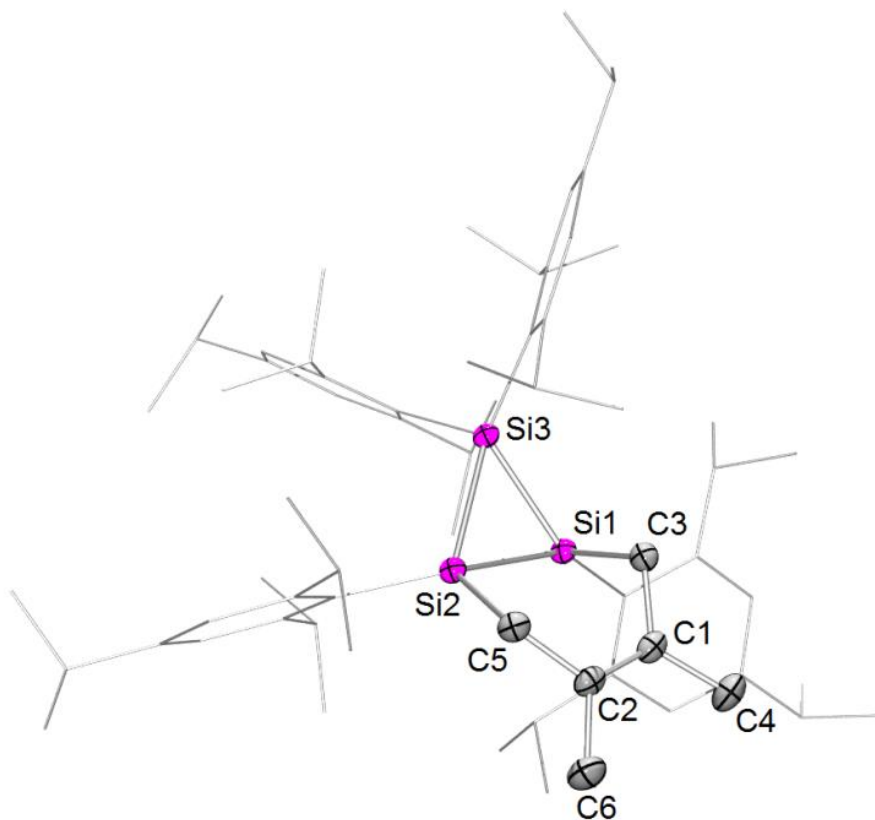


Figure 30. Determination of ϵ ($14350 \text{ L mol}^{-1}\text{cm}^{-1}$) at $\lambda = 328 \text{ nm}$ through a graphical draw of absorptions of **105** against their concentrations.

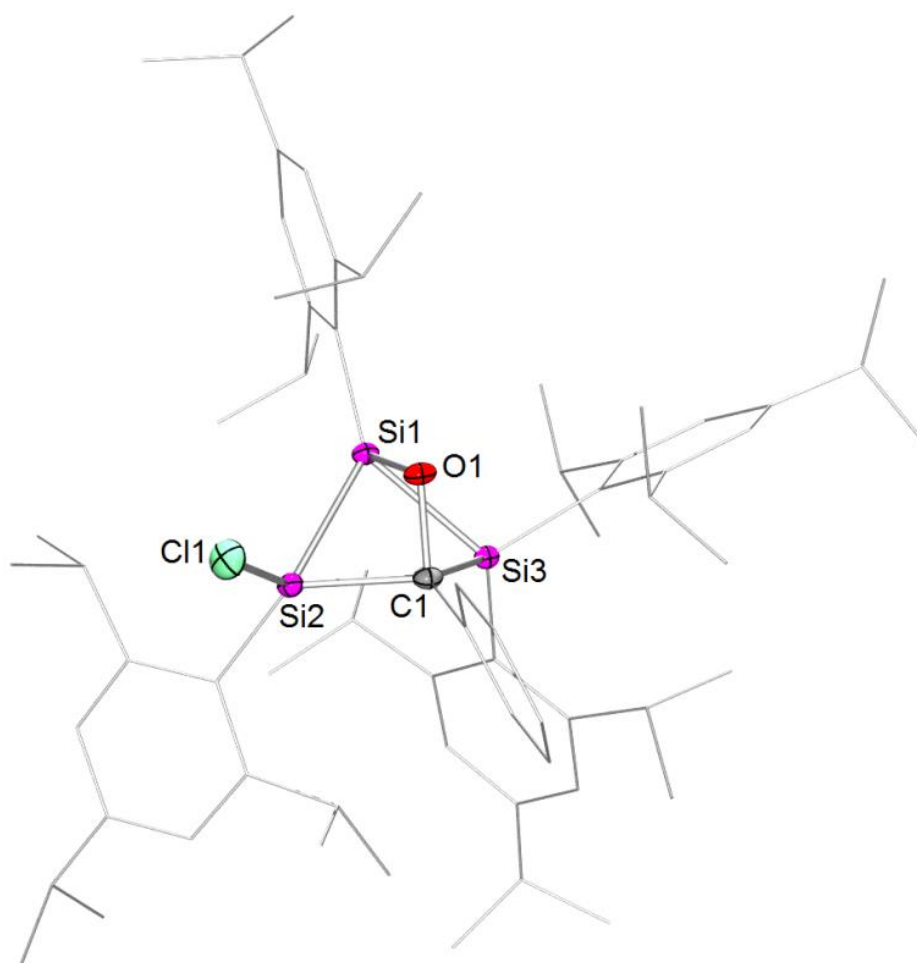
9.3 X-ray Structure Determination

9.3.1 Crystal Data and Structure Refinement for 82



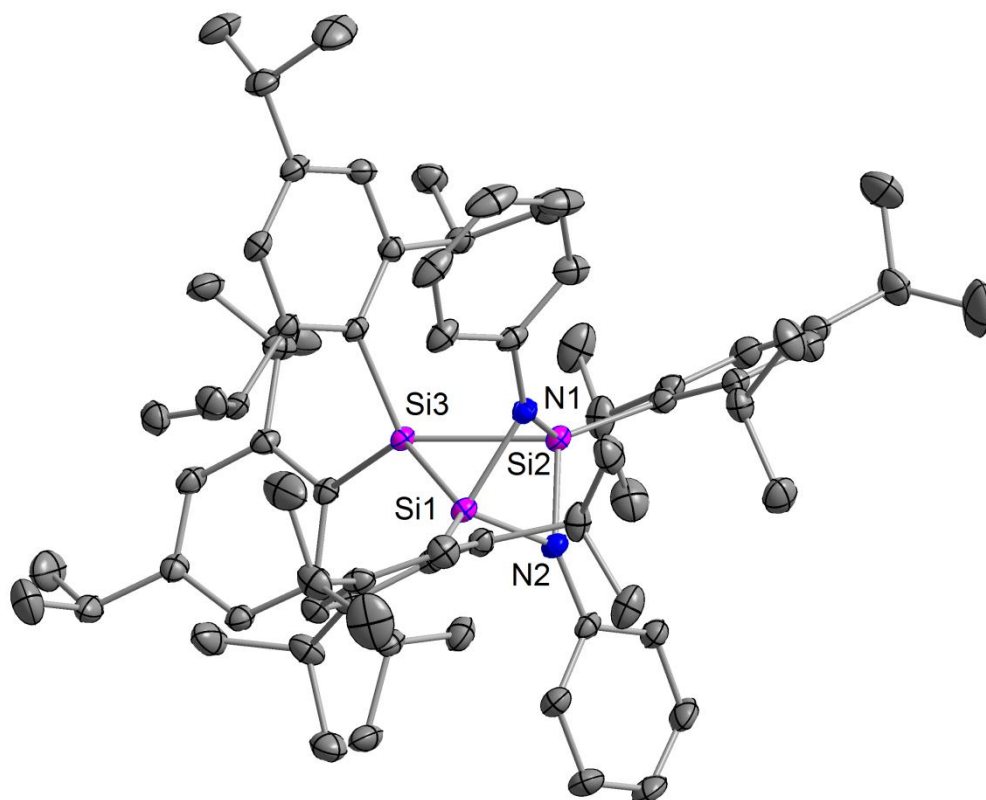
Identification code	sh3781
Empirical formula	C73 H110 Si3
Formula weight	1071.87
Temperature	152(2) K
Wavelength	0.71073 Å
Crystal system	Tetragonal
Space group	I 41/a
Unit cell dimensions	a = 40.0423(14) Å $\alpha = 90.000^\circ$. b = 40.0423(14) Å $\beta = 90.000^\circ$. c = 16.6447(7) Å $\gamma = 90.000^\circ$.
Volume	26688(2) Å ³
Z	16
Density (calculated)	1.067 Mg/m ³
Absorption coefficient	0.110 mm ⁻¹
F(000)	9440
Crystal size	0.542 x 0.096 x 0.092 mm ³
Theta range for data collection	1.017 to 26.486°.
Index ranges	-50 ≤ h ≤ 48, -50 ≤ k ≤ 50, -16 ≤ l ≤ 20
Reflections collected	198645
Independent reflections	13745 [R(int) = 0.1386]
Completeness to theta = 25.242°	100.0 %
Absorption correction	Semi-empirical from equivalents
Max. and min. transmission	0.7454 and 0.7100
Refinement method	Full-matrix least-squares on F ²
Data / restraints / parameters	13745 / 42 / 711
Goodness-of-fit on F ²	1.006
Final R indices [I > 2σ(I)]	R ₁ = 0.0548, ωR ₂ = 0.1071
R indices (all data)	R ₁ = 0.1126, ωR ₂ = 0.1301
Extinction coefficient	n/a
Largest diff. peak and hole	0.669 and -0.263 e.Å ⁻³

9.3.2 Crystal Data and Structure Refinement for 85



Identification code	sh3790
Empirical formula	C67 H97 Cl O Si3 x C6 H14
Formula weight	1124.33
Temperature	152(2) K
Wavelength	0.71073 Å
Crystal system	Triclinic
Space group	P-1
Unit cell dimensions	a = 12.8250(13) Å $\alpha = 73.024(5)^\circ$. b = 13.5014(14) Å $\beta = 85.230(5)^\circ$. c = 21.081(2) Å $\gamma = 78.689(5)^\circ$.
Volume	3422.1(6) Å ³
Z	2
Density (calculated)	1.091 Mg/m ³
Absorption coefficient	0.149 mm ⁻¹
F(000)	1232
Crystal size	0.376 x 0.260 x 0.132 mm ³
Theta range for data collection	1.010 to 27.228°.
Index ranges	-16<=h<=15, -17<=k<=17, -25<=l<=27
Reflections collected	53990
Independent reflections	14826 [R(int) = 0.0290]
Completeness to theta = 25.242°	99.2 %
Absorption correction	Semi-empirical from equivalents
Max. and min. transmission	0.7455 and 0.7138
Refinement method	Full-matrix least-squares on F ²
Data / restraints / parameters	14826 / 33 / 1061
Goodness-of-fit on F ²	1.035
Final R indices [I>2sigma(I)]	R ₁ = 0.0463, ω R ₂ = 0.1217
R indices (all data)	R ₁ = 0.0624, ω R ₂ = 0.1318
Extinction coefficient	n/a
Largest diff. peak and hole	0.845 and -0.404 e.Å ⁻³

9.3.3 Crystal Data and Structure Refinement for 88



Identification code	sh3604
Empirical formula	C ₇₂ H ₁₀₂ N ₂ Si ₃ x 0.5 (C ₅ H ₁₂)
Formula weight	1115.89
Temperature	142(2) K
Wavelength	0.71073 Å
Crystal system	Triclinic
Space group	P-1
Unit cell dimensions	a = 11.8008(5) Å α = 77.6128(12)°. b = 13.4826(6) Å β = 79.5939(12)°. c = 24.0224(11) Å γ = 68.0984(12)°.
Volume	3442.3(3) Å ³
Z	2
Density (calculated)	1.077 Mg/m ³
Absorption coefficient	0.110 mm ⁻¹
F(000)	1222
Crystal size	0.632 x 0.262 x 0.204 mm ³
Theta range for data collection	1.649 to 27.148°.
Index ranges	-14 ≤ h ≤ 15, -17 ≤ k ≤ 17, -30 ≤ l ≤ 30
Reflections collected	54972
Independent reflections	14792 [R(int) = 0.0298]
Completeness to theta = 25.242°	97.6 %
Absorption correction	Semi-empirical from equivalents
Max. and min. transmission	0.7455 and 0.6963
Refinement method	Full-matrix least-squares on F ²
Data / restraints / parameters	14792 / 36 / 1148
Goodness-of-fit on F ²	1.021
Final R indices [I > 2σ(I)]	R ₁ = 0.0399, ωR ₂ = 0.0938
R indices (all data)	R ₁ = 0.0568, ωR ₂ = 0.1026
Extinction coefficient	n/a
Largest diff. peak and hole	0.486 and -0.346 e.Å ⁻³

Curriculum Vitae

PERSONAL DATA

Name: Hui Zhao

Gender: Female

Date/Place of Birth: 27.09.1989, Henan Province, P. R. China.

Nationality: Chinese

Contact: s8huzhao@stud.uni-saarland.de, heiikee@163.com

EDUCATION

10.2014-present **PhD candidate** in Allgemeine und Anorganische Chemie, Naturwissenschaftlich-Technischen Fakultät, Saarland University, Germany

- Thesis: *Peraryl-substituted Cyclotrisilene ($c\text{-Si}_3\text{R}_4$) as a Precursor for Ring opening and Expansion*
Supervisor: Prof. Dr. David Scheschkewitz

09.2011-07.2014 **M.S.** in Organic Chemistry, Key Laboratory of Organosilicon Chemistry and Material Technology, Ministry of Education, Hangzhou Normal University, P. R. China

- Thesis: *Synthesis, Characterization and Reactions of New Silicon-containing Reactive Intermediates*
Supervisor: Prof. Dr. Zhifang Li

09.2006-07.2010 **B.S.** in Chemistry, Department of Chemistry, Anyang Normal University, P. R. China

- Thesis: *Investigation on Degradation Mechanism of Diclofenac Sodium by Thermal Degradation Kinetics*

POSTER PRESENTATIONS

- *Reactivity of cyclotrisilene towards multiply-bonded molecules:* H. Zhao, M. J. Cowley, M. Majumdar, V. Huch, D. Scheschkewitz, 14th International Symposium on Inorganic Ring Systems, Regensburg, **Germany, 2015.**
- *Reactivity of cyclotrisilene towards Chalcogens and carbon disulfide:* H. Zhao, P. Bag, M. J. Cowley, V. Huch, D. Scheschkewitz, 8th Europe Silicon Days, **Poland, 2016.**
- *Reactivity of Cyclotrisilene Towards Divalent Group 14 Species: An access to functionalized small inorganic rings:* H. Zhao, M. J. Cowley, D. Andrada, V. Huch, M. Zimmer and D. Scheschkewitz, 4th European Conference on Smart Inorganic Polymers, **Croatia, 2018.**
- *Peraryl-substituted Cyclotrisilene ($c\text{-Si}_3\text{R}_4$) in Synthesis:* H. Zhao, M. J. Cowley, V. Huch, M. Zimmer, and D. Scheschkewitz, 9th Europe Silicon Days, Saarbrücken, **Germany, 2018.**

ORAL PRESENTATIONS

- *Reactivity of cyclotrisilene towards small organic molecules*: ECUST-UdS Summerschool on Materials Science and Chemistry, Saarbrücken, Germany, October 6th, **2015**.
- *Cyclotrisilenes: Heavier Analogues of Cyclopropenes*: Anorganisch Chemisches Kolloquium Programm Winter semester 2015/ 2016, Saarland University, Saarbrücken, December 09th, **2015**.
- *Cyclotrisilenes: From disilyl silylene like reactivity to cross-conjugated Si=Si systems*: the 18th International Symposium on Silicon Chemistry in Conjugation with 6th Asian Silicon Symposium, Shandong University, Ji'nan, August 6th, **2017**

PUBLICATIONS

- H. Zhao, K. Leszczyńska, L. Klemmer, V. Huch, M. Zimmer, D. Scheschkewitz. Disilyl silylene reactivity of a cyclotrisilene. *Angew. Chem. Int. Ed.* **2018**, *57*, 2445-2449. [DOI 10.1002/anie.201711833](https://doi.org/10.1002/anie.201711833)
- H. Zhao, J. Li, X.-Q. Xiao, M. Kira, Z. F. Li, T. Müller. Cation-triggered stannate(II)/stannylene/stannylene conversion. *Chem. Eur. J.* **2018**, *24*, 5967-5973. [DOI 10.1002/chem.201800602](https://doi.org/10.1002/chem.201800602)
- H. Zhao, L. Klemmer, M. J. Cowley, M. Majumdar, V. Huch, M. Zimmer, D. Scheschkewitz. Phenylene-bridged cross-conjugated 1,2,3-trisilacyclopentadiene, *Chem. Commun.*, **2018**, *54*, 8399-8402. [DOI 10.1039/C8CC03297A](https://doi.org/10.1039/C8CC03297A)
- H. Zhao, L. Klemmer, M. J. Cowley, V. Huch, M. Zimmer and D. Scheschkewitz. Reactivity of a peraryl cyclotrisilene (*c*-Si₃R₄) toward chalcogens. *Z. Anorg. Allg. Chem.* **2018**, *644*, 999-1005. *Dedicated to Prof. Alexander Filippou on occasion of his 60th birthday.* [DOI 10.1002/zaac.201800182](https://doi.org/10.1002/zaac.201800182)
- K. Abersfelder, H. Zhao, A. J. P. White, C. Praesang, D. Scheschkewitz. Synthesis of the first homoleptic trisilaallyl chloride: 3-chloro-1,1,2,3,3-pentakis(2',4',6'-triisopropylphenyl)trisil-1-ene. *Z. Anorg. Allg. Chem.* **2015**, *641*, 2051-2055. *Dedicated to Professor F. Ekkehardt Hahn on the Occasion of His 60th Birthday.* [DOI 10.1002/zaac.201500561](https://doi.org/10.1002/zaac.201500561)
- X.-Q. Xiao, H. Zhao, Z. Xu, G. Q. Lai, X.-L. He and Z. F. Li. Reduction of the dihalocyclopentasilanes. A quest for a homocyclic silylene. *Chem. Commun.* **2013**, *49*, 2706-2708. *Back Cover* [DOI: 10.1039/C3CC00114H](https://doi.org/10.1039/C3CC00114H)
- X.-Q. Xiao, H. Zhao, J. Luo, Z. Xu, G. Q. Lai and Z. F. Li, Synthesis and characterization of heterocyclic disilylchalcogenides. *Dalton Trans.*, **2013**, *42*, 3994. [DOI: 10.1039/C2DT32406G](https://doi.org/10.1039/C2DT32406G)
- J. Luo, E.-H. Yan, H. Zhao, X.-Q. Xiao, Z. F. Li. Synthesis, structure and reactivity of sterically demanding oligosilanylmagnesium compounds. *Polyhedron* **2015**, *102*, 233-238. [DOI 10.1016/j.poly.2015.09.058](https://doi.org/10.1016/j.poly.2015.09.058)

